

國立交通大學

電信工程研究所

博士論文

以排隊理論為基礎對  
感知無線網路頻譜管理技術之研究  
Queueing-Theoretical Spectrum Management  
Techniques for Cognitive Radio Networks

研究生：王中瑋

指導教授：王蒞君

中華民國九十九年九月

以排隊理論為基礎對  
感知無線網路頻譜管理技術之研究

Queueing-Theoretical Spectrum Management  
Techniques for Cognitive Radio Networks

研究生：王中瑋

Student: Chung-Wei Wang

指導教授：王蒞君 博士

Advisor: Dr. Li-Chun Wang

國立交通大學

電信工程研究所

博士論文

A Dissertation

Submitted to Institute of Communication Engineering  
College of Electrical and Computer Engineering  
National Chiao Tung University  
in Partial Fulfillment of the Requirements  
for the Degree of Doctor of Philosophy  
in  
Communication Engineering  
Hsinchu, Taiwan

2010 年 9 月

# 以排隊理論為基礎對 感知無線網路頻譜管理技術之研究

研究生：王中璋

指導教授：王蒞君 博士

國立交通大學  
電信工程研究所

## 摘要

本論文探討感知無線網路的頻譜管理問題。在此網路中，來自主要使用者的『多次中斷』將大大地影響次要使用者的通訊效能。每當次要使用者被主要使用者中斷時，次要使用者必須選擇一個適合的通道進行頻譜切換，以便繼續未完成的傳輸。很明顯地，『多次中斷』將造成多次的頻譜切換，並且增加次要使用者連線的傳輸延遲。為了從一個宏觀的角度來分析感知無線網路下『多次中斷』行為對『次要使用者連線』所造成的傳輸延遲，本論文提出一個優先權排隊理論的分析模型替感知無線網路的頻譜使用行為進行建模。藉由此模型，我們分析次要使用者的一個重要服務品質參數：『完整系統時間』。

在此論文中，基於排隊理論分析模型，我們發展具服務品質考量的頻譜管理機制，其中包括 (1) 頻譜選擇機制、(2) 頻譜切換機制、和 (3) 頻譜分享機制的設計與討論。針對這些機制的具體研究成果敘述如下：(1) 針對頻譜選擇問題，我們提出一個具有負載平衡功效的頻譜選擇機制來優化次要使用者的『完整系統時間』；(2) 針對頻譜切換問題，我們量化在多通道下多次頻譜切換對次要使用者所造成的『完整系統時間』增加量；(3) 針對頻譜分享問題，我們提出一個允入控制機制來避免主要使用者被次要使用者干擾並優化次要使用者的『完整系統時間』。我們完整探討這三種頻譜管理機制對次要使用者所造成的傳輸延遲。基於這些分析結果，在不同資料到達率與服務時間分佈下，我們可以設計相對應的頻譜管理機制來增強次要使用者連線的傳輸品質。

總而言之，本論文的主要貢獻是提出一個以排隊理論為基礎的分析模型並用多樣化的角度與觀點來對感知無線網路效能進行分析。本論文所建議之模型可以提供一個很好的感知無線網路效能之分析架構。

# Queueing-Theoretical Spectrum Management Techniques for Cognitive Radio Networks

Student: Chung-Wei Wang

Advisor: Dr. Li-Chun Wang

Department of Electrical Engineering  
National Chiao Tung University

## Abstract

In this dissertation, we investigate spectrum management techniques in cognitive radio (CR) networks with quality of service (QoS) provisioning. One fundamental issue in enhancing QoS performance for the secondary users is the multiple interruptions from the primary users during each secondary user's connection. These interruptions from the primary users result in the phenomenon of multiple spectrum handoffs within one secondary user's connection. Thus, a set of target channels for spectrum handoffs are needed to be selected sequentially. In order to characterize the general channel usage behaviors with multiple handoffs from a macroscopic viewpoint, an analytical framework based on the preemptive resumption priority (PRP) M/G/1 queueing theory is introduced. Based on the PRP M/G/1 queueing network model, we can evaluate the effects of multiple handoffs on the overall system time, which is an important QoS performance measure for the secondary connections in CR networks.

The proposed analytical framework can provide important insights into the design of spectrum management techniques in CR networks. In order to demonstrate the effectiveness of this analytical model, we discuss various spectrum management techniques, consisting of spectrum decision, spectrum sharing, and spectrum mobility. For the *spectrum decision* issue, we show how to determine which channels are required to probe and transmit. For the *spectrum mobility* issue, we illustrate how to characterize the effects of multiple handoffs, where the secondary users can have different operating channels before and after spectrum handoff. For the *spectrum sharing* issue, we explore how to determine the optimal admission probability to avoid the interference between primary and secondary users in the presence of false alarm and missed detection. From numerical results, we can develop traffic-adaptive spectrum management policies to enhance the QoS performance of the secondary users in CR networks with various traffic arrival rates and service distributions.

To summarize, the main contribution of this dissertation is to investigate the modeling techniques for CR networks from a macroscopic viewpoint based on the queueing theory. The proposed analytical framework can help analyze the performances of CR networks and provide important insights into the design of various spectrum management techniques with enhanced QoS performances.

# Acknowledgements

First of all, I want to express my deeply gratitude to my advisor, Prof. Li-Chun Wang. Not only the important insights to research problems, encouragement, and support, he also shows me a way of being optimistic to face difficulties. Without his advice, guidance, comments, and all that, this work could not have been done. He indeed opened a door to the future for me.

Special thanks to my mates of Wireless System Laboratory in National Chiao Tung University. They gave me kindly help in many aspects in my study. Drs. Chih-Wen Chang, Anderson Chen, Wei-Cheng Liu, and Jane-Hwa Huang gave me many valuable suggestions and ideas in my research. Messrs. Chu-Jung Yeh, Samer Talat, and Ang-Hsun Tsai encouraged me every time when I felt frustrated. I was so lucky to have all these lab mates.

Most importantly, I would like to thank Prof. Fumiyuki Adachi. During the study in Tohoku University from April, 2009 to March, 2010, he give me many valuable comments. Furthermore, I also wish to thank my mates of Wireless Signal Processing and Networking Laboratory in Tohoku University, especially for Prof. Wei Peng, Mr. Takeda, and Mr. Guan Gui.

Finally, my thanks would go to my wife, Hui-Cheng Chuang, and beloved family for their loving considerations and great confidence in me all through these years. I also want to thank Hsing Tian Kong Culture and Education Development Foundation. Because of their scholarship supports, I can con-

centrate our attention on my research. I also owe my sincere gratitude to my friends who gave me their help and time in listening to me and helping me work out my problems during the difficult course of the thesis.



# Contents

<b>Abstract</b>	<b>i</b>
<b>Acknowledgements</b>	<b>iii</b>
<b>Contents</b>	<b>v</b>
<b>List of Tables</b>	<b>xii</b>
<b>List of Figures</b>	<b>xiii</b>
<b>Glossary of Symbols</b>	<b>xx</b>
<b>1 Introduction</b>	<b>1</b>
1.1 Problems and Solutions . . . . .	6
1.1.1 Modeling Techniques for Cognitive Radio Networks . . . . .	6
1.1.2 Load-Balancing Spectrum Decision . . . . .	7
1.1.3 Proactive Spectrum Handoff . . . . .	8
1.1.4 Optimal Proactive Spectrum Handoff . . . . .	9
1.1.5 Reactive Spectrum Handoff . . . . .	10
1.1.6 Interference-Avoiding Spectrum Sharing . . . . .	10
1.2 Dissertation Outlines . . . . .	11



<b>2</b>	<b>Background and Literature Survey</b>	<b>14</b>
2.1	Modeling Techniques for Cognitive Radio Networks . . . . .	14
2.2	Load-Balancing Spectrum Decision . . . . .	16
2.2.1	Probability-based Spectrum Decision . . . . .	16
2.2.2	Sensing-based Spectrum Decision . . . . .	20
2.3	Proactive Spectrum Handoff . . . . .	20
2.4	Optimal Proactive Spectrum Handoff . . . . .	24
2.5	Reactive Spectrum Handoff . . . . .	25
2.6	Interference-Avoiding Spectrum Sharing . . . . .	28
2.6.1	Admission Control with Perfect Sensing . . . . .	28
2.6.2	Admission Control without Perfect Sensing . . . . .	31
<b>3</b>	<b>Queueing-Theoretical Modeling Techniques for Cognitive Ra-</b>	
	<b>dio Networks</b>	<b>32</b>
3.1	Motivation . . . . .	33
3.2	Transmission Processes with Multiple Handoffs for the Sec-	
	ondary Users' Connections . . . . .	34
3.3	Queueing Theoretical Framework for Spectrum Management .	37
3.3.1	Assumptions . . . . .	37
3.3.2	Overview of the PRP M/G/1 Queueing Network Model	37
3.3.3	Modeling of the Connection-based Channel Usage Be-	
	haviors . . . . .	41
3.3.4	Two Auxiliary Parameters: $\omega_i^{(k)}$ and $\Phi_i^{(k)}$ . . . . .	42
3.3.5	Constraint . . . . .	44
3.4	Summary . . . . .	44
<b>4</b>	<b>Load-Balancing Spectrum Decision</b>	<b>46</b>
4.1	Motivation . . . . .	47

4.2	System Model . . . . .	49
4.2.1	Assumptions . . . . .	49
4.2.2	Spectrum Decision Behavior Model . . . . .	49
4.3	Problem Formulation . . . . .	51
4.3.1	Performance Metric: Overall System Time . . . . .	51
4.3.2	Overall System Time Minimization Problem for Probability- based Channel Selection Scheme . . . . .	51
4.3.3	Overall System Time Minimization Problem for Sensing- based Channel Selection Scheme . . . . .	53
4.3.4	Performance Model . . . . .	54
4.4	Analysis of Overall System Time . . . . .	57
4.4.1	Extended Data Delivery Time . . . . .	57
4.4.2	Waiting Time . . . . .	59
4.5	Effects of Sensing Errors . . . . .	62
4.5.1	False Alarm . . . . .	63
4.5.2	Missed Detection . . . . .	64
4.6	Numerical Results . . . . .	66
4.6.1	Probability-based Spectrum Decision Scheme . . . . .	66
4.6.2	Sensing-based Spectrum Decision Scheme . . . . .	70
4.6.3	Comparison between Different Spectrum Decision Schemes	75
<b>5</b>	<b>Proactive Spectrum Handoff</b>	<b>77</b>
5.1	Motivation . . . . .	79
5.2	System Model . . . . .	79
5.2.1	Assumptions . . . . .	79
5.2.2	Illustrative Example of Proactive Multiple Handoffs with Multiple Interruptions . . . . .	80
5.3	Analytical Model . . . . .	82

5.4	Analysis of Extended Data Delivery Time . . . . .	84
5.5	Applications to Performance Analysis in IEEE 802.22 . . . . .	92
5.5.1	Derivation of Extended Data Delivery Time . . . . .	92
5.5.2	An Example for Homogeneous Traffic Loads . . . . .	93
5.6	Numerical Results . . . . .	95
5.6.1	Simulation Setup . . . . .	95
5.6.2	Effects of Various Service Time Distributions for Pri- mary Connections . . . . .	96
5.6.3	Traffic-adaptive Target Channel Selection Principle . . . . .	98
5.6.4	Performance Comparison between Different Channel Selection Methods . . . . .	103
<b>6</b>	<b>Optimal Proactive Spectrum Handoff</b>	<b>107</b>
6.1	Problem Formulation . . . . .	108
6.2	Cumulative Handoff Delay Analysis . . . . .	109
6.3	An Optimal Dynamical Programming Algorithm . . . . .	112
6.3.1	State Diagram for Target Channel Sequences . . . . .	113
6.3.2	Optimal Substructure Property . . . . .	115
6.3.3	Dynamic-Programming-Based Target Channel Selec- tion Algorithm . . . . .	116
6.4	A Suboptimal Low-Complexity Greedy Algorithm . . . . .	117
6.4.1	Greedy Target Channel Selection Strategy . . . . .	117
6.4.2	Greedy Target Channel Selection Algorithm . . . . .	123
6.5	Numerical Results . . . . .	123
6.5.1	Effects of Traffic Statistics for Arriving Secondary User's Service Time . . . . .	124
6.5.2	Effects of Traffic Statistics of Existing Secondary Users' Connections . . . . .	125

6.5.3	Effects of Traffic Statistics of Existing Primary Users' Connections . . . . .	131
<b>7</b>	<b>Reactive Spectrum Handoff</b>	<b>134</b>
7.1	System Model . . . . .	136
7.1.1	Assumptions . . . . .	136
7.1.2	Illustrative Example of Reactive Multiple Handoffs with Multiple Interruptions . . . . .	136
7.2	Analytical Model . . . . .	138
7.2.1	Notations . . . . .	139
7.3	Analysis of Channel Utilization Factor . . . . .	143
7.3.1	Derivations of $\omega_{i,\eta}^{(k)}$ and $\mathbf{E}[\Phi_{i,\eta}^{(k)}]$ . . . . .	145
7.3.2	An Example for the Exponentially Distributed Service Time . . . . .	148
7.4	Analysis of Extended Data Delivery Time . . . . .	149
7.4.1	Derivations of $\Pr\{\mathbf{S}^{(\eta)} = \mathbf{s}_N\}$ and $\mathbf{E}[D \mathbf{S}^{(\eta)} = \mathbf{s}_N]$ . . . . .	149
7.4.2	An Example for the Exponentially Distributed Service Time . . . . .	152
7.5	Numerical Results . . . . .	155
7.5.1	Simulation Setting . . . . .	155
7.5.2	Effects of Various Arrival Rates for the Secondary Users' Connections . . . . .	155
7.5.3	Effects of Heterogeneous Arrival Rates for the Primary Users' Connections . . . . .	158
7.5.4	Effects of Handoff Processing Time . . . . .	161
7.5.5	Comparison between Proactive and Reactive Spectrum Handoff Scheme . . . . .	164

<b>8</b>	<b>Interference-Avoiding Spectrum Sharing</b>	<b>168</b>
8.1	Motivation . . . . .	169
8.2	System Model . . . . .	171
8.2.1	Assumptions . . . . .	171
8.2.2	Admission Control Mechanism . . . . .	172
8.3	Problem Formulation and Analytical Model . . . . .	172
8.3.1	Problem Formulation . . . . .	172
8.3.2	Analytical Model . . . . .	174
8.4	Analysis of Constraint Functions in the Utilization Maximiza- tion Problem . . . . .	175
8.4.1	Analysis of Actual Service Time of the Primary Con- nection in the Physical Channel . . . . .	175
8.4.2	Analysis of Overall System Time of the Secondary Con- nections . . . . .	178
8.5	Numerical Results . . . . .	181
<b>9</b>	<b>Conclusions</b>	<b>185</b>
9.1	Modeling Techniques for Cognitive Radio Networks . . . . .	186
9.2	Load-Balancing Spectrum Decision . . . . .	187
9.3	Proactive Spectrum Handoff . . . . .	188
9.4	Optimal Proactive Spectrum Handoff . . . . .	188
9.5	Reactive Spectrum Handoff . . . . .	189
9.6	Interference-Avoiding Spectrum Sharing . . . . .	190
9.7	Suggestions for Future Research . . . . .	190
	<b>Bibliography</b>	<b>194</b>
	<b>Appendices</b>	<b>209</b>

A	Distribution Probability Vector for the Sensing-based Channel Selection Scheme . . . . .	209
B	Derivation of $\omega_i^{(k)}$ . . . . .	210
C	Derivations of $\mathbf{E}[\Phi_i^{(k)}]$ and $\mathbf{E}[(\Phi_i^{(k)})^2]$ . . . . .	211
D	Derivation of $\mathbf{Pr}(\tilde{X}_p = x)$ . . . . .	214
<b>Vita</b>		<b>215</b>
<b>Publication List</b>		<b>216</b>



# List of Tables

2.1	Comparison of Various Analytical Models for CR Networks. . .	15
2.2	Comparison of Various Load-balancing Spectrum Decision Schemes for Cognitive Radio Networks, where PP, GT, and LA stand for the packet-wise probabilistic, game-theoretic, and learning automata approaches, respectively. . . . .	17
2.3	Comparison of Various Proactive Handoff Models. . . . .	21
2.4	Comparison of Various Channel Usage Models. . . . .	26
2.5	Comparison of Various Objective Functions. . . . .	29
9.1	Summary of This Dissertation . . . . .	191

# List of Figures

1.1	An illustrative example of CR network, which consists a primary network and a secondary network. There are three primary users (PUs) and one secondary user (SU) in the primary and secondary networks, respectively. . . . .	2
1.2	During the transmission period of secondary user (SU), it experiences multiple handoffs. . . . .	3
1.3	Relationships between spectrum sensing, spectrum decision, spectrum mobility, and spectrum sharing functionalities. . . .	5
1.4	Outline of this dissertation. . . . .	12
3.1	Illustration of transmission procedures in a two-channel system. The gray areas indicate that the channels are occupied by the existing primary users' connections (PCs) or the other secondary users' connections (SCs). . . . .	35
3.2	The PRP M/G/1 queueing network model with three channels. $\lambda_p^{(k)}$ , $\lambda_s^{(k)}$ , and $\omega_n^{(k)}$ are the arrival rates of the primary connections, the secondary connections, and the type- $n$ secondary connections ( $n \geq 1$ ) at channel $k$ . Note that $\omega_0^{(k)} = \lambda_s^{(k)}$ . Furthermore, $f_p^{(k)}(x)$ and $f_i^{(k)}(\phi)$ are the pmfs of $X_p^{(k)}$ and $\Phi_i^{(k)}$ , respectively. . . . .	39



3.3	Illustration of the physical meaning of random variable $\Phi_i^{(k)}$ . For example, $\Phi_2^{(1)}$ is one of the third segments (gray areas) of the first, the third, and the fourth secondary connections. . . .	45
4.1	Spectrum decision behavior model. . . . .	50
4.2	Example of the overall system time of the secondary connection $SC_A$ . The white areas indicate that channel is occupied by $SC_A$ . Furthermore, the gray areas indicate that channel is occupied by the primary connections (PCs) and its duration is the busy period resulting from transmissions of the primary connections. Here, $SC_A$ encounters two interruptions from the primary connections during its transmission period. . . . .	52
4.3	Performance model for the probability-based channel selection scheme where the channel usage behaviors are characterized by the PRP M/G/1 queueing systems. . . . .	55
4.4	Performance model for the sensing-based channel selection scheme where the channel usage behaviors are characterized by the PRP M/G/1 queueing systems. . . . .	56
4.5	Optimal distribution probability vector for the probability-based spectrum decision with various arrival rates of the secondary connections, where $P_F = 0.1$ , $P_M = 0.1$ , and $\mathbf{E}[X_s] = 10$ . . . . .	68
4.6	Channel busy probability for the probability-based spectrum decision with various arrival rates of the secondary connections, where $P_F = 0.1$ , $P_M = 0.1$ , and $\mathbf{E}[X_s] = 10$ . . . . .	69
4.7	Channel busy probability for the probability-based spectrum decision with various arrival rates of the secondary connections, where $P_F = 0$ , $P_M = 0$ , and $\mathbf{E}[X_s] = 15$ . . . . .	71

4.8	Optimal distribution probability vector for the probability-based spectrum decision with various arrival rates of the secondary connections, where $P_M = 0.1$ , $\lambda_s = 0.03$ , and $\mathbf{E}[X_s] = 15$ .	72
4.9	Overall system time for the sensing-based spectrum decision with various numbers of candidate channels $n$ , where $P_F = 0.1$ , $P_M = 0.1$ , $\tau = 2$ , and $\mathbf{E}[X_p] = 20$ .	73
4.10	Overall system time for the sensing-based spectrum decision with various numbers of candidate channels $n$ , where $P_M = 0.1$ , $\tau = 2$ , $\mathbf{E}[X_p] = 20$ , and $\mathbf{E}[X_s] = 5$ .	74
4.11	Comparison of the overall system time for three considered spectrum decision schemes, where $P_F = 0.1$ , $P_M = 0.1$ , and $\mathbf{E}[X_s] = 10$ .	76
5.1	An example of transmission process for the secondary connection $SC_A$ , where $t_s$ is the channel switching time, $T$ is the extended data delivery time of $SC_A$ , and $D_i$ is the handoff delay of the $i^{th}$ interruption. The gray areas indicate that the channels are occupied by the existing primary connections (PCs) or secondary connections (SCs). Because $SC_A$ is interrupted three times in total, the overall data connection is divided into four segments.	83
5.2	The PRP M/G/1 queueing network model with three channels where $\lambda_p^{(k)}$ , $\lambda_s^{(k)}$ , and $\omega_n^{(k)}$ are the arrival rates of the primary connections, the secondary connections, and the type- $n$ secondary connections ( $n \geq 1$ ) at channel $k$ . Note that $\omega_0^{(k)} = \lambda_s^{(k)}$ . Furthermore, $f_p^{(k)}(x)$ and $f_i^{(k)}(\phi)$ are the pdfs of $X_p^{(k)}$ and $\Phi_i^{(k)}$ , respectively.	85

5.3	Effects of Pareto and exponential service time distributions for primary connections on the extended data delivery time ( $\mathbf{E}[T_{change}]$ ) of the secondary connections when the <b>always-changing</b> spectrum handoff sequence is adopted, where $t_s = 1$ (slot), $\lambda_s = 0.01$ (arrivals/slot), $\mathbf{E}[X_s] = 10$ (slots/arrival), and $\mathbf{E}[X_p] = 20$ (slots/arrival). . . . .	99
5.4	Effects of Pareto and exponential service time distributions for primary connections on the extended data delivery time ( $\mathbf{E}[T_{stay}]$ ) of the secondary connections when the <b>always-staying</b> spectrum handoff sequence is adopted, where $t_s = 1$ (slot), $\lambda_s = 0.01$ (arrivals/slot), $\mathbf{E}[X_s] = 10$ (slots/arrival), and $\mathbf{E}[X_p] = 20$ (slots/arrival). . . . .	100
5.5	Comparison of the extended data delivery time for the always-staying and always-changing spectrum handoff sequences as well as the traffic-adaptive channel selection approach, where $t_s = 1$ (slot), $\lambda_s = 0.01$ (arrivals/slot), $\mathbf{E}[X_p] = 20$ (slots/arrival), and $\mathbf{E}[X_s] = 10$ (slots/arrival). . . . .	101
5.6	Effects of secondary connections' service time $\mathbf{E}[X_s]$ on the cross-point for the traffic-adaptive channel selection approach, where $t_s = 1$ (slot), $\mathbf{E}[X_p] = 20$ (slots/arrival), and $\lambda_s = 0.01$ (arrivals/slot). . . . .	102
5.7	Admissible region for the normalized traffic workloads $(\rho_p, \rho_s)$ , where the average cumulative delay constraint can be satisfied when $t_s = 0$ (slot), $\mathbf{E}[X_p] = 20$ (slots/arrival) and $\mathbf{E}[X_s] = 10$ (slots/arrival). . . . .	104
5.8	Comparison of average extended data delivery time for different target channel selection sequences. . . . .	106

6.1	An example of state diagram of the target channel sequences for a newly arriving secondary user, where the default channel $\eta = 1$ , the number of total channels $M = 3$ , and the required length of the target channel sequence $L = 4$ . Furthermore, $(k, i)$ stands for the state of operating at the channel $k$ with the $i^{th}$ interruption. . . . .	113
6.2	Six kinds of candidate sequences for the <b>Cumulative Handoff Delay Minimization Problem</b> when the greedy shortest-handoff-delay target channel selection strategy is adopted. . .	118
6.3	Effects of the newly arriving secondary user's average service time $\mathbf{E}[\chi_s]$ on the cumulative handoff delay for $\lambda_p^{(k)} = 0.02$ and $\lambda_s^{(k)} = 0.01$ when $1 \leq k \leq 4$ . . . . .	127
6.4	Effect of the average service time $\mathbf{E}[X_s]$ and the arrival rate $\lambda_s$ of the secondary users' connections on the cumulative handoff delay of the newly arriving secondary user's connection for $(\lambda_p^{(1)}, \lambda_p^{(2)}, \lambda_p^{(3)}, \lambda_p^{(4)}) = (0.019, 0.02, 0.02, 0.02)$ and $\mathbf{E}[X_p^{(k)}] = 15$ when $1 \leq k \leq 4$ . . . . .	130
6.5	Effect of the average service time $\mathbf{E}[X_p]$ and the arrival rate $\lambda_p$ of the primary users' connections on the cumulative handoff delay of the newly arriving secondary user's connection for $\lambda_s^{(k)} = 0.01$ and $\mathbf{E}[X_s^{(k)}] = 15$ when $1 \leq k \leq 4$ . . . . .	133

7.1	An example of transmission process for the secondary connection $SC_A$ , where $T$ is the extended data delivery time of $SC_A$ and $D_i$ is the handoff delay of the $i^{th}$ interruption. The gray areas indicate that the channels are occupied by the existing primary connections (PCs) or secondary connections (SCs). Because $SC_A$ is interrupted three times in total, the overall data connection is divided into four segments. Note that $D_1 = \delta_c$ , $D_2 = \delta_s$ , and $D_3 = \delta_c$ . . . . .	138
7.2	The PRP M/G/1 queueing network model with three channels where $\lambda_p^{(k)}$ , $\lambda_s^{(k)}$ , and $\omega_n^{(k)}$ are the arrival rates of the primary connections, the secondary connections, and the type- $n$ secondary connections ( $n \geq 1$ ) at channel $k$ . Note that $\lambda_s^{(k)} = \omega_0^{(k)}$ . Furthermore, $f_p^{(k)}(x)$ and $f_i^{(k)}(\phi)$ are the probability density functions (pdfs) of $X_p^{(k)}$ and $\Phi_i^{(k)}$ , respectively. . . . .	140
7.3	Illustration of the physical meaning of random variable $\Phi_i^{(k)}$ . For example, $\Phi_2^{(1)}$ is one of the third segments (gray areas) of the first and the third secondary connections in (a) as well as the second secondary connection in (b). Note that the third secondary connection in (b) does not have the third segment because it is interrupted only once. . . . .	144
7.4	State diagram of target channel sequence for a secondary connection, where default channel $\eta = 1$ . . . . .	150
7.5	Tree-structured representations of the proposed state diagram where the grounding symbols represent the ending of state transition. Note that this figure considers the secondary connections whose default channels are $Chk$ . . . . .	154

7.6	Effects of the arrival rate of the primary connections ( $\lambda_p$ ) on the channel utilizations at the channels 1 and 2, where $\delta_s = 1$ and $\delta_c = 2$ . . . . .	156
7.7	Effects of the arrival rate of the primary connections ( $\lambda_p$ ) on the extended data delivery time of the secondary connections whose default channels are channels 1 and 2, where $\delta_s = 1$ and $\delta_c = 2$ . . . . .	157
7.8	Effects of the initial arrival rate of the secondary connections ( $\lambda_s$ ) on the channel utilizations at the channels 1 and 2, where $\delta_s = 1$ and $\delta_c = 2$ . . . . .	159
7.9	Effects of the initial arrival rate of the secondary connections ( $\lambda_s$ ) on the extended data delivery time of the secondary connections whose default channels are the channels 1 and 2, where $\delta_s = 1$ and $\delta_c = 2$ . . . . .	160
7.10	Comparison of average extended data delivery time for different target channel selection schemes. . . . .	162
7.11	Admissible region ( $\lambda_p, \lambda_s$ ), where the average extended data delivery time constraint can be satisfied when $\tau = 0$ . . . . .	165
7.12	Comparison of the average extended data delivery time for different spectrum handoff schemes, where $\mathbf{E}[X_s] = 10$ , $t_s = 0$ , and $t_h = 0$ . . . . .	167
8.1	Interference ratio ( $\Theta_p$ ) for various arrival rates of the secondary connections, where $P_M = 0.1$ . . . . .	182
8.2	Average overall system time ( $\mathbf{E}[S_s]$ ) for various arrival rates of the secondary connections, where $P_F = 0.1$ . . . . .	183
8.3	Optimal traffic admission probability for various arrival rates of the secondary connections where $\Theta_{max} = 1.13$ and $S_{max} = 75$ .184	

# Glossary of Symbols

- type- $i$  secondary connection: the secondary user's connection that has experienced  $i$  interruptions.
- $\lambda_p^{(k)}$ : the arrival rate of the primary users' connections whose default channels are channel  $k$ .
- $\lambda_s$ : the arrival rate of the secondary users' connections.
- $\lambda_s^{(k)}$ : the initial arrival rate of the secondary users' connections whose initial channels are channel  $k$ .
- $\omega_i^{(k)}$ : the arrival rate of the type- $i$  secondary connections at channel  $k$ .
- $X_p^{(k)}$ : the service time of the primary users' connections whose default channels are channel  $k$ .
- $X_s$ : the service time of the secondary users' connections.
- $X_s^{(k)}$ : the service time of the secondary users' connections whose default channels are channel  $k$ .
- $\Phi_i^{(k)}$  is the effective service time for the  $i^{th}$  interruption at channel  $k$ . It is the transmission duration of a secondary connection between the  $i^{th}$  and the  $(i + 1)^{th}$  interruptions at channel  $k$ .

- $\tilde{X}_s$ : the actual service time of the secondary users' connections when the effects of sensing errors are considered.
- $f_p^{(k)}(x)$ : probability density function of  $X_p^{(k)}$ .
- $f_s(x)$ : probability density function of  $X_s$ .
- $f_s^{(k)}(x)$ : probability density function of  $X_s^{(k)}$ .
- $f_i^{(k)}(\phi)$ : probability density function of  $\Phi_i^{(k)}$ .
- $P_M$ : missed detection probability.
- $P_F$ : false alarm probability.
- $\pi_p$ : outage probability for the primary connections.
- $\pi_s$ : outage probability for the secondary connections.



# Chapter 1

## Introduction

Recent measurements show that the licensed spectrum is under-utilized [1]. In order to solve this spectrum waste issue, many technologies have been proposed. Cognitive radio (CR) is one of the promising approaches to improve spectrum utilization [2–8]. A CR network consists of the primary and the secondary networks as shown in Fig. 1.1. The primary networks are defined as the systems that own the licensed spectrum, such as the cellular mobile networks or the TV broadcast networks. By contrast, the secondary networks do not have any licensed frequency. By allowing the secondary users to temporarily access the primary user’s under-utilized licensed spectrum, CR can significantly improve spectrum efficiency and enhance the quality of service (QoS) performance of the secondary users.

One fundamental issue for enhancing QoS performance of the secondary users in CR networks is the spectrum handoff issue. When the high-priority primary user appears at its licensed channel being occupied by the low-priority secondary users, these secondary users must vacate the occupied channel. In order to vacate the occupied channel to the primary user and discover the suitable target channel to resume the unfinished transmission,

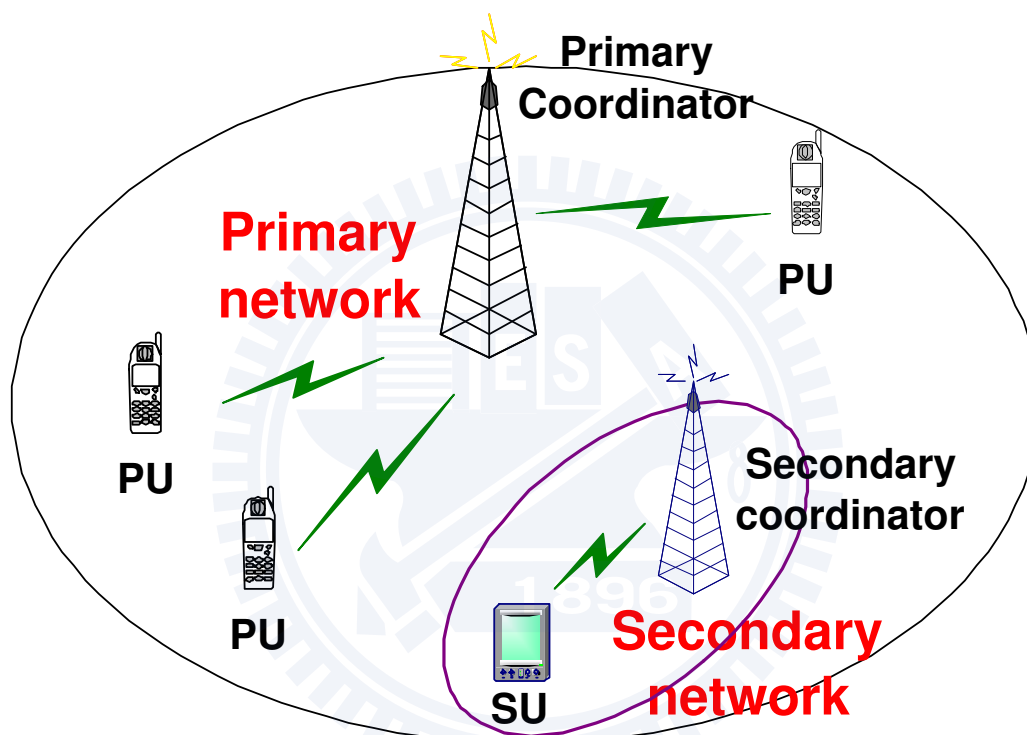


Figure 1.1: An illustrative example of CR network, which consists a primary network and a secondary network. There are three primary users (PUs) and one secondary user (SU) in the primary and secondary networks, respectively.

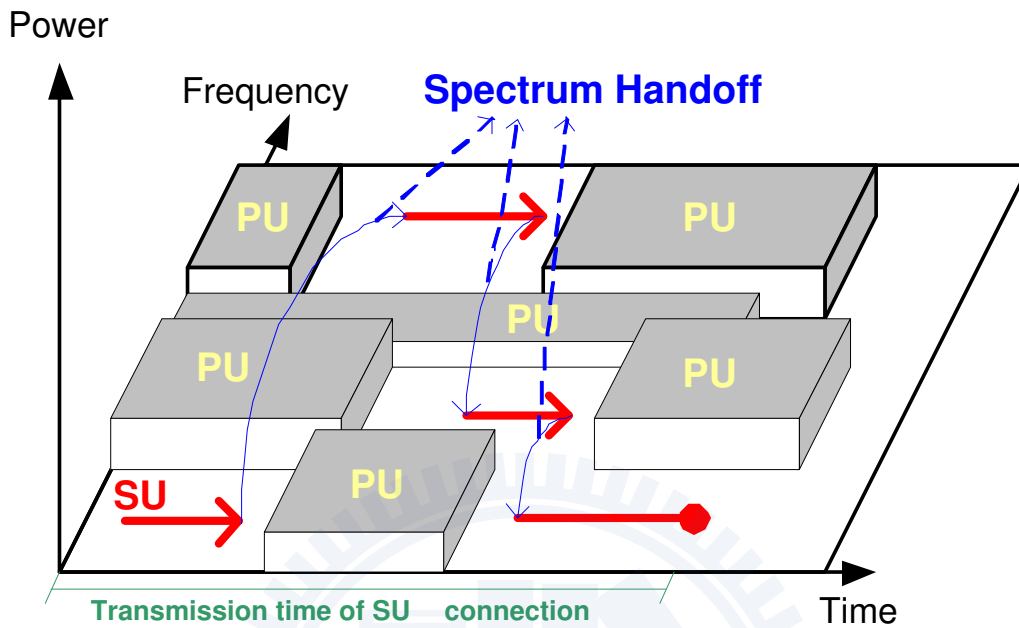


Figure 1.2: During the transmission period of secondary user (SU), it experiences multiple handoffs.

the *spectrum handoff* procedures are initiated for the secondary users [9, 10]<sup>1</sup>. During the transmission period of a secondary connection, multiple interruptions from the primary users result in multiple spectrum handoffs as show in Fig. 1.2. These spectrum handoffs will degrade the QoS performance of the secondary users.

In order to overcome the performance degradation issue due to multiple

<sup>1</sup>Spectrum handoff in CR networks is different from the conventional handoff mechanisms in cellular mobile networks. Spectrum handoff considers two types of users with different priorities, where the high-priority primary users have the right to interrupt the transmission of the low-priority secondary users. When the interruption event occurs, the secondary user must stop using the current channel even though the received signal strength is still acceptable. In contrast, all users in the conventional handoff mechanisms have the same priority to access channels and they change their operating channels mainly due to deterioration of signal quality [11].

spectrum handoffs for the secondary users, various spectrum management techniques in CR networks are re-examined from a link connection quality perspective. There are four spectrum management functionalities in CR networks [12]:

1. Spectrum sensing: The secondary users should monitor all channels in order to capture channel characteristic and detect spectrum holes. Based on sensing results, the secondary users can find some candidate channels to transmit data. In this dissertation, we consider a fully-connected CR network. Hence, the transmitter and receiver of a secondary connection can have the same consensus on sensing results.
2. Spectrum decision: The secondary users can select the best channel from many candidate channels to transmit data. This decision should take the traffic statistics of the primary users as well as the secondary users into account.
3. Spectrum mobility: The secondary users must vacate the occupied channel when the primary user appears because the primary users have the preemptive priority to access channels. In order to return the occupied channel to the primary users and resume the unfinished transmission at the suitable channel, the *spectrum handoff* procedures are initiated for the interrupted secondary user.
4. Spectrum sharing: The secondary users must coordinate their transmissions and avoid interfering with transmission of the primary users.

Referring to [13], the relationships of these four spectrum management functionalities are shown in Fig. 1.3. In the beginning, the traffic requests of secondary users arrive at the CR network. With the spectrum decision

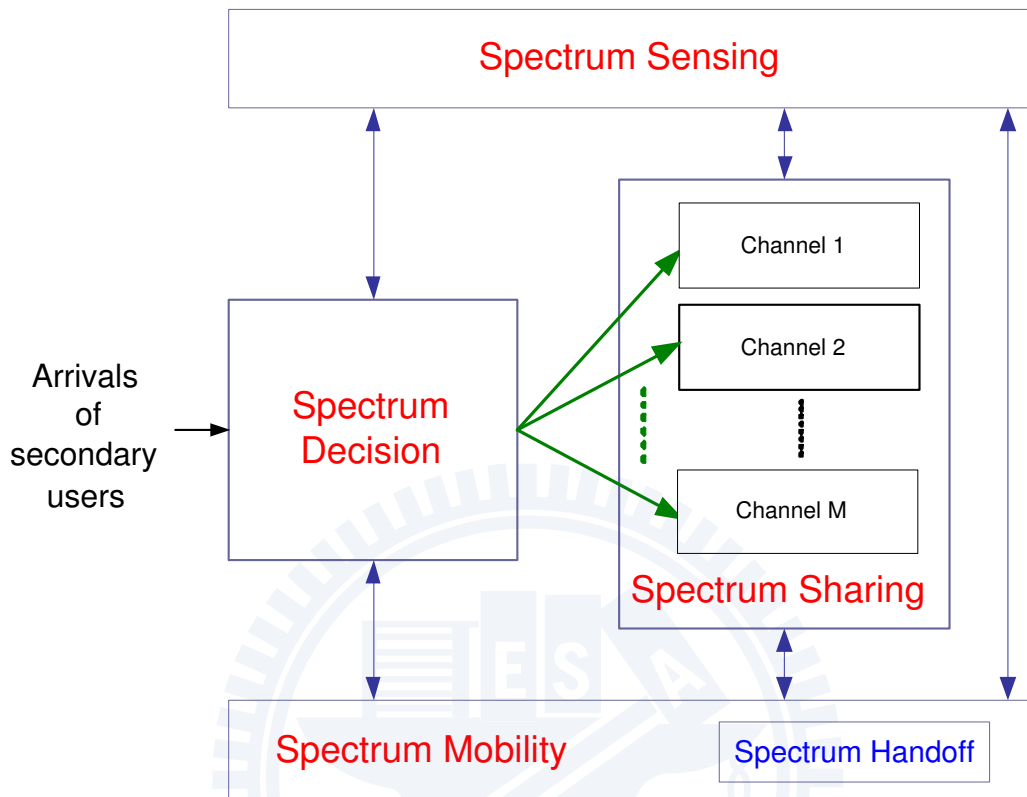


Figure 1.3: Relationships between spectrum sensing, spectrum decision, spectrum mobility, and spectrum sharing functionalities.

functionality, they can determine their initial operating channels from all  $M$  candidate channels, which can be found by the spectrum sensing functionality. In order to alleviate the channel contention when multiple secondary users select the same channel and the interference on the primary users when missed detection occur, the spectrum sharing functionality must be implemented. Furthermore, if the primary user appears at the occupied channel, the *spectrum handoff* procedures in the spectrum mobility functionality must be initiated. Based on this dynamic spectrum management, spectrum efficiency can be improved. Note that the multiple handoff issue should be taken into account when designing these spectrum management functionalities.

In this dissertation, we focus on the spectrum decision, spectrum mobility, and spectrum sharing issues. In order to evaluate the system performance of the proposed spectrum management techniques, an analytical framework based on the preemptive resumption priority (PRP) M/G/1 queueing theory is developed to characterize the connection-based channel usage behaviors with multiple handoffs. We investigate the effects of multiple handoffs on the QoS performance and study the performance limitation of various spectrum management techniques in different traffic loads. Different from the traditional work which investigated the effects of multiple handoffs on the network throughput, this dissertation concentrates on the effects of latency performance of the secondary users. Based on the proposed analytical framework, some useful insights into the design of the spectrum management techniques can be provided and the traffic-adaptive spectrum management schemes can be developed according to traffic conditions such as traffic arrival rates and service time distributions.

## **1.1 Problems and Solutions**

In this section, we will briefly describe our problem formulations and the corresponding solutions, including modeling technique for CR networks, traffic-adaptive spectrum mobility issues, load-balancing spectrum decision issues, and interference-avoiding spectrum sharing issues.

### **1.1.1 Modeling Techniques for Cognitive Radio Networks**

In this part, we outline the fundamental modeling issues of opportunistic spectrum access in cognitive radio (CR) networks. In particular, we identify

the effects of the general behaviors for the connection-based channel usage on the quality of service (QoS) performances of spectrum management techniques. During the transmission period of a secondary user's connection, the phenomenon of multiple spectrum handoffs resulted from the interruptions of the primary users arises quite often. In addition to multiple interruptions, the connection-based channel usage behaviors are also affected by other factors, including spectrum sensing time, channel switching between different channels, generally distributed service time, and channel contention between multiple secondary users. An analytical framework based on the preemptive resumption priority M/G/1 queueing theory is introduced to characterize these effects simultaneously. The proposed analytical framework can provide important insights into the design of spectrum management techniques in CR networks and can be adapted more flexibly for various traffic arrival rates and service time distributions.

### 1.1.2 Load-Balancing Spectrum Decision

In this part, we present an analytical framework to design system parameters for load-balancing multiuser spectrum decision schemes in cognitive radio (CR) networks. Unlike the non-load-balancing methods that multiple secondary users may contend for the same channel, the considered load-balancing schemes can evenly distribute the traffic loads of secondary users to multiple channels. Based on the preemptive resume priority (PRP) M/G/1 queueing theory, a spectrum decision analytical model is proposed to evaluate the effects of multiple interruptions from the primary user during each link connection and the sensing errors of the secondary users. With the objective of minimizing the overall system time (i.e., waiting time plus data delivery time) of the secondary users, we derive the optimal number of candidate

channels and the optimal channel selection probability for the sensing-based and the probability-based spectrum decision schemes, respectively. We find that the probability-based scheme can yield a shorter overall system time compared to the sensing-based scheme when the traffic loads of the secondary users is light, whereas the sensing-based scheme performs better in the condition of heavy traffic loads. If the secondary users can intelligently adopt the best spectrum decision scheme according to sensing time and traffic parameters, the overall system time can be improved by 50% compared to the existing methods. Furthermore, the proposed analytical model also takes into account of the probability of missed detection and false alarm for the appearance of the primary users, and can help evaluate the impacts of imperfect sensing on the spectrum decision schemes for CR networks.

### 1.1.3 Proactive Spectrum Handoff

In this part, we present an analytical framework to evaluate the latency performance of connection-based spectrum handoffs in cognitive radio (CR) networks. During the transmission period of a secondary connection, multiple interruptions from the primary users result in multiple spectrum handoffs and the need of predetermining a set of target channels for spectrum handoffs. To quantify the effects of channel obsolete issue on the target channel predetermination, we should consider the three key design features: (1) generally distributed service time of the primary and secondary connections; (2) different operating channels in multiple handoffs; and (3) queueing delay due to channel contention from multiple interrupted secondary connections. To this end, we propose the preemptive resume priority (PRP) M/G/1 queueing network model to characterize the spectrum usage behaviors with all the three design features. This model aims to analyze the extended data delivery



time of the secondary connections with proactively designed target channel sequences under various traffic arrival rates and service time distributions. These analytical results are applied to evaluate the latency performance of the connection-based spectrum handoff based on target channel sequences used in the IEEE 802.22 wireless regional area networks standard. Then, to reduce the extended data delivery time, a traffic-adaptive spectrum handoff is proposed, which changes the target channel sequence of spectrum handoffs based on traffic conditions. Compared to the existing target channel selection methods, this traffic-adaptive target channel selection approach can reduce the extended data transmission time by 35%, especially for the heavy traffic loads of the primary users.

#### 1.1.4 Optimal Proactive Spectrum Handoff

In this part, we investigate how to determine an optimal target channel sequence for multiple spectrum handoffs with the minimum cumulative handoff delay for the secondary users in cognitive radio networks. In addition to multiple interruptions from the high-priority primary users, the optimal sequence for spectrum handoffs incorporates the effects of various traffic statistics of both the primary and the secondary users. Compared to the exhaustive search with time complexity of  $O(M^L)$ , where  $L$  is the total number of elements in the target channel sequence and  $M$  is the total number of candidate channels for spectrum handoffs, a dynamic programming algorithm with the complexity of  $O(LM^2)$  is proposed to determine the optimal target channel sequence for spectrum handoffs. Furthermore, we propose a greedy algorithm with time complexity of  $O(M)$  for spectrum handoffs and prove that it only requires to compare six permutations of the target channel sequences. Numerical results show that the cumulative handoff delay of the low-complexity

greedy algorithm can approach that of the optimal solution.

### **1.1.5 Reactive Spectrum Handoff**

Spectrum handoff is an important functionality in cognitive radio (CR) networks. Whenever a primary user appears, transmission of the secondary users must be interrupted. In this case, spectrum handoff procedures are initiated for the secondary users in order to search the idle channel to resume the unfinished transmission. Although this dynamic spectrum access scheme can enhance channel utilization, multiple interruptions from the primary users will result in multiple handoffs and thereby increase the transmission latency of the secondary users. Hence, two fundamental issues in CR networks are how much channel utilization can be improved and how long transmission latency is extended for the secondary users due to multiple spectrum handoffs. To solve the first problem, we introduce the preemptive resume priority (PRP) M/G/1 queueing network to characterize the channel usage behaviors of CR networks. Based on this queueing network, channel utilization under various traffic arrival rates and service time distributions can be evaluated. Furthermore, on top of the proposed queueing network, a state diagram is developed to characterize the effects of multiple handoff delay on the transmission latency of the secondary users. The analytical results can provide a helpful insight to study the effects of traffic arrival rates and service time on the transmission latency and then facilitate the designs of admission control rules for the secondary users subject to their latency requirements.

### **1.1.6 Interference-Avoiding Spectrum Sharing**

In this part, we present an analytical framework to design key system parameters for an interference-avoiding admission control mechanism to enhance

channel utilization, while maintaining the quality of service (QoS) requirements for both the primary users and secondary users in cognitive radio (CR) networks. Intuitively, a larger admission probability for the secondary users can increase channel utilization, but it leads to more contention between the secondary users and thus affects the latency performance of the secondary users. More importantly, if the missed detection for the presence of the primary user happen, the larger the admission probability of the secondary user, the more the interference to the primary user. In order to find the optimal traffic admission probability, a cross-layer optimization problem is formulated. Our cross-layer design can incorporate the following effects: (1) false alarm and missed detection, power outage in the physical layer; (2) admission probability in the medium access control (MAC) layer; and (3) the traffic statistics as well as the QoS constraints of both the primary and the secondary users in the application layer. The analytical results proposed in this part can calculate the optimal traffic admission probability under various cross-layer parameters and provide useful insights into the tradeoff design of channel utilization and the QoS performance for both the primary and the secondary users.

## 1.2 Dissertation Outlines

This dissertation consists of four themes as shown in Fig. 1.4. The first part is to outline the fundamental modeling issues of various spectrum management techniques in CR networks. Then, an analytical framework based on the preemptive resumption priority M/G/1 queueing theory is introduced to characterize these modeling issues simultaneously. In order to demonstrate the effectiveness of this model, three illustrative examples are presented in

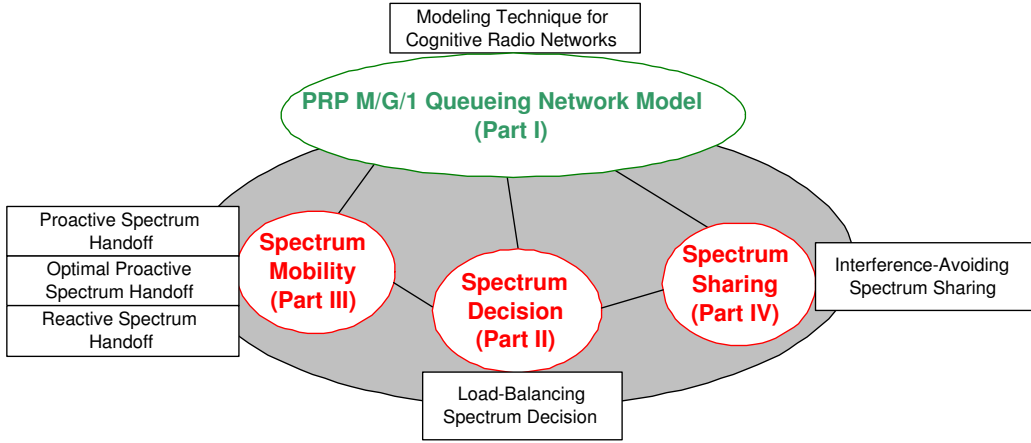


Figure 1.4: Outline of this dissertation.

the second, third, and fourth parts as follows. The second part investigates the spectrum decision issue. We determine which channels to probe and transmit in a load-balancing manner. The third part focuses on the spectrum mobility issue. We illustrate how to model the effects of multiple handoffs, where the secondary users can have different operating channels before and after spectrum handoff. The final part considers the spectrum sharing issue. The optimal admission probability for the secondary users is determined to satisfy the interference constraint to the primary users.

The remaining chapters of this dissertation are organized as follows. In Chapter 2, we first give a literature survey of the state-of-the-art techniques. Chapter 3 provides an analytical framework to characterize the general channel usage behaviors with multiple handoffs from a macroscopic viewpoint. Based on the proposed analytical framework, Chapter 4 designs system parameters for load-balancing multiuser spectrum decision schemes in CR networks. Furthermore, Chapters 5 and 6 evaluate the latency performance and determine the optimal target channel sequence for the proactive spectrum handoff, respectively. Next, the effect of sensing time on the latency per-

formance of the reactive spectrum handoff is investigated in Chapter 7. In Chapter 8, an admission control mechanism for the secondary users' spectrum sharing is discussed. Finally, the concluding remarks and some suggestions for future research topics are given in Chapter 9.



# Chapter 2

## Background and Literature

### Survey

In this chapter, we firstly survey related work to the modeling techniques of the connection-based channel usage behaviors with multiple handoffs. Then, the existing spectrum management techniques, which consist of spectrum decision, spectrum mobility, and spectrum sharing, also are discussed.

#### 2.1 Modeling Techniques for Cognitive Radio Networks

Most of the modeling techniques of channel usage behaviors in CR networks can be classified into three categories: the partially observable Markov decision process (POMDP), the two-dimensional Markov chain (TDMC), and the PRP M/G/1 queueing model (QM). However, these models have not simultaneously considered all of the five design features. Table 2.1 classifies the existing modeling techniques, where the signs “○” and “×” indicate that the proposed model “does” and “does not” consider the corresponding

Table 2.1: Comparison of Various Analytical Models for CR Networks.

Model Name	Multiple Spectrum Handoff	Spectrum Sensing Time	Various Operating Channels	General Service Time	Multiple Secondary Connections
POMDP [14]	○	×	○	×	×
TDMC [15]	○	×	○	×	○
QM [16–18]	○	×	×	○	○
Proposed Model	○	○	○	○	○

feature, respectively.

In [14], the evolutions of the channel usage of the primary network is characterized by a discrete-time Markov chain which has two occupancy states (the busy and the idle states). The framework of partially observable Markov decision process (POMDP) was developed to preselect the best action (target channel) to maximize the immediate reward (expected per-slot throughput) of the decision maker (secondary user) at the next time slot [14]. Unlike [14] considered only the effects of the traffic loads of the primary network, the authors in [15] considered the effects of the traffic loads of both the primary and the secondary users on the statistics of channel occupancy. In [15], the channel usage behaviors of a CR network is modeled by a two-dimensional Markov chain where the two dimensions represent the total numbers of the primary and the secondary users in a CR network, respectively. When the secondary users are interrupted, it is assumed that they can immediately find the idle channel if at least one idle channel exists. Hence, the spectrum sensing time is neglected in this model. Note that the two Markov chain models are suitable for the exponentially distributed service time, and how to extend

them to the case with generally distributed service time is not clear.

Some researchers used the PRP M/G/1 queueing model to characterize the spectrum usage behaviors of each channel. For example, the effects of multi-user contention and multiple interruptions on the latency performance of the secondary users' connections were studied in [16–18]. This PRP M/G/1 queueing model assumed that the secondary user must stay on its current operating channel to resume its unfinished transmission when it is interrupted. That is, there is one candidate channel for spectrum handoff and thus the sensing time issue has not been addressed.

## 2.2 Load-Balancing Spectrum Decision

The load-balancing spectrum decision schemes can be categorized into two methods: the sensing-based spectrum decision and the probability-based spectrum decision. Table 2.2 compares the existing load-balancing spectrum decision schemes. In the following, we discuss the features of these spectrum decision methods in more details.

### 2.2.1 Probability-based Spectrum Decision

In the literature, many probability-based spectrum decision schemes were proposed to balance the traffic loads of secondary users in multi-channel CR networks, which can be categorized into three types: (1) packet-wise probabilistic (PP) approach [19–23]; (2) game-theoretic (GT) approach [24–26]; and (3) learning automata (LA) approach [27].

- Packet-wise probabilistic spectrum decision approaches [19–23] aim at maximizing the expected throughput of the secondary users at each slot by determining the probability of selecting each channel from the



Table 2.2: Comparison of Various Load-balancing Spectrum Decision Schemes for Cognitive Radio Networks, where PP, GT, and LA stand for the packet-wise probabilistic, game-theoretic, and learning automata approaches, respectively.

	Channel Occupancy Model of a Primary Network		Multiple Interruptions	Sensing Errors
Probability- based Methods	PP	Bernoulli Process [19]	×	×
		Bernoulli Process [20–23]	×	○
	GT	Deterministic Process [24]	×	×
		M/M/1 [25] or M/G/1 [26]	○	×
	LA	General Distribution [27]	○	×
Sensing- based Methods	Deterministic Process [28]		×	×
	Two-state Markov Chain [29]		×	×
	Bernoulli Process [30–32]		×	×
Proposed Model	M/G/1		○	○

pool of candidate channel. Based on busy probability and capacity of each channel, [19] suggested a method to determine the probability for selecting channels on top of  $p$ -persistent carrier sense multiple access (CSMA) medium access control (MAC) protocol in a decentralized manner. They claimed that their proposed sub-optimal channel probability assignment can achieve the Nash equilibrium as the number of secondary users tends to infinity. Furthermore, [20, 21] considered the effects of sensing errors in terms of false alarm and missed detection on the throughput of the secondary users in a two-channel system, and proposed a probabilistic channel selection approach to maximize the throughput of the secondary users in each slot while maintaining the latency constraint of the primary users. Moreover, [22] formulated an optimization problem for channel selection probability to maximize the throughput of the secondary users in each slot while maintaining the interference constraint of the primary users when the primary and secondary networks are asynchronous. Unlike [20–22] considered only the case that one single secondary user can select the channel at each time instant, [23] further extended the probabilistic channel selection approach of [20, 21] to the case that multiple users can simultaneously select their operating channels from the pool of candidate channels, and analyzed the throughput of the secondary users based on the probabilistic channel selection approach taking into account of the effects of channel contention as well as sensing errors. Note that the packet-wise probabilistic spectrum decision approaches in [19–23] were executed in a slot-by-slot manner, which may lead to many channel-switching behaviors during each secondary user’s link connection. Moreover, it is assumed that the traffic loads of the secondary users are saturated.

Further, the channel occupancy model of a primary network is modeled as a Bernoulli process and thus the length of busy and idle periods are exponentially distributed.

- Game-theoretic approaches were proposed to solve the spectrum decision problem in CR networks [24–26]. Based on the game theory model, each player (secondary user) can decide the best strategy (channel selection probability) to maximize its utility function. [24] proposed a game-theoretic load-balancing approach to find a set of channel selection probabilities so that no secondary user has incentive to unilaterally change his/her action. To converge to such the Nash equilibrium, a best-reply algorithm was designed for each user to calculate each channel’s selection probability as well as its transmission duration based on a utility function related to the load-balancing channel selection. Beside the load-balancing issue, [25] suggested that the utility function in the game-theoretic spectrum decision should also incorporate the channel bandwidth and its idle period as well as the cost of spectrum handoff because the spectrum decision procedure must be executed many times due to multiple interruptions. They emphasized that the channel selection game shall be repeated many times to capture the scenario when primary users stochastically activate or deactivate at each epoch. Unlike the pervious work that considered the homogeneous secondary users, [26] assumed that the secondary users can have different priorities. They proposed a dynamic strategy learning algorithm to determine the channel selection strategies that can converge to the Nash equilibrium. Noteworthily, the Nash equilibrium solution of the game-theoretic approach is not necessary the globally optimal solution from the viewpoint of the overall network [33].

- In [27], a learning automata (LA) approach was suggested to determine the channel selection probabilities by exploring the uncertainty of traffic patterns in CR networks. After a huge number of trials, the secondary users can estimate the optimal channel selection probability. However, the problem for this method is its converging speed, especially for a large number of users.

### 2.2.2 Sensing-based Spectrum Decision

The sensing-based spectrum decision scheme requires scanning all the candidate channels to determine the most suitable operating channel. Thus, the total number of candidate channels significantly affects the overall system time in the sensing-based spectrum decision scheme. In [28–30], the optimal number of candidate channels to maximize the spectrum accessibility and the procedures to determine the optimal set of candidate channels were investigated. Furthermore, the authors in [31, 32] formulated the sequential channel sensing problem as an optimal stopping problem with the objective of maximizing the throughput of the secondary users. They studied when the secondary users shall stop sensing and start transmitting data. Nevertheless, the effects of multiple interruptions from the primary user and the sensing errors for the primary user’s occurrence on the overall system time of the secondary users in the CR networks have not been addressed in these existing sensing-based spectrum decision methods.

## 2.3 Proactive Spectrum Handoff

In order to characterize the multiple handoff behaviors in CR networks, we should consider the three key design features, consisting of (1) generally

Table 2.3: Comparison of Various Proactive Handoff Models.

Model Name	General Service Time	Various Operating Channels	Multiple Secondary Connections
TMC [29, 34–39]	×	○	×
OORP [40–42]	○	○	×
BRP [43]	×	○	×
MMC [44]	×	×	○
QM [16–18, 26, 45–49]	○	×	○
Proposed Model	○	○	○

distributed service time; (2) various operating channels; and (3) queueing delay due to channel contention from multiple secondary connections. Based on these three features, Table 2.3 classifies the existing modeling techniques for the proactive spectrum handoff. In the literature, the modeling techniques for spectrum handoff behaviors can be categorized into the following five types: (1) the two-state Markov chain; (2) the Bernoulli random process; (3) the arbitrary ON/OFF random process; (4) the birth-death process with multi-dimensional Markov chain; and (5) the PRP M/G/1 queueing model. One can observe that the current modeling techniques have not considered all the aforementioned three design features. In the following, we briefly discuss the features of these analytical models for spectrum handoff behaviors.

- **Two-state Markov chain (TMC):** In [29, 34–39], the evolutions of the channel usage of the primary networks at each channel were characterized by a discrete-time Markov chain which has two occupancy states: busy (ON) and idle (OFF) states. The idle (OFF) state can be regarded as a potential spectrum opportunity for the secondary users.

Note that the Markov chain model is suitable for the exponentially distributed service time, and it is not clear how to extend it to the case with generally distributed service time. In this model, the target channel selection problem in every time slot is modeled as a Markov decision process. According to the channel occupancy state at the current time slot, a decision maker (secondary user) can preselect the best action (target channel) to maximize its immediate reward at the next time slot such as expected per-slot throughput [29,34–37], expected idle period [38], or expected waiting time [39]. Note that this model belongs to the slot-based modeling technique because the secondary user shall decide its target channel at each time slot. In this scheme, even though the primary users do not appear at the current operating channel, the secondary user may still need to change its target channel, resulting in frequent spectrum handoffs.

- **Arbitrary ON/OFF random process (OORP):** Unlike [29,34–39] assumed that the channel usage behaviors of the primary networks have the Markov property, the authors in [40–42] used the ON/OFF random process with arbitrary distributed ON/OFF period to characterize the channel usage behaviors of the primary networks at each channel. It was assumed that the secondary user can estimate the distributions of the ON period and the OFF period based on long-term observations. In each time slot, the secondary user must calculate the expected remaining idle periods of all channels and then will immediately switch to the channel with the longest remaining idle period. This model also belongs to the slot-based modeling technique because the target channel is decided in each time slot.

- **Bernoulli random process (BRP)**: The authors in [43] examined the effects of multiple interruptions from the primary users on the connection maintenance probability in a connection-based environment, where the spectrum usage behaviors of the primary networks on each channel were characterized by a Bernoulli random process. Because both the busy and idle periods of the considered primary networks follow the geometrical distributions, it is more difficult to extend this modeling technique to the cases with other generally distributed service time.
- **Multi-dimensional Markov chain (MMC)**: In [44], the spectrum usage behaviors of both the primary and secondary networks were modeled by the multi-dimensional Markov chain. Each state in the Markov chain indicates the identity number for the serving users and the waiting users for the channel. It was assumed that the secondary user must stay on its current operating channel after the primary user's interruption. This analytical model is suitable for the single channel network, and the issue of different operating channels in multiple handoffs has not been addressed.
- **M/G/1 queueing model (QM)**: Some researchers used the preemptive resume priority (PRP) M/G/1 queueing model to characterize the spectrum usage behaviors in a single-channel CR network. The effects of multi-user sharing and multiple interruptions on the extended data delivery time of the secondary users were studied in [16–18, 26, 45–49]. Note that the authors in [16–18, 26, 45–49] also assumed that the secondary users must stay on the current operating channel to resume their unfinished transmissions when they are interrupted.

To summarize, the first three analytical models, two-state Markov chain, arbitrary ON/OFF random process, and bernoulli random process, did not incorporate the effects of the traffic loads of the secondary users on the statistics of channel occupancy. How to extend these models to consider the queueing delay due to channel contention from multiple secondary connections is unclear. The last two models, multi-dimensional Markov chain and M/G/1 queueing model, can characterize the effects of spectrum sharing between multiple secondary users. However, these two models assumed that the interrupted secondary user must stay on the current operating channel. and have not dealt with the handoff interaction issue among different channels.

## 2.4 Optimal Proactive Spectrum Handoff

In the literature, some predetermined target channel selection methods for spectrum handoffs have been proposed and can be categorized into two kinds: probability-based channel selection methods and Markov decision process.

- In [20,21,23], the probability-based channel selection methods were developed to predetermine the probability that each channel is selected to the target channel. Based on the predetermine probabilities, the optimal channel hopping sequence can be decided in packet-by-packet or slot-by-slot manners. The work in [20,21] designed of the optimal channel hopping sequence in the single-user case, while [23] extended the similar problem to the multiple user case. The above approaches for channel hopping sequence design are optimal in the sense of maximizing the per-slot throughput. However, the latency issue in spectrum handoff has not been considered yet. Clearly, the cumulative delay in one connection due to multiple spectrum handoffs is an important QoS



performance measure for CR networks.

- Besides the probability-based channel selection methods, another kind of target channel selection approach is to apply the theory of Markov decision process. In [29, 34–39], the target channel selection problem in every time slot is modeled as a Markov decision process. According to the channel occupancy state at the current time slot, a decision maker (secondary user) can preselect the best action (target channel) to maximize its immediate reward at the next time slot. The considered reward or objective function includes the expected per-slot throughput [29, 34–37], expected idle period [38], and expected waiting time [39]. However, only the effects of channel usage behaviors of the primary users are considered on the channel occupancy. In fact, the traffic loads of the secondary users are also needed to be considered in channel selection.

## 2.5 Reactive Spectrum Handoff

A key property of reactive spectrum handoff is that the interrupted secondary user can actually find the idle if at least one idle channel exists at the moment of link transition. In order to characterize the channel usage behaviors with this property, we should consider the three key design features, consisting of (1) heterogeneous arrival rates of the primary users (PUs); (2) various arrival rates of the secondary users (SUs); (3) handoff processing time. Based on these three features, Table 2.4 classifies the existing modeling techniques for the reactive spectrum handoff. In the literature, the modeling techniques for spectrum handoff behaviors can be categorized into the following four types: (1) ON/OFF random process; (2) M/M/m queueing Model; (3) two-

Table 2.4: Comparison of Various Channel Usage Models.

Model Name	Heterogeneous Arrival Rates of PUs	Various Arrival Rates of SUs	Handoff Processing Time
OORP [50, 51]	×	×	×
OORP [43]	×	×	○
M/M/m [52]	×	×	×
MDMC [15, 53–66]	×	×	×
M/G/1 [67, 68]	○	○	×
Proposed Unifying Model	○	○	○

dimensional Markov chain; and (4) M/G/1 queueing model. One can observe that the current modeling techniques have not considered all the aforementioned three design features. In the following, we briefly discuss the features of these analytical models for spectrum handoff behaviors.

- **ON/OFF random process (OORP):** In [43, 50, 51], the ON/OFF random process was used to characterize the channel usage behaviors of the primary networks at each channel, where the distributions of ON (busy) period- and OFF (idle) period at each channel are geometrical distributed. The OFF state can be regarded as a potential spectrum opportunity for the secondary users. The authors in [50] and [51] investigated the channel utilization factors and the extended data delivery time of the secondary users, respectively. Unlike [51] that did not address the effects of spectrum sensing time, the authors in [43] examined the effects of spectrum sensing time on the extended data delivery time of the secondary users. However, [43] assumed that at least one channel is certainly available after spectrum sensing, and the case that all

channels are busy after spectrum sensing did not been considered.

- **M/M/m queueing model:** In [52], the channel usage behaviors of the primary users are characterized by the M/M/m queueing model, where  $m$  is the total number of channels in the CR network. The author in [52] calculated the handoff delay of the secondary users. However, it is assumed that the handoff delay only results from the waiting time which is the duration from the instant that interruption event occurs until the instant that one idle channel is found. The sensing time had not been considered when calculating handoff delay.
- **Multiple-dimensional Markov chain (MDMC):** In [15,53–63], the spectrum usage behaviors of both the primary and secondary networks were modeled by a two-dimensional Markov chain, where the two dimensions represent the total numbers of the primary and the secondary users in a CR network, respectively. The blocking probability and forced termination probability for the secondary users' connections in the CR network without and with queue are studied in [15, 53–58] and [59–61], respectively. Different from [15, 53–61] that considered infinite user population, [62, 63] derived the blocking probability in a CR network with finite user population. Furthermore, the authors in [64–66] further extended the two-dimensional Markov chain model to the multiple-dimensional Markov chain, where the new dimension is used to describe the channel state or queue length. Note that these analytical models are suitable for the CR network with homogeneous traffic loads, and the issues of heterogeneous arrival rates of the primary and the secondary users has not been addressed.
- **M/G/1 queueing model:** [67,68] used the M/G/1 queueing model to

characterize the channel usage behaviors of a secondary network, where each secondary user can simultaneously use all idle channels to transmit its data. Because the total number of idle channels depends on how many channels are occupied by the primary users, the service rates of the secondary users are related to the traffic statistics of the primary users, which results in a non-trivially distributed service time. Thus, the authors suggested using the M/G/1 queueing system to characterize this system. However, authors did not show how to obtain this non-trivial service time distribution.

## 2.6 Interference-Avoiding Spectrum Sharing

In order to determine the optimal admission probability, we should consider four key design features: (1) interference on the primary users (PUs), where the transmission of the primary users may be stained by the secondary users due to missed detection; (2) channel contention between multiple secondary users (SUs), where channel contention will increase waiting time of the secondary users; (3) multiple handoffs, a secondary user may have multiple handoffs due to multiple interruptions from the primary users during its transmission period; and (4) generally distributed service time, where the probability mass functions (pmfs) of service time of the primary and secondary connections can be any distributions. Based on these four design features, Table 2.5 classifies the existing admission control techniques.

### 2.6.1 Admission Control with Perfect Sensing

- **Network-throughput-oriented approach:** The authors in [6,19,44] determined the optimal admission probability to maximize the overall

Table 2.5: Comparison of Various Objective Functions.

Objective Function	Interference on PUs	Channel Contention between SUs	Multiple Spectrum Handoffs	General Traffic Loads
Network Throughput [6, 19, 44]	×	○	×	×
User Throughput [49]	×	×	○	○
Dropping Probability [57]	×	○	×	×
Transmission Latency [64]	×	○	×	×
Network Throughput [20, 21]	○	×	×	×
User Throughput [69]	○	×	×	×
The Proposed Model	○	○	○	○

throughput of a secondary network. They found that a larger admission probability can enhance the per-secondary-user throughput. However, it results in more competition between the secondary users, thereby degrading the overall network throughput. In [6, 19], the authors provided the analytical approaches to determine the admission probability  $p$  on top of  $p$ -persistence carrier sense multiple access (CSMA) medium access control (MAC) protocol. They assumed that the secondary users have the saturated traffic load, i.e., the secondary users always have data to send. Unlike [6, 19] that assumed only one secondary user can transmit data at one slot, [44] considered the case that multiple secondary users can transmit data simultaneously. The interference from the coexistence of multiple secondary users is incorporated in the proposed analytical model, where each secondary user's service time is exponentially distributed.

- **User-throughput-oriented approach:** [49] determined the optimal payload length of the secondary users to maximize the throughput of each secondary user. They assumed that the interrupted secondary users must retransmit whole data connection instead of resume the unfinished transmission. They found that the longer payload length can increase per-secondary-user throughput when header length is a constant, but it also increase the interrupted probability, thereby degrading per-secondary-user throughput. Then, a preemptive repeat priority queueing model was proposed to solve this tradeoff issue.
- **Dropping-probability-oriented approach:** In [57], the optimal arrival rate (admission probability) is determined to minimize the dropping (or forced termination) probability of the secondary users by formulating it as a nonlinear optimization problem with the constraint of given the blocking probability for the secondary users. In order to derive the closed-form expressions for the dropping and blocking probabilities in terms of arrival rate, a two-dimensional Markov chain is used to characterize the channel usage behaviors of a CR network, where the two dimensions represent the total numbers of the primary and the secondary users, respectively. Note that this Markov chain model is suitable for the exponentially distributed service time, and how to extend it to the case with generally distributed service time it is not clear.
- **Latency-oriented approach:** In [64], authors proposed a Markov chain model to characterize channel usage behavior of both the primary users and the secondary users. Based on this model, the transmission latency of the secondary users under various arrival rates of the primary

users and the secondary users can be evaluated. Hence, when the arrival rate of the primary users is given, the maximum arrival rate of the secondary users can be determined to satisfy the transmission latency requirement of the secondary users.

### 2.6.2 Admission Control without Perfect Sensing

- **Network-throughput-oriented approach:** [20, 21] considered the effects of sensing errors in terms of false alarm and missed detection on the throughput of the secondary users in a two-channel system, and determined the optimal channel access probability for each channel to maximize the throughput of the secondary users in each slot while maintaining the latency constraint of the primary users. [20, 21] considered only the case that single secondary user can select the channel at each time instant and assumed that the secondary users have infinite amount of data to transmit.
- **User-throughput-oriented approach:** [69] further extended the analytical model of [20, 21] to determine the optimal false alarm probability to maximize the throughput of each secondary users, while maintaining the latency constraint of the primary users. They found that a lower false alarm probability can enhance per-secondary-user throughput. However, a lower false alarm probability results in higher missed detection probability and thus increasing interference to the primary users. Hence, an optimal false alarm probability exists.

## Chapter 3

# Queueing-Theoretical Modeling Techniques for Cognitive Radio Networks

Basically, according to the principle of selecting the target channel for spectrum handoff, the operating mode of the secondary networks can be categorized as either the non-hopping mode or the hopping mode. The secondary user always stays on its current operating channel when it is interrupted in the non-hopping mode, which is the basic mode of IEEE 802.22 systems [70]. In the hopping mode, the interrupted secondary user can either stay on its current operating channel or change to another channel, which is determined according to traffic statistics. An example of hopping mode is the phase-shifting hopping method of the IEEE 802.22 systems [70]. As a result, the non-hopping mode is a special case of the hopping mode. Note that the secondary users' connection may execute multiple handoffs during its transmission period due to the interruptions from the primary users [71]. Clearly, these handoffs will degrade the quality of service (QoS) performances of the



latency-sensitive traffic for the secondary users.

In this chapter, in order to evaluate the QoS performances of spectrum management techniques in the non-hopping or the hopping modes, an analytical framework based on the preemptive resumption priority (PRP) M/G/1 queueing theory is developed. The proposed analytical framework can provide important insights into the system parameter design of spectrum management techniques and can be adapted more flexibly for various traffic arrival rates and service time distributions. Finally, we also provide some new research directions and open issues on top of this model.

### 3.1 Motivation

Although it is conceptually simple, the proposed PRP M/G/1 queueing network model faces the new challenges. Specifically, it is needed to consider the general behaviors of the connection-based channel usage, including the following key design features: (1) multiple interruptions and handoffs; (2) spectrum sensing time; (3) various operating channels, the operating channels before and after spectrum handoff can be different; (4) generally distributed service time, where the probability mass functions (pmfs) of service time of the primary and the secondary connections can be any distributions; and (5) channel waiting time due to multiple secondary connections' contention.

How to find a unifying analytical model to characterize the effects of the five key design features is important. Because there are many approaches for target channel selection in the hopping model, it is challenging to find a unifying model to facilitate the QoS performance evaluation for various spectrum management techniques. Based on the proposed analytical framework, we provide a systematic approach to catch the randomness property of the

target channel selection and can evaluate its effects on system performance metrics such as transmission latency and channel utilization. Many analytical models have been proposed to characterize the channel usage behaviors in the CR networks [14–18]. However, these five key design features have not been considered simultaneously. To our knowledge, an analytical model which is integrated with these design features has rarely been discussed in the literature.

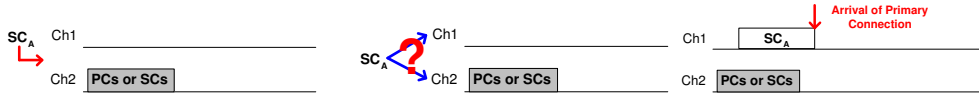
### 3.2 Transmission Processes with Multiple Handoffs for the Secondary Users' Connections

Figure 3.1 illustrates the transmission processes of a secondary connection in a two-channel CR network. The procedures consist of the following steps:

1. In Fig. 3.1(a), a secondary user plans to establish a new connection flow  $SC_A$  to its intend receiver.
2. Next, in Fig. 3.1(b), the transmitter and receiver of  $SC_A$  select the initial operating channel. In this example, they can select channel Ch1 or Ch2.
3. In Fig. 3.1(c),  $SC_A$  is established at Ch1. During the transmission period of  $SC_A$ , a request of primary connection may arrive at Ch1.
4. Next, in Fig. 3.1(d),  $SC_A$  detects the appearance of the primary user<sup>1</sup>.

---

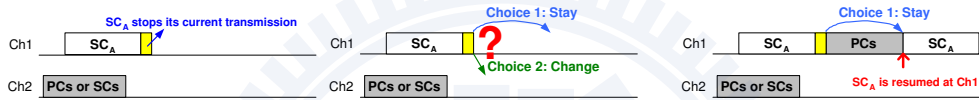
<sup>1</sup>In this dissertation, we assume that the considered CR network is a time-slotted system. In order to detect the presence of primary users, each secondary user must perform spectrum sensing at the beginning of each time slot. If the current operating channel is idle, the secondary user can transmit one slot-sized frame in this time slot. Otherwise, the secondary user must perform spectrum handoff procedures to resume its unfinished



(a) The transmitter of the secondary connection  $SC_A$  plans to establish a connection flow to the intended receiver.

(b) The transmitter and receiver of  $SC_A$  can select channel Ch1 or Ch2 for its initial operating channel.

(c) During the transmission period of  $SC_A$ , a primary connection arrives at Ch1.



(d) The transmission of  $SC_A$  is stopped.

(e) The target channel of  $SC_A$  is decided for spectrum handoff. They can either stay on Ch1 or change to Ch2.

(f)  $SC_A$  vacates Ch1 and then resumes the unfinished transmission when Ch1 becomes idle.



(g)  $SC_A$  vacates Ch1 and changes its operating channel to the idle channel Ch2.

(h)  $SC_A$  vacates Ch1 and changes its operating channel to the busy channel Ch2.

Figure 3.1: Illustration of transmission procedures in a two-channel system. The gray areas indicate that the channels are occupied by the existing primary users' connections (PCs) or the other secondary users' connections (SCs).

Then, the spectrum handoff procedures are initiated to vacate Ch1 and discover the suitable target channel to resume the unfinished transmission.

5. Then, in Fig. 3.1(e), the target channel of  $SC_A$  must be decided for spectrum handoff. If the non-hopping mode is adopted, the operating channel of  $SC_A$  cannot be changed and thus  $SC_A$  must select Ch1 to be its target channel. However,  $SC_A$  can select Ch1 or Ch2 for its target channel when the hopping mode is adopted. There are many methods to select the target channel. For example, the target channel can be searched by instantaneous spectrum sensing at this moment of interruption. In this case, the effect of spectrum sensing time  $\tau$  on the latency performance of  $SC_A$  must be considered.
6. Finally, if  $SC_A$  chooses to stay on Ch1, its remaining transmission will be resumed after all traffic loads of the primary users at Ch1 have been served as shown in Fig.3.1(f). On the other hand, if the decision is change to Ch2, there are two possible situations. If Ch2 is idle,  $SC_A$  can transmit remaining data immediately as shown in Fig.3.1(g). Otherwise,  $SC_A$  must wait at the queue until all secondary users in the present queue of Ch2 are served as shown in Fig.3.1(h).
7. Note that the similar spectrum handoff behaviors may be executed many times because a secondary connection may experience multiple interruptions from the primary users during its transmission period. Hence, the procedures from Figs. 3.1(c) to 3.1(h) will be executed

---

transmission at the target channel. Furthermore, The secondary user can differentiate the appearance of the primary user or the secondary user by exiting spectrum sensing techniques such as feature detection.

repeatedly. In this case, a set of target channels will be selected sequentially, called the *target channel sequence* in this dissertation.

### 3.3 Queueing Theoretical Framework for Spectrum Management

#### 3.3.1 Assumptions

Assume that the considered CR network is a time-slotted system as [34, 72–75]. In order to detect the presence of primary users, each secondary user must perform spectrum sensing at the beginning of each time slot. If the current operating channel is idle, the secondary user can transmit one slot-sized frame in this time slot. Otherwise, the secondary user must perform spectrum handoff procedures to resume its unfinished transmission at the preselected target channel. This kind of listen-before-talk channel access scheme is implemented in many wireless techniques, such as the quiet period of the IEEE 802.22 standard [76] and the clear channel assessment (CCA) of the IEEE 802.11 standard [77].

#### 3.3.2 Overview of the PRP M/G/1 Queueing Network Model

Now we propose a preemptive resume priority (PRP) M/G/1 queueing network model to characterize the connection-based spectrum usage behaviors in CR networks. This queueing network analytical framework is quite general and can be easily adjusted to evaluate the performance of various spectrum management techniques under different traffic conditions. Furthermore, it can also be applied to general CR network architectures, including ad hoc

CR network and centralized CR networks such as the IEEE 802.22 standard. Key features of the proposed PRP M/G/1 queueing network model are listed below:

- Each server (channel) has two types of customers (connections). Before transmitting data, the traffic of the primary and the secondary users enter to the high-priority queue and the low-priority queue<sup>2</sup>, respectively. Then, according to the traffic arrival time at queues, the *primary connections* and the *secondary connections* can be established without any collision. Here, we assume that the connections with the same priority follow the first-come-first-served (FCFS) scheduling discipline<sup>3</sup>.
- The primary users have the preemptive priority to interrupt the transmission of the secondary users. The interrupted secondary user can resume the unfinished transmission on the selected target channel, instead of retransmitting the whole data. Note that the target channel of an interrupted secondary connection can be different from its current operating channel. This is a key difference from the spectrum usage model based on the conventional PRP M/G/1 queueing theory [16–18].
- A secondary connection may experience multiple interruptions from the primary users during its transmission period. This model can characterize the effects of multiple spectrum handoffs.

Note that this model can be also extended to characterize the effects of sensing errors (i.e., missed detection and false alarm) and the heterogeneous

---

<sup>2</sup>Note that we assume the considered two queues have an infinite length.

<sup>3</sup>In fact, the analytical results of mean values obtained based the proposed framework can be applied to other scheduling discipline which is independent of the service time of the primary and secondary connections because the averages of system performance metrics will be invariant to the order of service in this case (see page 113 in [78]).

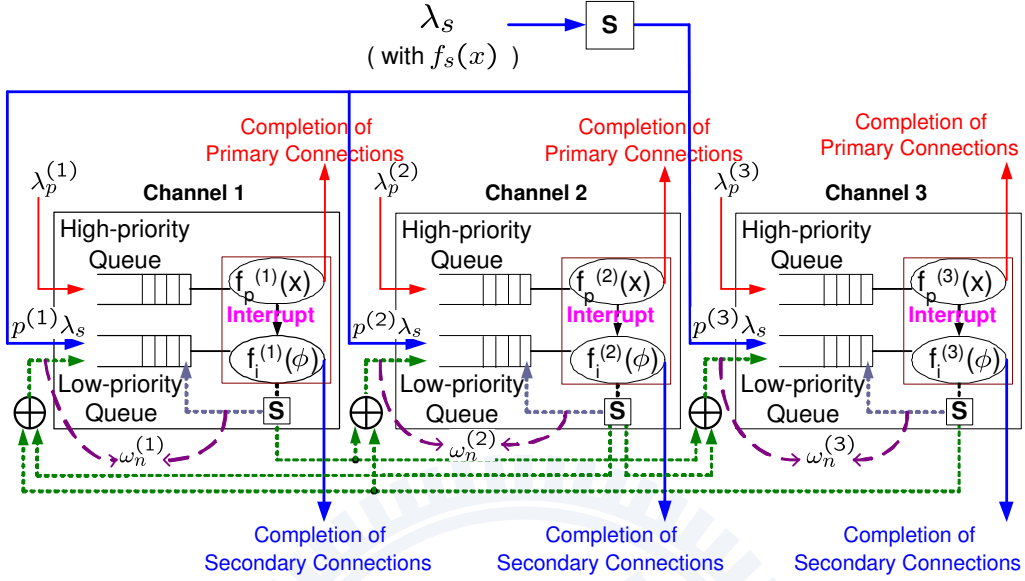


Figure 3.2: The PRP M/G/1 queueing network model with three channels.  $\lambda_p^{(k)}$ ,  $\lambda_s^{(k)}$ , and  $\omega_n^{(k)}$  are the arrival rates of the primary connections, the secondary connections, and the type- $n$  secondary connections ( $n \geq 1$ ) at channel  $k$ . Note that  $\omega_0^{(k)} = \lambda_s^{(k)}$ . Furthermore,  $f_p^{(k)}(x)$  and  $f_i^{(k)}(\phi)$  are the pmfs of  $X_p^{(k)}$  and  $\Phi_i^{(k)}$ , respectively.

channel bandwidth [79]. Some assumptions are adopted for ease of analysis.

- The arrival processes of the primary and the secondary connections are Poisson.
- Only one user can transmit on each channel at any time instant.
- The secondary transmitter can notify its corresponding receiver of the interruption event by certain spectrum handoff protocols [80].

Figure 3.2 shows an example of the PRP M/G/1 queueing network model with three channels. Let  $\lambda_s$  (arrivals/slot) be the arrival rates of the secondary connections in CR network. When a secondary connection arrives

at CR network, it can select its initial operating channel from one of three channels. Let  $p^{(k)}$  be the probability that it selects channel  $k$  for its initial operating channel. Thus, the effective arrival rate of the secondary connection at channel  $k$  is  $\lambda_s^{(k)} = p^{(k)}\lambda_s$ . Note that various spectrum decision algorithms will yield different values of  $p^{(k)}$ .

When a newly arriving secondary connection is connected to the low-priority of its initial operating channel, it can be transmitted immediately if the selected channel is idle. Otherwise, it must wait until this channel becomes idle. Furthermore, when a secondary connection is transmitting at channel  $k$ , it will be interrupted if a primary user appears at channel  $k$ . In this case, the secondary connection can either stay on the current operating channel or change to another channel through different feedback paths. The decision depends on which operating mode and spectrum handoff scheme are adopted. If the secondary connection chooses to stay on its current operating channel, the remaining data of the interrupted secondary connection must wait at the head of the low-priority queue of the current operating channel. If the decision is to change its operating channel, its remaining data will be connected to the tail of the low-priority queue of another channel. Note that  $\oplus$  represents that the traffic of the interrupted secondary connection is merged. Furthermore, when the interrupted secondary connection transmits its remaining data on the selected target channel, it may be interrupted again. Hence, this model can describe the effects of multiple handoffs.

In Fig. 3.2,  $\boxed{S}$  represents the channel selection point, where the newly arriving secondary connection must select its initial operating channel or the interrupted secondary connection must select its target channel for spectrum handoff. There are many methods to select these channels. For example, the secondary connection can decide its initial operating channel or target



channel according to the predetermined probability or the outcomes from instantaneous spectrum sensing. If the spectrum sensing is executed to search the idle channels,  $\boxed{\text{S}}$  can be regarded as a tapped delay line or a server with constant service time, which related to sensing time. Hence, the effect of spectrum sensing time on the latency performance of the secondary connections can be characterized.

### 3.3.3 Modeling of the Connection-based Channel Usage Behaviors

Now, we explain why the proposed model can characterize the connection-based channel usage behaviors in a CR network. In order to accurately characterize the transmission processes of a secondary connection, we must take the seven events as discussed in Section 3.2 into account.

1. Secondary connection arrival event as shown in Fig. 3.1(a): We assume that the arrival process of the secondary connections is Poisson. Let  $X_s$  be the service time of the secondary connections and  $f_s(x)$  be the probability mass function (pmf) of  $X_s$ .
2. Initial channel selection event of the secondary connections as shown in Fig. 3.1(b): We use  $p^{(k)}$  to represent the probability that the secondary connection selects channel  $k$  for its initial operating channel. Furthermore, if the spectrum sensing is executed to decide the initial operating channel, the effect of sensing time can be modeled by  $\boxed{\text{S}}$ .
3. Primary connection arrival event as shown in Fig. 3.1(c): We assume that the arrival process of the primary connections is Poisson. Denote  $\lambda_p^{(k)}$  as the arrival rate of the primary connections whose default channels are channel  $k$ . Furthermore, let  $X_p^{(k)}$  be the service time of the

primary connections whose default channels are channel  $k$  and  $f_p^{(k)}(x)$  be the pmf of  $X_p^{(k)}$ .

4. Interruption event as shown in Fig. 3.1(d): In the PRP M/G/1 queueing network model, the primary users have the preemptive priority and thus they can interrupt transmission of the secondary users. In other words, the secondary users must vacate the occupied channel when the primary users appear.
5. Target channel selection event as shown in Fig. 3.1(e): An interrupted secondary connection can either stay on its current channel or change to another channel. To this end, its remaining transmission must be connected to the low-priority queue of current channel or another channel through different feedback paths. Furthermore, if the spectrum sensing is executed to search the target channel, the effect of sensing time can be modeled by  $\boxed{S}$ .
6. Resumption event as shown in Figs. 3.1(f)-(h): The interrupted secondary connection can resume its unfinished transmission on the target channel, instead of retransmitting the whole data.
7. Multiple handoff events: Two auxiliary parameters ( $\omega_i^{(k)}$  and  $\Phi_i^{(k)}$ ) are suggested to characterize the traffic flows of the interrupted secondary connections.

### 3.3.4 Two Auxiliary Parameters: $\omega_i^{(k)}$ and $\Phi_i^{(k)}$

In Fig. 3.2, we use two auxiliary parameters to characterize the traffic flows of the interrupted secondary connections. We call the secondary connections which have experienced  $i$  interruptions the type- $i$  secondary connec-

tions where  $i \geq 0$ . At channel  $k$ , denote  $\omega_i^{(k)}$  as the arrival rate of traffic flows redirected from the type- $(i - 1)$  secondary connections. That is,  $\omega_i^{(k)}$  is the arrival rate of the type- $i$  secondary connections at channel  $k$ . Note that  $\omega_0^{(k)} = \lambda_s^{(k)}$ . Furthermore, let  $\Phi_i^{(k)}$  be the transmission duration of a secondary connection between the  $i^{th}$  and the  $(i + 1)^{th}$  interruptions at channel  $k$  and  $f_i^{(k)}(\phi)$  be the pmf of  $\Phi_i^{(k)}$ . That is,  $\Phi_i^{(k)}$  is the effective service time of the type- $i$  secondary connections at channel  $k$ .

Figure 3.3 illustrates the physical meaning of random variable  $\Phi_i^{(k)}$ . Recall that  $X_s$  is the service time of the secondary connections. We generate  $X_s$  five times in Fig. 3.3. The five realizations are divided into many segments due to multiple primary users' interruptions. For example, the first secondary connection (realization) is divided into four segments because it experiences three interruptions in total. The first, second, third, and fourth segments are transmitted at channels 1, 1, 1, and 2, respectively. Thus, this secondary connection's initial operating channel is Ch1 and its target channel sequence is (Ch1, Ch1, Ch2). In Fig. 3.3, random variable  $\Phi_2^{(1)}$  is one of the gray regions, representing the transmission duration of a secondary connection between the 2<sup>nd</sup> and the 3<sup>rd</sup> interruptions at Ch1. That is,  $\Phi_2^{(1)}$  is one of the third segments of the first, the third, and the fourth secondary connections in Fig. 3.3. Note that the fifth secondary connection in Fig. 3.3 does not have the third segment because it is interrupted only once.

In the hopping mode, it is quite complex to find the probability mass function of the effective service time of each segment because the effective service time is dependent on the traffic statistics of the primary and other secondary users of each channels and the operating channels for these segments can be different. Fortunately, based on the proposed analytical framework, we provide a systematic approach to study the effects of various system pa-

rameters on the effective service time and then can derive the closed-form expression for the probability mass function of the effective service time of each segment.

### 3.3.5 Constraint

Finally, we denote  $\rho^{(k)}$  as the busy probability of channel  $k$ . In an  $M$ -channel network, the following constraint shall be satisfied:

$$\rho^{(k)} \triangleq \lambda_p^{(k)} \mathbf{E}[X_p^{(k)}] + \sum_{i=0}^{\infty} \omega_i^{(k)} \mathbf{E}[\Phi_i^{(k)}] < 1 , \quad (3.1)$$

Note that  $\rho^{(k)}$  can be also interpreted as the utilization factor of channel  $k$ .

## 3.4 Summary

In the following chapters, we will discuss various spectrum management techniques to demonstrate the effectiveness of this analytical model. For the *spectrum decision* issue, we show how to determine which channels are required to probe and transmit. For the *spectrum mobility* issue, we illustrate how to characterize the effects of multiple handoffs, where the secondary users can have different operating channels before and after spectrum handoff. For the *spectrum sharing* issue, we explore how to determine the optimal admission probability to avoid the interference between primary and secondary users in the presence of false alarm and missed detection.

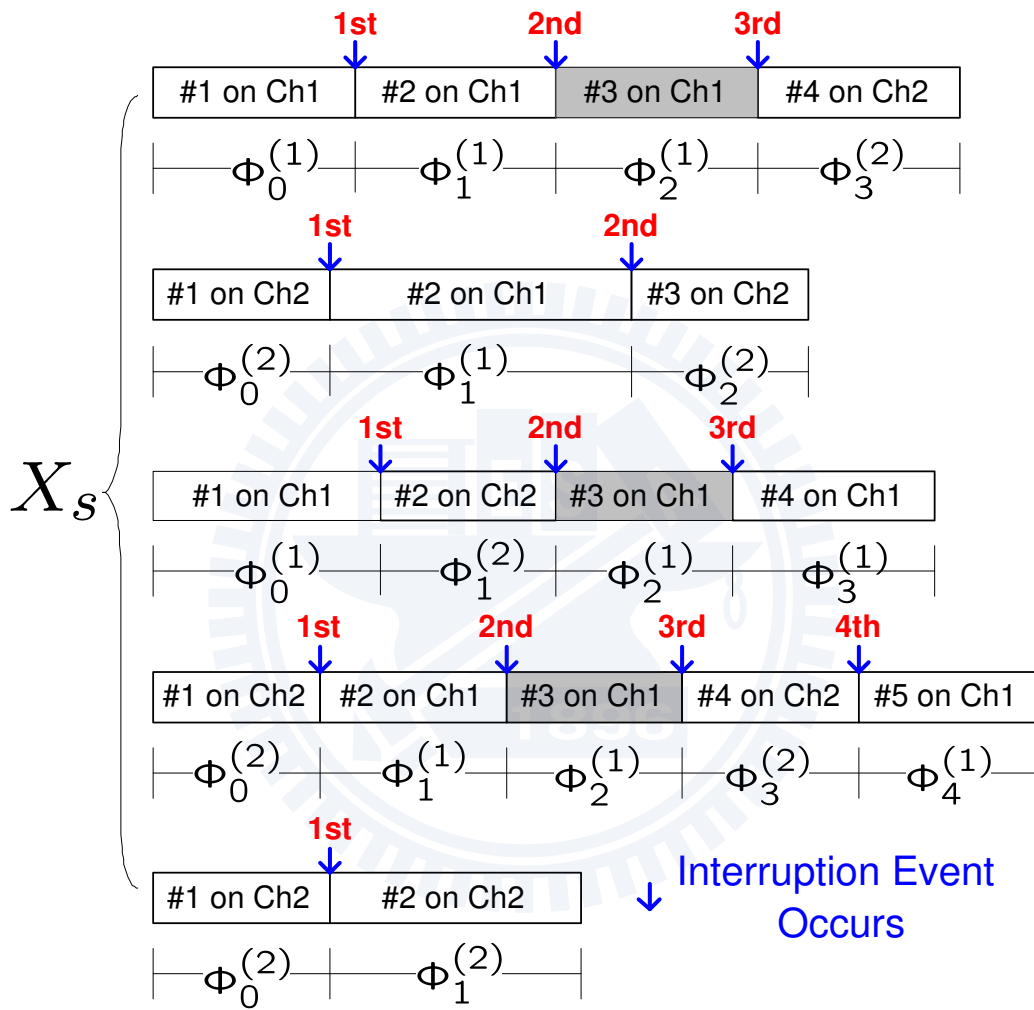


Figure 3.3: Illustration of the physical meaning of random variable  $\Phi_i^{(k)}$ . For example,  $\Phi_2^{(1)}$  is one of the third segments (gray areas) of the first, the third, and the fourth secondary connections.

# Chapter 4

## Load-Balancing Spectrum

### Decision

Spectrum decision is a crucial process in CR networks [13], which helps the secondary user select the best channel to transmit data from candidate channels. In order to distribute the traffic loads of the secondary users evenly to these candidate channels, an effective spectrum decision scheme should take the traffic statistics of the primary users as well as the secondary users into account. In this chapter, we introduce a performance measure for evaluating various spectrum decision schemes – the overall system time of the secondary connection, which is defined as the duration from the instant that data arrives at system until the instant of finishing the whole transmission.

In this chapter, we investigate how to evaluate the overall system time for the sensing-based and the probability-based spectrum decision schemes in the CR network when multiple interruptions from the primary user and sensing errors are taken into account. To this end, we design our multiuser spectrum decision schemes on top of the preemptive resume priority (PRP) M/G/1 queueing model. Based on the proposed analysis-based framework,

we can design the suitable parameters to shorten the overall system time. Unlike the non-load-balancing methods that multiple secondary users may contend for the same channel, the channel selection schemes based on the designed parameters of the proposed analytical model can evenly distribute the traffic loads of secondary users to multiple channels, thereby reducing the average overall system time. The major contributions of this chapter are summarized in the following:

- Derive the optimal selection probability for the probability-based channel selection scheme.
- Develop a method to determine the optimal number of candidate channels for the sensing-based channel selection scheme.
- Compare the sensing-based and the probability-based channel selection methods and suggest which spectrum decision scheme can result in shorter overall system time with various sensing error probabilities and traffic parameters.
- Characterize the effects of sensing errors on the spectrum decision schemes of CR networks in terms of the overall system time of the primary and the secondary connections.

## 4.1 Motivation

The overall system time of the secondary users' connections is affected by the multiple interruptions from the primary users and the sensing errors like missed detection and false alarm for the primary users. Within the transmission period of the secondary users' connection, it is likely to have multiple spectrum handoffs due to the interruptions from the primary users.

Clearly, multiple spectrum handoffs will increase the overall system time [71]. In the meanwhile, false alarm occurs when the detector mistakenly reports the presence of a primary user. In this situation, the overall system time of the secondary user's connections becomes longer because the secondary users cannot transmit data even with an idle channel. When the detection of a primary user is missed, data collision of both the primary user and the secondary user occurs, resulting in retransmitting and prolonging the overall system time of the secondary users' connections. Hence, it is crucial is incorporating the effects of multiple handoffs and the sensing errors of false alarm and missed detection in spectrum decision methods for CR networks.

In this chapter, two kinds of spectrum decision schemes are considered: (1) the sensing-based spectrum decision scheme; and (2) the probability-based channel selection scheme. For the sensing-based spectrum decision method, a secondary user selects its operating channel according to the *instantaneous* sensing results from scanning the wideband spectrum. For the probability-based spectrum decision method, the operating channel is selected based on the predetermined probabilities which are determined according to traffic statistics from the *long-term* observation. Note that the sensing outcomes in both the methods are related to the traffic statistics of both the primary users and the secondary users. The two considered spectrum decision schemes have different design issues. For the sensing-based spectrum decision scheme, the total number of candidate channels for channel selection significantly affects the overall system time because this scheme requires scanning all the candidate channels. Intuitively, a narrowband sensing (or a smaller number of candidate channels) can reduce the total sensing time. However, it is difficult to find one idle channel from a small number of candidate channels. Hence, one challenge is to determine the optimal num-



ber of candidate channels to minimize the overall system time. On the other hand, the probability-based spectrum decision scheme needs to prevent the secondary users from selecting a busy channel. Hence, the most important issue is to determine the optimal channel selection probability to minimize the overall system time.

## 4.2 System Model

### 4.2.1 Assumptions

In practice, many reasons may lead to an error on sensing the presence of the primary users. If such a sensing error occurs, not only the primary user's connection will be stained, but the secondary user's transmission will be affected. There are two types of sensing errors regarding the detection of the primary users: false alarm and missed detection. False alarm occurs when the detector reports the presence of a primary user while it is absent, while missed detection occurs when the detector reports the absence of a primary user while it is present. In this chapter, the effects of false alarm and missed detection on CR network performance are discussed in Section 4.5.

### 4.2.2 Spectrum Decision Behavior Model

Fig. 4.1 illustrates the spectrum decision behavior model, which will be used to evaluate the overall system time of a secondary user's connection for different channel selection schemes. We assume that the arrival processes of the primary and the secondary connections<sup>1</sup> are Poisson. Let  $\lambda_p^{(k)}$  (arrivals/slot)

---

<sup>1</sup>When a secondary transmitter has data to send, how to establish a secondary connection to its intended receiver has been investigated in [81].

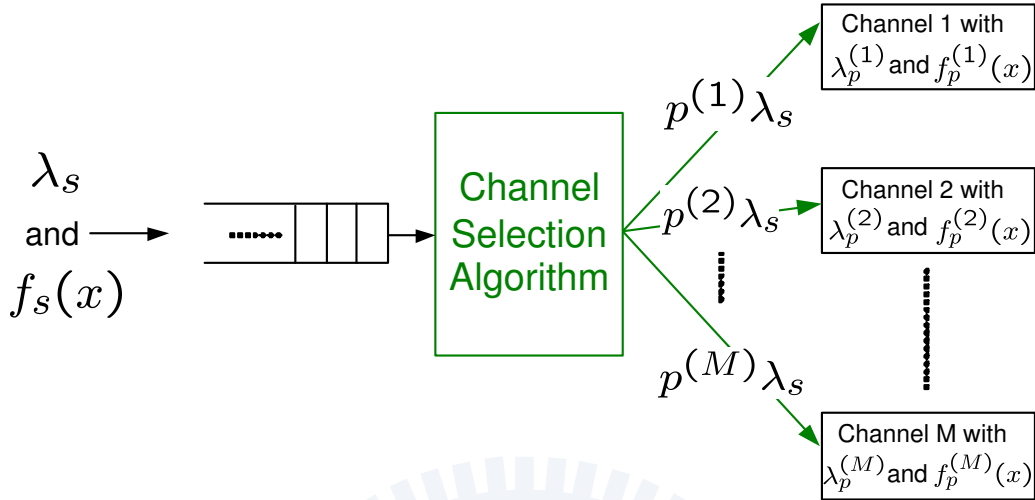


Figure 4.1: Spectrum decision behavior model.

and  $\lambda_s$  (arrivals/slot) be the average arrival rates of the primary connections at channel  $k$  and the secondary connections of CR network, respectively. Also, denote  $X_p^{(k)}$  (slots/arrival) and  $X_s$  (slots/arrival) the service time of the primary connections of channel  $k$  and the secondary connections, respectively; and let  $f_p^{(k)}(x)$  and  $f_s(x)$  be the probability mass functions (pmf) of  $X_p^{(k)}$  and  $X_s$ , respectively. It is assumed that  $\lambda_p^{(k)}$ ,  $\lambda_s$ ,  $f_p^{(k)}(x)$ , and  $f_s(x)$ , which can be estimated by the existing methods [82], are known to all the secondary users.

As shown in Fig. 4.1, each secondary connection can select one of  $M$  candidate channels for its operating channel. Based on our proposed analytical framework, which will be discussed in more detail later, all the secondary users can dynamically select their operating channels with suitable probability that can balance the traffic loads of secondary users in multiple channels. The distribution probability vector (denoted by  $\mathbf{p} = (p^{(1)}, p^{(2)}, \dots, p^{(M)})$ ) represents the set of probabilities for selecting all the candidate channels, in which  $p^{(k)}$  denotes the probability of a secondary connection selecting channel

$k$  for its operating channel. Thus, the effective arrival rate of the secondary connection at channel  $k$  is  $\lambda_s^{(k)} = p^{(k)}\lambda_s$ . Note that various channel selection algorithms yield different distribution probability vectors.

## 4.3 Problem Formulation

### 4.3.1 Performance Metric: Overall System Time

The overall system time (denoted by  $S$ ) is an important quality of service (QoS) metric for the connection-based service of the secondary users. It consists of the waiting time (denoted by  $W$ ) and the extended data delivery time (denoted by  $T$ ) as shown in Fig. 4.2. Hence, we have

$$\mathbf{E}[S] = \mathbf{E}[W] + \mathbf{E}[T] , \quad (4.1)$$

where  $\mathbf{E}[\cdot]$  is the expectation function. Here, the waiting time is defined as the duration from the instant that a data transmission request arrives at the system until the instant of starting transmitting data. The duration of waiting time depends on the channel selection scheme that the secondary users adopt. Furthermore, the extended data delivery time is defined as the duration from the beginning of transmitting the data in the first time slot until the completion of the data in the last time slot. Clearly, multiple handoff behaviors significantly affect the extended data delivery time.

### 4.3.2 Overall System Time Minimization Problem for Probability-based Channel Selection Scheme

For the probability-based channel selection method, each secondary user selects its operating channel from all the  $M$  candidate channels based on a

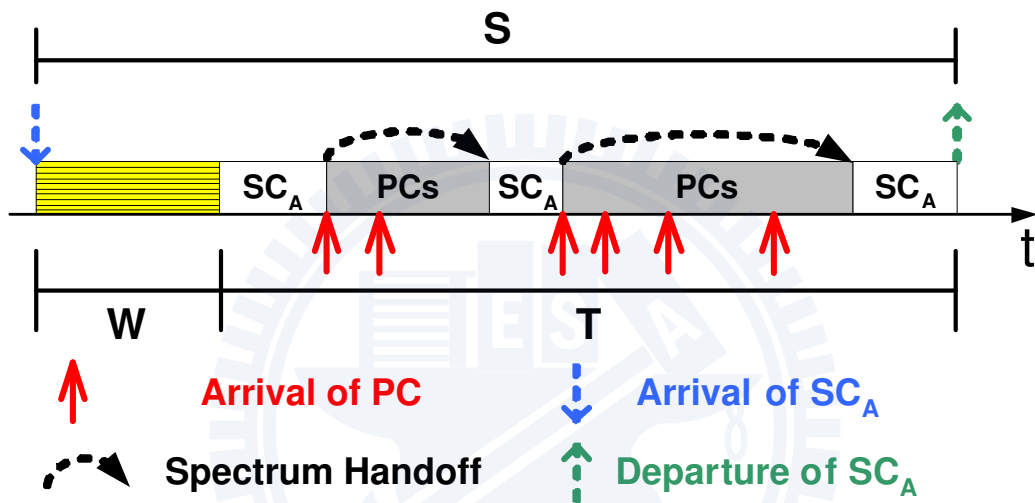


Figure 4.2: Example of the overall system time of the secondary connection  $SC_A$ . The white areas indicate that channel is occupied by  $SC_A$ . Furthermore, the gray areas indicate that channel is occupied by the primary connections (PCs) and its duration is the busy period resulting from transmissions of the primary connections. Here,  $SC_A$  encounters two interruptions from the primary connections during its transmission period.

predetermined distribution probability vector  $\mathbf{p}_{pb}$ . In this case, an **Overall System Time Minimization Problem for Probability-based Channel Selection Scheme** can be formulated as follows. Given the set of candidate channels  $\Omega = \{1, 2, \dots, M\}$ , we aim to find the optimal distribution probability vector (denoted by  $\mathbf{p}^*$ ) to minimize the average overall system time of the secondary connections (denoted by  $\mathbf{E}[S_{pb}]$ ). Formally,

$$\mathbf{p}^* = \arg \min_{\forall \mathbf{p}_{pb}} \mathbf{E}[S_{pb}(\mathbf{p}_{pb})] , \quad (4.2)$$

subject to:

$$0 \leq p_{pb}^{(k)} \leq 1, \quad \forall k \in \Omega , \quad (4.3)$$

$$\sum_{k \in \Omega} p_{pb}^{(k)} = \sum_{k=1}^M p_{pb}^{(k)} = 1 . \quad (4.4)$$

and

$$\rho^{(k)} = \rho_p^{(k)} + \rho_s^{(k)} < 1 , \quad (4.5)$$

where  $\rho^{(k)}$  is the busy probability of channel  $k$ . Furthermore,  $\rho_p^{(k)}$  and  $\rho_s^{(k)}$  are the busy probabilities resulting from the primary and the secondary connections at channel  $k$  when sensing errors are considered, respectively. In Section 4.4, we will derive the closed-form expressions for  $\rho_p^{(k)}$  and  $\rho_s^{(k)}$ .

### 4.3.3 Overall System Time Minimization Problem for Sensing-based Channel Selection Scheme

For the sensing-based channel selection scheme, the secondary users perform wideband sensing to find an idle channel from all the candidate channels. If more than one idle channel is found, the secondary user randomly selects one channel from the idle channels for its operating channel. Furthermore, if all the candidate channels are busy, the secondary user still randomly select one

channel from all the candidate channels and wait for the available time slot of the selected channel.

In order to decrease the total sensing time, the secondary users shall reduce the number of candidate channels by sensing only the best  $n$  channels among  $M$  channels. Without loss of generality, we assume that the channel preference of the secondary users follows the lexicographic order. That is, channel  $i$  is not better than channel  $j$  if  $i > j$ . Note that the ordering issue for channel preference has been discussed in [83]. Let  $\Omega$  be the set of candidate channels. Then, we can have  $\Omega = \{1, 2, \dots, n\}$ , where  $n = |\Omega| \leq M$ . Next, we formulate an **Overall System Time Minimization Problem for Sensing-based Channel Selection Scheme** as follows. Given the total number of channels  $M$ , we aim to find the optimal number of candidate channels (denoted by  $n^*$ ) to minimize the average overall system time of the secondary connections (denoted by  $\mathbf{E}[S_{sb}]$ ). Formally,

$$n^* = \arg \min_{1 \leq n \leq M} \mathbf{E}[S_{sb}(n)] . \quad (4.6)$$

#### 4.3.4 Performance Model

In order to calculate the overall system time of various spectrum decision schemes, we extend the general model in Fig. 4.1 to characterize the sensing- and the probability-based channel selection schemes. Fig. 4.3 shows the performance model for the probability-based scheme. When the traffic of the secondary user (i.e., the secondary connection) arrives at the system, it can be directly connected to the selected channel based on the predetermined distribution probability vector. On the other hand, Fig. 4.4 shows the performance model of the sensing-based scheme. When the traffic of a secondary user arrives at the system, the secondary user performs spectrum sensing to find idle channels. The total sensing time can be modeled by a tapped delay

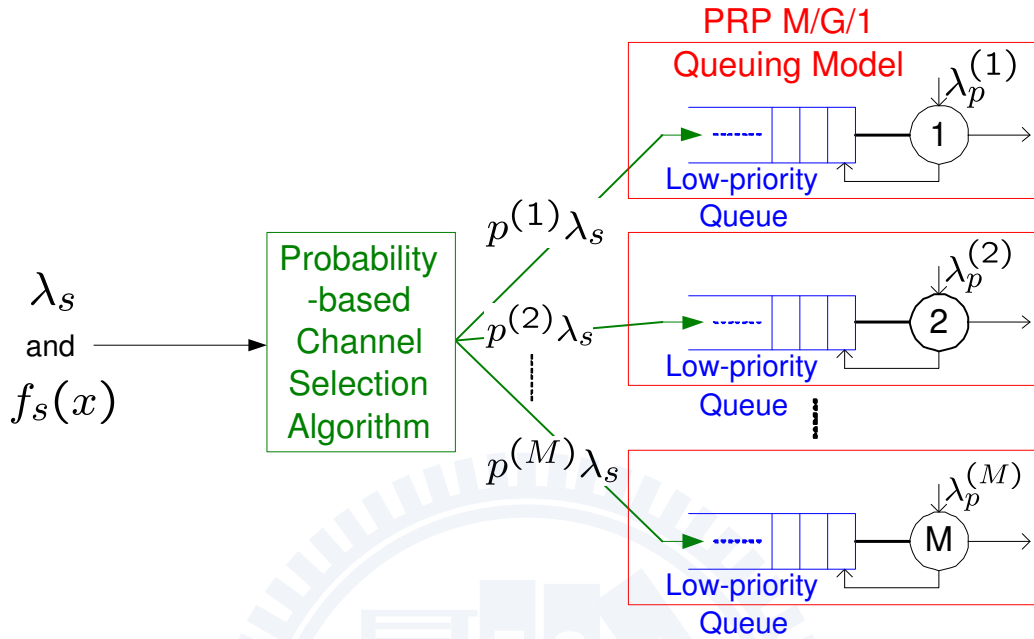


Figure 4.3: Performance model for the probability-based channel selection scheme where the channel usage behaviors are characterized by the PRP M/G/1 queueing systems.

line  $\boxed{S}$ . In this case,  $\boxed{S}$  can be regarded as a server with constant service time, which equals to sensing time. If an idle channel can be found, the secondary connection can be served immediately. Finally, in Figs. 4.3 and 4.4, the channel usage behaviors of each channel is characterized by a PRP M/G/1 queueing model, which had been presented in Chapter 3. Here, we assume that the non-hopping mode is adopted. Hence, the secondary user must stay on its current channel when it is interrupted.

Based on the proposed performance models, we can analytically compare the overall system time resulting from both the spectrum decision schemes for various sensing time and traffic parameters. Then, each secondary user can intelligently adopt the best channel selection scheme to minimize its overall

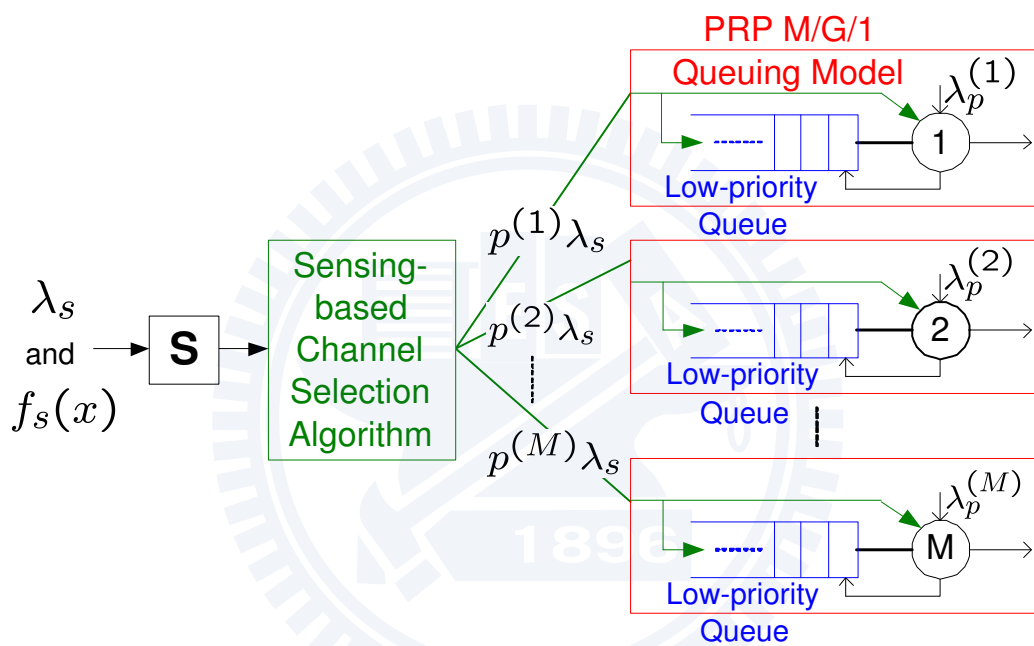


Figure 4.4: Performance model for the sensing-based channel selection scheme where the channel usage behaviors are characterized by the PRP M/G/1 queueing systems.



system time. Thus, the optimal overall system time (denoted by  $S^*$ ) can be expressed as follows:

$$S^* = \min(\mathbf{E}[S_{pb}], \mathbf{E}[S_{sb}]) . \quad (4.7)$$

In the next section, we will show how to derive  $\mathbf{E}[S_{pb}]$  and  $\mathbf{E}[S_{sb}]$ .

## 4.4 Analysis of Overall System Time

As discussed in Section 4.3.1, the overall system time consists of the waiting time and the extended data delivery time. Let  $\mathbf{E}[T_{pb}]$  and  $\mathbf{E}[T_{sb}]$  be the average data delivery time for the probability- and sensing-based spectrum decision methods, respectively. Furthermore, denote  $\mathbf{E}[W_{pb}]$  and  $\mathbf{E}[W_{sb}]$  as the average waiting time for the probability- and sensing-based spectrum decision methods, respectively. Then, we can have

$$\mathbf{E}[S_{pb}] = \mathbf{E}[W_{pb}] + \mathbf{E}[T_{pb}] , \quad (4.8)$$

and

$$\mathbf{E}[S_{sb}] = \mathbf{E}[W_{sb}] + \mathbf{E}[T_{sb}] . \quad (4.9)$$

In the following, we will investigate how to obtain the average extended data delivery time and the average waiting time.

### 4.4.1 Extended Data Delivery Time

First, we investigate the effects of multiple interruptions on the extended data delivery time. Within the transmission period of a secondary connection, it is likely to have multiple spectrum handoffs due to the interruptions from the primary users. The spectrum handoff procedure helps the secondary users vacate the occupied channel and then resume the unfinished transmission

when this channel becomes idle. Clearly, multiple spectrum handoffs will increase the extended data delivery time and degrade the QoS for the latency-sensitive traffic of the secondary users [84].

Based on the PRP M/G/1 queueing model, we can derive the extended data delivery time of the secondary connections as follows. Let  $N^{(k)}$  be the total number of interruptions for a secondary connection at channel  $k$ . Furthermore, denote  $Y_p^{(k)}$  as the duration from the time instant that channel  $k$  is occupied by the primary connections until the time instant that the high-priority queue becomes empty. This duration is called the *busy period* resulting from transmissions of multiple primary connections at channel  $k$ . When a secondary connection is interrupted by primary users, it must stop transmitting on the current operating channel until all the primary connections in the high-priority queue have been served. In this case, the secondary connections of channel  $k$  must wait for the duration of  $\mathbf{E}[Y_p^{(k)}]$  on average after the interruption event occurs. Denote  $\tilde{X}_s$  as the actual service time of the secondary connections when the effects of sensing errors are considered<sup>2</sup> and  $T^{(k)}$  as the extended data delivery time of the secondary connections at channel  $k$ . We can have

$$\mathbf{E}[T^{(k)}] = \mathbf{E}[\tilde{X}_s] + \mathbf{E}[N^{(k)}]\mathbf{E}[Y_p^{(k)}] . \quad (4.10)$$

Let  $\tilde{X}_p^{(k)}$  be the actual service time of the primary connections at channel  $k$  when the effects of sensing errors are considered. One can obtain  $\mathbf{E}[N^{(k)}] =$

---

<sup>2</sup>Although this chapter assumes that all  $M$  channels have the same data transmission rate (or equivalently service rate), the proposed model can be applied to the CR network where all channels have different data rates. In the CR network with heterogeneous data rates, the secondary connections at different channels have different average service time. Hence, they will have different average actual service time. In this case, the notation  $\tilde{X}_s$  in (4.10) should be replaced by the notation  $\tilde{X}_s^{(k)}$ , which is the actual service time of the secondary connections at channel  $k$ . More discussions had been shown in [79].

$\lambda_p^{(k)} \mathbf{E}[\tilde{X}_s]$  and  $\mathbf{E}[Y_p^{(k)}] = \frac{\mathbf{E}[\tilde{X}_p^{(k)}]}{1 - \lambda_p^{(k)} \mathbf{E}[\tilde{X}_p^{(k)}]}$  according to [85]. Note that  $\mathbf{E}[\tilde{X}_s]$  and  $\mathbf{E}[\tilde{X}_p^{(k)}]$  will be derived in Section 4.5.

Finally, the average extended data delivery time for the probability- and sensing-based channel selection methods can be expressed as follows:

$$\mathbf{E}[T_{pb}] = \sum_{k=1}^M p_{pb}^{(k)} \mathbf{E}[T^{(k)}] , \quad (4.11)$$

and

$$\mathbf{E}[T_{sb}] = \sum_{k=1}^n p_{sb}^{(k)} \mathbf{E}[T^{(k)}] . \quad (4.12)$$

For various channel selection algorithms, we use different methods to evaluate the corresponding distribution probability vectors  $\mathbf{p}$ . For the probability-based scheme, the distribution probability vector  $\mathbf{p}_{pb}$  can be designed by solving the **Overall System Time Minimization Problem for Probability-based Channel Selection Scheme** in (4.2). For the sensing-based scheme, the distribution probability vector  $\mathbf{p}_{sb}$  is determined inherently based on the given traffic patterns. Intuitively, a channel with larger idle probability will be selected more frequently through spectrum sensing. How to derive  $\mathbf{p}_{sb}$  from the given traffic parameters will be discussed in Appendix A.

#### 4.4.2 Waiting Time

Next, we focus on the derivations of the average waiting time for the probability-based and sensing-based channel selection schemes.

##### Probability-based Channel Selection Scheme

For the probability-based channel selection scheme, a secondary connection selects its operating channel based on the predetermined probability. Then, it is directly connected to the low-priority queue of the selected channel. It

cannot be served until all the primary and the secondary connections in the high-priority queue and the present low-priority queue of the selected channel have been served. Hence, the waiting time is the required duration from the time instant that a secondary connection arrives at the low-priority queue of the selected channel until the time instant that the selected channel becomes idle. That is, the waiting time is the duration spent in the waiting queue by a secondary connection. Hence,  $\mathbf{E}[W_{pb}]$  can be expressed as follows:

$$\mathbf{E}[W_{pb}] = \sum_{k=1}^M p_{pb}^{(k)} \mathbf{E}[W_{pb}^{(k)}] , \quad (4.13)$$

where  $W_{pb}^{(k)}$  is the waiting time of the secondary connections at channel  $k$  for the probability-based channel selection scheme. Applying the PRP M/G/1 queueing theory [86], one can obtain

$$\mathbf{E}[W_{pb}^{(k)}] = \frac{\mathbf{E}[R^{(k)}]}{(1 - \rho_p^{(k)})(1 - \rho_p^{(k)} - \rho_s^{(k)})} , \quad (4.14)$$

where  $\rho_p^{(k)}$  and  $\rho_s^{(k)}$  are the busy probabilities resulting from the primary and the secondary connections at channel  $k$  when sensing errors are considered, respectively. Hence, we can have  $\rho_p^{(k)} = \lambda_p^{(k)} \mathbf{E}[\tilde{X}_p^{(k)}]$  and  $\rho_s^{(k)} = \lambda_s^{(k)} \mathbf{E}[\tilde{X}_s]$ . Furthermore,  $\mathbf{E}[R^{(k)}]$  is the average remaining time to complete the service of the connection being served at channel  $k$ . Referring to [86], we have

$$\mathbf{E}[R^{(k)}] = \frac{1}{2} \lambda_p^{(k)} \mathbf{E}[(\tilde{X}_p^{(k)})^2] + \frac{1}{2} p_{pb}^{(k)} \lambda_s \mathbf{E}[(\tilde{X}_s)^2] . \quad (4.15)$$

Then, substituting (4.14) and (4.15) into (4.13), we can obtain the closed-form expression for  $\mathbf{E}[W_{pb}]$ .

Finally, substituting (4.11) and (4.13) into (4.8), we can obtain the relationship between the average overall system time and the distribution probability vector  $\mathbf{p}_{pb}$  for the probability-based channel selection scheme. Then, the optimal distribution probability vector  $\mathbf{p}^*$  can be determined by solving

the **Overall System Time Minimization Problem for Probability-based Channel Selection** in (4.2).

### Sensing-based Channel Selection Scheme

The waiting time  $W_{sb}$  for the sensing-based channel selection method consists of the total sensing time and the queueing time (denoted by  $W'_{sb}$ ). Let  $\tau$  be the sensing time for scanning one candidate channel. Hence,  $n\tau$  is the total sensing time for scanning all the  $n$  candidate channels. After wideband sensing, the secondary user can decide channel availability and then transmits data at one of the idle channels. Moreover, if the idle channel cannot be found, the secondary user cannot transmit immediately. In this case, the secondary user's connection will be put into the low-priority queue of the randomly selected channel. Hence, we can have

$$\mathbf{E}[W_{sb}] = n\tau + \mathbf{Pr}(\mathcal{E}) \times 0 + \mathbf{Pr}(\mathcal{E}^c) \times \mathbf{E}[W'_{sb}] , \quad (4.16)$$

where  $\mathcal{E}$  is the event that at least one idle channel can be found after sensing, and  $\mathcal{E}^c$  is the compliment of  $\mathcal{E}$ .

Next, the closed-form expressions for  $\mathbf{Pr}(\mathcal{E})$  and  $\mathbf{Pr}(\mathcal{E}^c)$  can be derived by the following two observations. First, a channel is called actual idle if and only if (1) this channel is not occupied by the primary connections and (2) the low-priority queue of this channel is empty. Note that the second condition should be contained because the FCFS scheduling discipline is adopted. Secondly, an actual idle channel is assessed as idle through spectrum sensing if and only if false alarm does not occur. Hence, we can have

$$\begin{aligned} \mathbf{Pr}(\mathcal{E}) &= \sum_{k=1}^n [\mathbf{Pr}(\mathcal{E} | k \text{ channels are actually idle}) \times \mathbf{Pr}(k \text{ channels are actually idle})] \\ &= \sum_{k=1}^n \left[ [1 - (P_F)^k] \times \sum_{\mathfrak{S} \subseteq \Omega, |\mathfrak{S}|=k} \left[ \prod_{i \in \mathfrak{S}} (1 - \rho^{(i)}) \prod_{j \in \Omega - \mathfrak{S}} \rho^{(j)} \right] \right] , \end{aligned} \quad (4.17)$$

where  $\rho^{(k)} = \rho_p^{(k)} + \rho_s^{(k)}$  and  $P_F$  is the false alarm probability. On the other hand,  $\mathcal{E}^c$  is the compliment of  $\mathcal{E}$ . That is,

$$\Pr(\mathcal{E}^c) = 1 - \Pr(\mathcal{E}) . \quad (4.18)$$

Moreover, when all channels are assessed as busy, each channel is selected by the secondary users with probability  $1/n$ . Hence, in this case, one can derive the average queueing time based on the PRP M/G/1 queueing theory as follows [86] :

$$\mathbf{E}[W'_{sb}] = \sum_{k=1}^n \left[ \frac{1}{n} \cdot \frac{\mathbf{E}[R^{(k)}]}{(1 - \rho_p^{(k)})(1 - \rho_p^{(k)} - \rho_s^{(k)})} \right] . \quad (4.19)$$

Finally, substituting (4.12) and (4.16) into (4.9), we can obtain the relationship between the average overall system time and the number of candidate channels  $n$  for the sensing-based channel selection scheme.

Determining the optimal number of candidate channels (denoted by  $n^*$ ) is the key issue for sensing-based spectrum decision scheme. Intuitively, a small number of candidate channels can reduce the total sensing time  $n\tau$  in (4.16). However, it is harder to find one idle channel from fewer candidate channels, resulting in a larger value of  $\Pr(\mathcal{E}^c)$  in (4.16) and thus increasing the overall system time. The optimal number of candidate channels  $n^*$  can be determined by solving the **Overall System Time Minimization Problem for Sensing-based Channel Selection** in (4.6).

## 4.5 Effects of Sensing Errors

Sensing errors such as false alarm and missed detection will degrade the performance of the secondary users and the primary users<sup>3</sup>. This section in-

---

<sup>3</sup>The relationship between the missed detection probability  $P_M$  and the false alarm probability  $P_F$  can be characterized by the receiver operating characteristic curve [87].

investigates the effects of false alarm and missed detection on the transmission time of the secondary and the primary connections. Specifically, we will show how to derive the first and the second moments of  $\tilde{X}_s$  and  $\tilde{X}_p^{(k)}$ .

### 4.5.1 False Alarm

First, we study the effect of false alarm on the actual service time of the secondary connections. When a false alarm occurs, a secondary user cannot transmit data even with an idle channel. Hence, the actual service time of a secondary connection will be extended to  $\tilde{X}_s$  (slots/arrival) from  $X_s$  (slots/arrival). The first and the second moments of  $\tilde{X}_s$  can be expressed as follows:

$$\mathbf{E}[\tilde{X}_s] = \sum_{x=1}^{\infty} \mathbf{E}[\tilde{X}_s | X_s = x] \mathbf{Pr}(X_s = x) , \quad (4.20)$$

and

$$\mathbf{E}[(\tilde{X}_s)^2] = \sum_{x=1}^{\infty} \mathbf{E}[(\tilde{X}_s)^2 | X_s = x] \mathbf{Pr}(X_s = x) . \quad (4.21)$$

Note that because the false-alarm slot cannot be exploited by any secondary or primary connections, it can be regarded as a busy slot. Hence, we can have  $\rho_s^{(k)} = \lambda_s^{(k)} \mathbf{E}[\tilde{X}_s]$ .

When a false alarm occurs, the data transmission is postponed to the next slot. Hence, for a connection with  $x$  slots, its actual service time will be extended to  $x + i$  slots if and only if false alarms occur in  $i$  slots out of the first  $x + i - 1$  slots and false alarms do not occur at the  $(x + i)^{th}$  slot. Thus, the conditional expectation of the actual service time follows the negative binomial distribution with parameter  $P_F$ . That is,

$$\mathbf{E}[\tilde{X}_s | X_s = x] = \sum_{i=0}^{\infty} (x + i) \binom{x + i - 1}{i} (1 - P_F)^x (P_F)^i , \quad (4.22)$$

and

$$\mathbf{E}[(\tilde{X}_s)^2|X_s = x] = \sum_{i=0}^{\infty} (x+i)^2 \binom{x+i-1}{i} (1-P_F)^x (P_F)^i, \quad (4.23)$$

where  $P_F$  is the false alarm probability. Because  $\mathbf{Pr}(X_s = x)$  is given by  $f_s(x)$ , we can obtain  $\mathbf{E}[\tilde{X}_s]$  and  $\mathbf{E}[(\tilde{X}_s)^2]$  by substituting (4.22) and (4.23) into (4.20) and (4.21), respectively. For example, if  $f_s(x)$  is the geometric distribution, i.e.,

$$f_s(x) = \left(1 - \frac{1}{\mathbf{E}[X_s]}\right)^{x-1} \left(\frac{1}{\mathbf{E}[X_s]}\right), \quad (4.24)$$

we can have

$$\mathbf{E}[\tilde{X}_s] = \frac{\mathbf{E}[X_s]}{1-P_F}, \quad (4.25)$$

and

$$\mathbf{E}[(\tilde{X}_s)^2] = \frac{\mathbf{E}[X_s](2\mathbf{E}[X_s] - 1 + P_F)}{(1-P_F)^2}. \quad (4.26)$$

## 4.5.2 Missed Detection

The data frame of the primary connection will be stained by the secondary connection when a missed detection occurs. Thus the primary user will request to retransmit this stained data frame in the next slot. Hence, the actual service time of a primary connection will be extended from  $X_p^{(k)}$  (slots/arrival) to  $\tilde{X}_p^{(k)}$  (slots/arrival). The first and the second moments of  $\tilde{X}_p^{(k)}$  can be expressed as follows:

$$\mathbf{E}[\tilde{X}_p^{(k)}] = \sum_{x=1}^{\infty} \mathbf{E}[\tilde{X}_p^{(k)}|X_p^{(k)} = x] \mathbf{Pr}(X_p^{(k)} = x), \quad (4.27)$$

and

$$\mathbf{E}[(\tilde{X}_p^{(k)})^2] = \sum_{x=1}^{\infty} \mathbf{E}[(\tilde{X}_p^{(k)})^2|X_p^{(k)} = x] \mathbf{Pr}(X_p^{(k)} = x). \quad (4.28)$$

Basically, there are two types of missed detections in CR networks [58,60]. Firstly, when a primary user transmits data, a newly arriving secondary connection may incorrectly determine that this specific channel is available in



its first sensing phase. We call this situation the class-A missed detection. After a secondary user arrives at a CR network for a while, it may also fail to detect the presence of primary users. In this case, the class-B missed detection occurs. The authors in [58,60] found that the class-B missed detection is small because the sensing results at the first sensing phase can be employed to improve the accuracy of the sensing results at the following sensing phases.

Next, we explain the effect of class-A missed detection on the actual service time of the primary connection at channel  $k$ . We consider a transmission slot of this primary connection. During this slot, more than one arrival of the secondary connection appears with probability  $1 - e^{-\lambda_s^{(k)}\Delta}$ , where  $\Delta$  is the slot duration. For these arrivals of secondary connections, each of them will assess this busy slot as idle if and only if (1) a missed detection occurs and (2) the low-priority queue of channel  $k$  is empty. Let  $Q_s^{(k)}$  be the length of the low-priority queue at channel  $k$ . Hence, the first arrival at the considered slot will make an error channel assessment with probability  $P_M \Pr\{Q_s^{(k)} = 0\}$ , where  $P_M$  is the missed detection probability for spectrum sensing and  $\Pr\{Q_s^{(k)} = 0\}$  has been derived in [88]. However, for the remaining arrivals in the considered slot, we have  $\Pr\{Q_s^{(k)} = 0\} = 0$  because the first arrival has been put into the low-priority queue of channel  $k$ . Thus, the remaining arrivals do not make the error channel assessment. From above observations, we can conclude that a primary connection's transmission slot is stained by the arrivals of the secondary connections with probability

$$P_I^{(k)} = (1 - e^{-\lambda_s^{(k)}\Delta})P_M \Pr\{Q_s^{(k)} = 0\} . \quad (4.29)$$

Similar to the case of missed detection, we find that the random variables  $\tilde{X}_p^{(k)}$  and  $(\tilde{X}_p^{(k)})^2$  follows the negative binomial distribution with parameter  $P_I^{(k)}$  when  $X_p^{(k)} = x$ . Then, because  $\Pr(X_p^{(k)} = x)$  can be determined by  $f_p^{(k)}(l)$ , we can calculate the values of  $\mathbf{E}[\tilde{X}_p^{(k)}]$  and  $\mathbf{E}[(\tilde{X}_p^{(k)})^2]$  in (4.27) and

(4.28), respectively. For example, if  $f_p^{(k)}(l)$  is the geometric distribution, i.e.,

$$f_p^{(k)}(x) = \left(1 - \frac{1}{\mathbf{E}[X_p^{(k)}]}\right)^{x-1} \left(\frac{1}{\mathbf{E}[X_p^{(k)}]}\right), \quad (4.30)$$

we can have

$$\mathbf{E}[\tilde{X}_p^{(k)}] = \frac{\mathbf{E}[X_p^{(k)}]}{1 - P_I^{(k)}}, \quad (4.31)$$

and

$$\mathbf{E}[(\tilde{X}_p^{(k)})^2] = \frac{\mathbf{E}[X_p^{(k)}](2\mathbf{E}[X_p^{(k)}] - 1 + P_I^{(k)})}{(1 - P_I^{(k)})^2}. \quad (4.32)$$

## 4.6 Numerical Results

In this section, numerical results are presented to show how to design the system parameters for the load-balancing spectrum decision methods, including the probability-based and the sensing-based spectrum decision schemes. We adopt the system parameters in the IEEE 802.22 standard in our simulation [89], where the time slot duration is 10 msec,  $P_M = 0.1$ , and  $P_F = 0.1$ . Because this dissertation focuses on the latency-sensitive traffic, we can assume that the service time distributions of primary and secondary connections are geometrically distributed (see page 135 in [86]). Note that we only use the geometric distribution as an example here. Indeed, the proposed analytical framework can be applied to any distributions. It only requires the knowledge of the first and the second moments of the service time distributions for the primary and the secondary connections.

### 4.6.1 Probability-based Spectrum Decision Scheme

Figure 4.5 shows the effect of various arrival rates of the secondary connections on the optimal distribution probability vector, where the distribution

probability vector is plotted in each bar and the summation of all probabilities in each bar is 1. In the figure, we consider a four-channel system with the following traffic parameters:  $\lambda_p^{(1)} = 0.01$ ,  $\lambda_p^{(2)} = 0.01$ ,  $\lambda_p^{(3)} = 0.02$ , and  $\lambda_p^{(4)} = 0.02$  as well as  $\mathbf{E}[X_p^{(1)}] = 20$ ,  $\mathbf{E}[X_p^{(2)}] = 30$ ,  $\mathbf{E}[X_p^{(3)}] = 20$ , and  $\mathbf{E}[X_p^{(4)}] = 25$ . When  $\lambda_s = 0.01$ , all the secondary users prefer selecting channel 1 to be their operating channels because channel 1 has the lightest traffic loads. Furthermore, as  $\lambda_s$  increases, some secondary users tend to select other channels to transmit data in order to balance the traffic loads in each channel. For example, when  $\lambda_s = 0.1$ , the optimal distribution probability vector is  $(0.4142, 0.2784, 0.2131, 0.0943)$ . Inevitably, channel 1 is still selected to be the operating channel with the largest probability.

Furthermore, Fig. 4.6 shows the channel busy probability under various arrival rates of the secondary connections. In the beginning, channel 1 has the lowest busy probability. However, when  $\lambda_s \geq 0.05$ , channel 1 has the highest busy probability because most secondary users prefer to select channel 1 to transmit data. Although channel 1 has the highest busy probability in this case, one can find that the secondary users still favor channel 1 from the viewpoint of the overall system time. The performance advantages of the choosing the probability vector based on the proposed analytical framework over the traditional channel selection methods will be illustrated in Fig. 4.11 from the perspective of the overall system time.

Figure 4.7 shows that most secondary connections prefer selecting a channel with the largest arrival rate and the shortest service time of the primary connections even though all the channels have the same busy probability of the primary connections. Here, we consider the following traffic parameters:  $\lambda_p^{(1)} = 0.01$ ,  $\lambda_p^{(2)} = 0.02$ ,  $\lambda_p^{(3)} = 0.04$ , and  $\lambda_p^{(4)} = 0.08$  as well as  $\mathbf{E}[X_p^{(1)}] = 40$ ,  $\mathbf{E}[X_p^{(2)}] = 20$ ,  $\mathbf{E}[X_p^{(3)}] = 10$ , and  $\mathbf{E}[X_p^{(4)}] = 5$ . Hence, all channels have

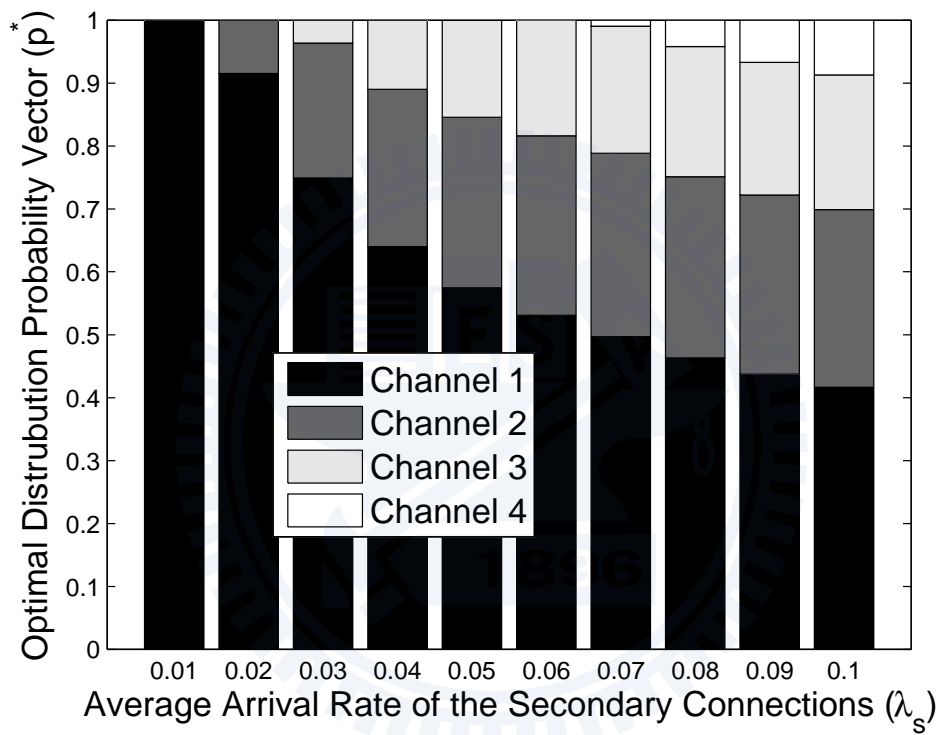


Figure 4.5: Optimal distribution probability vector for the probability-based spectrum decision with various arrival rates of the secondary connections, where  $P_F = 0.1$ ,  $P_M = 0.1$ , and  $\mathbf{E}[X_s] = 10$ .

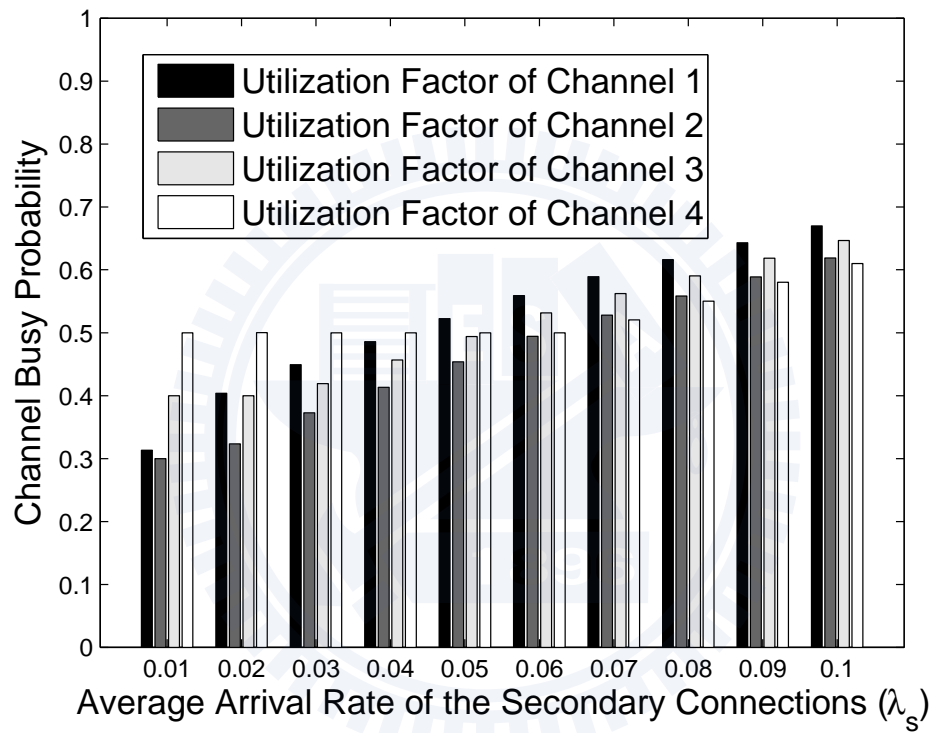


Figure 4.6: Channel busy probability for the probability-based spectrum decision with various arrival rates of the secondary connections, where  $P_F = 0.1$ ,  $P_M = 0.1$ , and  $\mathbf{E}[X_s] = 10$ .

the same busy probability, which is equal to 0.4, when  $\lambda_s = 0$ . According to (4.13) and (4.14), we know that selecting channel 4 can result in shorter average waiting time ( $\mathbf{E}[W_{pb}]$ ) because channel 4 has the smallest value of  $\mathbf{E}[R^{(k)}]$ . Consequently, most secondary connections prefer selecting channel 4 and thus it has the highest busy probability when  $\lambda_s > 0$ .

Figure 4.8 shows the effects of false alarms on the optimal distribution probability vector. When  $P_F = 0.05$ , only three channels can be the candidate channels. However, all the four channels can be the candidate channels when  $P_F \geq 0.1$ . This phenomenon can be interpreted as follows. When  $P_F$  becomes higher,  $\mathbf{E}[\tilde{X}_s]$  increases due to more false alarms. Hence, the actual traffic loads ( $\rho_s = \lambda_s \mathbf{E}[\tilde{X}_s]$ ) of the secondary connections become heavy. Then, the secondary connections must distribute overall traffic loads to more channels in order to prevent channel contention.

#### 4.6.2 Sensing-based Spectrum Decision Scheme

Figures 4.9 and 4.10 show the effects of  $\mathbf{E}[X_s]$  and  $P_F$  on the optimal number of candidate channels  $n^*$ , respectively. Here, we consider a four-channel system with the following traffic parameters:  $(\lambda_p^{(1)}, \lambda_p^{(2)}, \lambda_p^{(3)}, \lambda_p^{(4)}) = (0.01, 0.015, 0.02, 0.025)$ ,  $\lambda_s = 0.02$  and  $\tau = 2$ . Moreover,  $\mathbf{E}[X_p^{(k)}] = 20$  for any  $k$ . From Fig. 4.9, one can see that when  $P_F = 0.1$ ,  $n^* = 1$  and 2 for  $\mathbf{E}[X_s] = 5$  and 10, respectively. In Fig. 4.10, we see that  $n^* = 1$  and 2 for  $P_F = 0.1$  and 0.5 when  $\mathbf{E}[X_s] = 5$ . It is observed that the optimal value of  $n$  monotonically increases as  $\mathbf{E}[X_s]$  or  $P_F$  increases. This is because a larger value of  $\mathbf{E}[X_s]$  or  $P_F$  can lead to a larger value of  $\mathbf{E}[\tilde{X}_s]$  according to (4.25). From (4.19) one can expect that the queueing time will become longer for a larger value of  $\mathbf{E}[\tilde{X}_s]$ . In this case, the secondary users shall sense more channels to increase the probability of finding idle channels  $\mathbf{Pr}(\mathcal{E})$ , which will reduce the waiting time.

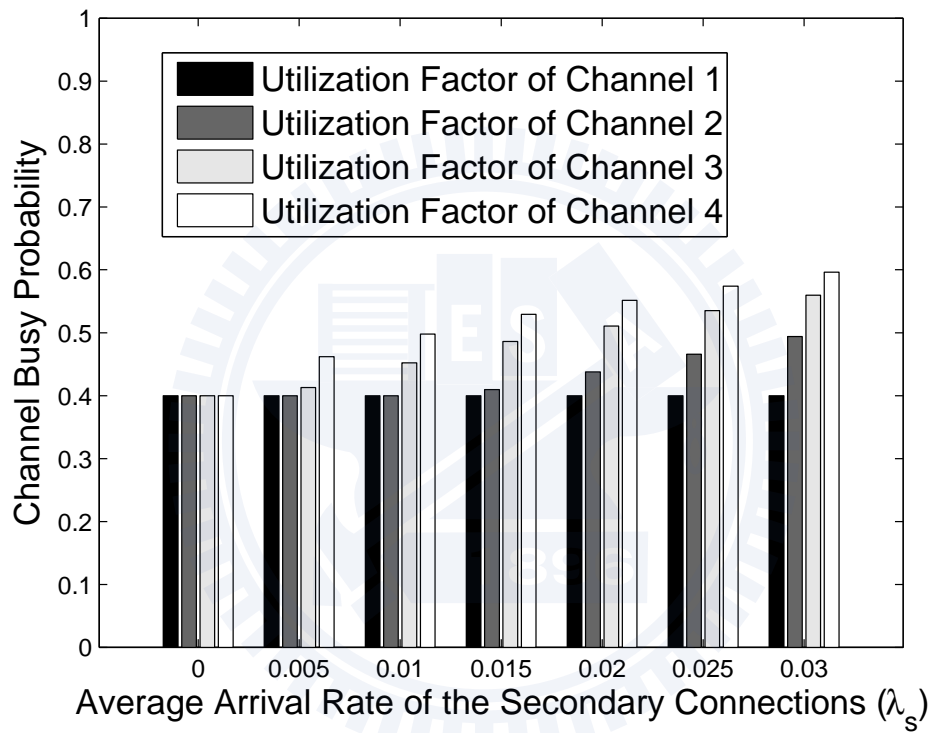


Figure 4.7: Channel busy probability for the probability-based spectrum decision with various arrival rates of the secondary connections, where  $P_F = 0$ ,  $P_M = 0$ , and  $\mathbf{E}[X_s] = 15$ .

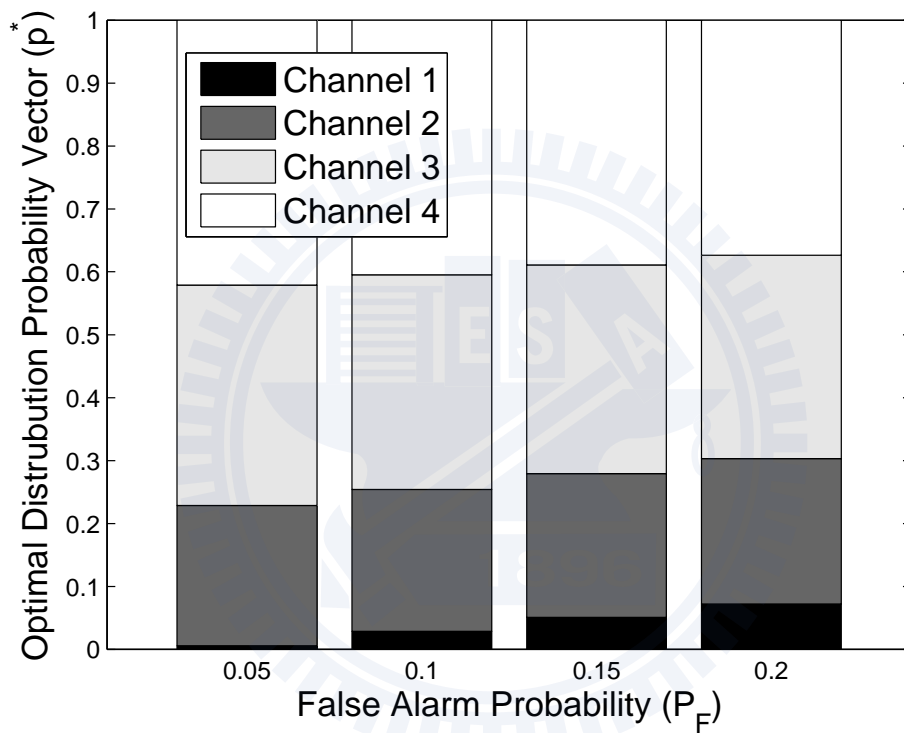


Figure 4.8: Optimal distribution probability vector for the probability-based spectrum decision with various arrival rates of the secondary connections, where  $P_M = 0.1$ ,  $\lambda_s = 0.03$ , and  $\mathbf{E}[X_s] = 15$ .



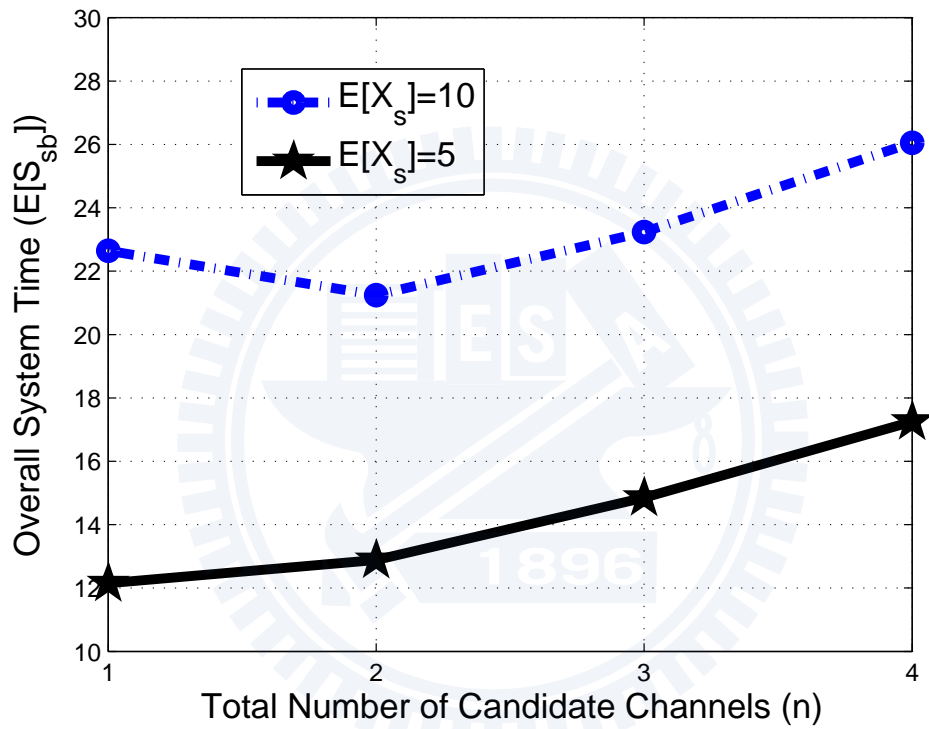


Figure 4.9: Overall system time for the sensing-based spectrum decision with various numbers of candidate channels  $n$ , where  $P_F = 0.1$ ,  $P_M = 0.1$ ,  $\tau = 2$ , and  $\mathbf{E}[X_p] = 20$ .

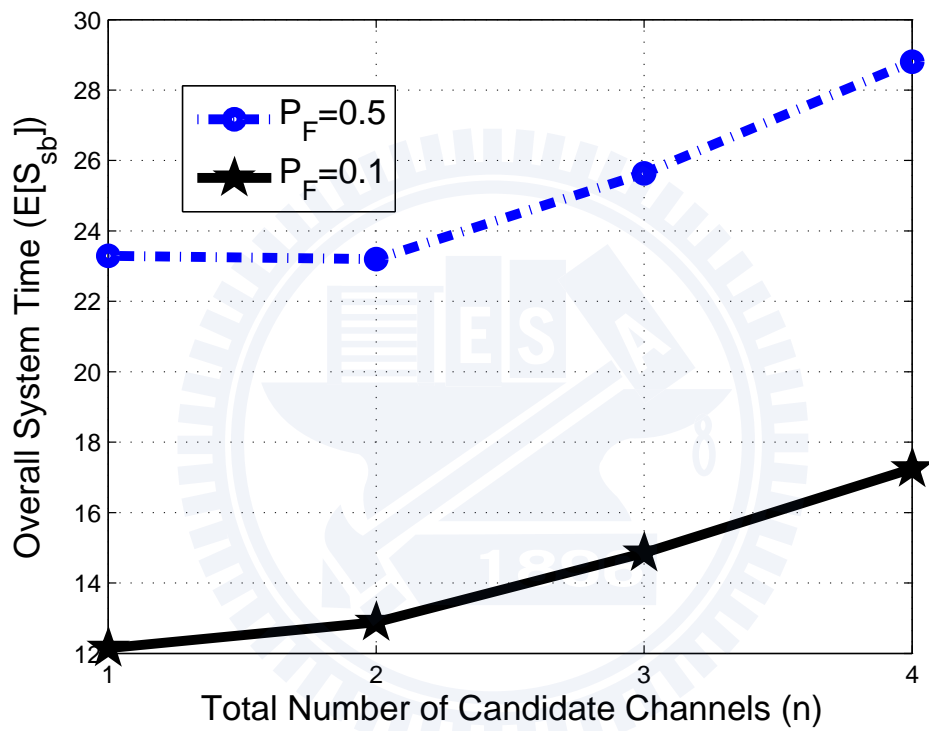


Figure 4.10: Overall system time for the sensing-based spectrum decision with various numbers of candidate channels  $n$ , where  $P_M = 0.1$ ,  $\tau = 2$ ,  $\mathbf{E}[X_p] = 20$ , and  $\mathbf{E}[X_s] = 5$ .

### 4.6.3 Comparison between Different Spectrum Decision Schemes

Figure 4.11 shows the effects of  $\lambda_s$  on the average overall system time for three different channel selection schemes: (1) sensing-based method; (2) probability-based method; and (3) non-load-balancing method. Consider a three-channel system with the following traffic parameters:  $(\lambda_p^{(1)}, \lambda_p^{(2)}, \lambda_p^{(3)}) = (0.02, 0.02, 0.03)$ ,  $(\mathbf{E}[X_p^{(1)}], \mathbf{E}[X_p^{(2)}], \mathbf{E}[X_p^{(3)}]) = (20, 25, 20)$ , and  $\mathbf{E}[X_s] = 10$ . The overall system time of the probability-based and sensing-based channel selection schemes are calculated from (4.8) and (4.9), respectively. For the non-load-balancing method, all the secondary connections will select channel 1 to be their operating channels because channel 1 has the lowest busy probability. One can find that both the load-balancing channel selection schemes can significantly reduce the average overall system time compared to the non-load-balancing scheme, especially for larger  $\lambda_s$ . When  $\tau$  is small (e.g. 5 slots), the sensing-based spectrum decision scheme can result in the shortest overall system time. As  $\tau$  increases, the improvement of the sensing-based spectrum decision over other schemes decreases. In addition, we also observe that when  $\tau = 17$  and  $\lambda_s < 0.026$ , the probability-based scheme has better overall system time performance than the sensing-based scheme. This is because the probability-based spectrum decision scheme can select the channels with lower interrupted probability. By contrast, if  $\lambda_s > 0.026$ , the sensing-based scheme can result in shorter overall system time because the sensing-based scheme can significantly reduce waiting time through wide-band sensing. Based on (4.7), each secondary user can intelligently adopt the best channel selection scheme to minimize its overall system time. The two considered load-balancing spectrum decision methods can reduce the overall system time by over 50% compared to the existing non-load-balancing

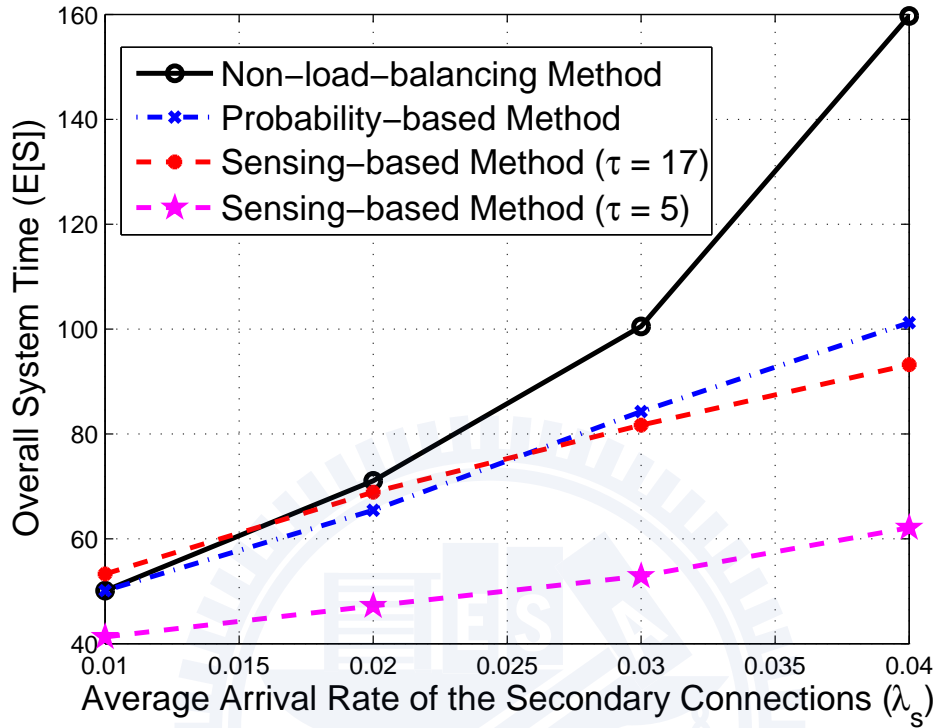


Figure 4.11: Comparison of the overall system time for three considered spectrum decision schemes, where  $P_F = 0.1$ ,  $P_M = 0.1$ , and  $\mathbf{E}[X_s] = 10$ .

method when  $\lambda_s = 0.04$ .

# Chapter 5

## Proactive Spectrum Handoff

Spectrum handoff mechanisms can be generally categorized into two kinds according to the decision timing of selecting target channels [85]. The first kind is called the proactive spectrum handoff<sup>1</sup>, which decides the target channels for future spectrum handoffs based on the long-term traffic statistics before data connection is established [72, 90, 91]. The second kind is called the reactive spectrum handoff scheme [92]. For this scheme, the target channel is searched in an on-demand manner [93, 94]. After a spectrum handoff is requested, spectrum sensing is performed to help the secondary users find idle channels to resume their unfinished data transmission. Both spectrum handoff schemes have their own advantages and disadvantages. A quantitative comparison of the two spectrum handoff schemes was provided in [95].

In this chapter, we focus on the modeling technique and performance

---

<sup>1</sup>In this dissertation, we assume that spectrum handoff request is initiated only when the primary user appears as discussed in the IEEE 802.22 wireless regional area networks (WRAN) standard. In this scheme, the proactive spectrum handoff represents the spectrum handoff scheme with the proactively designed target channel sequences. It is different from the proactive spectrum handoff in [29, 34–42] that assumes spectrum handoff can be performed before the appearance of the primary users.

analysis for the proactive spectrum handoff scheme, while leave the related studies on the reactive spectrum handoff in Chapter 6. Compared to the reactive spectrum handoff scheme, the proactive spectrum handoff is easier to achieve a consensus on their target channels between the transmitter and its intended receiver because both the transmitter and receiver can know their target channel sequence for future spectrum handoffs before data transmission. Furthermore, the change switching delay of the proactive spectrum handoff is shorter than that of the reactive spectrum handoff because scanning wide spectrum to determine the target channel is not necessary at the moment of link transition. Nevertheless, the proactive spectrum handoff scheme shall resolve the obsolescent channel issue because the predetermined target channel may not be available any more when a spectrum handoff is requested.

The contribution of this chapter is to propose a preemptive resume priority (PRP) M/G/1 queueing network model to characterize the spectrum usage behaviors of the connection-based multiple-channel spectrum handoffs. Based on the proposed model, we derive the closed-form expression for the extended data delivery time of different proactively designed target channel sequences under various traffic arrival rates and service time distributions. We apply the developed analytical method to analyze the latency performance of spectrum handoffs based on the target channel sequences specified in the IEEE 802.22 wireless regional area networks (WRAN). We also suggest a traffic-adaptive target channel selection principle for spectrum handoffs under different traffic conditions.

## 5.1 Motivation

To characterize the channel obsolescence effects and the spectrum usage behaviors with a series of interruptions in the secondary connections, we suggest a new performance metric - the extended data delivery time of the secondary connections. It is defined as the duration from the instant of starting transmitting data until the instant of finishing the whole connection, during which multiple interruptions from the primary users may occur. In the context of the connection-based spectrum handoffs, how to analyze the extended data delivery time is challenging because three key design features must be taken into account: (1) generally distributed service time, where the probability density functions (pdfs) of service time of the primary and secondary connections can be any distributions; (2) different operating channels before and after spectrum handoff; and (3) queueing delay due to channel contention from multiple secondary connections. To the best of our knowledge, an analytical model for characterizing all these three features for multiple handoffs has rarely been seen in the literature.

## 5.2 System Model

### 5.2.1 Assumptions

In this chapter, we make the following assumptions:

- A default channel is preassigned to each secondary user through spectrum decision algorithms in order to balance the overall traffic loads of the secondary users to all the channels [79]. When a secondary transmitter has data, it can transmit handshaking signal at the default channel of the intended receiver to establish a secondary connection [96].

If the corresponding receiver's default channel is busy, the secondary transmitter must wait at this channel until it becomes available [34].

- Each primary connection is assigned with a default or licensed channel.
- Each secondary user can detect the presence of the primary user. In fact, this model can be also extended to consider the effects of false alarm and missed detection as discussed in Chapter 7.
- Any time only one user can transmit data at one channel.

### 5.2.2 Illustrative Example of Proactive Multiple Handoffs with Multiple Interruptions

A secondary connection may encounter multiple interruption requests during its transmission period. Because spectrum handoff procedures must be performed whenever a primary user appears, a set of target channels will be sequentially selected, called the *target channel sequence* in this dissertation. Fig. 5.1 shows an example that three spectrum handoff requests occur during the transmission period of the secondary connection  $SC_A$ . In this example,  $SC_A$ 's initial (default) channel is Ch1 and its *target channel sequence* for spectrum handoffs is (Ch2, Ch2, Ch3,  $\dots$ ). The extended data delivery time of  $SC_A$  is denoted by  $T$ . Furthermore,  $D_i$  is the handoff delay of the  $i^{th}$  interruption. Here, the handoff delay is the duration from the instant when the transmission is interrupted until the instant when the unfinished transmission is resumed.

We assume that the transmitter of  $SC_A$  plans to establish a connection flow consisting of the 28 slot-sized frames to the corresponding receiver. Then, the transmission process with multiple handoffs is described as fol-



lows:

1. In the beginning,  $SC_A$  is established at its default channel Ch1. When an interruption event occurs,  $SC_A$  decides its target channel according to the predetermined target channel sequence.
2. At the first interruption,  $SC_A$  changes its operating channel to the idle channel Ch2 from Ch1 because the first predetermined target channel is Ch2. In this case, the handoff delay  $D_1$  is the channel switching time (denoted by  $t_s$ ).
3. At the second interruption,  $SC_A$  stays on its current operating channel Ch2 because the second target channel is Ch2.  $SC_A$  cannot be resumed until all the high-priority primary connections finish their transmissions at Ch2. In this case, the handoff delay  $D_2$  is the duration from the time instant that Ch2 is used by the primary connections until the time instant that the high-priority queue becomes empty. This duration (denoted by  $Y_p^{(2)}$ ) is called the *busy period* resulting from the transmissions of multiple primary connections at Ch2.
4. At the third interruption,  $SC_A$  changes its operating channel to Ch3 because the third target channel is Ch3. In this example, because Ch3 is busy,  $SC_A$  must wait in the low-priority queue until all the data in the present high-priority and low-priority queues of Ch3 are served<sup>2</sup>.

---

<sup>2</sup>Here, the 1-persistent waiting policy is adopted. That is, the interrupted secondary user must stay on the selected target channel even though the selected channel is busy and then transmit unfinished data when channel becomes idle. Another possible approach is to reselect a new channel at the next time slot when a busy channel is selected. However, this approach is more impractical because it will lead to many channel-switching behaviors during a secondary connection.

Hence, the handoff delay  $D_3$  is the sum of this waiting time and the channel switching time  $t_s$ .

5. Finally,  $SC_A$  is completed on Ch3.

When a secondary connection changes its operating channel from channel  $k$  to  $k'$  where  $k' \neq k$ , the expected handoff delay is the sum of the channel switching time  $t_s$  and the average waiting time of channel  $k'$  (denoted by  $\mathbf{E}[W_s^{(k')}]$ ) for the secondary connections. Note that this waiting time  $W_s^{(k')}$  is the duration from the time instant that a secondary connection enters the low-priority queue of channel  $k'$  until it gets a chance to transmit at channel  $k'$ . After the secondary connection's operating channel is changed to channel  $k'$ , one of two situations will occur. If channel  $k'$  is idle as the first interruption in Fig. 5.1, the expected handoff delay is  $t_s$  since  $\mathbf{E}[W_s^{(k')} | \text{channel } k' \text{ is idle}] = 0$ . On the other hand, the expected handoff delay is  $t_s + \mathbf{E}[W_s^{(k')} | \text{channel } k' \text{ is busy}]$  if channel  $k'$  is busy as the third interruption in Fig. 5.1.

### 5.3 Analytical Model

We use the PRP M/G/1 queueing network model proposed in Chapter 3 to characterize the channel usage behaviors of a CR network. Let  $X_s^{(\eta)}$  (slots/arrival) be the service time of the secondary connections whose default channels are channel  $\eta$  and let  $f_s^{(\eta)}(x)$  be the pdf of  $X_s^{(\eta)}$ . Figure 5.2 shows an example of the PRP M/G/1 queueing network model with three channels, in which the traffic flows of the primary connections and the secondary connections are directly connected to the high-priority queue and the low-priority queue, respectively. When a primary connection appears at the channel being occupied by the secondary connection, the interruption event occurs. The interrupted secondary connection decides its target chan-

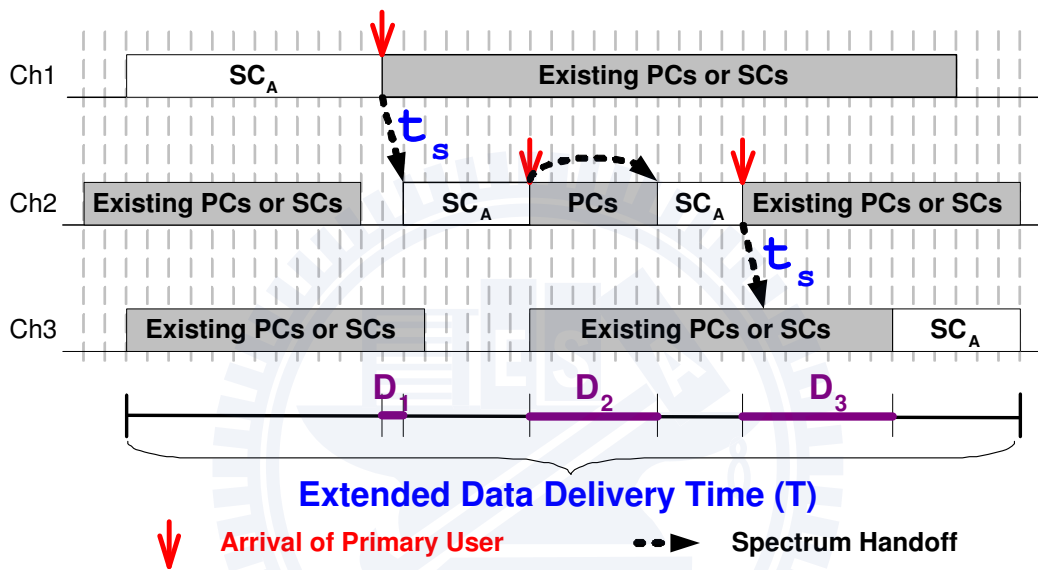


Figure 5.1: An example of transmission process for the secondary connection  $SC_A$ , where  $t_s$  is the channel switching time,  $T$  is the extended data delivery time of  $SC_A$ , and  $D_i$  is the handoff delay of the  $i^{th}$  interruption. The gray areas indicate that the channels are occupied by the existing primary connections (PCs) or secondary connections (SCs). Because  $SC_A$  is interrupted three times in total, the overall data connection is divided into four segments.

nel for spectrum handoff according to the target channel predetermination algorithm which is implemented in the channel selection point  $\boxed{S}$ . In our queueing network model, the interrupted secondary connection can either stay on its current channel or change to another channel through different feedback paths. If a secondary connection chooses to stay on its current operating channel, its remaining data will be connected to the head of the low-priority queue of its current operating channel. On the other hand, if the decision is to change its operating channel, the remaining data of the interrupted secondary connection will be connected to the tail of the low-priority queue of the selected channel after channel switching time  $t_s$ . In order to characterize the handoff delay from channel switching time  $t_s$ ,  $\boxed{S}$  must be regarded as a server with constant service time  $t_s$ . Note that  $\oplus$  in the figure represents that the traffic of the interrupted secondary connection is merged. Furthermore, when the interrupted secondary connection transmits the remaining data on the target channel, it may be interrupted again. Hence, this model can incorporate the effects of multiple interruptions in multi-channel spectrum handoffs.

## 5.4 Analysis of Extended Data Delivery Time

Based on the proposed PRP M/G/1 queueing network model, we can evaluate many performance metrics of the secondary connections with various target channel sequences. In this chapter, we focus on the analysis of the extended data delivery time, which is an important performance measure for the latency-sensitive traffic of the secondary connections.

A secondary connection may encounter many interruptions during its transmission period. Without loss of generality, we consider a secondary

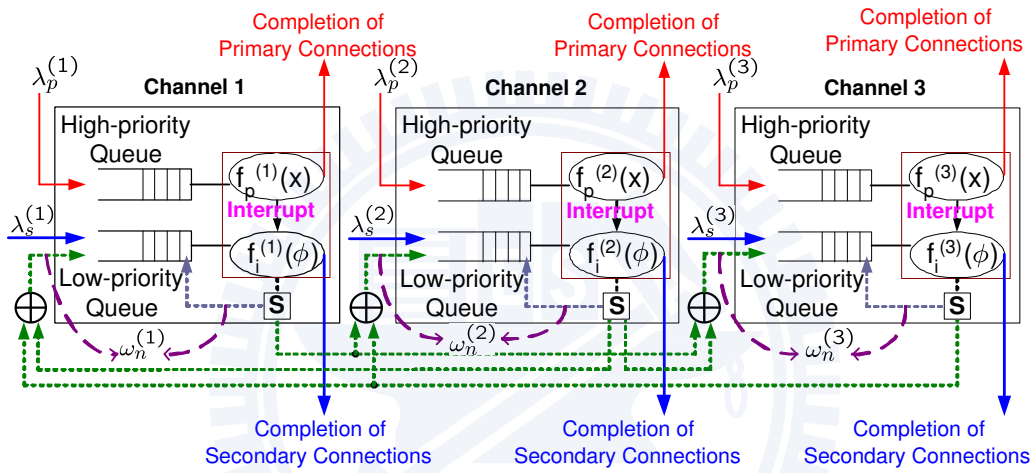


Figure 5.2: The PRP M/G/1 queueing network model with three channels where  $\lambda_p^{(k)}$ ,  $\lambda_s^{(k)}$ , and  $\omega_n^{(k)}$  are the arrival rates of the primary connections, the secondary connections, and the type- $n$  secondary connections ( $n \geq 1$ ) at channel  $k$ . Note that  $\omega_0^{(k)} = \lambda_s^{(k)}$ . Furthermore,  $f_p^{(k)}(x)$  and  $f_i^{(k)}(\phi)$  are the pdfs of  $X_p^{(k)}$  and  $\Phi_i^{(k)}$ , respectively.

connection whose default channel is channel  $\eta$  in the following discussions. Let  $N$  be the total number of interruptions of this secondary connection. Then, the average extended data delivery time of this secondary connection can be expressed as

$$\mathbf{E}[T] = \sum_{n=1}^{\infty} \mathbf{E}[T|N = n] \mathbf{Pr}(N = n) . \quad (5.1)$$

First, we show how to derive the value of  $\mathbf{E}[T|N = n]$  of (5.1). The considered secondary connection can be divided into many segments due to multiple interruptions as discussed in Fig. 5.1. Hence, the extended data delivery time of this secondary connection consists of the original service time and the cumulative delay resulting from multiple handoffs. Let  $D_i$  be the handoff delay of the considered secondary connection for the  $i^{\text{th}}$  interruption. When  $N = n$ , we have  $D_i = 0$  if  $i \geq n + 1$ . Then, the conditional expectation of the extended data delivery time of the considered secondary connection given the event  $N = n$  can be derived as

$$\mathbf{E}[T|N = n] = \mathbf{E}[X_s^{(\eta)}] + \sum_{i=1}^n \mathbf{E}[D_i] . \quad (5.2)$$

Next, we investigate how to derive the value of  $\mathbf{Pr}(N = n)$  of (5.1). For the considered secondary connection, denote  $s_{0,\eta}$  and  $s_{i,\eta}$  as its default channel and its target channel at the  $i^{\text{th}}$  interruption, respectively. Thus, we have  $s_{0,\eta} = \eta$  and this secondary connection's target channel sequence can be expressed as  $(s_{1,\eta}, s_{2,\eta}, s_{3,\eta}, \dots)$ . Let  $p_i^{(s_{i,\eta})}$  be the probability that the considered secondary connection is interrupted again at channel  $s_{i,\eta}$  when it has experienced  $i$  interruption. Then, the probability that the considered secondary connection is interrupted exactly  $n$  times can be expressed as

$$\mathbf{Pr}(N = n) = (1 - p_n^{(s_{n,\eta})}) \prod_{i=0}^{n-1} p_i^{(s_{i,\eta})} . \quad (5.3)$$

Finally, substituting (5.2) and (5.3) into (5.1) yields

$$\mathbf{E}[T] = \mathbf{E}[X_s^{(\eta)}] + \sum_{n=1}^{\infty} \left[ \left( \sum_{i=1}^n \mathbf{E}[D_i] \right) (1 - p_n^{(s_n, \eta)}) \prod_{i=0}^{n-1} p_i^{(s_i, \eta)} \right], \quad (5.4)$$

where the values of  $\mathbf{E}[D_i]$  and  $p_i^{(k)}$  can be obtained from the Propositions 1 and 2, respectively.

**Proposition 1.**

$$\mathbf{E}[D_i] = \begin{cases} \mathbf{E}[Y_p^{(s_{i, \eta})}] & , \quad s_{i-1, \eta} = s_{i, \eta} \\ \mathbf{E}[W_s^{(s_{i, \eta})}] + t_s & , \quad s_{i-1, \eta} \neq s_{i, \eta} \end{cases}, \quad (5.5)$$

where

$$\mathbf{E}[Y_p^{(k)}] = \frac{\mathbf{E}[X_p^{(k)}]}{1 - \rho_p^{(k)}} = \frac{\mathbf{E}[X_p^{(k)}]}{1 - \lambda_p^{(k)} \mathbf{E}[X_p^{(k)}]}, \quad (5.6)$$

and

$$\mathbf{E}[W_s^{(k)}] = \frac{\lambda_p^{(k)} \mathbf{E}[(X_p^{(k)})^2] + \sum_{i=0}^{\infty} \omega_i^{(k)} \mathbf{E}[(\Phi_i^{(k)})^2] + \frac{(\lambda_p^{(k)})^2 \mathbf{E}[(X_p^{(k)})^2]}{1 - \lambda_p^{(k)} \mathbf{E}[X_p^{(k)}]} \mathbf{E}[X_p^{(k)}]}{2(1 - \lambda_p^{(k)} \mathbf{E}[X_p^{(k)}] - \sum_{i=0}^{\infty} \omega_i^{(k)} \mathbf{E}[\Phi_i^{(k)}])}. \quad (5.7)$$

*Proof.* The handoff delay  $\mathbf{E}[D_i]$  depends on which channel is selected for the target channel at the  $i^{\text{th}}$  interruption. For the secondary connection with  $(i - 1)$  interruptions, its current operating channel is  $s_{i-1, \eta}$ . When it is interrupted again, its new operating channel is  $s_{i, \eta}$ . When  $s_{i-1, \eta} = s_{i, \eta}$ , it means that the considered secondary connection will stay on the current channel. When  $s_{i-1, \eta} \neq s_{i, \eta}$ , it represents that the considered secondary connection will change its operating channel to another channel. Both cases are discussed as follows.

**(1) Staying case:** When the considered secondary connection stays on its current operating channel  $s_{i, \eta} = k$ , it cannot be resumed until all the

high-priority primary connections of channel  $k$  finish their transmissions. Hence, the handoff delay is the busy period resulting from multiple primary connections of channel  $k$  (denoted by  $Y_p^{(k)}$ ) as discussed in Section 5.2.2. That is, we can have  $\mathbf{E}[D_i] = \mathbf{E}[Y_p^{(k)}]$ .

The value of  $\mathbf{E}[Y_p^{(k)}]$  can be derived as follows. Denote  $I_p$  as the idle period resulting from the primary connections. This idle period is the duration from the termination of the busy period to the arrival of the next primary connection. Because of the memoryless property, the idle period follows the exponential distribution with rate  $\lambda_p^{(k)}$ . Hence, we have

$$\mathbf{E}[I_p^{(k)}] = \frac{1}{\lambda_p^{(k)}} . \quad (5.8)$$

Next, according to the definition of the utilization factor at channel  $k$ , we have

$$\rho_p^{(k)} = \lambda_p^{(k)} \mathbf{E}[X_p^{(k)}] . \quad (5.9)$$

Because  $\rho_p^{(k)}$  is also the busy probability resulting from the primary connections of channel  $k$ , we have

$$\rho_p^{(k)} = \frac{\mathbf{E}[Y_p^{(k)}]}{\mathbf{E}[Y_p^{(k)}] + \mathbf{E}[I_p^{(k)}]} . \quad (5.10)$$

Then, substituting (5.8) and (5.9) into (5.10), we can obtain (5.6).

**(2) Changing case:** In this case, the considered secondary connection will change to channel  $s_{i,\eta} = k'$ . After switching channel from channel  $k$  to  $k'$ , it must wait in the low-priority queue of channel  $k'$  until all the traffic in the high-priority and the present low-priority queues of channel  $k'$  are served as discussed in Section 5.2.2. Denote  $W_s^{(k')}$  as this waiting time for the secondary connections at channel  $k'^3$ . Hence, we have  $\mathbf{E}[D_i] = \mathbf{E}[W_s^{(k')}] + t_s$ .

---

<sup>3</sup>A secondary connection needs to change its operating channel only when a primary connection appears. Because the arrivals of the primary connections follow Poisson dis-



The value of  $\mathbf{E}[W_s^{(k')}]$  can be derived as follows. Let  $\mathbf{E}[Q_p^{(k')}]$  be the average number of the primary connections which are waiting in the high-priority queue of channel  $k'$  and  $\mathbf{E}[Q_i^{(k')}]$  be the average number of the type- $i$  secondary connections which are waiting in the low-priority queue of channel  $k'$ . Because the newly arriving secondary connections cannot be established until all the secondary connections in the low-priority queue and the primary connections in the high-priority queue have been served, the average waiting time of channel  $k'$  is expressed as

$$\mathbf{E}[W_s^{(k')}] = \mathbf{E}[R_s^{(k')}] + \mathbf{E}[Q_p^{(k')}] \mathbf{E}[X_p^{(k')}] + \sum_{i=0}^{\infty} \mathbf{E}[Q_i^{(k')}] \mathbf{E}[\Phi_i^{(k')}] + \lambda_p^{(k')} \mathbf{E}[W_s^{(k')}] \mathbf{E}[X_p^{(k')}] , \quad (5.11)$$

where  $\mathbf{E}[R_s^{(k')}]$  is the average residual effective service time of channel  $k'$ . That is,  $\mathbf{E}[R_s^{(k')}]$  is the remaining time to complete the service of the connection being served at channel  $k'$ . This connection being served can be the primary connection or the type- $i$  secondary connection. Furthermore,  $\mathbf{E}[Q_p^{(k')}] \mathbf{E}[X_p^{(k')}]$  and  $\sum_{i=0}^{\infty} \mathbf{E}[Q_i^{(k')}] \mathbf{E}[\Phi_i^{(k')}]$  in (5.11) are the cumulative workload resulting from the primary connections and the secondary connections in the present queues of channel  $k'$ , respectively. Moreover, the fourth term ( $\lambda_p^{(k')} \mathbf{E}[W_s^{(k')}] \mathbf{E}[X_p^{(k')}]$ ) in (5.11) is the cumulative workload resulting from the arrivals of the primary connections during  $W_s^{(k')}$ .

In (5.11), the closed-form expression for  $\mathbf{E}[\Phi_i^{(k')}]$  is derived in Appendix C. Next, we will derive  $\mathbf{E}[R_s^{(k')}]$ ,  $\mathbf{E}[Q_p^{(k')}]$ , and  $\mathbf{E}[Q_i^{(k')}]$ . Firstly, according to tribution, the arrivals of the interrupted secondary connections at channel  $k'$  also follow Poisson distribution. Applying the property of Poisson arrivals see time average (PASTA) on the arrivals of the interrupted secondary connections at channel  $k'$  [97], all of them must spend time duration  $\mathbf{E}[W_s^{(k')}]$  on average to wait for an idle channel  $k'$ . This waiting time is uncorrelated to the number of interruptions.

the definition of residual time in [98], we have

$$\mathbf{E}[R_s^{(k')}] = \frac{1}{2}\lambda_p^{(k')} \mathbf{E}[(X_p^{(k')})^2] + \frac{1}{2} \sum_{i=0}^{\infty} \omega_i^{(k')} \mathbf{E}[(\Phi_i^{(k')})^2] , \quad (5.12)$$

where  $\omega_i^{(k')}$  is derived in Appendix B. Secondly, according to Little's formula, it follows that

$$\mathbf{E}[Q_p^{(k')}] = \lambda_p^{(k')} \mathbf{E}[W_p^{(k')}] , \quad (5.13)$$

where  $\mathbf{E}[W_p^{(k')}]$  is the average waiting time of the primary connections at channel  $k'$ . It is the duration from the time instant that a primary connection enters the high-priority queue of channel  $k'$  until it gets a chance to transmit at channel  $k'$ . Hence, it follows that

$$\mathbf{E}[W_p^{(k')}] = \mathbf{E}[R_p^{(k')}] + \mathbf{E}[Q_p^{(k')}] \mathbf{E}[X_p^{(k')}] , \quad (5.14)$$

where  $\mathbf{E}[R_p^{(k')}]$  is the average residual service time resulting from only the primary connections of channel  $k'$  and  $\mathbf{E}[Q_p^{(k')}] \mathbf{E}[X_p^{(k')}]$  is the total workload of the primary connections in the present high-priority queue of channel  $k'$ . According to [98], we have  $\mathbf{E}[R_p^{(k')}] = \frac{1}{2}\lambda_p^{(k')} \mathbf{E}[(X_p^{(k')})^2]$ . Then, solving (5.13) and (5.14) simultaneously yields

$$\mathbf{E}[W_p^{(k')}] = \frac{\mathbf{E}[R_p^{(k')}]}{1 - \rho_p^{(k')}} = \frac{\lambda_p^{(k')} \mathbf{E}[(X_p^{(k')})^2]}{2(1 - \lambda_p^{(k')} \mathbf{E}[X_p^{(k')}]})} , \quad (5.15)$$

and

$$\mathbf{E}[Q_p^{(k')}] = \frac{\lambda_p^{(k')} \mathbf{E}[R_p^{(k')}]}{1 - \rho_p^{(k')}} = \frac{(\lambda_p^{(k')})^2 \mathbf{E}[(X_p^{(k')})^2]}{2(1 - \lambda_p^{(k')} \mathbf{E}[X_p^{(k')}]})} . \quad (5.16)$$

Next, according to Little's formula, we can obtain

$$\mathbf{E}[Q_i^{(k')}] = \omega_i^{(k')} \mathbf{E}[W_s^{(k')}] . \quad (5.17)$$

Finally, substituting (5.12), (5.16), and (5.17) into (5.11), we can obtain (5.7). □

**Proposition 2.**

$$p_i^{(k)} = \begin{cases} \lambda_p^{(k)} \mathbf{E}[\Phi_i^{(k)}] & , \quad k = s_{i,\eta} \\ 0 & , \quad k \neq s_{i,\eta} \end{cases} . \quad (5.18)$$

*Proof.* The value of  $p_i^{(k)}$  can be evaluated as follows. Because the considered secondary connection will operate at channel  $s_{i,\eta}$  after  $i^{th}$  interruption, we have  $p_i^{(k)} = 0$  when  $k \neq s_{i,\eta}$ . Furthermore, for the case that  $k = s_{i,\eta}$ , we consider the time interval  $[0, t]$  at channel  $k$ . Total  $\lambda_p^{(k)} t$  primary connections and  $\omega_i^{(k)} t$  type- $i$  secondary connections arrive at channel  $k$  during this interval. Hence, there are total  $\omega_i^{(k)} t p_i^{(k)}$  type- $i$  secondary connections will be interrupted on average during this interval. Furthermore, applying the property of Poisson arrivals see time average (PASTA) on the arrivals of the primary connections [97], we can obtain the probability of a primary connection finding channel  $k$  being occupied by the type- $i$  secondary connections is  $\rho_i^{(k)}$ . Thus, during this interval, the total  $\lambda_p^{(k)} t \rho_i^{(k)}$  primary connections can see a busy channel being occupied by the type- $i$  secondary connections. For each primary connection, it can interrupt only one secondary connection when it arrives at a busy channel being occupied by the secondary connection because only one secondary user can transmit at any instant of time. Thus, the total number of the interrupted secondary connections at channel  $k$  is also  $\lambda_p^{(k)} t \rho_i^{(k)}$ . Hence, we have  $\omega_i^{(k)} t p_i^{(k)} = \lambda_p^{(k)} t \rho_i^{(k)}$ . That is,

$$\rho_i^{(k)} = \frac{\omega_i^{(k)}}{\lambda_p^{(k)}} p_i^{(k)} . \quad (5.19)$$

Next, we consider a type- $i$  secondary connection at channel  $k$ . Before the  $(i+1)^{th}$  interruption event occurs, its effective service time is  $\mathbf{E}[\Phi_i^{(k)}]$ . Thus, from queueing theory, we can have

$$\rho_i^{(k)} = \omega_i^{(k)} \mathbf{E}[\Phi_i^{(k)}] . \quad (5.20)$$

Comparing (5.19) and (5.20), we can obtain (5.18).  $\square$

## 5.5 Applications to Performance Analysis in IEEE 802.22

To demonstrate the usefulness of the developed analytical method, we apply these analytical results in Section 5.4 on two typical target channel sequences used in the IEEE 802.22 WRAN standard<sup>4</sup>. Specifically, we consider the *always-staying* and *always-changing* spectrum handoff sequences, which are respectively introduced in the non-hopping mode and the phase-shifting hopping mode of the IEEE 802.22 standard [70]. From the analytical results, an adaptive target channel selection approach can be provided.

### 5.5.1 Derivation of Extended Data Delivery Time

For the *always-staying* sequence, a secondary connection always stays on its default channel  $\eta$  when it is interrupted. That is, its target channel sequence can be expressed as  $(\text{Ch}\eta, \text{Ch}\eta, \text{Ch}\eta, \dots)$  and thus  $s_{i,\eta} = \eta$  for each  $i$ . Hence, we can have  $\mathbf{E}[D_i] = \mathbf{E}[Y_p^{(\eta)}]$  for each  $i$  in (5.4). Then, the average extended data delivery time of the secondary connections for the *always-staying* sequence can be expressed as follows:

$$\mathbf{E}[T_{\text{stay}}] = \mathbf{E}[X_s^{(\eta)}] + \sum_{n=1}^{\infty} \left( \sum_{i=1}^n \mathbf{E}[Y_p^{(\eta)}] \right) (1 - p_i^{(\eta)}) \prod_{i=0}^{n-1} p_i^{(\eta)}. \quad (5.21)$$

Next, we consider the *always-changing* sequence. In this case, the secondary connection sequentially changes its operating channel to the next

---

<sup>4</sup>In fact, the analytical results can help the secondary users find the best target channel sequence to minimize its extended data delivery time by comparing the extended data delivery time resulting from all possible target channel sequences.

neighboring channel. Without loss of generality, its corresponding target channel sequence can be expressed as  $(\text{Ch}\eta + 1, \text{Ch}\eta + 2, \dots, \text{Ch}M, \text{Ch}1, \text{Ch}2, \dots, \text{Ch}\eta, \text{Ch}\eta + 1, \dots)$ , where channel  $\eta$  is the default channel of the secondary connection. That is, at the  $i^{\text{th}}$  interruption, the target channel of the interrupted secondary connection is channel  $s_{i,\eta} \equiv \mathcal{MOD}(i+\eta, M)$  where  $\mathcal{MOD}(a, b)$  is the Modulus function and it returns the remainder resulting when  $a$  is divided by  $b$ . Hence, we have  $\mathbf{E}[D_i] = \mathbf{E}[W_s^{(s_{i,\eta})}] + t_s$  for each  $i$  in (5.4). Thus, the average extended data delivery time of the secondary connections for the always-changing sequence can be expressed as follows:

$$\mathbf{E}[T_{change}] = \mathbf{E}[X_s^{(\eta)}] + \sum_{n=1}^{\infty} \left[ \left( \sum_{i=1}^n (\mathbf{E}[W_s^{(s_{i,\eta})}] + t_s) \right) (1 - p_i^{(s_{n,\eta})}) \prod_{i=0}^{n-1} p_i^{(s_{i,\eta})} \right]. \quad (5.22)$$

Based on the analytical results, the secondary connection can adaptively adopt the better target channel sequence to reduce its extended data delivery time. Thus, the average extended data delivery time with this adaptive channel selection principle (denoted by  $\mathbf{E}[T^*]$ ) can be expressed as follows:

$$\mathbf{E}[T^*] = \min(\mathbf{E}[T_{stay}], \mathbf{E}[T_{change}]) . \quad (5.23)$$

### 5.5.2 An Example for Homogeneous Traffic Loads

Now, we give an example to explain how to apply our analytical results to find the better target channel sequence when traffic parameters are given. We consider a special case that the primary and the secondary connections have the same traffic parameters in a three-channel system (i.e.,  $\lambda_p^{(1)} = \lambda_p^{(2)} = \lambda_p^{(3)} \equiv \lambda_p$ ,  $\lambda_s^{(1)} = \lambda_s^{(2)} \equiv \lambda_s$ , and  $\mathbf{E}[X_p^{(1)}] = \mathbf{E}[X_p^{(2)}] = \mathbf{E}[X_p^{(3)}] \equiv \mathbf{E}[X_p]$ ). Because the three channels are identical, three channels have the same performance metrics. Thus, the superscript ( $k$ ) can be dropped to ease the notations. Furthermore, we assume that the service time of the secondary connections

follows the same exponential distribution, i.e.,  $f_s^{(1)}(x) = f_s^{(2)}(x) = f_s^{(3)}(x) \equiv f_s(x) = \mu_s e^{-\mu_s x}$ . Hence, we have  $\mathbf{E}[X_s^{(1)}] = \mathbf{E}[X_s^{(2)}] = \mathbf{E}[X_s^{(3)}] \equiv \mathbf{E}[X_s] = \frac{1}{\mu_s}$ .

### Derivation of $p_i^{(\eta)}$ and $\mathbf{E}[Y_p^{(\eta)}]$ in (5.21)

First, according to Appendix C, we can derive  $\mathbf{E}[\Phi_i^{(\eta)}]$  as follows:

$$\mathbf{E}[\Phi_i^{(\eta)}] = \mathbf{E}[\Phi_i] = \frac{1}{\lambda_p + \mu_s} . \quad (5.24)$$

Then, the value of  $p_i^{(\eta)}$  can be derived from (5.18) as follows:

$$p_i^{(\eta)} = \lambda_p^{(\eta)} \mathbf{E}[\Phi_i^{(\eta)}] = \frac{\lambda_p}{\lambda_p + \mu_s} \equiv p_i . \quad (5.25)$$

Next, referring to (5.6), it follows that

$$\mathbf{E}[Y_p^{(\eta)}] = \mathbf{E}[Y_p] = \frac{\mathbf{E}[X_p]}{1 - \lambda_p \mathbf{E}[X_p]} . \quad (5.26)$$

Finally, substituting (5.25) and (5.26) into (5.21), we can obtain the closed-form expression for the extended data delivery time with the always-staying target channel sequence.

### Derivation of $\mathbf{E}[W_s^{(s_i, \eta)}]$ and $p_i^{(s_i, \eta)}$ in (5.22)

Referring to Appendixes B and C, we can have

$$\omega_i^{(s_i, \eta)} = \omega_i = \lambda_s \left( \frac{\lambda_p}{\lambda_p + \mu_s} \right)^i , \quad (5.27)$$

and

$$\mathbf{E}[(\Phi_i^{(s_i, \eta)})^2] = \mathbf{E}[(\Phi_i)^2] = \frac{2}{(\lambda_p + \mu_s)^2} . \quad (5.28)$$

Next, substituting (5.24), (5.27), and (5.28) into (5.7), we can have

$$\mathbf{E}[W_s^{(s_i, \eta)}] = \mathbf{E}[W_s] = \frac{\lambda_p \mathbf{E}[(X_p)^2] + \frac{2\lambda_s \mathbf{E}[X_s]}{(\lambda_p + \mu_s)} + \frac{(\lambda_p)^2 \mathbf{E}[(X_p)^2]}{1 - \lambda_p \mathbf{E}[X_p]} \mathbf{E}[X_p]}{2(1 - \lambda_p \mathbf{E}[X_p] - \lambda_s \mathbf{E}[X_s])} . \quad (5.29)$$

Then, referring to (5.18), it follows that

$$p_i^{(s_i, \eta)} = p_i = \frac{\lambda_p}{\lambda_p + \mu_s} . \quad (5.30)$$

Finally, substituting (5.29) and (5.30) into (5.22), we can obtain the closed-form expression for the extended data delivery time with the always-changing target channel sequence. Note that this closed-form expression for  $p_i$  in this special case had been discussed in [71]. However, [71] cannot extend to the case with the generally distributed service time.

In summary, the average extended data delivery time with our adaptive target channel selection approach can be expressed as follows:

$$\mathbf{E}[T^*] = \begin{cases} \mathbf{E}[T_{stay}] & , \quad \mathbf{E}[Y_p] \leq \mathbf{E}[W_s] + t_s \\ \mathbf{E}[T_{change}] & , \quad \mathbf{E}[Y_p] \geq \mathbf{E}[W_s] + t_s \end{cases} . \quad (5.31)$$

Note that the always-staying and the always-changing sequences have the same extended data delivery time when  $\mathbf{E}[Y_p] = \mathbf{E}[W_s] + t_s$ .

## 5.6 Numerical Results

We show numerical results to reveal the importance of the three key design features for modeling spectrum handoffs as discussed in Section 5.1, which consist of (1) generally distributed service time; (2) various operating channels; and (3) queueing behaviors of multiple secondary connections.

### 5.6.1 Simulation Setup

In order to validate the proposed analytical model, we perform simulations in non-slot-based (continuous-time) cognitive radio systems, where the inter-arrival time and service time can be the duration of non-integer time slots. We consider a three-channel CR system with Poisson arrival processes of rates

$\lambda_p$  and  $\lambda_s$  for the high-priority primary connections and the low-priority secondary connections, respectively. The high-priority connections can interrupt the transmissions of the low-priority connections, and the connections with the same priority follow the first-come-first-served (FCFS) scheduling discipline<sup>5</sup>. Referring to the IEEE 802.22 standard, we adopt time slot duration of 10 msec in our simulations [89].

### 5.6.2 Effects of Various Service Time Distributions for Primary Connections

Firstly, we investigate the effects of various service time distributions for primary connections on the extended data delivery time of the secondary connections. The truncated Pareto distribution and the exponential distribution are considered in our simulations. Referring to [86], these two distributions match the actual data and voice traffic measurements very well, respectively. The truncated Pareto distribution is expressed as follows:

$$f_X(x) = \begin{cases} \alpha \frac{K^\alpha}{x^{\alpha+1}} & , \quad K \leq x \leq m \\ \frac{K^\alpha}{m^\alpha} & , \quad x = m \end{cases} . \quad (5.32)$$

According to [99], the traffic shaping parameter  $\alpha = 1.1$  and the scale parameter  $K = 81.5$ , and the truncated upper bound  $m = 66666$  bytes in (5.32). Then, the average connection length is 480 bytes for the primary connections. If the exponentially distributed primary connections are considered, the average connection length is also 480 bytes. Moreover, we assume that  $\mathbf{E}[X_s^{(1)}] = \mathbf{E}[X_s^{(2)}] = \mathbf{E}[X_s^{(3)}] \equiv \mathbf{E}[X_s] = 10$  (slots/arrival), and

---

<sup>5</sup>In fact, the analytical results of mean values obtained in this dissertation can be applied to other scheduling discipline which is independent of the service time of the primary and secondary connections because the averages of system performance metrics will be invariant to the order of service in this case (see page 113 in [78]).



$\mathbf{E}[X_p^{(1)}] = \mathbf{E}[X_p^{(2)}] = \mathbf{E}[X_p^{(3)}] \equiv \mathbf{E}[X_p]$ . When the data rate of the primary connections is 19.2 Kbps, we have  $\mathbf{E}[X_p] = \frac{480 \times 8 \text{ bits}}{19.2 \text{ Kbps}} \div \frac{10 \text{ msec}}{\text{slot}} = 20$  (slots/arrival) for the Pareto and the exponential distributions. Furthermore, we consider that  $\lambda_s = 0.01$  (arrivals/slot). Recall that  $\rho_p$  is the channel busy probability resulting from the transmissions of the primary connections. We only consider the case that  $0 \leq \rho_p < 1 - \lambda_s \mathbf{E}[X_s] = 0.9$  in the following numerical results. When  $\rho_p + \lambda_s \mathbf{E}[X_s] \geq 1$  (or equivalently  $\lambda_p \geq \frac{\lambda_s \mathbf{E}[X_s]}{\mathbf{E}[X_p]} = 0.045$  (arrivals/slot)), the secondary connections will encounter the infinite extended data delivery time on average.

Figure 5.3 compares the effects of Pareto and exponential service time distributions for primary connections when the always-changing spectrum handoff sequence is adopted. First, we find that the simulation results match the analytical results quite well, which can validate the slot-based assumption used in our analysis. Next, compared to the exponentially distributed service time for primary connections, the Pareto distributed service time results in longer average extended data delivery time in the secondary connections. This phenomenon can be interpreted as follows. Because of the heavy tail property of Pareto distribution, the second moment  $\mathbf{E}[(X_p)^2]$  of service time with Pareto distribution is larger than that with exponential distribution. According to (5.29) and (5.22), an interrupted secondary connection will encounter longer waiting time and extended data delivery time when the primary connections' service time distribution is Pareto. For example, when  $\rho_p = 0.44$  or equivalently  $\lambda_p = \frac{\rho_p}{\mathbf{E}[X_p]} = 0.022$  (arrivals/slot), the average extended data delivery time with the Pareto-typed primary connection service time is four times longer than that with the exponential-typed primary connection service time. Because the developed analytical framework can characterize the effects of generally distributed service time, it is

quite useful.

When the always-staying spectrum handoff sequence is adopted, Fig. 5.4 shows the average extended data delivery time of the secondary connections. According to (5.21), the extended data delivery time in this case is related to the average busy period  $E[Y_p]$  for the primary connections. Because the considered Pareto and exponential distributions have the same average service time, these two distributions result in the same average busy period  $E[Y_p]$  for the primary connections according to (5.26), resulting in the same average extended data delivery time as well.

### 5.6.3 Traffic-adaptive Target Channel Selection Principle

Figure 5.5 compares the extended data delivery time of the always-staying and the always-changing spectrum handoff sequences when the service time of the primary connections is exponentially distributed. Based on (5.31), the traffic-adaptive channel selection approach can appropriately change to better target channel sequence according to traffic conditions. We can see that both the always-staying and the always-changing sequences result in the same extended data delivery time when  $\rho_p = 0.44$  or equivalently  $\lambda_p = \frac{\rho_p}{E[X_p]} = 0.022$  (arrivals/slot). When  $\rho_p > 0.44$ , the interrupted user prefers the always-staying sequence. This phenomenon can be interpreted as follows. A larger value of  $\rho_p$  (or equivalently a larger value of  $\lambda_p$ ) will increase the probability that an interrupted secondary user experiences long waiting time when it changes its operating channel. As a result, the average handoff delay for changing operating channel (i.e.,  $E[W_s] + t_s$ ) will be extended. Then, the average extended data delivery time will be also prolonged. In our case, the secondary user prefers staying on the current

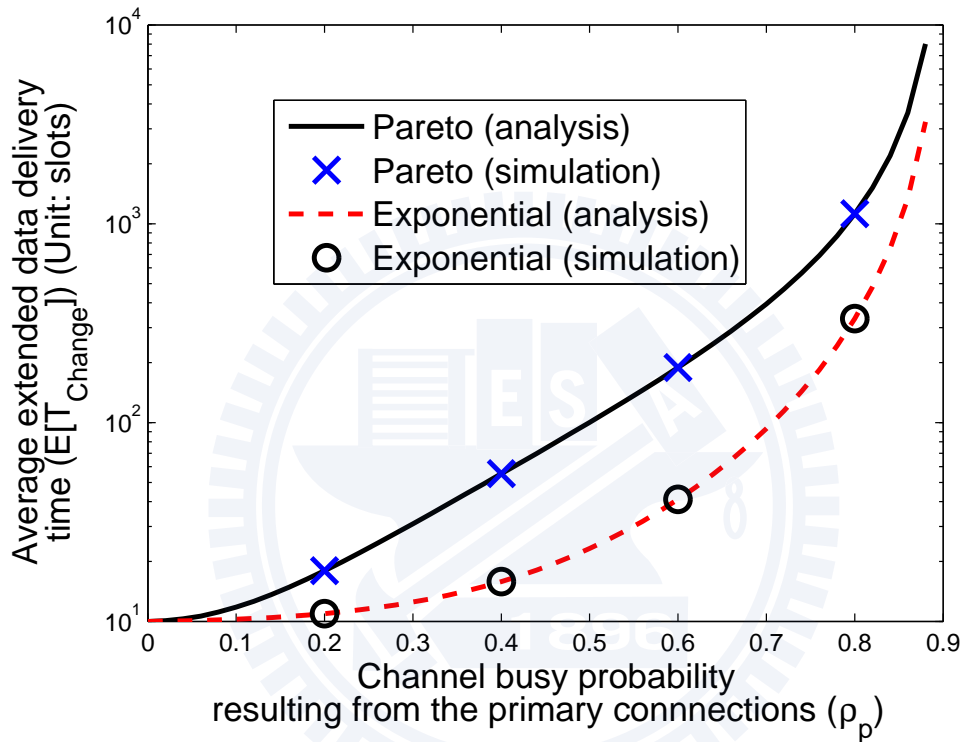


Figure 5.3: Effects of Pareto and exponential service time distributions for primary connections on the extended data delivery time ( $\mathbf{E}[T_{change}]$ ) of the secondary connections when the **always-changing** spectrum handoff sequence is adopted, where  $t_s = 1$  (slot),  $\lambda_s = 0.01$  (arrivals/slot),  $\mathbf{E}[X_s] = 10$  (slots/arrival), and  $\mathbf{E}[X_p] = 20$  (slots/arrival).

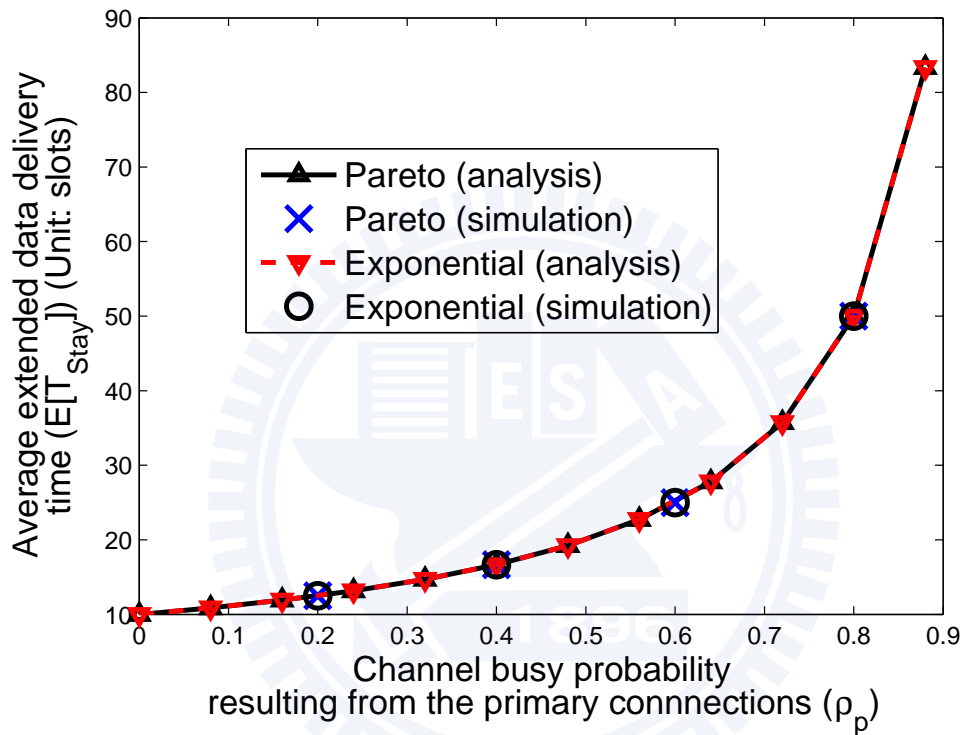


Figure 5.4: Effects of Pareto and exponential service time distributions for primary connections on the extended data delivery time ( $\mathbf{E}[T_{stay}]$ ) of the secondary connections when the **always-staying** spectrum handoff sequence is adopted, where  $t_s = 1$  (slot),  $\lambda_s = 0.01$  (arrivals/slot),  $\mathbf{E}[X_s] = 10$  (slots/arrival), and  $\mathbf{E}[X_p] = 20$  (slots/arrival).

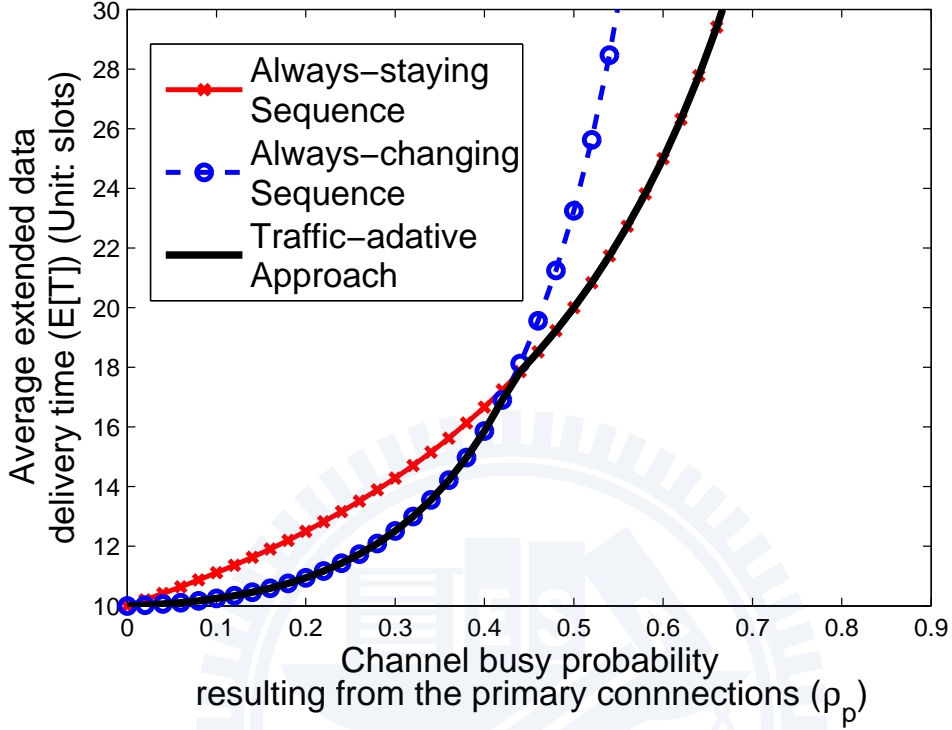


Figure 5.5: Comparison of the extended data delivery time for the always-staying and always-changing spectrum handoff sequences as well as the traffic-adaptive channel selection approach, where  $t_s = 1$  (slot),  $\lambda_s = 0.01$  (arrivals/slot),  $\mathbf{E}[X_p] = 20$  (slots/arrival), and  $\mathbf{E}[X_s] = 10$  (slots/arrival).

operating channel when  $\rho_p > 0.44$ . By contrast, when  $\rho_p < 0.44$ , the traffic-adaptive channel selection approach can improve latency performance by changing to the always-changing sequence. For example, when  $\rho_p = 0.2$ , the traffic-adaptive approach can improve the extended data delivery time by 15% compared to the always-staying sequence. Compared to the single-channel spectrum handoff model [16–18, 26, 45–49], the developed analytical framework for multi-channel spectrum handoff is more general because it can incorporate the effects of changing operating channels.

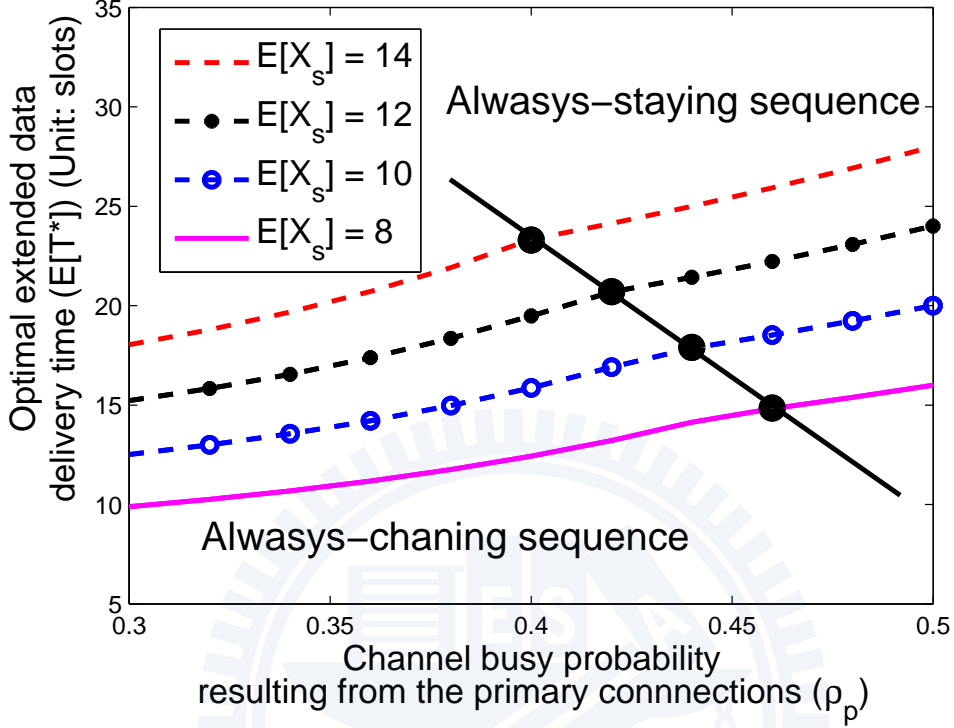


Figure 5.6: Effects of secondary connections' service time  $\mathbf{E}[X_s]$  on the cross-point for the traffic-adaptive channel selection approach, where  $t_s = 1$  (slot),  $\mathbf{E}[X_p] = 20$  (slots/arrival), and  $\lambda_s = 0.01$  (arrivals/slot).

Figure 5.6 shows the effect of secondary connections' service time  $\mathbf{E}[X_s]$  on the cross-point for traffic-adaptive channel selection approach. According to (5.31), for a larger value of  $\mathbf{E}[X_s]$ , the interrupted secondary connection prefers staying on the current channel because the average handoff delay for changing its operating channel is longer than that for staying on the current channel. Thus, the cross-point of "always-staying" and "always-changing" sequences moves toward left-hand side as  $\mathbf{E}[X_s]$  increases as seen in the figure.

The analytical results developed in this chapter can be used to design the admission control rule for the arriving secondary users subject to their latency

requirement. Fig. 5.7 shows the admissible region for the normalized traffic workloads (or channel utilities)  $(\rho_p, \rho_s)$ <sup>6</sup> for the Voice over IP (VoIP) services. The maximum allowable average cumulative delay resulting from multiple handoffs is 20 ms for the VoIP traffic [100]. Assume  $\mathbf{E}[X_p] = 20$  (slots/arrival) and  $\mathbf{E}[X_s] = 10$  (slots/arrival). The admission control policy can be designed according to this figure. When  $\rho_p < 0.166$ , a CR network can accept all arrival requests from the secondary users until the CR network is saturated, i.e.,  $\rho_p + \rho_s \simeq 1$ . Furthermore, when  $0.166 < \rho_p < 0.312$ , a part of traffic workloads of the secondary users must be rejected in order to satisfy the delay constraint for the secondary users. In this case,  $0.31 < \rho_p + \rho_s < 0.645$ . For example, when  $\rho_p = 0.25$ , a CR network can support at most 0.214 workload for the secondary users. That is, a CR network can accept at most  $\lambda_s = 0.0214$  (arrivals/slot) based on the results shown in the figure when  $\lambda_p = 0.0125$  (arrivals/slot). In order to design the most allowable  $\lambda_s$  to achieve this arrival rate upper bound for the secondary connections, many arrival-rate control methods can be considered, such as the p-persistent carrier sense multiple access (CSMA) protocol in [19] and the call admission control mechanisms in [44, 57, 101]. Finally, when  $\rho_p > 0.312$ , no secondary user can be accepted.

#### 5.6.4 Performance Comparison between Different Channel Selection Methods

Now we compare the extended data delivery time of the following three schemes: (1) the slot-based target channel selection scheme; (2) the random-based target channel selection scheme; and (3) the traffic-adaptive target channel selection scheme. We consider a three-channel network with various

<sup>6</sup> $\rho_p = \lambda_p \mathbf{E}[X_p]$  and  $\rho_s = \lambda_s \mathbf{E}[X_s]$ .

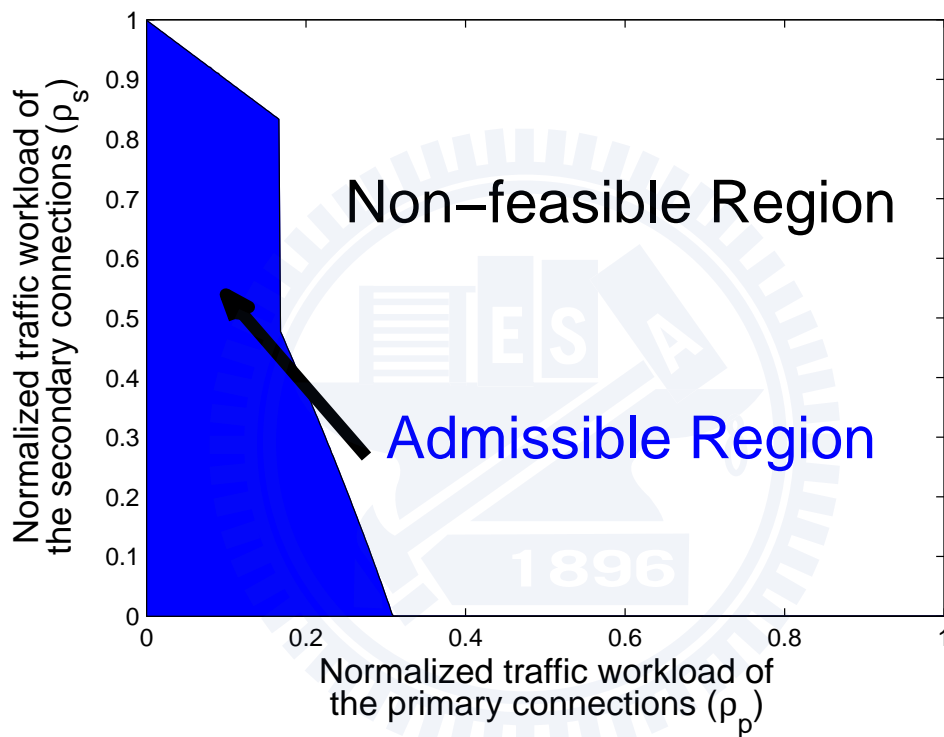


Figure 5.7: Admissible region for the normalized traffic workloads  $(\rho_p, \rho_s)$ , where the average cumulative delay constraint can be satisfied when  $t_s = 0$  (slot),  $\mathbf{E}[X_p] = 20$  (slots/arrival) and  $\mathbf{E}[X_s] = 10$  (slots/arrival).



traffic loads, where  $\lambda_p^{(1)} = \lambda_p^{(2)} = \lambda_p^{(3)} \equiv \lambda_p$ ,  $\lambda_s^{(1)} = \lambda_s^{(2)} = \lambda_s^{(3)} \equiv 0.01$  (arrivals/slot),  $(\mathbf{E}[X_p^{(1)}], \mathbf{E}[X_p^{(2)}], \mathbf{E}[X_p^{(3)}]) = (5, 15, 25)$  (slots/arrival), and  $(\mathbf{E}[X_s^{(1)}], \mathbf{E}[X_s^{(2)}], \mathbf{E}[X_s^{(3)}]) = (15, 15, 15)$  (slots/arrival). For the slot-based scheme, the secondary connections prefer selecting the channel which has the lowest busy probability resulting from the primary connections in each time slot. That is, when handoff procedures are initiated in the beginning of each time slot, all the secondary connections will select channel 1 to be their target channels. Furthermore, the random-based scheme selects one channel out of all the three channels for the target channel. Hence, each channel is selected with probability 1/3. Moreover, based on the considered traffic parameters, the traffic-adaptive scheme will adopt the always-changing sequence and the always-staying sequence when  $\lambda_p \leq 0.018$  (arrivals/slot) and  $\lambda_p \geq 0.018$  (arrivals/slot), respectively. The three target channel selection schemes result in various target channel sequences. Based on the proposed analytical model, we can evaluate the average extended data delivery time resulting from these target channel sequences.

Figure 5.8 compares the extended data delivery time of the three target channel selection methods. We have the following three important observations. First, we consider  $\lambda_p < 0.018$  (arrivals/slot). Because the probability of changing operating channel is higher than that of staying on the current operating channel for the interrupted secondary user in the random-based scheme, we can find that the average extended data delivery time for the random-based target channel selection scheme is similar to that for the traffic-adaptive target channel selection scheme, which adopts the always-changing sequence. Secondly, when  $\lambda_p > 0.018$  (arrivals/slot), the traffic-adaptive scheme can shorten the average extended data delivery time because it adopts the always-staying sequence. For a larger value of  $\lambda_p$ , the

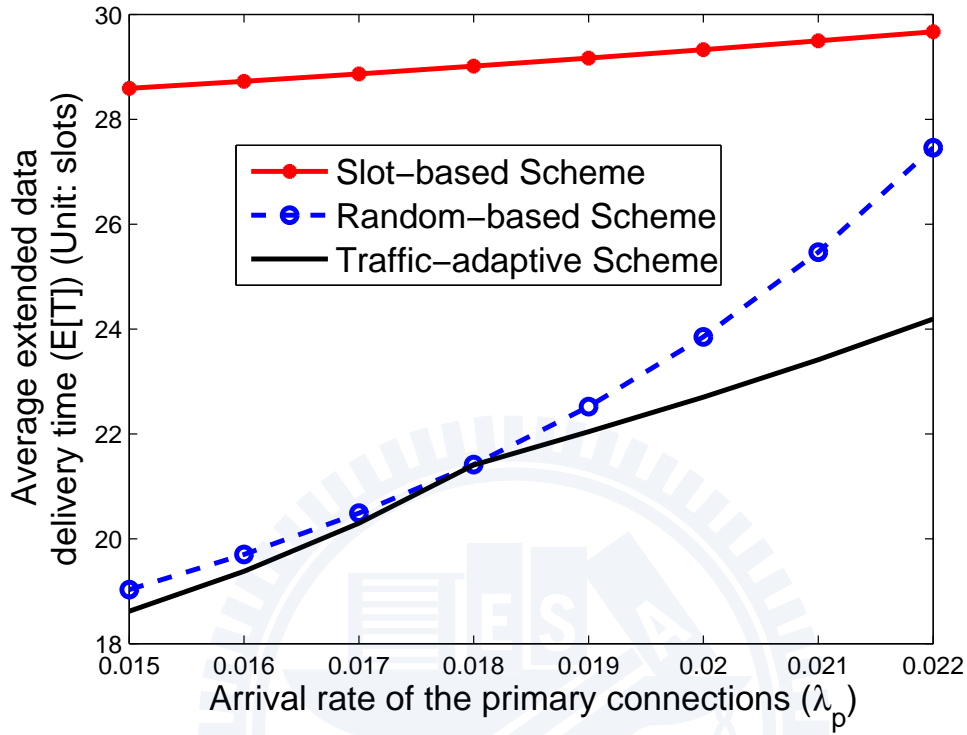


Figure 5.8: Comparison of average extended data delivery time for different target channel selection sequences.

traffic-adaptive scheme can improve the extended data delivery time more significantly. Thirdly, it is shown that the random-based and traffic-adaptive schemes can result in shorter extended data delivery time compared to the slot-based scheme. For example, when  $\lambda_p = 0.018$ , the random-based and traffic-adaptive schemes can improve the extended data delivery time by 35% compared to the slot-based scheme. This is because the slot-based scheme ignores the queuing behaviors of the secondary connections.

## Chapter 6

# Optimal Proactive Spectrum Handoff

Extended to the discussions of the proactive spectrum handoff in Chapter 5, we further investigate how to predetermine the optimal target channel sequence for future handoffs. We incorporate two important features in the design of spectrum handoff to ensure the quality of service (QoS) for the secondary users. First, due to multiple interruptions from the primary users in each secondary user's connection, a series of spectrum handoffs are considered in our model. Secondly, we consider the impacts of the traffic statistics of both the primary and secondary users on the handoff delay.

In this chapter, we formulate an optimization problem of finding a target channel sequence for multiple handoffs with the objective of minimizing the cumulative delay per connection for a newly arriving secondary user. We will simultaneously consider two design features in spectrum handoffs: (1) multiple spectrum handoffs and (2) various service time of the primary and secondary users. The contributions of this chapter can be summarized in the following:

- We propose a dynamic-programming-based algorithm with time complexity of  $O(LM^2)$  to find an optimal target channel sequence with minimum cumulative spectrum handoff delay, where  $L$  and  $M$  are the length of the target channel sequence and the total number of candidate channels for spectrum handoffs, respectively.
- Furthermore, a low-complexity greedy algorithm is proposed to find the suboptimal solution with time complexity of  $O(M)$ . We prove that only six permutations of the target channel sequences are required to be compared, and demonstrate that it can approach the optimal solution.

## 6.1 Problem Formulation

The extended data delivery time is an important QoS performance metric for secondary users from a connection viewpoint. The extended data delivery time per connection consists of the service time of one connection and the cumulative handoff delay resulting from multiple handoffs. Because the cumulative handoff delay depends on which channels are selected when the primary users' interruptions occur, one of important issue for the secondary users is to search the best *target channel sequence*.

We consider a CR network  $\mathcal{G}$  with  $M$  independent channels, where the target channel sequence for future spectrum handoffs is determined proactively for each newly arriving secondary user. For a secondary user with default channel  $s_0 \triangleq \eta$ , we denote its target channel sequence as  $\mathbf{s}(\eta) \triangleq (s_1, s_2, s_3, \dots)$  where  $s_{i,\eta}$  is the target channel for spectrum handoff at the  $i^{\text{th}}$  interruption. Next, we formulate a **Cumulative Handoff Delay Minimization Problem** for multiple spectrum handoffs. Given a set of candidate channels  $\Omega = \{1, 2, \dots, M\}$  and the required length  $L$  of the target channel

sequence for  $L$  spectrum handoffs, we aim to determine a target channel sequence (denoted by  $\mathbf{s}(\eta)^*$ ) to minimize the average cumulative handoff delay  $\mathbf{E}[D(\mathbf{s}(\eta))]$  for a newly arriving secondary user's connection. Formally, we have

$$\mathbf{s}(\eta)^* = \arg \min_{\forall \mathbf{s}(\eta) \in \Omega^L} \mathbf{E}[D(\mathbf{s}(\eta))] , \quad (6.1)$$

where  $\mathbf{E}[\cdot]$  is the expectation function. In the next section, the closed-form expression for  $\mathbf{E}[D(\mathbf{s}(\eta))]$  will be derived given the arrival rates and service time distributions of both primary and secondary users.

## 6.2 Cumulative Handoff Delay Analysis

In this section, we derive the closed-form expression for the average cumulative handoff delay with different target channel sequence  $\mathbf{s}(\eta)$  of the newly arriving secondary user's connection. To ease notation, we denote  $\mathbf{s}$  for  $\mathbf{s}(\eta)$  in the rest of this chapter. Let  $N$  be the total number of interruptions in the considered connection. According to the total probability principle, it follows that

$$\begin{aligned} \mathbf{E}[D(\mathbf{s})] &= \sum_{n=1}^L \Pr\{N = n\} \mathbf{E}[D(\mathbf{s})|N = n] \\ &= \sum_{n=1}^L \left[ \Pr\{N = n\} \sum_{i=1}^n \mathbf{E}[d(s_{i-1}, s_i)] \right] , \end{aligned} \quad (6.2)$$

where  $d(s_{i-1}, s_i)$  is the handoff delay when the interrupted secondary users change their operating channel from channel  $s_{i-1}$  to  $s_i$ .

Firstly, we evaluate  $\mathbf{E}[d(s_{i-1}, s_i)]$  in (6.2). When a primary user's connection appears at the channel being occupied by the newly arriving secondary user's connection, an interruption event occurs. The spectrum handoff delay depends on which channel is selected for the target channel. The interrupted

secondary users can either stay on the current channel or change to another channel. If the considered secondary user's connection chooses to stay on its current operating channel (i.e.,  $s_{i-1} = s_i$ ), the expected handoff delay is the duration from the time instant that current operating channel is used by the primary users' connections until this channel becomes idle. This duration is called the *busy period* (denoted by  $Y_p^{(s_i)}$ ) resulting from the transmissions of multiple primary users' connections at channel  $s_{i-1}$ . In the other case, the considered secondary user's connection may change its operating channel (i.e.,  $s_{i-1} \neq s_i$ ). After switching channel from channel  $s_{i-1}$  to  $s_i$ , the considered secondary user's connection cannot be resumed until all the present primary and secondary users' connections at channel  $s_i$  are served. Let  $\mathbf{E}[W_s^{(s_i)}]$  be the waiting time<sup>1</sup> for the secondary users' connections at channel  $s_i$ . Then, the expected handoff delay is the sum of  $\mathbf{E}[W_s^{(s_i)}]$  and the channel switching time  $t_s$ . Thus,

$$\mathbf{E}[d(s_{i-1}, s_i)] = \begin{cases} \mathbf{E}[Y_p^{(s_i)}] & , \quad s_{i-1} = s_i \\ \mathbf{E}[W_s^{(s_i)}] + t_s & , \quad s_{i-1} \neq s_i \end{cases} . \quad (6.3)$$

Next, we evaluate  $\mathbf{Pr}\{N = n\}$  in (6.2). Denote  $p_i^{(s_i)}$  as the probability that a secondary user's connection is interrupted by the arrival of primary user's connection again at channel  $s_i$  after  $i$  interruptions. Then, the probability that the considered secondary user's connection is interrupted exactly

---

<sup>1</sup>A secondary user's connection needs to change its operating channel only when a primary user's connection appears. Because the arrivals of the primary users' connections follow Poisson distribution, the arrivals of the interrupted secondary users' connections at channel  $s_i$  also follow Poisson distribution. Applying the property of Poisson arrivals see time average (PASTA) on the arrivals of the interrupted secondary users' connections at channel  $s_i$  [97], all of them must spend time duration  $\mathbf{E}[W_s^{(s_i)}]$  on average to wait for an idle channel  $s_i$ . This waiting time is uncorrelated to the number of interruptions.

$n$  times can be expressed as

$$\Pr\{N = n\} = (1 - p_n^{(s_n)}) \prod_{i=0}^{n-1} p_i^{(s_i)} . \quad (6.4)$$

Now, we apply the proposed preemptive resume priority (PRP) M/G/1 queueing network model in Chapters 3 and 4 [102] to derive the closed-form expressions for  $\mathbf{E}[d(s_{i-1}, s_i)]$  and  $\Pr\{N = n\}$ . Let  $\lambda_p^{(\eta)}$  (arrivals/slot) and  $\lambda_s^{(\eta)}$  (arrivals/slot) be the initial arrival rates of the primary users' and secondary users' connections at channel  $\eta$  in  $\mathcal{G}$ , respectively, and  $X_p^{(\eta)}$  (slots/arrival) and  $X_s^{(\eta)}$  (slots/arrival) be their corresponding service time, respectively. Furthermore, we assume that the existing secondary users' connections in  $\mathcal{G}$  must stay on the current operating channel when they are interrupted. Then, referring to [79], a newly arriving secondary user's connection will experience the following performance measures:

$$\mathbf{E}[Y_p^{(s_i)}] = \frac{\mathbf{E}[X_p^{(s_i)}]}{1 - \lambda_p^{(s_i)} \mathbf{E}[X_p^{(s_i)}]} , \quad (6.5)$$

$$\mathbf{E}[W_s^{(s_i)}] = \frac{\lambda_p^{(s_i)} \mathbf{E}[X_p^{(s_i)}]^2 + \lambda_s^{(s_i)} \mathbf{E}[X_s^{(s_i)}]^2}{(1 - \lambda_p^{(s_i)} \mathbf{E}[X_p^{(s_i)}])(1 - \lambda_p^{(s_i)} \mathbf{E}[X_p^{(s_i)}] - \lambda_s^{(s_i)} \mathbf{E}[X_s^{(s_i)}])} , \quad (6.6)$$

and

$$p_i^{(s_i)} = \lambda_p^{(s_i)} \mathbf{E}[\Phi_i^{(s_i)}] , \quad (6.7)$$

where  $\mathbf{E}[\Phi_i^{(k)}]$  is the considered newly arriving secondary connection's transmission duration between the  $i^{th}$  and the  $(i+1)^{th}$  interruptions at channel  $k$ . When the service time (denoted by  $\chi_s$ ) of the considered newly arriving secondary connection is given, we can derive the closed-form expression for  $\mathbf{E}[\Phi_i^{(k)}]$  according to [103] and thus  $p_i^{(s_i)}$  can be evaluated. For example, when  $\chi_s$  is geometrically distributed, we can have

$$p_i^{(s_i)} = \frac{\lambda_p^{(s_i)} \mathbf{E}[\chi_s]}{\lambda_p^{(s_i)} \mathbf{E}[\chi_s] + 1} . \quad (6.8)$$

Note that the distributions of service time  $\chi_s$  for the newly arriving secondary user's connection and  $X_s^{(n)}$  for the existing secondary users' connections can be different in our model. Finally, we can obtain the values of  $\mathbf{E}[d(s_{i-1}, s_i)]$  and  $\mathbf{Pr}\{N = n\}$  by substituting (6.5) and (6.6) into (6.3) and (6.7) into (6.4), respectively.

The **Cumulative Handoff Delay Minimization Problem** can be solved by exhaustively searching all the possible target channel sequences. Because this brute force must enumerate all  $M^L$  possible permutations of the target channel sequences and compute how long each permutation will take to find a target channel sequence with the minimum cumulative handoff delay, the exhaustive search method has the time complexity of  $O(M^L)$  and it is infeasible when  $M$  is large. Hence, it is critical to design a low-complexity algorithm to solve this optimization problem.

### 6.3 An Optimal Dynamical Programming Algorithm

In this section, we propose a low-complexity algorithm to solve the **Cumulative Handoff Delay Minimization Problem**. First, we develop a state diagram to characterize the evolution of target channel sequences and their corresponding cumulative handoff delay. We observe that the considered optimization problem has the optimal substructure property, and thus propose a dynamic programming algorithm for the **Cumulative Handoff Delay Minimization Problem** with a time complexity of  $O(LM^2)$ .



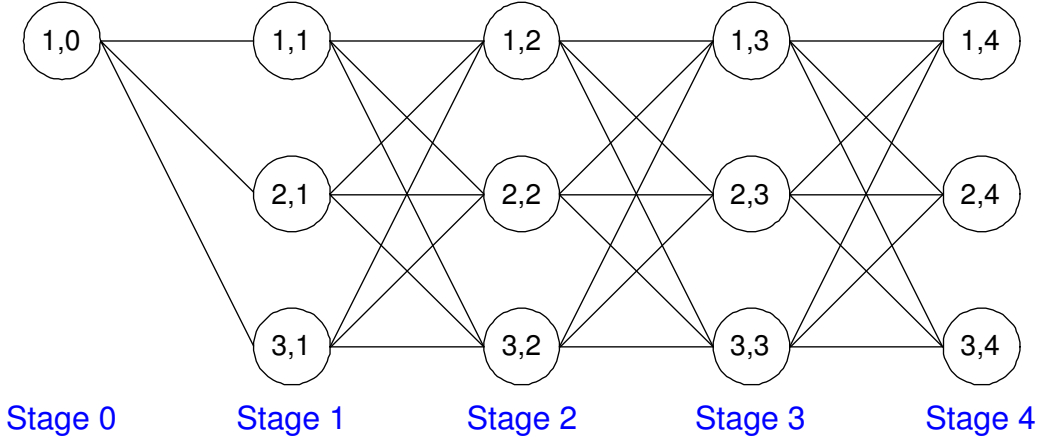


Figure 6.1: An example of state diagram of the target channel sequences for a newly arriving secondary user, where the default channel  $\eta = 1$ , the number of total channels  $M = 3$ , and the required length of the target channel sequence  $L = 4$ . Furthermore,  $(k, i)$  stands for the state of operating at the channel  $k$  with the  $i^{\text{th}}$  interruption.

### 6.3.1 State Diagram for Target Channel Sequences

The proposed state diagram is a two-dimensional chain where state  $(k, i)$  represents that channel  $k$  is selected for the target channel at the  $i^{\text{th}}$  interruption. Because the default channel is channel  $\eta$ , the initial state of this state diagram model is  $(\eta, 0)$ . Furthermore, the set of all possible states for the  $i^{\text{th}}$  interruption is called stage  $i$ . The state transitions occur only at the states between the adjacent stages. Specifically, a transition link from  $(k, i)$  to  $(k', i')$  exists if  $i' = i + 1$ , and vice versa. An example of state diagram is shown in Fig. 6.1, where  $\eta = 1$ ,  $M = 3$ , and  $L = 4$ .

The cost of state transition shall be proportional to the handoff delay of the interrupted secondary user's connection. For example, the transition from states  $(k, i - 1)$  to  $(k, i)$  represents the situation that the considered secondary user's connection stays on the current channel  $k$  when the  $i^{\text{th}}$

interruption event occurs. Hence, in this case, the transition cost shall be proportional to  $\mathbf{E}[d(k, k)] = \mathbf{E}[Y_p^{(k)}]$ . Furthermore, the transition from states  $(k, i-1)$  to  $(k', i)$  represents the situation that the considered secondary user's connection changes its operating channel from channel  $k$  to  $k'$  when the  $i^{\text{th}}$  interruption event occurs. Hence, the transition cost shall be proportional to  $\mathbf{E}[d(k, k')] = \mathbf{E}[W_s^{(k')}] + t_s$ . Let  $w(k; k', i)$  be the transition cost from state  $(k, i-1)$  to state  $(k', i)$ . Because transition cost is proportional to the handoff delay of the interrupted secondary user's connections, it follows that

$$w(k; k', i) = \nu_i \cdot \mathbf{E}[d(k, k')] , \quad (6.9)$$

where  $\nu_i$  is a normalized factor. It can be obtained by Propositions 3.

**Proposition 3.** *For the considered secondary user's connections, given the total number of interruptions  $N$  and the interrupted probability  $p_i^{(s_i)}$  at channel  $s_i$  after  $i$  interruptions. It follows that*

$$\nu_i = \Pr\{N \geq n\} = \prod_{i=0}^{n-1} p_i^{(s_i)} . \quad (6.10)$$

*Proof.* Recall that  $\mathbf{E}[D(\mathbf{s})]$  is defined as the average cumulative handoff delay of the considered newly arriving secondary user's connection with the target channel sequence  $\mathbf{s}$ .  $\mathbf{E}[D(\mathbf{s})]$  can be also interpreted as the cumulative cost for the state transition path  $(s_0 \rightarrow s_1 \rightarrow s_2 \rightarrow s_3 \rightarrow \cdots \rightarrow s_L)$ . Hence, it follows that

$$\begin{aligned} \mathbf{E}[D(\mathbf{s})] &= \sum_{i=1}^L w(s_{i-1}; s_i, i) \\ &= \sum_{i=1}^L [\mathbf{E}[d(s_{i-1}, s_i) \cdot \nu_i]] . \end{aligned} \quad (6.11)$$

Furthermore, from (6.2), we can have

$$\begin{aligned}\mathbf{E}[D(\mathbf{s})] &= \sum_{i=1}^L [\mathbf{E}[d(s_{i-1}, s_i)] \cdot \mathbf{Pr}\{N \geq n\}] \\ &= \sum_{i=1}^L \left[ \mathbf{E}[d(s_{i-1}, s_i)] \cdot \prod_{i=0}^{n-1} p_i^{(s_i)} \right].\end{aligned}\quad (6.12)$$

Comparing (6.11) and (6.12), we can obtain (6.10).  $\square$

### 6.3.2 Optimal Substructure Property

Next, we show that this optimization problem has the optimal substructure property based on the proposed state diagram. Let  $m(k', i)$  be the cumulative cost of the minimum cost path from the initial state  $(\eta, 0)$  to the state  $(k', i)$  where  $i \geq 1$ . Then, we have the following recursive relationship:

$$m(k', i + 1) = \min_{k \in \Omega} \{m(k, i) + w(k; k', i + 1)\}, \quad (6.13)$$

where

$$\begin{aligned}m(k', 1) &= w(\eta; k', 1) \\ &= \begin{cases} \mathbf{E}[Y_p^{(k')}]p_0^{(\eta)}, & k' = \eta \\ (\mathbf{E}[W_s^{(k')}] + t_s)p_0^{(\eta)}, & k' \neq \eta \end{cases}.\end{aligned}\quad (6.14)$$

Based on this optimal substructure, we can build an optimal solution to the considered optimization problem from the optimal solutions to the subproblems. Then, the shortest cumulative handoff delay (denoted by  $m^*$ ) can be obtained as follows:

$$m^* = \min_{k' \in \Omega} m(k', L). \quad (6.15)$$

### 6.3.3 Dynamic-Programming-Based Target Channel Selection Algorithm

Based on the optimal substructure, we propose a dynamic programming algorithm with time complexity of  $O(LM^2)$  to search the minimum cost path in the state diagram to minimize the cumulative handoff delay of the considered secondary user's connection. The detail is shown in Algorithm 1.

---

**Algorithm 1:** Dynamic Programming Algorithm

---

**Input:**  $M, L, \eta$ , and  $w$

**Output:**  $m(k', L)$

```

for  $k' = 1 : M$  do
  |  $m(k', 1) = w(\eta; k', 1)$  ;
end
for  $i = 2 : L$  do
  | for  $k' = 1 : M$  do
    |  $m(k', i) = \infty$  ;
    | for  $k = 1 : M$  do
      |  $m'(k', i) = m(k, i - 1) + w(k; k', i)$  ;
      | if  $m(k', i) > m'(k', i)$  then
        | |  $m(k', i) = m'(k', i)$  ;
      | end
    | end
  | end
end
end

```

---

Our ultimate goal is to find an optimal target channel sequence to minimize the average cumulative handoff delay (or equivalently to find a minimum cost path). To this end, when evaluating the cumulative cost  $m(k, i)$ , we must keep track of how to construct an optimal solution to find the corresponding

minimum cost path.

## 6.4 A Suboptimal Low-Complexity Greedy Algorithm

In the section we present a suboptimal greedy algorithm to further reduce the time complexity of solving the **Cumulative Handoff Delay Minimization Problem**. Based on the suggested greedy target channel selection strategy, the proposed greedy algorithm has time complexity of  $O(M)$ .

### 6.4.1 Greedy Target Channel Selection Strategy

In each spectrum handoff, the greedy target channel selection strategy is suggested to select the channel with *the shortest expected handoff delay*. Some permutations of the target channel sequences will never occur when this shortest-handoff-delay strategy is adopted. Here, we give such an example. Consider a secondary user's connection whose default channel is channel 1 (*Ch1*). In a two-channel system, it can select either channel 1 or channel 2 (*Ch2*) for its target channel when an interruption event occurs. Now, we assume that the average busy period of *Ch1* (denoted by  $\mathbf{E}[Y_p^{(1)}]$ ) is shorter than the sum of channel switching time (denoted by  $t_s$ ) and the average waiting time of *Ch2* (denoted by  $\mathbf{E}[W_s^{(2)}]$ ). Hence, when the first interruption occurs and the greedy target channel selection strategy is adopted, the secondary user selects *Ch1* as its target channel for spectrum handoff. The similar argument can be held again for all the upcoming interruptions. That is, the target channel sequence will be (*Ch1, Ch1, Ch1, Ch1, Ch1, ...*). In this case, some permutations of the target channel sequences, such as

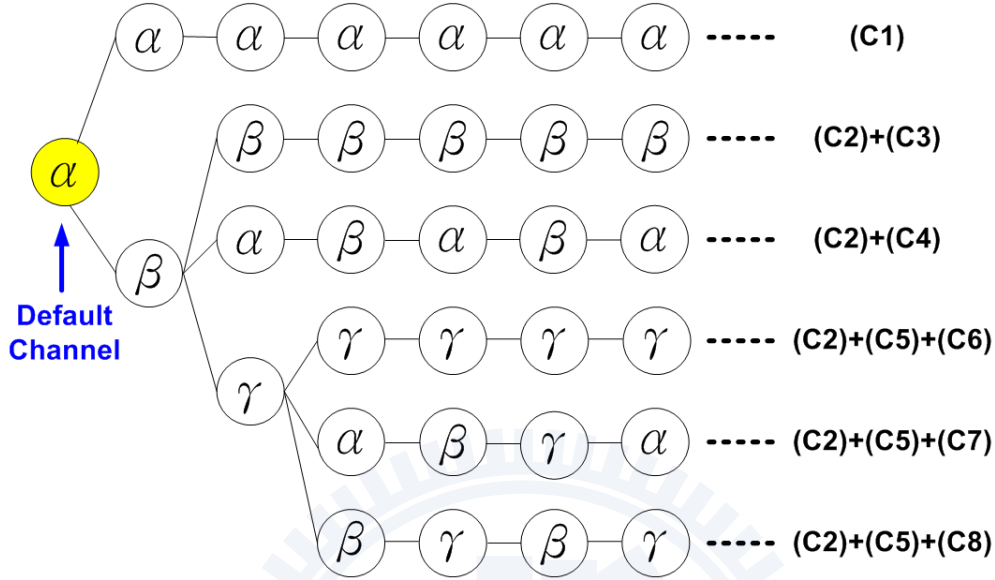


Figure 6.2: Six kinds of candidate sequences for the **Cumulative Hand-off Delay Minimization Problem** when the greedy shortest-handoff-delay target channel selection strategy is adopted.

$(Ch1, Ch2, Ch2, Ch2, Ch2, \dots)$  or  $(Ch1, Ch2, Ch1, Ch1, Ch1, \dots)$ , will never occur. In Theorem 4, we prove that only six permutations of the target channel sequences are required to be compared when the greedy shortest-handoff-delay target channel selection strategy is employed.

**Theorem 4.** *The shortest-handoff-delay target channel selection strategy only requires to compare six permutations of the target channel sequences, as shown in Fig. 6.2.*

*Proof.* Consider a secondary user's connection whose default channel is  $\alpha$  ( $\alpha \in \Omega$ ). If the strategy is to select a channel with the shortest handoff delay when an interruption event occurs, the secondary user will compare the expected handoff delay of staying on the same channel and that of changing

to a new channel. Now, we discuss what conditions will cause target channel sequences not to be considered by the greedy target channel selection strategy.

**(1) At the first interruption:** The secondary user can select channel  $\alpha$  or channel  $k$  ( $k \in \Omega/\{\alpha\}$ ) for the target channel. If staying on channel  $\alpha$ , the expected delay for the non-hopping spectrum handoff equals the average busy period of the primary users' connections at channel  $\alpha$  (denoted by  $\mathbf{E}[Y_p^{(\alpha)}]$ ). If changing its operating channel to channel  $k$ , the secondary user will experience the delay of the hopping spectrum handoff, which is equal to the sum of the channel switching time (denoted by  $t_s$ ) and the average waiting time on channel  $k$  (denoted by  $\mathbf{E}[W_s^{(k)}]$ ). On the one hand, if the following condition **(C1)** is satisfied,

$$\text{(C1)} : \mathbf{E}[Y_p^{(\alpha)}] \leq \min_{\forall k \in \Omega/\{\alpha\}} \{ \mathbf{E}[W_s^{(k)}] + t_s \} ,$$

channel  $\alpha$  is the first element in the target channel sequence. This implies that the interrupted secondary user must wait until all the primary users' connections leave channel  $\alpha$ . When the traffic statistics of all channels are stationary, the interrupted secondary user will always stay on channel  $\alpha$  because **(C1)** always can be satisfied for all the upcoming interruptions. That is, the target channel sequence becomes  $(\alpha, \alpha, \alpha, \alpha, \alpha, \alpha, \dots)$ , as shown in Fig. 6.2. On the other hand, if the condition

$$\text{(C2)} : \begin{cases} \beta = \arg \min_{\forall k \in \Omega/\{\alpha\}} \mathbf{E}[W_s^{(k)}] \\ \mathbf{E}[W_s^{(\beta)}] + t_s < \mathbf{E}[Y_p^{(\alpha)}] \end{cases}$$

is satisfied, the first element in the target channel sequence is channel  $\beta$ . Clearly, **(C2)** is not sufficient to determine the remaining elements in the target channel sequence.

**(2) At the second interruption:** When **(C2)** is satisfied, the secondary user will encounter one of the following three conditions at the second interruption. Denote  $\mathbf{E}[Y_p^{(\beta)}]$ ,  $\mathbf{E}[W_s^{(\gamma)}] + t_s$ , and  $\mathbf{E}[W_s^{(\alpha)}] + t_s$  as the average handoff delay for staying on channel  $\beta$ , that for changing to channel  $\gamma$  ( $\gamma \neq \alpha$  and  $\beta$ ), and that for switching back to channel  $\alpha$ , respectively.

- First, we consider the case

$$\text{(C3)} : \mathbf{E}[Y_p^{(\beta)}] \leq \min_{\forall k \in \Omega / \{\beta\}} \{\mathbf{E}[W_s^{(k)}] + t_s\} .$$

Similar to **(C1)**, the interrupted secondary user prefers staying on channel  $\beta$  when **(C3)** is satisfied. Thus, **(C2)** and **(C3)** lead to the target channel sequence  $(\beta, \beta, \beta, \dots)$ .

- Next, we consider the condition

$$\text{(C4)} : \mathbf{E}[W_s^{(\alpha)}] + t_s < \min\left\{ \min_{\forall k \in \Omega / \{\alpha, \beta\}} \{\mathbf{E}[W_s^{(k)}] + t_s\}, \mathbf{E}[Y_p^{(\beta)}] \right\} .$$

When **(C4)** is satisfied, the interrupted secondary user will switch back to channel  $\alpha$ . After that, the third interruption event may occur. If so, this interrupted secondary user will switch back to channel  $\beta$  due to **(C2)**. Hence, **(C2)** and **(C4)** yields the target channel sequence  $(\beta, \alpha, \beta, \alpha, \beta, \alpha, \dots)$ .

- When **(C3)** and **(C4)** are not satisfied, it implies that there exists channel  $\gamma$  ( $\gamma \neq \alpha$ ) such that

$$\text{(C5)} : \begin{cases} \gamma = \arg \min_{\forall k \in \Omega / \{\alpha, \beta\}} \mathbf{E}[W_s^{(k)}] \\ \mathbf{E}[W_s^{(\gamma)}] + t_s < \mathbf{E}[Y_p^{(\beta)}] \\ \mathbf{E}[W_s^{(\gamma)}] < \mathbf{E}[W_s^{(\alpha)}] \end{cases} .$$

Then, the second element in the target channel sequence is channel  $\gamma$ . Since **(C2)** and **(C5)** are not sufficient to determine the remaining



elements in the target channel sequence, the third interruption event will be considered.

**(3) At the third interruption:** In this case, we need to compare the expected handoff delay of staying on channel  $\gamma$  and that of switching back to channels  $\alpha$  and  $\beta$ , i.e.,  $\mathbf{E}[Y_p^{(\gamma)}]$ ,  $\mathbf{E}[W_s^{(\alpha)}] + t_s$ , and  $\mathbf{E}[W_s^{(\beta)}] + t_s$ , respectively. Given **(C2)** and **(C5)**, three different situations exist.

- First of all, if the condition

$$\text{(C6)} : \mathbf{E}[Y_p^{(\gamma)}] \leq \min_{\forall k \in \Omega/\{\gamma\}} \{\mathbf{E}[W_s^{(k)}] + t_s\}$$

is satisfied, the interrupted secondary user prefers staying on channel  $\gamma$ . Hence, **(C2)**, **(C5)**, and **(C6)** result in the the target channel sequence  $(\beta, \gamma, \gamma, \gamma, \dots)$ .

- Furthermore, if the condition

$$\text{(C7)} : \mathbf{E}[W_s^{(\alpha)}] + t_s < \min\left\{\min_{\forall k \in \Omega/\{\alpha, \gamma\}} \{\mathbf{E}[W_s^{(k)}] + t_s\}, \mathbf{E}[Y_p^{(\gamma)}]\right\}$$

is satisfied, the interrupted secondary user switches back to channel  $\alpha$ . Then, **(C2)** and **(C5)** will make this secondary user switches to channel  $\beta$  and channel  $\gamma$  at the fourth and fifth interruptions, respectively. Thus, when **(C2)**, **(C5)** and **(C7)** are satisfied, the target channel sequence becomes  $(\beta, \gamma, \alpha, \beta, \gamma, \alpha, \beta, \gamma, \alpha, \dots)$ .

- Similarly, when

$$\text{(C8)} : \mathbf{E}[W_s^{(\beta)}] + t_s < \min\left\{\min_{\forall k \in \Omega/\{\beta, \gamma\}} \{\mathbf{E}[W_s^{(k)}] + t_s\}, \mathbf{E}[Y_p^{(\gamma)}]\right\}$$

is satisfied, one can show that the target channel sequence is  $(\beta, \gamma, \beta, \gamma, \beta, \gamma, \dots)$ .

Now, we will prove that it is not necessary to consider other channels except for channels  $\alpha$ ,  $\beta$ , and  $\gamma$  when the third interruption event occurs. Assume that there exists channel  $\xi = \arg \min_{\forall k \in \Omega / \{\alpha, \beta, \gamma\}} \mathbf{E}[W_s^{(k)}]$  such that

$$\begin{cases} \mathbf{E}[W_s^{(\xi)}] + t_s < \mathbf{E}[Y_p^{(\gamma)}] \\ \mathbf{E}[W_s^{(\xi)}] < \mathbf{E}[W_s^{(\alpha)}] \\ \mathbf{E}[W_s^{(\xi)}] < \mathbf{E}[W_s^{(\beta)}] \end{cases} .$$

Then, it follows that

$$\mathbf{E}[W_s^{(\xi)}] + t_s < \mathbf{E}[W_s^{(k)}] + t_s, \quad \forall k \neq \xi, \gamma . \quad (6.16)$$

However, from **(C2)**, we know that

$$\mathbf{E}[W_s^{(\beta)}] + t_s < \mathbf{E}[W_s^{(k)}] + t_s, \quad \forall k \neq \alpha, \beta . \quad (6.17)$$

Since (6.16) yields  $\mathbf{E}[W_s^{(\xi)}] < \mathbf{E}[W_s^{(\beta)}]$ , but (6.17) yields  $\mathbf{E}[W_s^{(\beta)}] < \mathbf{E}[W_s^{(\xi)}]$ , it leads to a contradiction and proves that no other channels need to be considered further.

From the above discussions, **(C1)**-**(C8)** have considered all the conditions between  $\mathbf{E}[W_s^{(k)}]$  and  $\mathbf{E}[Y_p^{(k)}]$ . Hence, we can conclude that the greedy shortest-handoff-delay target channel selection strategy results in only six permutations of the target channel sequences that are needed to be further compared in the **Cumulative Handoff Delay Minimization Problem**, are shown in Fig. 6.2.  $\square$

Based on Theorem 4, the transmitter and receiver need to consider only three channels for spectrum handoff as long as the greedy shortest-handoff-delay target channel selection strategy is considered. Thus, it relieves channel consensus issue in CR networks. Theorem 4 can be extended to other greedy strategies for the target channel selection based on various criteria, such as the longest expected remaining idle period.

### 6.4.2 Greedy Target Channel Selection Algorithm

The shortest-handoff-delay strategy is adopted to select the target channel in the proposed greedy algorithm, as shown in Algorithm 2. Hence, this Algorithm 2 has time complexity of  $O(M)$ .

---

**Algorithm 2:** Suboptimal Greedy Algorithm

---

**Input:**  $M, L, \eta, \mathbf{E}[W_s^{(k)}]$ , and  $\mathbf{E}[Y_p^{(k)}]$

**Output:**  $m(k', L)$

**for**  $j = 1 : 8$  **do**

    | Checking whether the condition (Cj) can be satisfied by comparing  
    | the values of  $\mathbf{E}[W_s^{(k)}]$  and  $\mathbf{E}[Y_p^{(k)}]$  for any  $k$ , where  $1 \leq k \leq M$ .

**end**

According to Fig. 6.2, determining the target channel sequence.

---

## 6.5 Numerical Results

In this section, by applying the proposed analytical models to the environments with various statistics of service time distributions for both primary and secondary users, we show the cumulative spectrum handoff delay performance for the proposed target channel sequence design approaches subject to the effects of multiple handoffs. Five target channel selection schemes are compared, which consist of (1) the random selection strategy; (2) the throughput-orientated strategy; (3) the greedy shortest-handoff-delay target channel selection strategy; (4) the dynamic programming (DP)-based solution; and (5) the exhaustive search (ES)-based solution. For the random selection strategy, the secondary user randomly selects one channel for its target channel when an interruption event occurs. Furthermore, the throughput-

orientated strategy selects the channel that is accessed by the primary users with the lowest probability. Moreover, the suggested greedy strategy selects the channel with the shortest handoff delay for its target channel.

### 6.5.1 Effects of Traffic Statistics for Arriving Secondary User's Service Time

Firstly, we investigate the effects of the newly arriving secondary user's average service time ( $\mathbf{E}[\chi_s]$ ) on its cumulative handoff delay. Figure 6.3 compares the cumulative handoff delay of the five considered target channel selection schemes in a four-channel CR network with  $\lambda_p^{(k)} = 0.02$  and  $\lambda_s^{(k)} = 0.01$  for  $1 \leq k \leq 4$ . We have the following observations:

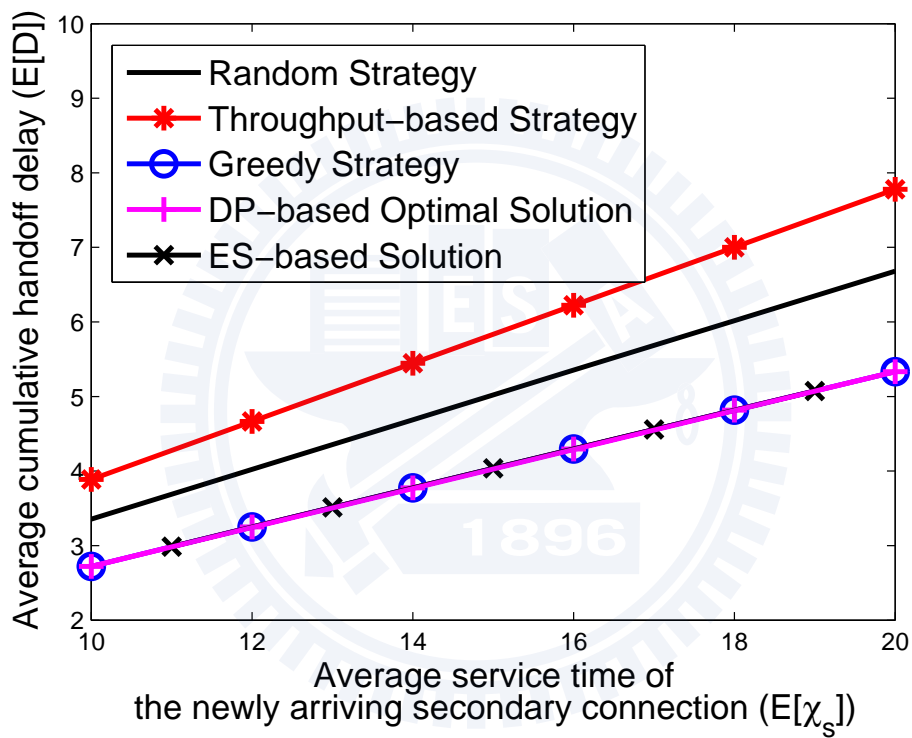
- When the average service time  $\mathbf{E}[\chi_s]$  increases, a secondary user experiences more interruptions on average and thus the cumulative handoff delay increases as shown in the figure.
- The dynamic programming approach yields almost the same result as the exhaustive search approach.
- Compared to the random strategy, the greedy strategy and the optimal solution can significantly reduce the cumulative handoff delay because it takes a priori traffic statistics into account when determining the target channel for spectrum handoff. For example, the greedy strategy and the optimal solution can reduce the cumulative handoff delay by over 20% and 58% compared to the random strategy when  $\mathbf{E}[\chi_s] = 20$  in Figs. 6.3(a) and 6.3(b), respectively.
- Figure 6.3(a) shows that the cumulative handoff delay of the low-complexity greedy target channel selection strategy is the same as the

optimal solution when the primary user service time has similar distributions in different channels, where  $(\mathbf{E}[X_p^{(1)}], \mathbf{E}[X_p^{(2)}], \mathbf{E}[X_p^{(3)}], \mathbf{E}[X_p^{(4)}]) = (14, 15, 15, 15)$ , and  $(\mathbf{E}[X_s^{(1)}], \mathbf{E}[X_s^{(2)}], \mathbf{E}[X_s^{(3)}], \mathbf{E}[X_s^{(4)}]) = (10, 12, 14, 16)$ . However, if the primary user's service time distributions of each channel are different, the cumulative handoff delay resulting from the suggested greedy strategy is slightly larger than the optimal solution. For example, when  $(\mathbf{E}[X_p^{(1)}], \mathbf{E}[X_p^{(2)}], \mathbf{E}[X_p^{(3)}], \mathbf{E}[X_p^{(4)}]) = (10, 15, 20, 25)$  and  $(\mathbf{E}[X_s^{(1)}], \mathbf{E}[X_s^{(2)}], \mathbf{E}[X_s^{(3)}], \mathbf{E}[X_s^{(4)}]) = (10, 10, 10, 10)$ , Fig. 6.3(b) shows that the cumulative handoff delay of the greedy strategy is 9% higher than that of the optimal solution at  $\mathbf{E}[\chi_s] = 20$ .

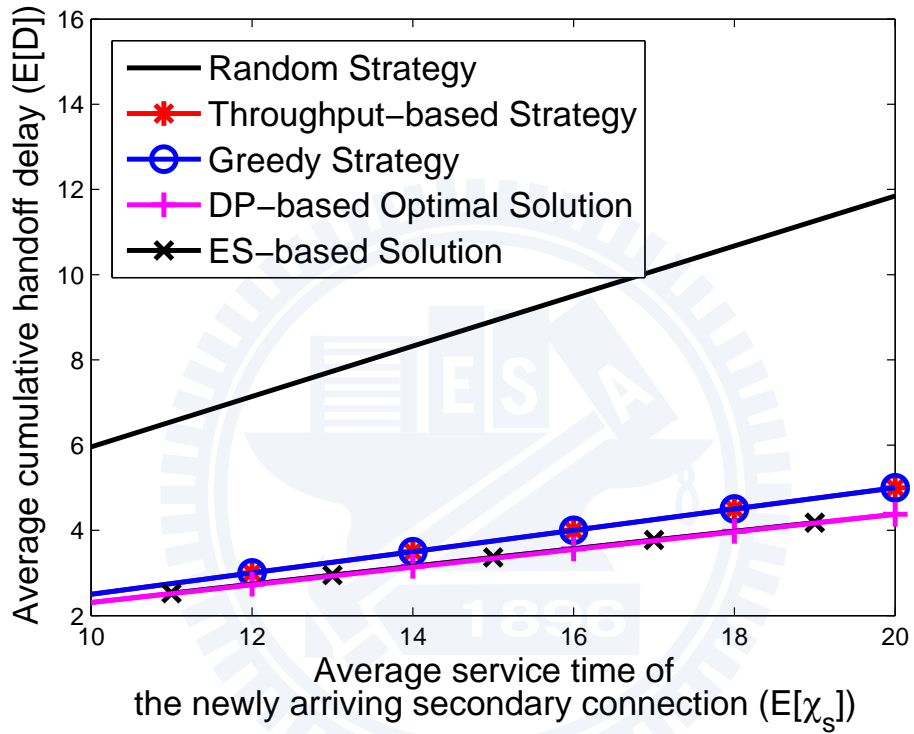
- When the arrival rates and service time of the secondary users' connections are the same at all the four channels as shown in Fig. 6.3(b), the throughput-orientated strategy and the suggested greedy strategy result in the same cumulative handoff delay. However, when the secondary users' connections have different traffic statistics as shown in Fig. 6.3(a), it is shown that at  $\mathbf{E}[\chi_s] = 20$  the greedy strategy improves the cumulative handoff delay of the throughput-orientated strategy by 46%. This is because the suggested greedy strategy takes into account of the traffic statistics of both the primary and secondary users when determining the target channel.

### 6.5.2 Effects of Traffic Statistics of Existing Secondary Users' Connections

Figure 6.4 shows how the existing secondary connections' traffic statistics, including the average service time  $\mathbf{E}[X_s]$  and the arrival rate  $\lambda_s$ , affect the cumulative handoff delay of the newly arriving secondary user's connection.



(a)  $(\mathbf{E}[X_p^{(1)}], \mathbf{E}[X_p^{(2)}], \mathbf{E}[X_p^{(3)}], \mathbf{E}[X_p^{(4)}]) = (14, 15, 15, 15)$ , and  $(\mathbf{E}[X_s^{(1)}], \mathbf{E}[X_s^{(2)}], \mathbf{E}[X_s^{(3)}], \mathbf{E}[X_s^{(4)}]) = (10, 12, 14, 16)$ .



(b)  $(\mathbf{E}[X_p^{(1)}], \mathbf{E}[X_p^{(2)}], \mathbf{E}[X_p^{(3)}], \mathbf{E}[X_p^{(4)}]) = (10, 15, 20, 25),$  and  
 $(\mathbf{E}[X_s^{(1)}], \mathbf{E}[X_s^{(2)}], \mathbf{E}[X_s^{(3)}], \mathbf{E}[X_s^{(4)}]) = (10, 10, 10, 10).$

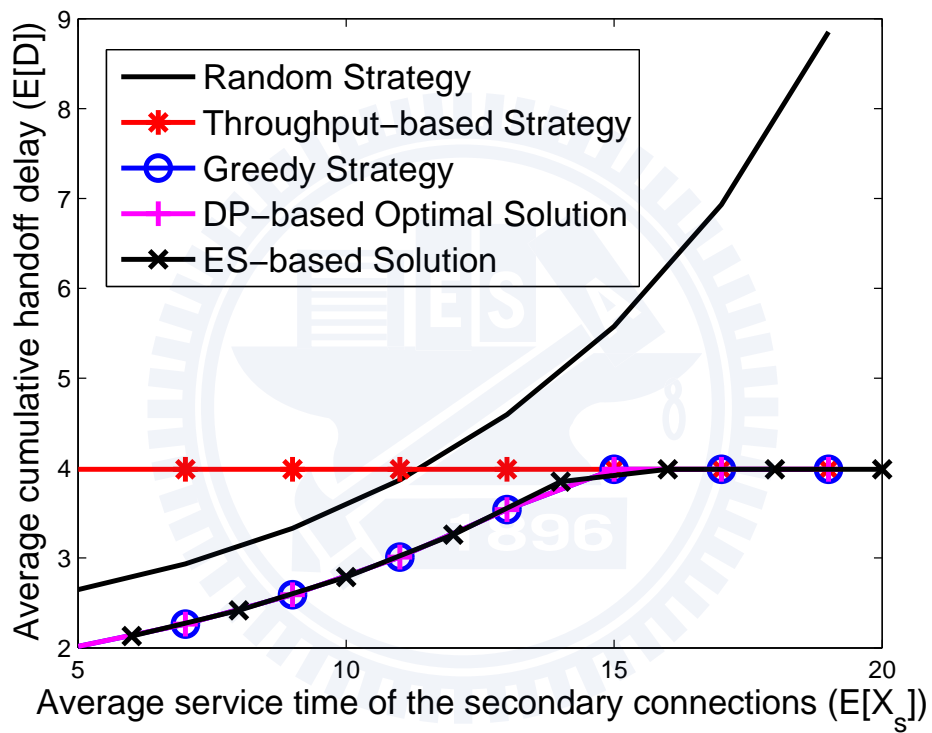
Figure 6.3: Effects of the newly arriving secondary user's average service time  $\mathbf{E}[\chi_s]$  on the cumulative handoff delay for  $\lambda_p^{(k)} = 0.02$  and  $\lambda_s^{(k)} = 0.01$  when  $1 \leq k \leq 4$ .

Assume that the service time  $\chi_s$  of the newly arriving secondary user's connection is geometrically distributed with  $\mathbf{E}[\chi_s] = 10$ , and the primary users have the similar traffic parameters in different channels. From Fig. 6.4(a) where  $\mathbf{E}[X_s^{(k)}] = \mathbf{E}[X_s]$  for  $1 \leq k \leq 4$ , we observe the following:

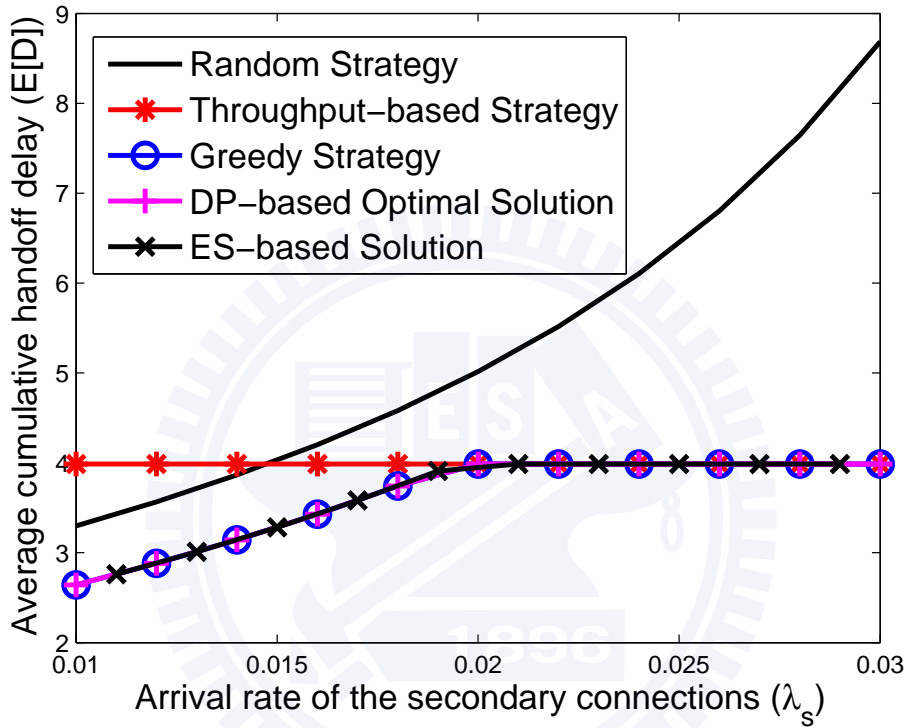
- In the range of small  $\mathbf{E}[X_s]$  (e.g.,  $\mathbf{E}[X_s] < 15$ ), the cumulative handoff delay increases as  $\mathbf{E}[X_s]$  increases for the random selection strategy, the greedy strategy, and the optimal solution.
- In the range of large  $\mathbf{E}[X_s]$  (e.g.,  $\mathbf{E}[X_s] \geq 15$ ), the secondary user will experience long waiting time when it changes its operating channel according to (6.6). Hence, the greedy strategy and the optimal solution prefer staying on the current operating channel when interruptions occur to reduce handoff delay. In this case, their average handoff delay for each handoff is a constant  $\mathbf{E}[Y_p]$ . Thus, the average cumulative handoff delay is also a constant. However, the random strategy still selects to change channel for spectrum handoff sometimes. Hence, the cumulative handoff delay of the random strategy still increases as  $\mathbf{E}[X_s]$  increases.
- Because the throughput-orientated strategy always selects channel 1 for the target channel, the corresponding average handoff delay is a constant  $\mathbf{E}[Y_p]$ . Hence, the throughput-orientated strategy results in the same average cumulative handoff delay for various  $\mathbf{E}[X_s]$ .

Note that the similar observations can be also found in Fig. 6.4(b), where  $\lambda_s^{(k)} = \lambda_s$  for  $1 \leq k \leq 4$ . When  $\lambda_s \geq 0.02$ , the interrupted secondary users will always stay on the current operating channel for the greedy strategy and the optimal solution.





(a) Effect of the average service time  $\mathbf{E}[X_s]$  on the cumulative handoff delay  $\mathbf{E}[D]$ , where  $(\lambda_s^{(1)}, \lambda_s^{(2)}, \lambda_s^{(3)}, \lambda_s^{(4)}) = (0.01, 0.015, 0.02, 0.025)$ .



(b) Effect of the arrival rate  $\lambda_s$  on the cumulative handoff delay  $\mathbf{E}[D]$ , where  $(\mathbf{E}[X_s^{(1)}], \mathbf{E}[X_s^{(2)}], \mathbf{E}[X_s^{(3)}], \mathbf{E}[X_s^{(4)}]) = (10, 12, 14, 16)$ .

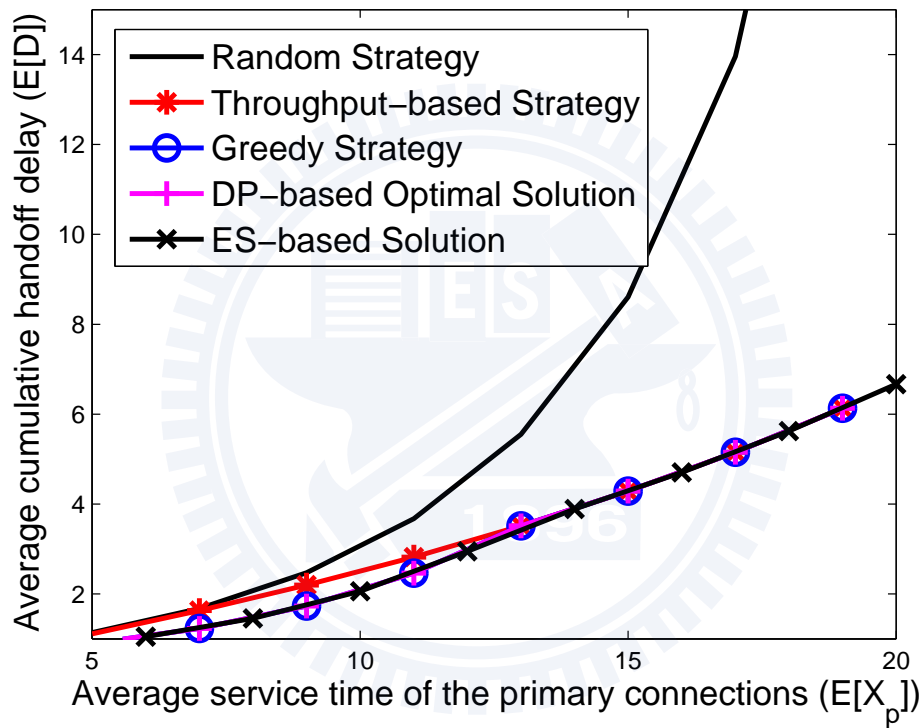
Figure 6.4: Effect of the average service time  $\mathbf{E}[X_s]$  and the arrival rate  $\lambda_s$  of the secondary users' connections on the cumulative handoff delay of the newly arriving secondary user's connection for  $(\lambda_p^{(1)}, \lambda_p^{(2)}, \lambda_p^{(3)}, \lambda_p^{(4)}) = (0.019, 0.02, 0.02, 0.02)$  and  $\mathbf{E}[X_p^{(k)}] = 15$  when  $1 \leq k \leq 4$ .

### 6.5.3 Effects of Traffic Statistics of Existing Primary Users' Connections

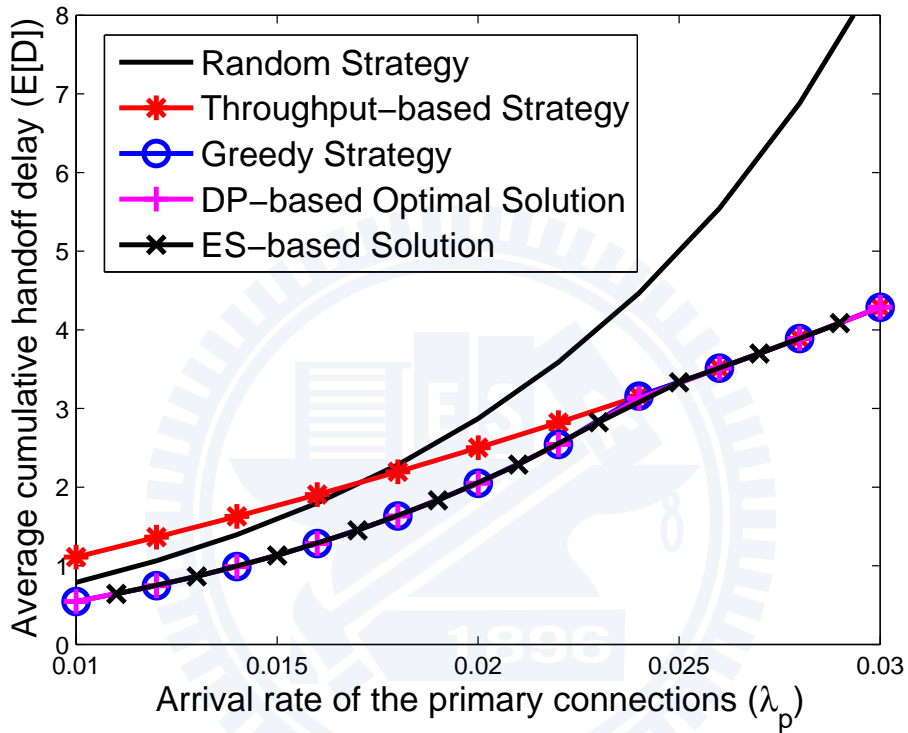
Figure 6.5 shows the effects of the average service time  $\mathbf{E}[X_p]$  and the arrival rate  $\lambda_p$  of the primary users' connections on the cumulative handoff delay of the newly arriving secondary user's connection. We consider that  $\lambda_s^{(k)} = \lambda_s$  and  $\mathbf{E}[X_s^{(k)}] = \mathbf{E}[X_s]$  for  $1 \leq k \leq 4$  as well as the service time  $\chi_s$  is geometrically distributed and  $\mathbf{E}[\chi_s] = 10$ . In Fig. 6.5(a), we assume that  $\mathbf{E}[X_p^{(k)}] = \mathbf{E}[X_p]$  for  $1 \leq k \leq 4$ . We can find the following:

- For all methods, the cumulative handoff delay increases as  $\mathbf{E}[X_p]$  increases because a larger value of  $\mathbf{E}[X_p]$  results in heavier traffic load.
- For the throughput-orientated strategy, the greedy strategy, and the optimal solution, their cumulative handoff delay at various  $\mathbf{E}[X_p]$  will ultimately converge to the same value as shown in the region of  $\mathbf{E}[X_p] \geq 13$  in Fig. 6.5(a). In the region, the handoff delay is only related to the busy period  $\mathbf{E}[Y_p]$  and uncorrelated to the value of  $\mathbf{E}[X_s]$  because the interrupted secondary users always stay on the current operating channel when  $\mathbf{E}[X_p] \geq 13$ .

Note that we can have the similar conclusions in Fig. 6.5(b), where  $\lambda_p^{(k)} = \lambda_p$  for  $1 \leq k \leq 4$ .



(a) Effect of the average service time  $\mathbf{E}[X_p]$  on the cumulative handoff delay  $\mathbf{E}[D]$ , where  $(\lambda_p^{(1)}, \lambda_p^{(2)}, \lambda_p^{(3)}, \lambda_p^{(4)}) = (0.02, 0.025, 0.03, 0.035)$ .



(b) Effect of the arrival rate  $\lambda_p$  on the cumulative handoff delay  $\mathbf{E}[D]$ , where  $(\mathbf{E}[X_p^{(1)}], \mathbf{E}[X_p^{(2)}], \mathbf{E}[X_p^{(3)}], \mathbf{E}[X_p^{(4)}]) = (10, 12, 14, 16)$ .

Figure 6.5: Effect of the average service time  $\mathbf{E}[X_p]$  and the arrival rate  $\lambda_p$  of the primary users' connections on the cumulative handoff delay of the newly arriving secondary user's connection for  $\lambda_s^{(k)} = 0.01$  and  $\mathbf{E}[X_s^{(k)}] = 15$  when  $1 \leq k \leq 4$ .

# Chapter 7

## Reactive Spectrum Handoff

As discussed in Chapter 5, spectrum handoff mechanisms can be categorized as either the proactive spectrum handoff or the reactive spectrum handoff schemes. In this chapter, we focus on the modeling technique and performance analysis for the reactive spectrum handoff scheme. Compared to the proactive spectrum handoff scheme that the preselected target channel may no longer be available at the instant that spectrum handoff procedures are initiated, the reactive spectrum handoff may have shorter handoff delay because it can reliably find an idle channel through spectrum sensing. Nevertheless, the reactive spectrum handoff scheme needs the sensing time to search the idle channels. In addition, it also needs the handshaking time to achieve a consensus on the target channel between the transmitter and receiver of a secondary connection. Hence, one important issue for the reactive spectrum handoff scheme is to characterize the effects of the sensing time and the handshaking time on the handoff delay. Obviously, when the sensing time and the handshaking time is too large, the reactive spectrum handoff is worse than the proactive spectrum handoff in terms of the extended data delivery time.

The goal of this chapter is to investigate the effects of spectrum handoffs

on the channel utilization and the extended data delivery time of the secondary users' connections with various traffic arrival rates and service time distributions. We consider the three key design features for spectrum handoff, consisting of (1) heterogeneous arrival rates of the primary users at different channels, where various channels have different traffic arrival rates of the primary users because these channels may belong to different primary system operators; (2) various arrival rates of the secondary users at different channels, where the arrival rates can be determined by the initial operating channel selection mechanisms [79]; and (3) handoff processing time, resulting from the sensing time, the handshaking time, and the channel switching time. How to model the channel utilization at each channel and the extended data delivery time in the context of multiple handoffs is challenging since the operating channels for multiple handoffs are selected according to the channel occupancy states at the moments of link transitions. To the best of our knowledge, an analytical model for characterizing all the three features for multiple handoffs has rarely been seen in the literature. The contributions of this chapter are summarized in the following:

- First, The preemptive resume priority (PRP) M/G/1 queueing network model is proposed to characterize the channel usage behaviors of CR networks. Based on this queueing model, we can evaluate the channel utilizations of different channels under various traffic arrival rates and service time distributions.
- Next, a state diagram is developed to characterize the effect of multiple handoff delay on the extended data delivery time of the secondary connections. Then, we can evaluate how long the extended data delivery time is prolonged due to multiple spectrum handoffs.

## 7.1 System Model

### 7.1.1 Assumptions

In this chapter, we consider the spectrum handoff protocol presented in [95]. When the spectrum handoff procedures are initiated, the secondary users must spend  $\tau$  slots on spectrum sensing to find the idle channels. Note that if more than one channel is assessed as idle, the interrupted secondary user will randomly select one idle channel from all idle channels to be its target channel for spectrum handoff. Here, we assume that this random selection follows the uniform distribution. Furthermore, the interrupted secondary user will stay on the current operating channel if all channels are busy. Next, the handshaking time of  $t_h$  slots is spent in order to achieve a consensus on the target channel between the transmitter and the receiver of a secondary connection. Hence, when a secondary user changes its operating channel to another channel, the total processing time for executing spectrum handoff procedures is  $\delta_c \triangleq \tau + t_h + t_s$  where  $t_s$  (slots) is the channel switching time. On the other hand, if the secondary user stays on the current operating channel, the total processing time is  $\delta_s \triangleq \tau + t_h$ .

### 7.1.2 Illustrative Example of Reactive Multiple Handoffs with Multiple Interruptions

A secondary user's connection may experience multiple interruption requests from the primary users during its transmission period. Because these interruptions result in multiple handoffs, a series of target channels is selected by spectrum sensing, called the *target channel sequence* in this dissertation. Fig. 7.1 shows an example that three spectrum handoffs occur during the



transmission period of the secondary connection  $SC_A$ , where  $SC_A$ 's initial (default) channel is Ch3. We assume that the transmitter of  $SC_A$  wants to establish a connection flow with 30 slots to the corresponding receiver. Its extended data delivery time is denoted by  $T$ . Furthermore,  $D_i$  is the handoff delay of the  $i^{th}$  interruption. Here, the handoff delay is defined as the duration from the instant that transmission is interrupted until the instant that the unfinished transmission is resumed. Then, the transmission process with multiple handoffs is described as follows:

1. In the beginning,  $SC_A$  is established at its default channel Ch3. When an interruption event occurs,  $SC_A$  performs spectrum sensing to search the idle channel for spectrum handoff.
2. At the first interruption,  $SC_A$  changes its operating channel to the idle channel Ch2 from Ch3. Thus, the handoff delay  $D_1$  is  $\delta_c$ .
3. At the second interruption,  $SC_A$  stays on its current operating channel Ch2 because all channels are busy.  $SC_A$  cannot be resumed until all the high-priority primary connections at Ch2 finish their transmissions. In this case, the handoff delay  $D_2$  is the sum of  $\delta_s$  and the duration from the time instant that Ch2 is used by the primary users' connections until the time instant that the high-priority queue becomes empty. This duration (denoted by  $Y_p^{(2)}$ ) is called the *busy period* resulting from the transmissions of multiple primary users' connections at Ch2.
4. At the third interruption,  $SC_A$  finds both Ch1 and Ch3 are idle. Then,  $SC_A$  randomly selects one channel to be the target channel. In this example,  $SC_A$  selects Ch1 to be its target channel. Note that the handoff delay  $D_3$  in this case is  $\delta_c$ .

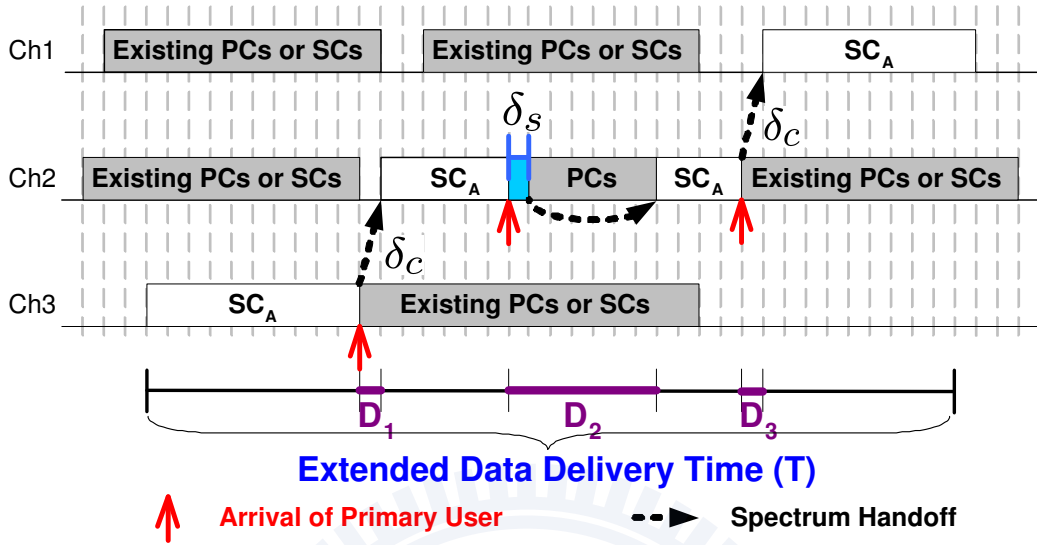


Figure 7.1: An example of transmission process for the secondary connection  $SC_A$ , where  $T$  is the extended data delivery time of  $SC_A$  and  $D_i$  is the handoff delay of the  $i^{th}$  interruption. The gray areas indicate that the channels are occupied by the existing primary connections (PCs) or secondary connections (SCs). Because  $SC_A$  is interrupted three times in total, the overall data connection is divided into four segments. Note that  $D_1 = \delta_c$ ,  $D_2 = \delta_s$ , and  $D_3 = \delta_c$ .

5. Finally,  $SC_A$  is completed on Ch3.

Hence,  $SC_A$ 's *target channel sequence* is (Ch2, Ch2, Ch1) in this example.

## 7.2 Analytical Model

We use the PRP M/G/1 queueing network model proposed in Chapter 3 to characterize the channel usage behaviors of a CR network. Let  $X_s^{(\eta)}$  (slots/arrival) be the service time of the secondary connections whose default channels are channel  $\eta$  and let  $f_s^{(\eta)}(x)$  be the probability density func-

tion (pdf) of  $X_s^{(\eta)}$ . Figure 7.2 shows an example of the PRP M/G/1 queueing network model with three channels. The traffic flows of the primary connections and the secondary connections are directly connected to the high-priority queue and the low-priority queue, respectively. A secondary connection will be interrupted when the primary connection appears. The interrupted secondary connection can decide its target channel for spectrum handoff according to the instantaneous spectrum sensing outcomes. Note that the required time for spectrum sensing is modeled in  $\boxed{\text{S}}$ . It can be regarded as a tapped delay line or a server with constant service time, which equals to the handoff processing time. In the proposed queueing network, the interrupted secondary connection can either stay on its current channel or change to another channel through different feedback paths. If the interrupted secondary connection chooses to stay on its current operating channel, its remaining data will be connected to the head of the low-priority queue of its current operating channel. On the other hand, if the decision is to change its operating channel, the remaining data of the interrupted secondary connection can be connected to the empty low-priority queue of the selected channel. In the figure,  $\oplus$  represents that the traffic of the interrupted secondary connection is merged. Furthermore, when the interrupted secondary connection transmits the remaining data on the target channel, it may be interrupted again. Hence, this model can incorporate the effects of multiple interruptions.

### 7.2.1 Notations

Now, we define some notations as follows. We call the secondary connection that has experienced  $i$  interruptions, where  $i \geq 0$ , the type- $i$  secondary connection. Firstly, we consider the type- $i$  secondary connections whose default

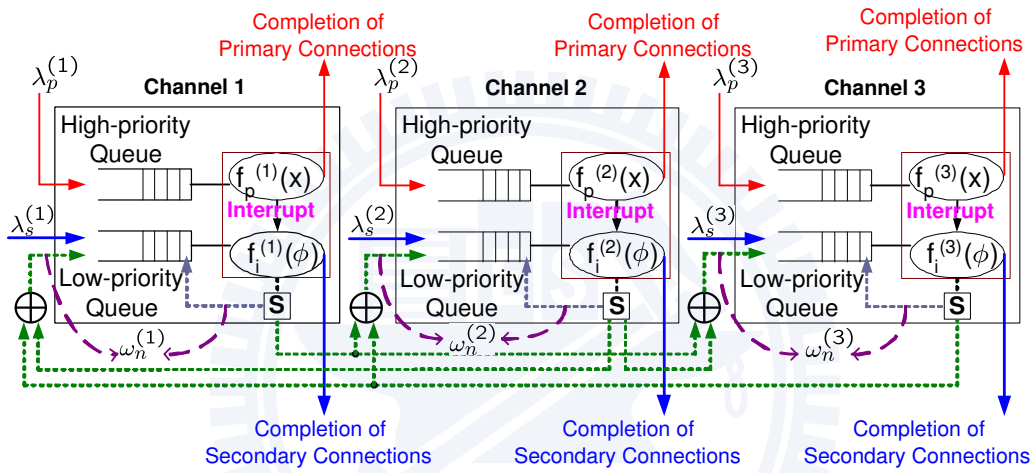


Figure 7.2: The PRP M/G/1 queueing network model with three channels where  $\lambda_p^{(k)}$ ,  $\lambda_s^{(k)}$ , and  $\omega_n^{(k)}$  are the arrival rates of the primary connections, the secondary connections, and the type- $n$  secondary connections ( $n \geq 1$ ) at channel  $k$ . Note that  $\lambda_s^{(k)} = \omega_0^{(k)}$ . Furthermore,  $f_p^{(k)}(x)$  and  $f_i^{(k)}(\phi)$  are the probability density functions (pdfs) of  $X_p^{(k)}$  and  $\Phi_i^{(k)}$ , respectively.

channels are the channel  $\eta$ . Two more important system parameters  $\omega_{i,\eta}^{(k)}$  and  $\Phi_{i,\eta}^{(k)}$  are defined as follows:

- $\omega_{i,\eta}^{(k)}$  is the arrival rate of the considered secondary connections at channel  $k$ . Note that  $\omega_{0,\eta}^{(\eta)} = \lambda_s^{(\eta)}$ . How to derive  $\omega_{i,\eta}^{(k)}$  from the four traffic parameters is discussed in Section 7.3.
- $\Phi_{i,\eta}^{(k)}$  is the effective service time of the considered secondary connections at channel  $k$ . That is,  $\Phi_{i,\eta}^{(k)}$  is the considered secondary connection's transmission duration between the  $i^{\text{th}}$  and the  $(i+1)^{\text{th}}$  interruptions at channel  $k$ . In Section 7.3, we will discuss how to derive  $\mathbf{E}[\Phi_{i,\eta}^{(k)}]$  from the four traffic parameters.

Next, let  $\omega_i^{(k)}$  and  $\Phi_i^{(k)}$  be the arrival rate and the effective service time of the type- $i$  secondary connections at channel  $k$ , respectively. We can have

$$\omega_i^{(k)} = \sum_{\eta=1}^M \omega_{i,\eta}^{(k)} , \quad (7.1)$$

and

$$\mathbf{E}[\Phi_i^{(k)}] = \sum_{\eta=1}^M \frac{\omega_{i,\eta}^{(k)}}{\omega_i^{(k)}} \mathbf{E}[\Phi_{i,\eta}^{(k)}] , \quad (7.2)$$

respectively.

Finally, we denote  $\rho_p^{(k)}$  and  $\rho_i^{(k)}$  as the channel busy probabilities resulting from the transmissions of the primary connections and the type- $i$  secondary connections whose current operating channels are the channel  $k$ , respectively. Then, in an  $M$ -channel network, we can have

$$\rho_p^{(k)} = \lambda_p^{(k)} \mathbf{E}[X_p^{(k)}] , \quad (7.3)$$

and

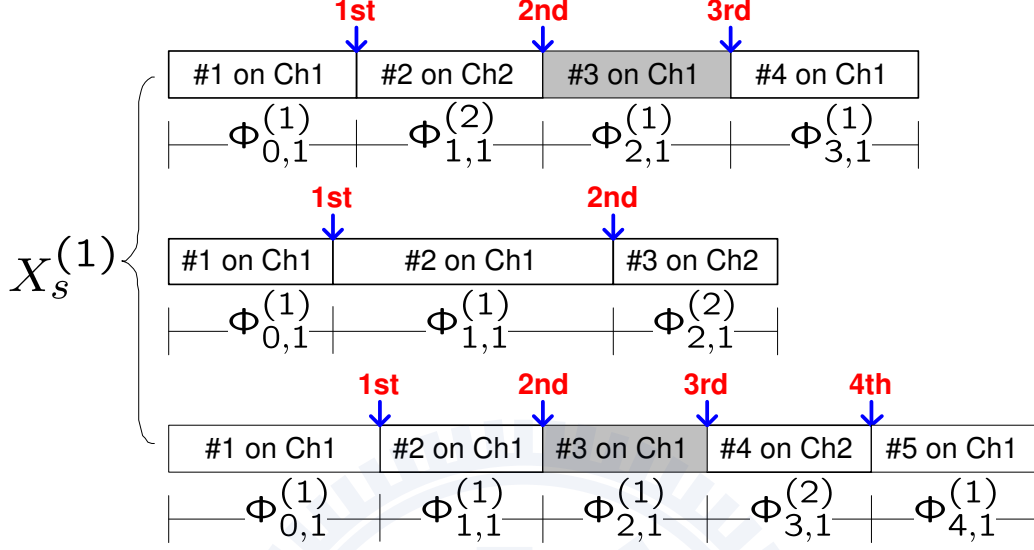
$$\rho_i^{(k)} = \omega_i^{(k)} \mathbf{E}[\Phi_i^{(k)}] = \sum_{\eta=1}^M \omega_{i,\eta}^{(k)} \mathbf{E}[\Phi_{i,\eta}^{(k)}] , \quad (7.4)$$

respectively. Furthermore, the busy probability of channel  $k$  (denoted by  $\rho^{(k)}$ ) shall satisfy the following constraint:

$$\rho^{(k)} \equiv \rho_p^{(k)} + \sum_{i=0}^{\infty} \rho_i^{(k)} < 1 \quad , \quad (7.5)$$

where  $1 \leq k \leq M$ . Note that  $\rho^{(k)}$  can be also interpreted as the utilization factor of channel  $k$ .

Figure 7.3 illustrates the physical meaning of random variable  $\Phi_{i,\eta}^{(k)}$ . Consider a two-channel network with the service time of the secondary connections  $X_s^{(1)}$  and  $X_s^{(2)}$  at the channels 1 and 2, respectively. In the channel 1, random variable  $X_s^{(1)}$  are generated three times in Fig. 7.3(a). Similarly, Fig. 7.3(b) shows the three realizations of  $X_s^{(2)}$  for the channel 2. Each secondary connection is divided into many segments due to multiple primary users' interruptions. For example, the first secondary connection in Fig. 7.3(a) is divided into four segments because it encounters three interruptions in total. The first, second, third, and fourth segments are transmitted at channels 1, 2, 1, and 1, respectively. Thus, this secondary connection's default channel is Ch1 and its target channel sequence is (Ch2, Ch1, Ch1). In Fig. 7.3(a), random variables  $\Phi_{2,1}^{(1)}$ , one of the gray regions, represents the transmission duration between the 2<sup>nd</sup> and the 3<sup>rd</sup> interruptions at the channel 1 for the secondary connection whose default channel is the channel 1. Similarly, random variables  $\Phi_{2,2}^{(1)}$ , one of the gray regions in Fig. 7.3(b), represents the transmission duration between the 2<sup>nd</sup> and the 3<sup>rd</sup> interruptions at the channel 1 for the secondary connection whose default channel is the channel 2. Furthermore, random variable  $\Phi_2^{(1)}$ , one of the gray regions in Fig. 7.3, represents the transmission duration of a secondary connection between the 2<sup>nd</sup> and the 3<sup>rd</sup> interruptions at channel 1. That is,  $\Phi_2^{(1)}$  is one of the third segments of the first and the third secondary connections in Fig. 7.3(a) as well



(a) Three realizations of  $X_s^{(1)}$ .

as the second secondary connection in Fig. 7.3(b).

### 7.3 Analysis of Channel Utilization Factor

Based on the proposed PRP M/G/1 queueing network model, we can evaluate many performance measures of CR networks with various traffic parameters. In this section, we show how to evaluate the channel utilization factor  $\rho^{(k)}$ . Referring to (7.5), for each channel  $k$  ( $1 \leq k \leq M$ ), it follows that

$$\rho^{(k)} = \lambda_p^{(k)} \mathbf{E}[X_p^{(k)}] + \sum_{i=0}^{\infty} \left[ \sum_{\eta=1}^M \omega_{i,\eta}^{(k)} \mathbf{E}[\Phi_{i,\eta}^{(k)}] \right]. \quad (7.6)$$

Note that  $\rho^{(k)}$  is unrelated to channel sensing time  $\tau$ , channel notification time  $t_n$ , and channel switching time  $t_s$ . In (7.6),  $\lambda_p^{(k)}$  and  $\mathbf{E}[X_p^{(k)}]$  are system parameters and can be known in advance. In the following, we will show how to derive  $\omega_{i,\eta}^{(k)}$  and  $\mathbf{E}[\Phi_{i,\eta}^{(k)}]$ .

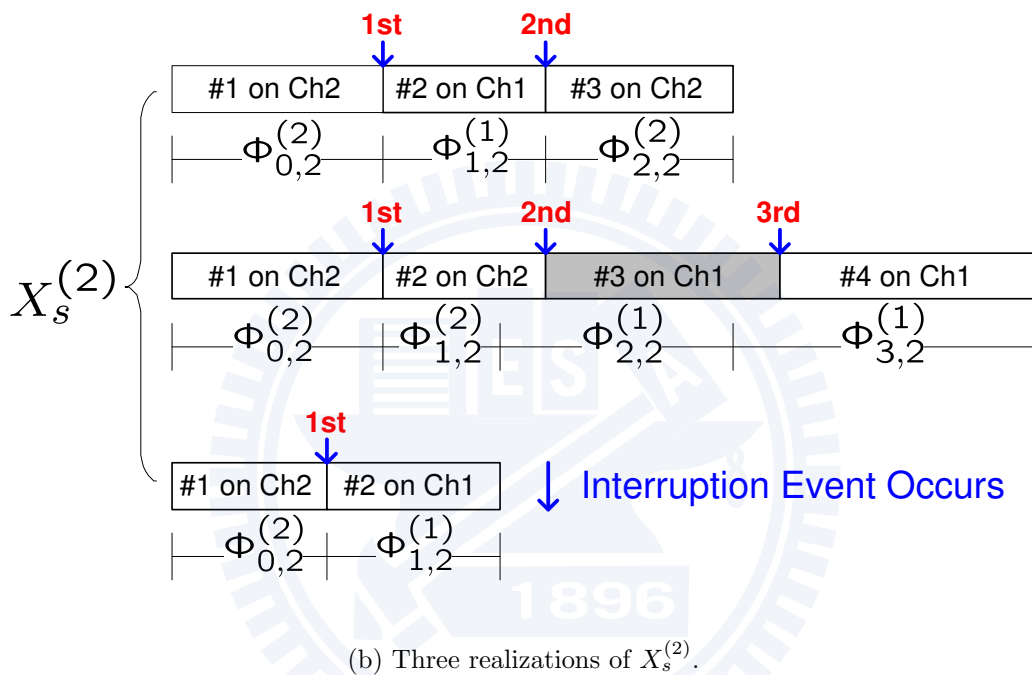


Figure 7.3: Illustration of the physical meaning of random variable  $\Phi_i^{(k)}$ . For example,  $\Phi_2^{(1)}$  is one of the third segments (gray areas) of the first and the third secondary connections in (a) as well as the second secondary connection in (b). Note that the third secondary connection in (b) does not have the third segment because it is interrupted only once.



### 7.3.1 Derivations of $\omega_{i,\eta}^{(k)}$ and $\mathbf{E}[\Phi_{i,\eta}^{(k)}]$

Without loss of generality, we consider a secondary connection whose default channel is channel  $\eta \triangleq s_0$  in the following discussions. Its target channel sequence is denoted by  $\mathbf{S}^{(\eta)} \triangleq (S_{1,\eta}, S_{2,\eta}, S_{3,\eta}, \dots)$ , where  $S_{i,\eta}$  is the target channel at the  $i^{\text{th}}$  interruption. Note that  $S_{i,\eta}$  is a random variable for each  $i \geq 1$ . It is decided according to the instantaneous sensing results after the  $i^{\text{th}}$  interruption event occurs. Thus,  $\mathbf{S}^{(\eta)}$  is a random sequence. Based on the definitions of these notations,  $\omega_{i,\eta}^{(k)}$  and  $\mathbf{E}[\Phi_{i,\eta}^{(k)}]$  can be derived from the Propositions 8 and 9, respectively. Then, the channel utilization  $\rho^{(k)}$  can be obtained.

**Lemma 5.** *Let  $p_{i,\eta}^{(k)}$  be the probability that the considered type- $i$  secondary connection is interrupted again at channel  $k$ . It follows that*

$$p_{i,\eta}^{(k)} = \lambda_p^{(k)} \mathbf{E}[\Phi_{i,\eta}^{(k)}] . \quad (7.7)$$

Proof of this lemma can be found in [103].

**Definition 6.** *Let  $\mathbf{s}_n \triangleq (s_1, s_2, s_3, \dots, s_n)$  be any target channel sequence which has  $n$  elements. That is,  $\mathbf{s}_n \in \Omega^n$ , where  $\Omega = \{1, 2, \dots, M\}$ .*

**Claim 7.** *Denote  $\Pr[S_{i,\eta} = s_i | S_{i-1,\eta} = s_{i-1}]$  as the probability that the considered secondary connection will select the channel  $s_i$  to be its target channel when an interruption event occurs at the channel  $s_{i-1}$ . Then, we have*

$$\begin{aligned} & \Pr[S_{i,\eta} = s_i | S_{i-1,\eta} = s_{i-1}] \\ = & \begin{cases} \prod_{1 \leq j \leq M, j \neq s_{i-1}} \rho^{(j)} & , \quad s_i = s_{i-1} \\ (1 - \rho^{(s_i)}) \sum_{\forall \mathbb{A} \subseteq \Omega / \{s_{i-1}, s_i\}} \left[ \frac{1}{1 + |\mathbb{A}|} \prod_{\forall v \in \mathbb{A}} (1 - \rho^{(v)}) \prod_{\forall v' \notin \mathbb{A}} \rho^{(v')} \right] & , \quad s_i \neq s_{i-1} \end{cases} , \end{aligned} \quad (7.8)$$

where  $1 \leq i \leq N$  and  $N$  is the total number of interruptions for the considered secondary connection during its transmission period.

*Proof.* When an interruption event occurs at channel  $s_{i-1}$ , the type- $(i-1)$  secondary connection must search its target channel  $s_i$  for spectrum handoff through spectrum sensing. The probability that one channel is selected to be the target channel is related to the channel busy probabilities of all channels. If all channels are busy, the type- $(i-1)$  secondary connection will stay on its current operating channel (i.e.,  $s_i = s_{i-1}$ ). On the other hand, if there exists one idle channel, the type- $(i-1)$  secondary connection will change to this idle channel from channel  $s_i$ . Note that this type- $(i-1)$  secondary connection will randomly and uniformly select one channel from all idle channels to be its target channel if more than one channel is idle. From these observations, we can have (7.8).  $\square$

**Proposition 8.** At channel  $k'$ , denote  $\omega_{i,\eta}^{(k \rightarrow k')}$  as the arrival rate of the type- $i$  secondary connections which be redirected from channel  $k$ . Then, we have

$$\omega_{i+1,\eta}^{(k')} = \sum_{k=1}^M \omega_{i+1,\eta}^{(k \rightarrow k')} , \quad (7.9)$$

where

$$\omega_{i+1,\eta}^{(k \rightarrow k')} = \omega_{i,\eta}^{(k)} \cdot p_{i,\eta}^{(k)} \Pr[S_{i+1,\eta} = k' | S_{i,\eta} = k] . \quad (7.10)$$

*Proof.* When a type- $i$  secondary connection is interrupted at channel  $k$ , it will turn into a new arrival of the type- $(i+1)$  secondary connection at channel  $k'$ . That is, the traffic loads of the type- $(i+1)$  secondary connections at channel  $k'$  can come from the remaining traffic loads of the type- $i$  secondary connections at any one of  $M$  channels. Thus, the arrival rate of the type- $(i+1)$  secondary connections at channel  $k'$  can be expressed as (7.9).

The values of  $\omega_{i+1,\eta}^{(k \rightarrow k')}$  can be evaluated as follows. For the type- $i$  secondary connection at the channel  $k$ , it will be interrupted again with probability  $p_{i,\eta}^{(k)}$ . When an interruption event occurs at the channel  $k$ , the type- $i$  secondary connection must search its target channel for spectrum handoff through spectrum sensing. Without loss of generality, we assume that the channel  $k'$  is selected to be the target channel. This situation occurs with probability  $\Pr[S_{i+1,\eta} = k' | S_{i,\eta} = k]$ . When channel  $k'$  is selected, the type- $i$  secondary connection will turn into a new arrival of the type- $(i+1)$  secondary connection at channel  $k'$ . Hence, we can have (7.10).  $\square$

**Proposition 9.** *Based on the proposed PRP M/G/1 queueing network model, we can derive the closed-form expression for  $\mathbf{E}[\Phi_{i,\eta}^{(k)}]$ .*

*Proof.* According to the total probability principle, we have

$$\mathbf{E}[\Phi_{i,\eta}^{(k)}] = \sum_{N=1}^L \sum_{\forall \mathbf{s}_N \in \Omega^N} \Pr[\mathbf{S}^{(\eta)} = \mathbf{s}_N] \mathbf{E}[\Phi_{i,\eta}^{(k)} | \mathbf{S}^{(\eta)} = \mathbf{s}_N], \quad (7.11)$$

where  $L$  is the maximum number of interruptions among all secondary users' connections, i.e., the maximum length of the target channel sequence. Based on the proposed queueing network, we can derive  $\mathbf{E}[\Phi_{i,\eta}^{(k)} | \mathbf{S}^{(\eta)} = \mathbf{s}_N]$  for any given  $\mathbf{s}_N$  can be derived when  $\lambda_p^{(k)}$ ,  $\lambda_s^{(k)}$ ,  $f_p^{(k)}(x)$ , and  $f_s^{(k)}(x)$  are given. The derivation detail can be found in [103]. As to  $\Pr[\mathbf{S}^{(\eta)}]$ , it can be expressed as follows:

$$\Pr[\mathbf{S}^{(\eta)} = \mathbf{s}_N] = (1 - p_{N,\eta}^{(s_N)}) \prod_{i=1}^N \Pr[S_{i,\eta} = s_i | S_{i-1,\eta} = s_{i-1}], \quad (7.12)$$

where  $S_{0,\eta}$  is the default channel  $s_0 = \eta$ . By substituting (7.7) and (7.8) into (7.12), the value of  $\Pr[\mathbf{S}^{(\eta)} = \mathbf{s}_N]$  can be obtained.  $\square$

### 7.3.2 An Example for the Exponentially Distributed Service Time

Now, we show how to derive channel utilization factor in the following special case. We assume that all secondary users' connections have the same service time distribution. Hence, we have  $f_s^{(k)}(x) = f_s(x)$  and  $\mathbf{E}[X_s^{(k)}] = \mathbf{E}[X_s]$ , where  $1 \leq k \leq M$ . Furthermore, because this dissertation focuses on the latency-sensitive traffic for the secondary users, it is reasonable to assume that the service time  $X_s$  is exponentially distributed (page 135 in [86]). Hence, we have  $f_s(x) = \mu_s e^{-\mu_s x}$ , where  $\mu_s = \frac{1}{\mathbf{E}[X_s]}$ .

Based on these traffic parameters, we derive  $\rho^{(k)}$  as follows. Firstly, referring to [103] and the Proposition 9, we can have

$$\mathbf{E}[\Phi_{i,\eta}^{(k)}] = \frac{1}{\lambda_p^{(k)} + \mu_s} . \quad (7.13)$$

Secondly, from (7.7), it follows that

$$p_{i,\eta}^{(k)} = \lambda_p^{(k)} \mathbf{E}[\Phi_{i,\eta}^{(k)}] = \frac{\lambda_p^{(k)}}{\lambda_p^{(k)} + \mu_s} . \quad (7.14)$$

Then, according to the Proposition 8, we can derive  $\omega_{i,\eta}^{(k')}$  as follows:

$$\omega_{i,\eta}^{(k')} = \sum_{k=1}^M \frac{\lambda_p^{(k)}}{\lambda_p^{(k)} + \mu_s} \cdot \omega_{i-1,\eta}^{(k)} \cdot \Pr[S_{i,\eta} = k' | S_{i-1,\eta} = k] . \quad (7.15)$$

Note that  $\omega_{i,\eta}^{(k')}$  is a function of  $\rho^{(k)}$  because  $\Pr[S_{i,\eta} = k' | S_{i-1,\eta} = k]$  is a function of  $\rho^{(k)}$ . Furthermore, according to (7.6), we can find that  $\rho^{(k)}$  is a function of  $\omega_{i,\eta}^{(k)}$ . Hence, we can determine  $\omega_{i,\eta}^{(k')}$  and  $\rho^{(k)}$  by solving (7.6) and (7.15) iteratively.

## 7.4 Analysis of Extended Data Delivery Time

In this section, we show how to evaluate the extended data delivery time, which is an important performance measure for the latency-sensitive traffic of the secondary connections. Without loss of generality, we consider the secondary connection whose default channel is the channel  $\eta$  in the following discussions. Its extended data delivery time consists of the original service time  $X_s^{(\eta)}$  and the cumulative delay resulting from multiple handoffs  $\mathbf{E}[D^{(\eta)}]$ . Let  $\mathbf{E}[D|\mathbf{S}^{(\eta)} = \mathbf{s}_N]$  be its cumulative handoff delay when its target channel is  $\mathbf{s}_N$ . Then, its average extended data delivery time (denoted by  $\mathbf{E}[T^{(\eta)}]$ ) can be expressed as

$$\begin{aligned} \mathbf{E}[T^{(\eta)}] &= \mathbf{E}[X_s^{(\eta)}] + \mathbf{E}[D^{(\eta)}] \\ &= \mathbf{E}[X_s^{(\eta)}] + \sum_{N=0}^L \sum_{\forall \mathbf{s}_N \in \Omega^N} \Pr\{\mathbf{S}^{(\eta)} = \mathbf{s}_N\} \mathbf{E}[D|\mathbf{S}^{(\eta)} = \mathbf{s}_N] \end{aligned} \quad (7.16)$$

Hence, in order to calculate  $\mathbf{E}[T^{(\eta)}]$ , we will show how to evaluate  $\Pr\{\mathbf{S}^{(\eta)} = \mathbf{s}_N\}$  and  $\mathbf{E}[D|\mathbf{S}^{(\eta)} = \mathbf{s}_N]$  in the following.

### 7.4.1 Derivations of $\Pr\{\mathbf{S}^{(\eta)} = \mathbf{s}_N\}$ and $\mathbf{E}[D|\mathbf{S}^{(\eta)} = \mathbf{s}_N]$

In order to evaluate  $\Pr\{\mathbf{S}^{(\eta)} = \mathbf{s}_N\}$  and  $\mathbf{E}[D|\mathbf{S}^{(\eta)} = \mathbf{s}_N]$ , a state diagram is developed by characterizing the evolutions of the target channel sequence and the corresponding cumulative handoff delay for the secondary connection. The proposed state diagram is a two-dimensional chain. Because the considered secondary's default channel is  $\eta$ , the initial state of this state diagram is  $(\eta, 0)$ . Next, the state  $(k, i)$ , where  $1 \leq k \leq M$ , represents that the channel  $k$  is selected for the target channel at the  $i^{\text{th}}$  interruption. The state  $(M+1, i)$  represents that the secondary user can finish its transmission after the  $(i-1)^{\text{th}}$  interruption, and thus the state  $(M+1, i)$  is the ending of state

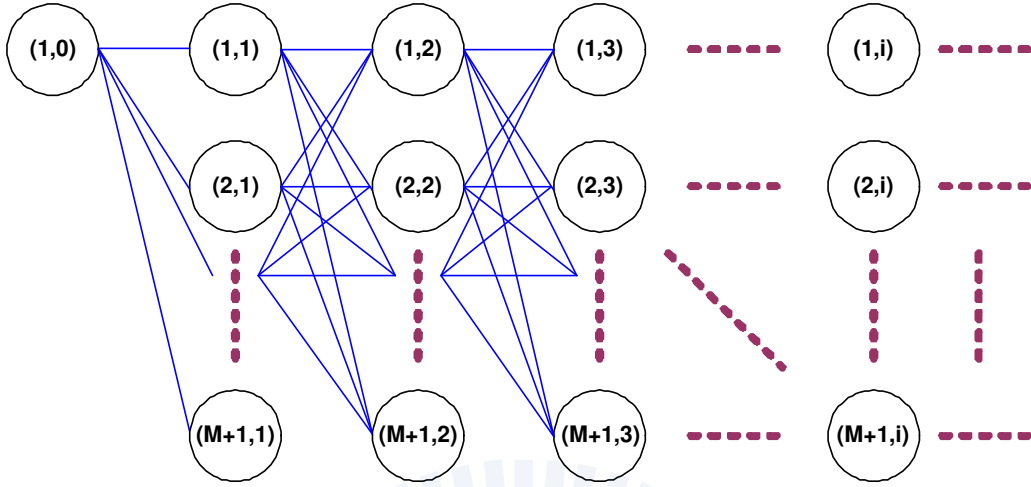


Figure 7.4: State diagram of target channel sequence for a secondary connection, where default channel  $\eta = 1$ .

transition. Note that the state transition occurs only at two adjacent states. Specifically, a transition link from  $(k, i)$  to  $(k', i')$  exists if  $i' = i + 1$ , and vice versa. An example of state diagram is shown in Fig. 7.4, where  $\eta = 1$ .

In this state diagram, the state transition path can be regarded as a target channel sequence. For example, for a target channel sequence  $\mathbf{s}_n \triangleq (s_1, s_2, s_3, \dots, s_n)$ , the corresponding state transition path  $(\eta, 0) \rightarrow (s_1, 1) \rightarrow (s_2, 2) \rightarrow (s_3, 3) \rightarrow \dots \rightarrow (s_n, n) \rightarrow (M + 1, n + 1)$ . Hence, calculating the average cumulative handoff delay over all possible target channel sequences can be regarded as calculating the cumulative transition cost over all possible state transition paths. In the following, we show how to design the state transition probability and cost in the developed state diagram.

### State Transition Probability

When an interruption event occurs, the interrupted secondary connection must search its target channel for spectrum handoff through spectrum sens-

ing. The probability that each channel is selected to be the target channel is related to the statistics of channel occupancy. Let  $P[(k', i)|(k, i - 1)]$  be the transition probability from states  $(k, i - 1)$  to  $(k', i)$ . At channel  $k$ , the considered secondary connection may do not experience interruption again and can finish its transmission at channel  $k$ . In this case, the transition from states  $(k, i - 1)$  to  $(M + 1, i)$  will occur. On the other hand, the transition from states  $(k, i - 1)$  to  $(k', i)$  where  $1 \leq k' \leq M$  will occur when the considered secondary connection is interrupted again at channel  $k$ . Thus,  $P[(k', i)|(k, i - 1)]$  can be expressed as follows:

$$P[(k', i)|(k, i - 1)] = \begin{cases} 1 - p_{i-1, \eta}^{(k)} & , \quad k' = M + 1 \\ p_{i-1, \eta}^{(k)} \cdot \Pr[S_{i, \eta} = k' | S_{i-1, \eta} = k] & , \quad k' \neq M + 1 \end{cases} . \quad (7.17)$$

### State Transition Cost

The cost of state transition is defined as the handoff delay of the interrupted secondary connection. The handoff delay from channels  $k$  to  $k'$  depends on the state of channel occupancy. Recall that  $\delta_s$  and  $\delta_c$  are the total processing time for executing spectrum handoff procedure when the secondary users stay on the current channel and change to another channel, respectively. If one idle channel exists after spectrum sensing, the interrupted secondary connection will change to this idle channel. Hence, the handoff delay in this case is  $\delta_c$ . Furthermore, if all channels are busy, the interrupted secondary connection will stay on its current operating channel (i.e.,  $k = k'$ ). Hence, the expected handoff delay is the sum of  $\delta_s$  and the duration from the time instant that channel  $k$  is used by the primary connections until the time instant that channel  $k$  becomes idle. This duration is called the *busy period* resulting from the transmissions of multiple primary connections at channel

$k$  and denoted by  $Y_p^{(k)}$ . Let  $C[k'|k]$  be the transition cost from states  $k$  to  $k'$  in the state diagram. Then, we can have

$$C[k'|k] = \begin{cases} 0 & , \quad k' = M + 1 \\ \delta_s + \mathbf{E}[Y_p^{(k)}] & , \quad k' = k \\ \delta_c & , \quad \text{others} \end{cases} . \quad (7.18)$$

Note that, referring to [103], we can have

$$\mathbf{E}[Y_p^{(k)}] = \frac{\mathbf{E}[X_p^{(k)}]}{1 - \lambda_p^{(k)} \mathbf{E}[X_p^{(k)}]} . \quad (7.19)$$

From this developed state diagram,  $\Pr\{\mathbf{S}_N^{(\eta)} = \mathbf{s}_N\}$  and  $\mathbf{E}[D|\mathbf{S}^{(\eta)} = \mathbf{s}_N]$  can be expressed as follows:

$$\Pr\{\mathbf{S}_N^{(\eta)} = \mathbf{s}_N\} = P[(M + 1, N + 1)|(s_N, N)] \prod_{i=0}^{N-1} P[(s_{i+1}, i + 1)|(s_i, i)] , \quad (7.20)$$

and

$$\mathbf{E}[D|\mathbf{S}^{(\eta)} = \mathbf{s}_N] = \sum_{i=0}^N C[s_{i+1}|s_i] . \quad (7.21)$$

Note that (7.20) is equivalent to (7.12). Finally, substituting (7.20) and (7.21) into (7.16), we can obtain the closed-form expression for the extended data delivery time  $\mathbf{E}[T^{(\eta)}]$  of the secondary connections with any service time distribution  $f_s^{(\eta)}$  based on this developed state diagram.

## 7.4.2 An Example for the Exponentially Distributed Service Time

Now, we investigate how to derive the cumulative handoff delay when the secondary connection's service time is exponentially distributed as adopted in Section 7.3.2. Intuitively, we can evaluate the cumulative handoff delay by examining all possible transition paths in the state diagram, which is quite



complex. Fortunately, the derivations of the cumulative handoff delay can be simplified due to the memoryless property of the exponential distribution.

Without loss of generality, we consider the secondary connection whose default channel is the channel  $k$ . Its cumulative handoff delay  $\mathbf{E}[D^{(k)}]$  in (7.16) can be derived as follows. Because the considered secondary connection's service time distribution is the exponential distribution, its remaining service time after an interruption event occurs also follows the identical exponential distribution. Hence, for the secondary connections at state  $(k, i)$  and  $(k', i')$ , they will experience the same cumulative handoff delay and interrupted probability in their remaining transmissions if  $k = k'$ ,  $k \neq M + 1$ , and  $k' \neq M + 1$ .

From the aforementioned discussions, we can re-plot the state diagram expression for the target channel selection as a tree-structured representation as shown in Fig. 7.5, where  $\text{Ch}k$  represents that channel  $k$  is selected for the target channel and the “grounding symbols” represent the endings of state transition. Note that at the second stage of Fig. 7.5, the average cumulative handoff delay of the type-1 secondary connection is equal to  $\mathbf{E}[D^{(k)}]$  when this type-1 secondary connection's current operating channel is the channel  $k$ . Furthermore, because the state transition probability is independent of the the number of interruptions for the secondary connections due to memoryless property, we can have  $P[(k', i + 1)|(k, i)] = P[k'|k]$  for each  $i \geq 0$ . Hence, it follows that

$$\mathbf{E}[D^{(k)}] = P[M + 1|k] \cdot C[M + 1|k] + \sum_{k'=1}^M P[k'|k] \cdot (C[k'|k] + \mathbf{E}[D^{(k')}]) \quad , \quad (7.22)$$

for any  $k$  where  $1 \leq k \leq M$ . Finally, substituting (7.17) and (7.18) into (7.22), we can obtain  $M$  independent equations. Hence, the closed-form expressions for the cumulative handoff delay  $\mathbf{E}[D^{(k)}]$  can be derived by solving these simultaneous equations iteratively.

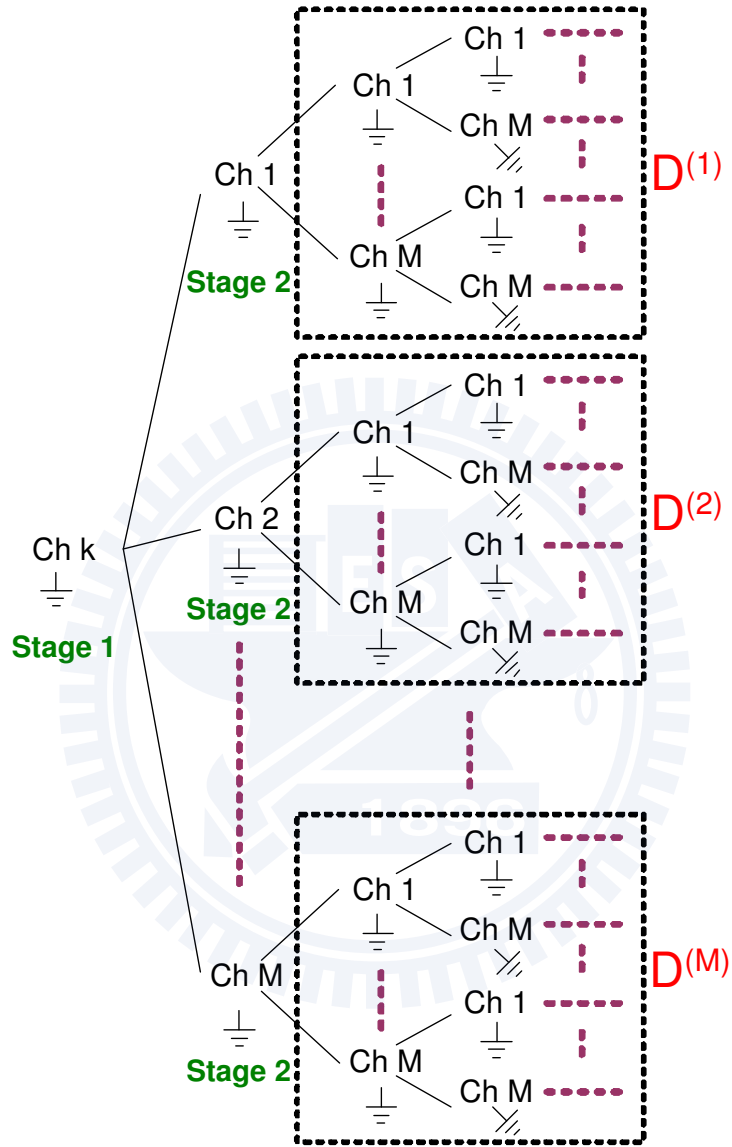


Figure 7.5: Tree-structured representations of the proposed state diagram where the grounding symbols represent the ending of state transition. Note that this figure considers the secondary connections whose default channels are  $Chk$ .

## 7.5 Numerical Results

We show numerical results to reveal the importance of the three key design features for modeling spectrum handoffs, which consist of (1) various arrival rates of the secondary users' connections; (2) heterogeneous arrival rates of the primary users' connections; and (3) the handoff processing time.

### 7.5.1 Simulation Setting

In order to validate the proposed analytical model, we perform simulations based on the Monte-carlo method in non-slot-based (continuous-time) cognitive radio systems, where the inter-arrival time and service time can be the duration of non-integer time slots. We consider a two-channel CR system with Poisson arrival processes of rates  $\lambda_p$  and  $\lambda_s$  for the high-priority primary connections and the low-priority secondary connections, respectively. The high-priority connections can interrupt the transmissions of the low-priority connections, and the connections with the same priority follow the first-come-first-served (FCFS) scheduling discipline<sup>1</sup>. Referring to the IEEE 802.22 standard, we adopt time slot duration of 10 msec in our simulations [89].

### 7.5.2 Effects of Various Arrival Rates for the Secondary Users' Connections

Firstly, we investigate the effects of various arrival rate for secondary users' connections on the channel utilization and the extended data delivery time

---

<sup>1</sup>In fact, the analytical results of mean values obtained in this dissertation can be applied to other scheduling discipline which is independent of the service time of the primary and secondary connections because the averages of system performance metrics will be invariant to the order of service in this case (see page 113 in [78]).

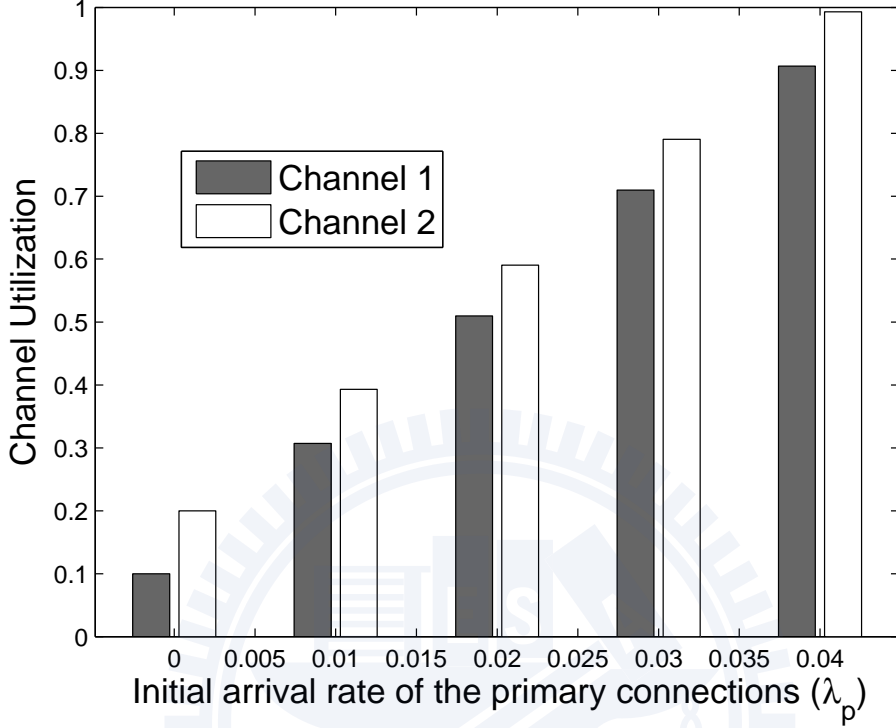


Figure 7.6: Effects of the arrival rate of the primary connections ( $\lambda_p$ ) on the channel utilizations at the channels 1 and 2, where  $\delta_s = 1$  and  $\delta_c = 2$ .

of the secondary connections. We consider a two-channel CR network, where  $\lambda_p^{(1)} = \lambda_p^{(2)} \triangleq \lambda_p$ ,  $(\lambda_s^{(1)}, \lambda_s^{(2)}) = (0.01, 0.02)$  (arrivals/slot),  $(\mathbf{E}[X_p^{(1)}], \mathbf{E}[X_p^{(2)}]) = (20, 20)$  (slots/arrival), and  $(\mathbf{E}[X_s^{(1)}], \mathbf{E}[X_s^{(2)}]) = (10, 10)$  (slots/arrival). We only consider the case that  $0 \leq \lambda_p \leq 0.04$  (arrivals/slot) in the following numerical results. When  $\lambda_p \geq 0.05$  (arrivals/slot), the overall normalized traffic workloads in the considered CR network will be saturated because  $\lambda_p \mathbf{E}[X_p^{(1)}] + \lambda_p \mathbf{E}[X_p^{(2)}] + \lambda_s^{(1)} \mathbf{E}[X_s^{(1)}] + \lambda_s^{(2)} \mathbf{E}[X_s^{(2)}] > 2$ .

Figure 7.6 shows the effects of the arrival rate of the primary connections ( $\lambda_s$ ) on channel utilizations of the channels 1 and 2. As  $\lambda_p$  increases, the channel utilizations of the two channels also increase. Because the nor-

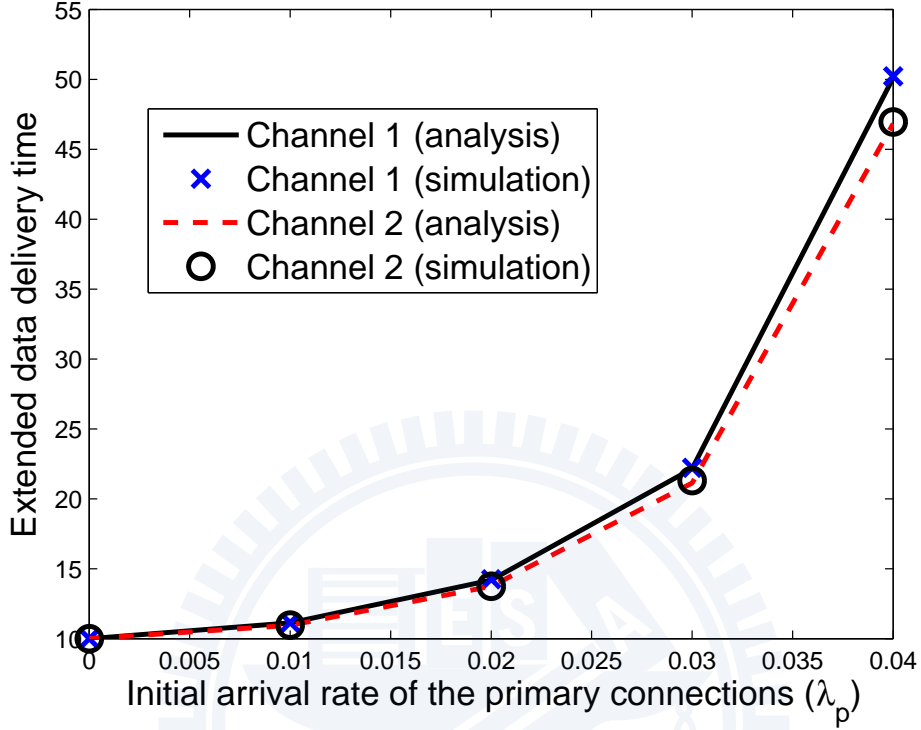


Figure 7.7: Effects of the arrival rate of the primary connections ( $\lambda_p$ ) on the extended data delivery time of the secondary connections whose default channels are channels 1 and 2, where  $\delta_s = 1$  and  $\delta_c = 2$ .

malized traffic workloads of the secondary connections are constant at each channel, the difference between channel utilizations of the two channels is also a constant, which equals to 0.1.

Figure 7.7 shows the effects of the arrival rate of the primary connections ( $\lambda_p$ ) on the extended data delivery time of the secondary connections whose initial default channels are the channels 1 and 2. We have three important observations. First of all, because the channels 1 and 2 have the same arrival rate of the primary connections, the secondary connections at the two channels will encounter same interrupted probability according to (7.14). Hence,

the secondary connections whose default channels are the channels 1 and 2 have similar extended data delivery time even though the channels 1 and 2 have different channel utilization. Next, it is shown that the extended data delivery time of the secondary connections increases as  $\lambda_p$  increases because a larger  $\lambda_s$  will lead to higher channel busy probabilities and longer average handoff delay. More importantly, we find that the simulation results match the analytical results quite well, which can validate the slot-based assumption used in our analysis.

### 7.5.3 Effects of Heterogeneous Arrival Rates for the Primary Users' Connections

Secondly, we demonstrate the effects of various arrival rate for primary users' connections on the channel utilization and the extended data delivery time of the secondary connections. We also consider a two-channel network, where  $\lambda_s^{(1)} = \lambda_s^{(2)} \triangleq \lambda_s$ ,  $(\lambda_p^{(1)}, \lambda_p^{(2)}) = (0.03, 0.01)$  (arrivals/slot),  $(\mathbf{E}[X_s^{(1)}], \mathbf{E}[X_s^{(2)}]) = (20, 20)$  (slots/arrival), and  $(\mathbf{E}[X_p^{(1)}], \mathbf{E}[X_p^{(2)}]) = (10, 30)$  (slots/arrival). Note that the two channels have the same channel utilizations resulting from the primary users' connections. Specifically, we have  $\rho_p^{(1)} = \rho_p^{(2)} = 0.3$  (arrivals/slot). We only consider the case that  $0 \leq \lambda_s \leq 0.03$  (arrivals/slot) in the following numerical results. When  $\lambda_s \geq 0.04$  (arrivals/slot), the overall normalized traffic workloads in the considered CR network will be saturated because  $\lambda_p^{(1)} \mathbf{E}[X_p^{(1)}] + \lambda_p^{(2)} \mathbf{E}[X_p^{(2)}] + \lambda_s \mathbf{E}[X_s^{(1)}] + \lambda_s \mathbf{E}[X_s^{(2)}] > 2$ .

The effects of the initial arrival rate of the secondary connections ( $\lambda_s$ ) on the channel utilizations of the channels 1 and 2 is shown in Fig. 7.8. When  $\lambda_s = 0$ , the two channels have the same channel utilizations of 0.3. As  $\lambda_s$  increases, the channel utilizations of the two channels also increase. However, the increases of the two channels are different even though the two chan-

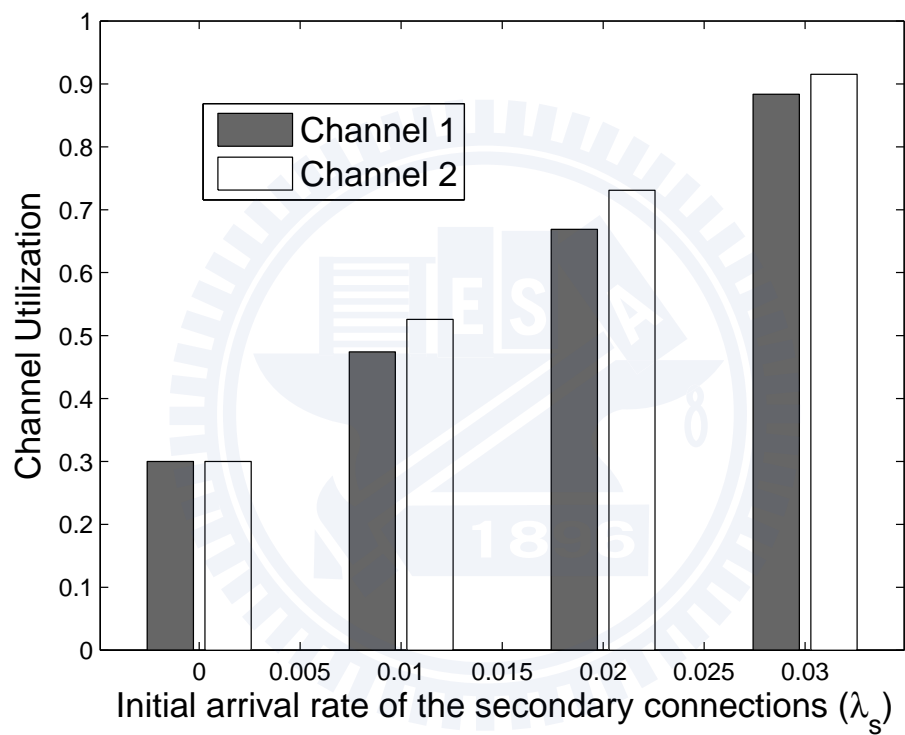


Figure 7.8: Effects of the initial arrival rate of the secondary connections ( $\lambda_s$ ) on the channel utilizations at the channels 1 and 2, where  $\delta_s = 1$  and  $\delta_c = 2$ .

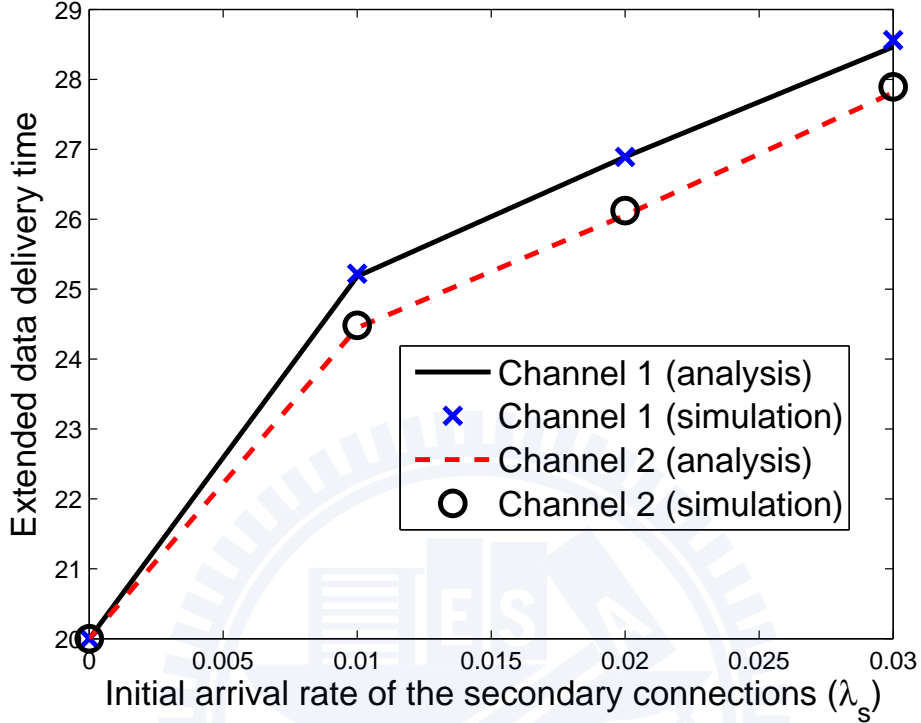


Figure 7.9: Effects of the initial arrival rate of the secondary connections ( $\lambda_s$ ) on the extended data delivery time of the secondary connections whose default channels are the channels 1 and 2, where  $\delta_s = 1$  and  $\delta_c = 2$ .

nels have the same busy probability resulting from the primary connections. Compared to the secondary connections at the channel 2, the secondary connections at the channel 1 will encounter higher interrupted probability because the channel 1 has larger arrival rate of the primary connections. Thus, the time that the secondary connections can use channel 1 is shorter than the time that the secondary connections can use channel 2. Hence, the increase of channel utilization at channel 2 is larger than that at channel 1.

Figure 7.9 shows the effects of the initial arrival rate of the secondary connections ( $\lambda_s$ ) on the extended data delivery time of the secondary con-



nections whose initial channels are the channels 1 and 2. We can find that the extended data delivery time of the secondary connections increases as  $\lambda_s$  increases because a larger  $\lambda_s$  will lead to a higher channel busy probabilities as shown in Fig. 7.8. Furthermore, the secondary connections whose initial channel is channel 2 has shorter extended data delivery time compared to the secondary connections whose initial channel is channel 1. This is because the secondary connections whose initial channel is channel 2 can have lower interrupted probability and the smaller number of interruptions during their transmission period.

#### 7.5.4 Effects of Handoff Processing Time

Finally, we discuss the effects of handoff processing time. A two-channel CR network is considered with the following parameters:  $t_n = 0$  (slot),  $t_s = 1$  (slot),  $\lambda_p^{(1)} = \lambda_p^{(2)} \triangleq \lambda_p$ ,  $\lambda_s^{(1)} = \lambda_s^{(2)} = 0.02$  (arrivals/slot),  $\mathbf{E}[X_p^{(1)}] = \mathbf{E}[X_p^{(2)}] = 5$  (slots/arrival) and  $\mathbf{E}[X_s^{(1)}] = \mathbf{E}[X_s^{(2)}] = 10$  (slots/arrival). Then, based on the proposed analytical model, we can evaluate the average extended data delivery time and then design the admission control rule for the secondary users as shown in Figs. 7.10 and 7.11.

Figure 7.10 compares the cumulative handoff delay of the following three target channel selection schemes: (1) the always-staying strategy; (2) the random selection strategy; and (3) the reactive selection strategy. For the always-staying approach, the interrupted secondary user always stays on its default channel to resume its unfinished data transmission. The method is one kind of proactive spectrum handoff [85] because the target channels are predetermined and it is similar to the non-hopping mode of IEEE 802.22 [70]. In the random selection approach, the interrupted user randomly selects a target channel from all channels. From this figure, we have the following

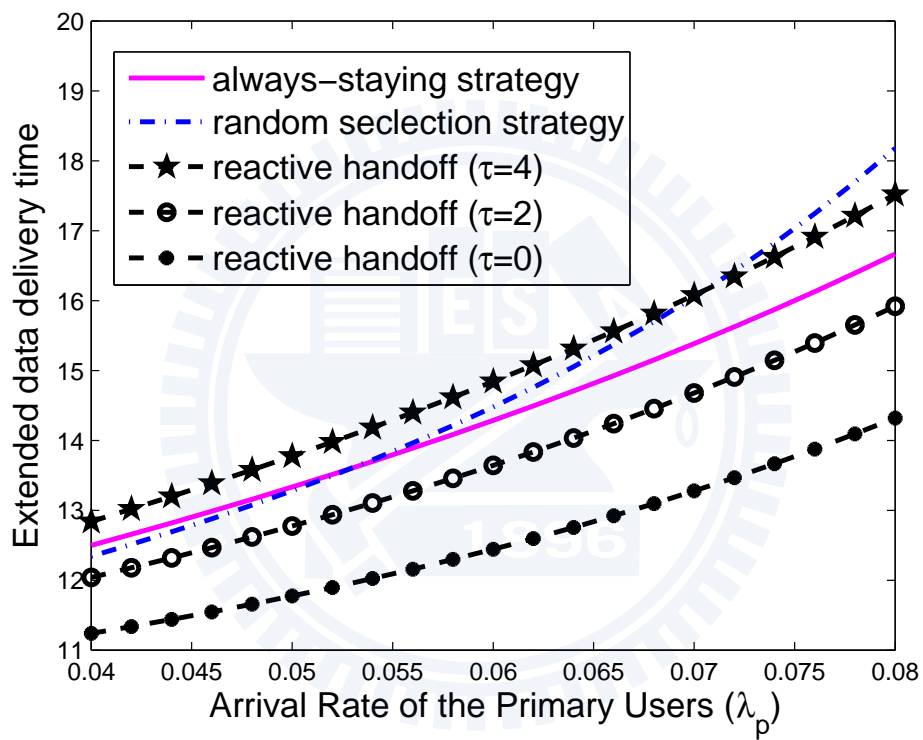


Figure 7.10: Comparison of average extended data delivery time for different target channel selection schemes.

three important observations. First, we find that the cumulative handoff delay resulting from the random selection method is longer than that resulting from the always-staying strategy when  $\lambda_p \geq 0.052$ . For a larger value of  $\lambda_p$ , the interrupted secondary users with the random selection method must spend much more time to wait when it changes its operating channel because this selected target channel is likely busy. Thus, the handoff delay of the random selection method becomes longer in this case. Next, it is shown that the reactive spectrum handoff can result in the shortest cumulative handoff delay in the ideal sensing case (i.e.,  $\tau = 0$ ) because it can reliably find idle channels by performing spectrum sensing. In this case, the cumulative handoff delay can be shortened around 40% compared to the other approaches under various arrival rates of the primary users' connections. However, when the spectrum sensing time becomes longer (e.g.,  $\tau = 4$ ), the reactive spectrum handoff is worse than the random selection method in terms of cumulative handoff delay when  $\lambda_p \leq 0.071$ . Finally, we find that the sensing technology can effectively shorten the average cumulative handoff delay only when  $\tau \leq 2$  compared to the always-staying strategy.

The analytical results developed in this chapter can be used to design the admission control rule for the arriving secondary users subject to their latency requirement. Fig. 7.11 shows the admissible region for the normalized traffic workloads (or channel utilities)  $(\rho_p, \rho_s)^2$  for the Voice over IP (VoIP) services when  $\tau = 0$  (slot). The maximum allowable average cumulative delay resulting from multiple handoffs is 20 ms for the VoIP traffic [100]. The admission control policy can be designed according to this figure. When  $\rho_p < 0.1667$ , a CR network can accept all arrival requests from the secondary users until the CR network is saturated, i.e.,  $\rho_p + \rho_s \simeq 1$ . Furthermore, when

---

<sup>2</sup> $\rho_p = \lambda_p \mathbf{E}[X_p]$  and  $\rho_s = \lambda_s \mathbf{E}[X_s]$ .

$0.1667 < \rho_p < 0.3397$ , a part of traffic workloads of the secondary users must be rejected in order to satisfy the delay constraint for the secondary users. For example, when  $\rho_p = 0.25$ , a CR network can support at most 0.279 workload for the secondary users. That is, a CR network can accept at most  $\lambda_s = 0.0279$  (arrivals/slot) based on the results shown in the figure when  $\lambda_p = 0.05$  (arrivals/slot). In order to design the most allowable  $\lambda_s$  to achieve this arrival rate upper bound for the secondary connections, many arrival-rate control methods can be considered, such as the p-persistent carrier sense multiple access (CSMA) protocol in [19] and the call admission control mechanisms in [44,57,101]. Finally, when  $\rho_p > 0.3397$ , no secondary user can be accepted. Note that the size of the admissible region decreases as  $\tau$  increases.

### 7.5.5 Comparison between Proactive and Reactive Spectrum Handoff Scheme

Figure 7.12 compares the extended data delivery time for the proactive and the reactive spectrum handoff schemes. Here, we consider a two-channel system with the following traffic parameters:  $\lambda_s^{(1)} = \lambda_s^{(2)} = 0.01$ ,  $\mathbf{E}[X_p^{(1)}] = \mathbf{E}[X_p^{(2)}] = 10$ , and  $\lambda_p^{(1)} = \lambda_p^{(2)} = \lambda_p$ . From this figure, we have the following important observations. First, the extended data delivery time of the reactive spectrum handoff has a singular point at  $\lambda_p = 0.043$ . This is because the two different predetermined target channel sequences are adopted in the cases of  $\lambda_p < 0.043$  and  $\lambda_p > 0.043$ . Based on the proposed model, the traffic-adaptive proactive spectrum handoff scheme can be designed to appropriately change to better target channel sequence according to traffic conditions in order to reduce the extended data delivery time of the secondary connections. Next, we focus on the reactive spectrum handoff scheme. In the ideal case that spectrum sensing time (denoted by  $\tau$ ) is 0 slot, the extended data

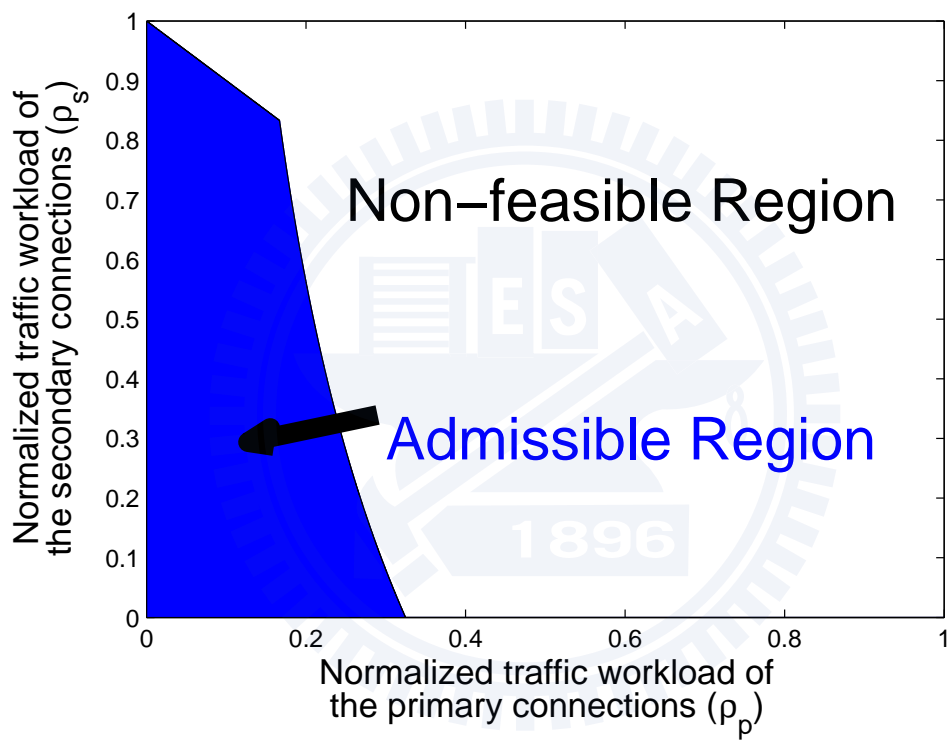


Figure 7.11: Admissible region  $(\lambda_p, \lambda_s)$ , where the average extended data delivery time constraint can be satisfied when  $\tau = 0$ .

delivery time can be shortened around 7%  $\sim$  20%, compared to the proactive spectrum handoff over various arrival rates of the primary connections, because the reactive spectrum handoff scheme can perform spectrum sensing to find the idle channels. Furthermore, the extended data delivery time of the reactive spectrum handoff scheme increases as sensing time increases. When  $\tau = 5$  (slots), the reactive handoff scheme is not always better than the proactive handoff scheme. As shown in this figure, when  $\lambda_p < 0.037$ , the proactive handoff scheme can result in shorter extended data delivery time. In this case, we can conclude that the proactive handoff scheme can yield shorter extended data delivery time compared to the reactive handoff scheme when the traffic loads of the primary users is light, whereas the reactive scheme performs better in the condition of heavy traffic loads. Finally, the reactive spectrum handoff scheme will result in the longest extended data delivery time when  $\tau = 10$  (slots). Based on the proposed model, we can provide a principle to determine which spectrum handoff scheme should be adopted in CR networks for various sensing time and traffic parameters.

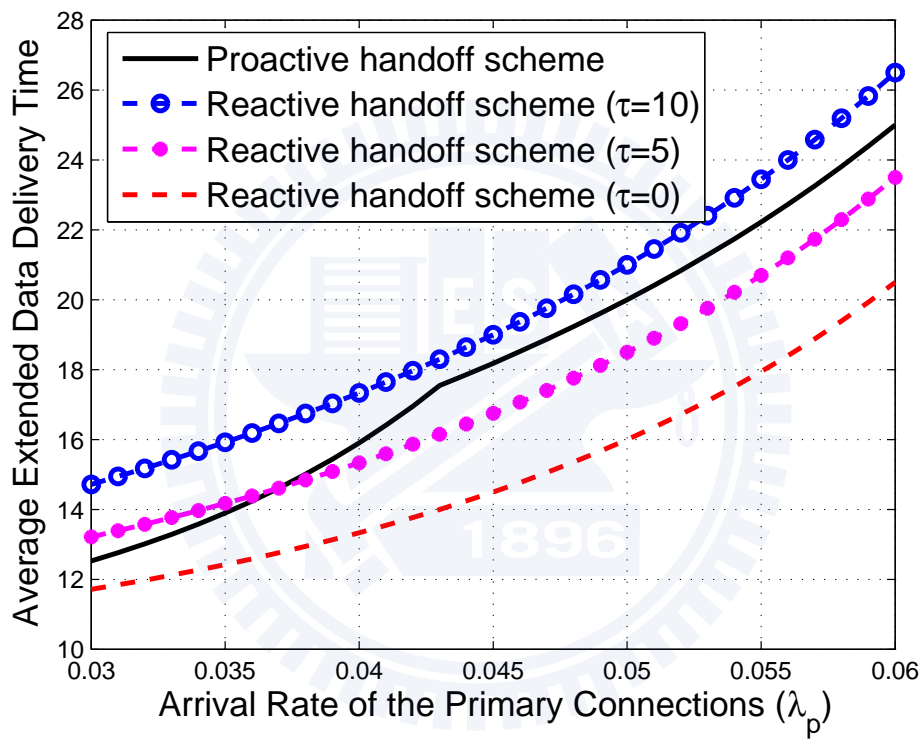


Figure 7.12: Comparison of the average extended data delivery time for different spectrum handoff schemes, where  $\mathbf{E}[X_s] = 10$ ,  $t_s = 0$ , and  $t_h = 0$

# Chapter 8

## Interference-Avoiding Spectrum Sharing

The goal of this part is to develop an analytical mechanism to design the admission control rule for the arriving secondary users subject to the following two quality of service (QoS) constraints:

- Interference avoidance for the primary users: Because the primary users have the highest priority to access channel, how to prevent the secondary users from interfering with the transmission of the primary users is the most important issue.
- Latency guarantee for the secondary users: The transmission latency of the secondary users is stained by many factors such as power outage due to fading channel, multiple handoffs due to interruptions from the primary users, and waiting time due to multiple secondary users.

In this chapter, we suggest a cross-layer approach to find the optimal traffic admission probability with the objective of maximizing channel utilization and maintaining the QoS requirements of the primary users and the



secondary users. Our cross-layer design can incorporate the effects in the physical, medium access control (MAC), and application layers. In the physical layer, we incorporate the sensing errors for missed detection as well as false alarm, and power outage. In the MAC layer, traffic admission probability for the secondary users is considered. In the application layer, we consider the traffic statistics and QoS constraints of both the primary and the secondary users. The proposed analytical approach can calculate the optimal traffic admission probability under various cross-layer parameters. Furthermore, it also provides useful insights into the tradeoff design between channel utilization and the QoS performances for the primary as well as secondary users. To our knowledge, such a PHY/MAC/APP cross-layer analytical approach to determine the optimal traffic admission probability for CR networks has rarely been seen in the literature.

## 8.1 Motivation

In order to satisfy the two QoS constraints, the secondary users must be able to accurately sense the presence of the primary users. However, missed detection and false alarm may occur because the perfect sensing is impossible. Missed detection occurs when the detector reports the absence of a primary user while it is present. In this case, the transmission of the primary users will be affected by the secondary users. On the contrary, false alarm occurs when the detector mistakenly reports the presence of a primary user. In this situation, the secondary users cannot transmit data even though channel is indeed idle, which cause the transmission latency of the secondary users. Basically, a smaller missed detection probability implies a larger false alarm probability, and vice versa, which is a performance tradeoff design issue [87].

In the literature, many methods have been proposed to improve the issues of interference avoidance and latency guarantee simultaneously for the CR network under the imperfect sensing situation, such as the optimal sensing parameters and the optimal admission control. On one hand, the authors in [73,74,104] found that the secondary users can decrease the missed detection and the false alarm probabilities by increasing spectrum sensing time. On the other hand, [105] suggested to control the arrival rate of the secondary users to maintain two aforementioned QoS constraints. A lower arrival rate can decrease the interference on the primary users and reduce the waiting time due to multiple secondary users' contention.

In this chapter, we focus on designing an admission control mechanism to adaptively control the arrival rate of the secondary users by adjusting their traffic admission probability  $\alpha$  in order to maintain the interference constraint of the primary users and the latency requirement of the secondary users. When the traffic of the secondary users arrives at system, it will be accepted with probability  $\alpha$  and be dropped with probability  $1-\alpha$ . Intuitively, a larger traffic admission probability for the secondary users can increase channel utilization. However, a larger traffic admission probability degrades the QoS performance of the primary users due to much more interference from the secondary users if missed detection happens. Furthermore, a larger traffic admission probability also degrades the QoS performance of the secondary users due to more contention between the secondary users. Hence, there exists an optimal tradeoff between channel utilization in the system-level performance measure and interference ratio as well as transmission latency in the user-level performance measures.

## 8.2 System Model

### 8.2.1 Assumptions

In CR networks, there are four key system parameters. Assume that the arrival processes of the primary and the secondary users' connections are Poisson. Denote  $\lambda_p$  (arrivals/slot) and  $\lambda_s$  (arrivals/slot) as the traffic arrival rates of the primary and the secondary users' connections, respectively. Furthermore, let  $X_p$  (slots/arrival) and  $X_s$  (slots/arrival) be the service time of the primary users' connections and the secondary users' connections, respectively. Then, the probability density functions of  $X_p$  and  $X_s$  are denoted by  $f_p(x)$  and  $f_s(x)$ , respectively.

The service time of the primary and secondary connections will be extended due to imperfect sensing and power outage. Denote  $P_M$  and  $P_F$  as missed detection and false alarm probabilities, respectively. Their relationship can be characterized by the receiver operating characteristic (ROC) curve [87]. When missed detections occur, the primary user must retransmit these stained data frames in the next slots. Thus, the service time of a primary connection will be extended from  $X_p$  (slots/arrival) to  $\tilde{X}_p$  (slots/arrival). Furthermore, a secondary user cannot transmit data even with an idle channel when a false alarm occurs. Hence, a secondary user needs to spend more time to complete its connection transmission. Then, the service time of a secondary connection will be extended to  $\tilde{X}_s$  (slots/arrival) from  $X_s$  (slots/arrival). Furthermore, power outage will extend the actual service time to  $Z_p$  (slots/arrival) and  $Z_s$  (slots/arrival) from  $\tilde{X}_p$  (slots/arrival) and  $\tilde{X}_s$  (slots/arrival), respectively. In the remaining part of this chapter, we call  $\tilde{X}_p$  and  $\tilde{X}_s$  the actual service time of the primary and secondary connections as well as  $Z_p$  and  $Z_s$  the actual service time of the primary and

secondary connections in the physical channel.

## 8.2.2 Admission Control Mechanism

An arrival rate control mechanism for the secondary connections can be used to satisfy the interference constraint of the primary users and the latency requirement of the secondary users. When a new traffic request arrives at system, it will be dropped with probability  $1 - \alpha$  and be accepted with probability  $\alpha$ . If this request is accepted, the secondary user will perform spectrum sensing to identify channel availability and then decide whether a secondary connection can be established. By contrary if this request is dropped, it will be retransmitted later by the upper layer protocol such as automatic repeat-request (ARQ) protocol. Here,  $\alpha$  is called the traffic admission probability of the secondary connections. Because  $0 \leq \alpha \leq 1$ , the effective arrival rate  $\alpha\lambda_s$  is not higher than the original arrival rate. This kind of arrival rate control mechanism is very similar to the concept of p-persistent carrier sense multiple access (CSMA) protocol as discussed in [19].

## 8.3 Problem Formulation and Analytical Model

### 8.3.1 Problem Formulation

In order to maximize channel utilization while maintaining the interference and latency requirements, we formulate the **Utilization Maximization Problem** for the secondary users as follows. Given the maximum allowable interference ratio  $\Theta_{max}$  on the primary connections and the longest allowable overall system time  $S_{max}$  of the secondary connections, we aim to find the optimal traffic admission probability (denoted by  $\alpha^*$ ) to maximize the

channel utilization (denoted by  $U$ ). Formally,

$$\alpha^* = \arg \max_{0 < \alpha \leq 1} U(\alpha) , \quad (8.1)$$

subject to

$$\Theta_p(\alpha) \triangleq \frac{\mathbf{E}[Z_p(\alpha)]}{\mathbf{E}[X_p]} \leq \Theta_{max} , \quad (8.2)$$

and

$$\mathbf{E}[S_s(\alpha)] \leq S_{max} , \quad (8.3)$$

where  $\mathbf{E}[\cdot]$  is the expectation function and  $S_s(\alpha)$  is the average overall system time of the secondary connections, which is defined as the duration from the instant that data arrives at system until the instant of finishing the whole transmission. Note that from queueing theory, it follows that

$$U(\alpha) = \lambda_p \mathbf{E}[X_p] + \alpha \lambda_s \mathbf{E}[X_s] . \quad (8.4)$$

From (8.4), we can found that  $U(\alpha)$  is a strictly increasing function of  $\alpha$ . Hence, our optimization problem can be solved by maximizing  $\alpha$  while maintaining the constraints (8.2) and (8.3).

In the **Utilization Maximization Problem**, (8.2) and (8.3) represent the interference and latency constraints of the primary and secondary connections in the application layer, respectively. Obviously,  $U$ ,  $\mathbf{E}[Z_p]$  and  $\mathbf{E}[S_s]$  are related to not only  $\alpha$  in the MAC layer and traffic statistics of the primary and secondary users in the application layer but also missed detection probability  $P_M$ , false alarm probability  $P_F$ , outage probability  $\pi_p$  for the primary users, and outage probability  $\pi_s$  for the secondary users in the physical layer. To solve this optimization problem, we use the preemptive resume priority (PRP) M/G/1 queueing model to evaluate these unknown system performance measures. We will detail this queueing mode in the following.

### 8.3.2 Analytical Model

In this chapter, we derive the closed-form expressions for  $\mathbf{E}[Z_p]$  and  $\mathbf{E}[S_s]$  based on the preemptive resume priority (PRP) M/G/1 queueing model [79]. Some important properties for the PRP M/G/1 queueing model are listed below:

- Each server (channel) has two types of customers (connections). The connections of the primary and secondary users are connected to the high-priority queue and the low-priority queue, respectively.
- The primary users have the preemptive priority to interrupt the transmission of the secondary users. The remaining transmission of the interrupted secondary user will be put into the head of the low-priority queue of the current operating channel. Furthermore, the interrupted secondary user can resume the unfinished transmission when the current channel becomes idle, instead of retransmitting the whole data.
- A secondary connection may encounter multiple interruptions from the primary connections during its transmission period. This model can characterize the effects of multiple spectrum handoffs.

Here, we assume that connections which have the same priority access channels with the first-come-first-served (FCFS) scheduling discipline. Based on this model, when the four traffic parameters  $\lambda_p$ ,  $\lambda_s$ ,  $f_p(x)$ , and  $f_s(x)$  are known,  $\mathbf{E}[Z_p]$  and  $\mathbf{E}[S_s]$  can be evaluated analytically in the next section.

## 8.4 Analysis of Constraint Functions in the Utilization Maximization Problem

This section show how to derive the closed-form expressions for  $\mathbf{E}[Z_p]$  and  $\mathbf{E}[S_s]$  in (8.2) and (8.3).

### 8.4.1 Analysis of Actual Service Time of the Primary Connection in the Physical Channel

#### Effect of Missed Detection

Basically, missed detections in CR networks can be categorized into two kinds [58, 60]. Firstly, when a primary user is transmitting data, a newly arriving secondary connection may incorrectly assess that this specific channel is available in its first sensing phase. In this case, the class-A missed detection occurs. Next, a secondary user may also fail to detect the presence of primary users after it arrives at a CR network for a while. This situation is called the class-B missed detection. The authors in [58, 60] found that the class-B missed detection is small because the sensing results at the first sensing phase can be employed to improve the accuracy of the sensing results at the following sensing phases.

Next, we explain the effect of class-A missed detection on the actual service time of the primary connections. We consider a transmission slot of this primary connection. During this slot, more than one arrival of the secondary connection appears with probability  $1 - e^{-\lambda_s \Delta}$ , where  $\Delta$  is the slot duration. For these arrivals of secondary connections, each of them will assess this busy slot as idle if and only if (1) a missed detection occurs and (2) the low-priority queue of the considered channel is empty. Let  $Q_s$  be the length

of the low-priority queue. Hence, the first arrival at the considered slot will make an error channel assessment with probability  $P_M \Pr\{Q_s = 0\}$ , where  $P_M$  is the missed detection probability for spectrum sensing and  $\Pr\{Q_s = 0\}$  has been derived in [88]. However, for the remaining arrivals in the considered slot, we have  $\Pr\{Q_s = 0\} = 0$  because the first arrival has been put into the low-priority queue. Thus, the remaining arrivals do not make the error channel assessment. From above observations, we can conclude that a primary connection's transmission slot is stained by the arrivals of the secondary connections with probability

$$P_I = (1 - e^{-\lambda_s \Delta}) P_M \Pr\{Q_s = 0\} . \quad (8.5)$$

Then, we consider an observation period with  $I + B$  slots, where  $I$  and  $B$  are the total numbers of idle and busy slots resulting from the primary connections when missed detections do not occur. Hence, we have  $\frac{B}{I+B} = \lambda_p \mathbf{E}[X_p]$ . For the primary connections, a total of  $BP_I$  slots out of  $B$  slots must be retransmitted at the next slot due to missed detection. Furthermore, when these retransmitted data are stained again, they must be retransmitted. On average, a total of  $B(P_I)^2$  slots out of  $BP_I$  slots must be retransmitted. The similar arguments can be applied for all the upcoming retransmissions. Hence, it follows that

$$\rho_p = \frac{B \sum_{i=0}^{\infty} (P_I)^i}{I + B} = \frac{\lambda_p \mathbf{E}[X_p]}{1 - P_I} . \quad (8.6)$$

Finally, because  $\rho_p = \lambda_p \mathbf{E}[\tilde{X}_p]$  in (8.6), the expected actual service time  $\mathbf{E}[\tilde{X}_p]$  can be written as

$$\mathbf{E}[\tilde{X}_p] = \frac{\mathbf{E}[X_p]}{1 - P_I} . \quad (8.7)$$



## Effect of Power Outage

When outage occurs, the users must retransmit the failed slot. Hence, the actual transmission time of the primary connections in the physical channel will be extended from  $\tilde{X}_p$  to  $Z_p$ . The first and the second moments of  $Z_p$  can be expressed as follows:

$$\mathbf{E}[Z_p] = \sum_{\tilde{x}=1}^{\infty} \mathbf{E}[(Z_p)|\tilde{X}_p = \tilde{x}] \mathbf{Pr}(\tilde{X}_p = \tilde{x}) , \quad (8.8)$$

and

$$\mathbf{E}[(Z_p)^2] = \sum_{\tilde{x}=1}^{\infty} \mathbf{E}[(Z_p)^2|\tilde{X}_p = \tilde{x}] \mathbf{Pr}(\tilde{X}_p = \tilde{x}) . \quad (8.9)$$

When outage occurs, the failed slots must be retransmitted in the next slot. Hence, for a connection with transmission duration  $\tilde{x}$ , its actual service time  $Z_p$  in the physical channel will be extended to  $z+i$  if and only if outages occur in  $i$  slots of the first  $\tilde{x}+i-1$  slots and outage does not occur at the  $(z+i)^{th}$  slot. Hence, the conditional expectation of the actual service time in the physical channel follows the negative binomial distribution. That is,

$$\mathbf{E}[Z_p|\tilde{X}_p = \tilde{x}] = \sum_{i=0}^{\infty} (\tilde{x}+i) \binom{\tilde{x}+i-1}{i} (1-\pi_p)^{\tilde{x}} \pi_p^i , \quad (8.10)$$

and

$$\mathbf{E}[Z_p^2|\tilde{X}_p = \tilde{x}] = \sum_{i=0}^{\infty} (\tilde{x}+i)^2 \binom{\tilde{x}+i-1}{i} (1-\pi_p)^{\tilde{x}} \pi_p^i . \quad (8.11)$$

where  $\pi_p$  is the outage probability for the primary connections.

Finally, when  $\mathbf{Pr}(\tilde{X}_p = \tilde{x})$  is given, we can obtain  $\mathbf{E}[Z_p]$  and  $\mathbf{E}[(Z_p)^2]$  by substituting (8.10) into (8.8) and (8.11) into (8.9), respectively. Note that how to derive  $\mathbf{Pr}(\tilde{X}_p = x)$  from  $f_p(x)$  has been discussed in Appendix D. For example, if  $f_p(x)$  is the geometric distribution, i.e.,

$$f_p(x) = \left(1 - \frac{1}{\mathbf{E}[X_p]}\right)^{x-1} \left(\frac{1}{\mathbf{E}[X_p]}\right) , \quad (8.12)$$

we can have

$$\mathbf{E}[Z_p] = \frac{\mathbf{E}[\tilde{X}_p]}{1 - \pi_p} = \frac{\mathbf{E}[X_p]}{(1 - P_I)(1 - \pi_p)} , \quad (8.13)$$

and

$$\mathbf{E}[(Z_p)^2] = \frac{\mathbf{E}[X_p](2\mathbf{E}[X_p] - 1 + P_I + \pi_p - P_I\pi_p)}{((1 - P_I)(1 - \pi_p))^2} , \quad (8.14)$$

where  $\pi_p$  is the outage probability of the primary connections.

## 8.4.2 Analysis of Overall System Time of the Secondary Connections

The overall system time (denoted by  $S_s$ ) is an important quality of service (QoS) metric for the the secondary users' connections. It consists of the waiting time (denoted by  $W$ ) and the extended data delivery time (denoted by  $T$ ). Hence, we have

$$\mathbf{E}[S_s] = \mathbf{E}[W] + \mathbf{E}[T] , \quad (8.15)$$

Here, the waiting time is defined as the duration from the instant that data arrives at system until the instant of starting transmitting data. Furthermore, the extended data delivery time is defined as the duration from the instant of starting transmitting data until the instant of finishing the whole transmission.

In addition to traffic admission probability  $\alpha$ , the overall system time of the secondary users is also affected by channel contention, multiple handoffs, false alarm, and power outage issues. Firstly, the secondary users' channel contention will increase waiting time. Furthermore, a secondary connection may have multiple interruptions from the primary user. Moreover, when false alarm occurs, the secondary users cannot transmit data even though channel is truly idle. Finally, power outage will make data retransmission. These

phenomenons will extend the overall system time. In the following subsections, we will investigate the effects of waiting time due to channel contention, multiple handoffs, false alarm probability  $P_F$ , and outage probability  $\pi_s$  on  $\mathbf{E}[S_s]$ .

### **Effect of Waiting Time Due to Multiple Secondary Users' Contention**

When a secondary connection arrives at system, it cannot be transmitted immediately until all the secondary connections in the low-priority queue and the primary connections in the high-priority queue have been served. Hence, when more secondary users access channel, waiting time will increase. Referring to [79], the average waiting time can be expressed as follows:

$$\mathbf{E}[W] = \frac{\frac{1}{2}\lambda_p\mathbf{E}[(Z_p)^2] + \frac{1}{2}\alpha\lambda_s\mathbf{E}[(Z_s)^2]}{(1 - \lambda_p\mathbf{E}[Z_p] - \alpha\lambda_s\mathbf{E}[Z_s])(1 - \lambda_p\mathbf{E}[Z_p])} . \quad (8.16)$$

### **Effects of Multiple Handoffs**

The extended data delivery time of each secondary connection consists of the actual service time  $Z_s$  in the physical channel and the cumulative delay resulting from multiple handoffs. Let  $N$  and  $D$  be the number of interruptions for the secondary connection and the handoff delay for each spectrum handoff. Then, we have

$$\mathbf{E}[T] = \mathbf{E}[Z_s] + \mathbf{E}[N]\mathbf{E}[D] . \quad (8.17)$$

Referring to [79], it follows that

$$\mathbf{E}[D] = \frac{\mathbf{E}[Z_p]}{1 - \lambda_p\mathbf{E}[Z_p]} , \quad (8.18)$$

and

$$\mathbf{E}[N] = \lambda_p\mathbf{E}[Z_s] . \quad (8.19)$$

### Effect of False Alarm

Now, we consider an observation period with  $I + B$  slots, where  $I$  and  $B$  are the total numbers of idle and busy slots resulting from the secondary connections when false alarms and power outages do not occur. Hence, we have  $\frac{B}{I+B} = \lambda_s \mathbf{E}[X_s]$ . Recall that  $\rho_s$  is the busy probability resulting from the secondary connections. Hence, in the duration of  $I + B$ , there are  $\rho_s(I + B)$  slots are busy, where  $\rho_s(I + B)P_F$  slots is the false-alarm busy slots. That is, the total number of busy slots resulting from the secondary connections is increased to  $B + \rho_s(I + B)P_F$ . From this observation, we have the following relationship:

$$\rho_s = \frac{B + (I + B)\rho_s P_F}{I + B}. \quad (8.20)$$

Solving (8.20), we can have

$$\rho_s = \frac{B}{(I + B)(1 - P_F)} = \frac{\lambda_s \mathbf{E}[X_s]}{1 - P_F}. \quad (8.21)$$

Finally, because  $\rho_s = \lambda_s \mathbf{E}[\tilde{X}_s]$  in (8.21), the expected actual service time  $\mathbf{E}[\tilde{X}_s]$  can be written as

$$\mathbf{E}[\tilde{X}_s] = \frac{\mathbf{E}[X_s]}{1 - P_F}. \quad (8.22)$$

### Effect of Power Outage

Referring to 8.4.1, if  $f_s(x)$  is the geometric distribution, i.e.,

$$f_s(x) = \left(1 - \frac{1}{\mathbf{E}[X_s]}\right)^{x-1} \left(\frac{1}{\mathbf{E}[X_s]}\right), \quad (8.23)$$

we can have

$$\mathbf{E}[Z_s] = \frac{\mathbf{E}[X_s]}{(1 - P_F)(1 - \pi_s)}, \quad (8.24)$$

and

$$\mathbf{E}[(Z_s)^2] = \frac{\mathbf{E}[X_s](2\mathbf{E}[X_s] - 1 + P_F + \pi_s - P_F\pi_s)}{((1 - P_F)(1 - \pi_s))^2}, \quad (8.25)$$

where  $\pi_s$  is the outage probability of the secondary connections.

## 8.5 Numerical Results

In this section, we show the impacts of different system parameters on  $\Theta_p$ ,  $\mathbf{E}[S_s]$ , and  $\alpha^*$ . We consider the following system parameters:  $\lambda_p = 0.02$  and  $\pi_p = \pi_s = 0.1$ . Furthermore, because this dissertation focuses on the latency-sensitive traffic, we can assume that the service time  $X_p$  and  $X_s$  of the primary and secondary connections follow the geometric distributions (see page 135 in [86]). Note that we only use the geometric distribution as an example here. Indeed, the proposed analytical framework can be applied to any distributions. It only requires the knowledge of the first and the second moments of the data transmission time distributions for the primary and the secondary connections.

Figure 8.1 compares the interference ratio ( $\Theta_p$ ) for various traffic admission probabilities ( $\alpha$ ). Obviously,  $\Theta_p$  increases as the arrival rate ( $\lambda_s$ ) of the secondary connections increases. Furthermore, because a larger  $\alpha$  will lead to much more traffic loads of the secondary connections, the primary connections will be stained with a larger probability. Based on the analytical results, we can design an admission control rule to satisfy the interference constraint on the primary connections. For example, we consider  $\lambda_s = 0.019$  and  $\Theta_{max} = 1.1175$ . In this case, when admission control had not implemented (i.e.  $\alpha = 1$ ), the interference ratio is 1.1325, which is larger than  $\Theta_{max}$ . In order to satisfy the interference constraint, we must lower the effective traffic loads of the secondary connections by setting  $\alpha = 0.3$ .

The effects of the traffic admission probability  $\alpha$  and the arrival rate  $\lambda_s$  of the secondary connections on the average overall system time ( $\mathbf{E}[S_s]$ ) of the secondary connections in shown in Fig 8.2. We can found that the average overall system time increases as  $\alpha$  or  $\lambda_s$  increases. Similarly, we can also develop the admission control rule for the arriving secondary users

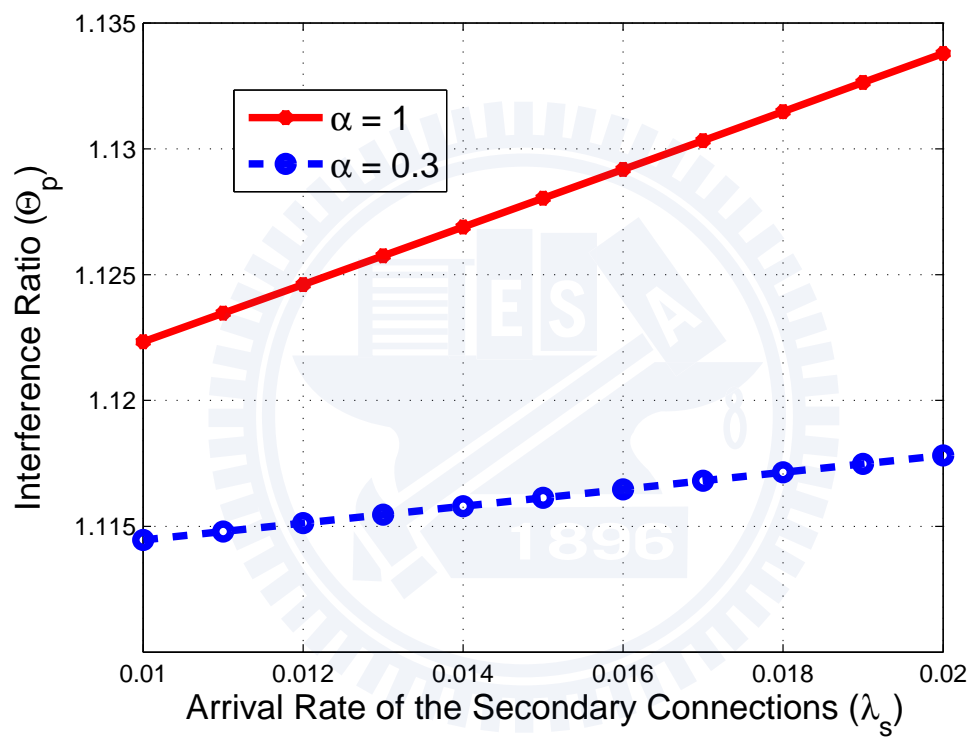


Figure 8.1: Interference ratio ( $\Theta_p$ ) for various arrival rates of the secondary connections, where  $P_M = 0.1$ .

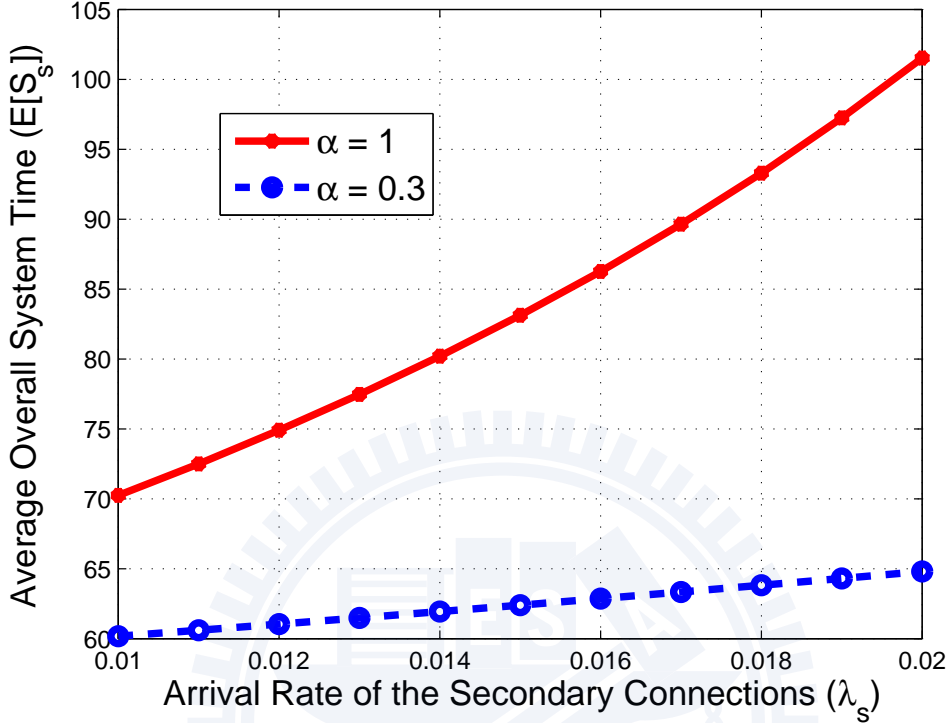


Figure 8.2: Average overall system time ( $\mathbf{E}[S_s]$ ) for various arrival rates of the secondary connections, where  $P_F = 0.1$ .

subject to their latency requirement. For example, we consider  $\lambda_s = 0.016$  and  $S_{max} = 63$ . If we do not use admission control mechanism, the average overall system time is 86, which is larger than  $S_{max}$ . Hence, a part of traffic workloads of the secondary users must be rejected in order to satisfy the delay constraint for the secondary users. In the considered case, we must set  $\alpha = 0.3$ .

The optimal traffic admission probability for various arrival rates of the secondary connections is shown in Fig. 8.3. This figure shows that  $\alpha^*$  decreases as  $\lambda_s$  increases because a larger  $\lambda_s$  implies much more interference and channel contention. Furthermore, a higher  $P_F$  will lead to longer ex-

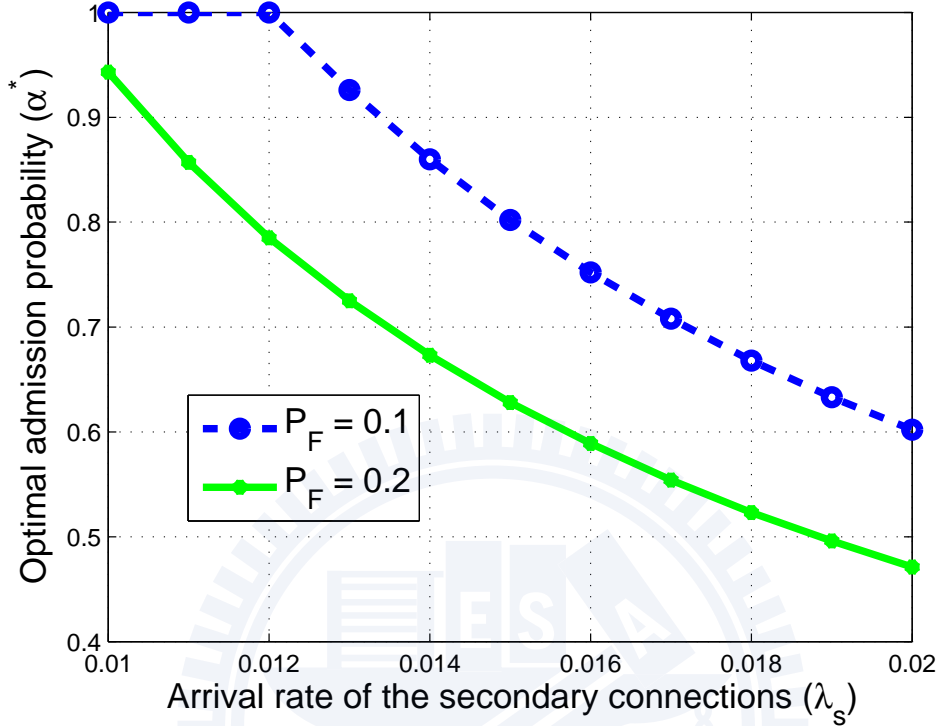


Figure 8.3: Optimal traffic admission probability for various arrival rates of the secondary connections where  $\Theta_{max} = 1.13$  and  $S_{max} = 75$ .

tended data delivery time. Hence, the secondary users must reduce their waiting time in order to maintain the same overall system time requirement. In order to alleviate channel contention between multiple secondary users, the total traffic loads of the secondary users must be lowered. Hence,  $\alpha^*$  decreases as  $P_F$  increases. For example, when  $\lambda_s = 0.014$ , we have  $\alpha^* = 0.86$  for  $P_F = 0.1$  and  $\alpha^* = 0.65$  for  $P_F = 0.2$ , respectively



# Chapter 9

## Conclusions

In this dissertation, we have developed analytical framework based on the preemptive resumption priority (PRP) M/G/1 queueing theory to characterize the general channel usage behaviors with multiple handoffs from a macroscopic viewpoint. Based on this model, we can evaluate the effects of multiple handoffs for the QoS performance of the secondary users, and then provide important insights into the designs of spectrum decision, spectrum mobility, and spectrum sharing algorithms. This dissertation includes the following research topics:

1. Modeling techniques for cognitive radio networks;
2. Load-balancing spectrum decision;
3. Proactive spectrum handoff;
4. Optimal proactive spectrum handoff;
5. Reactive spectrum handoff;
6. Interference-avoiding spectrum sharing.

The contributions from this research are listed as follows.

1. Introduce a queueing-theoretical framework to characterize the effects of the general channel usage behaviors with multiple handoffs.
2. Design system parameters for load-balancing multiuser spectrum decision schemes to evenly distribute the traffic loads of secondary users to multiple channels.
3. Propose a traffic-adaptive spectrum handoff scheme, which changes the target channel sequence of spectrum handoffs based on traffic conditions.
4. Determine the optimal target channel sequence for the proactive spectrum handoff.
5. Provide a framework to determine whether the spectrum sensing technology can effectively shorten the extended data delivery time under various sensing time and traffic parameters.
6. Develop a cross-layer admission control rule for the secondary users.

In the following, we summarize the results from the above contributions.

## **9.1 Modeling Techniques for Cognitive Radio Networks**

In this part, the preemptive resume priority (PRP) M/G/1 queueing network model has been proposed to evaluate the QoS performances for the connection-based spectrum management techniques in the non-hopping and

the hopping modes. This analytical framework provided a systematic viewpoint to integrate the designs of the spectrum management techniques and can help evaluate their QoS performances for various traffic arrival rates and service time distributions. There still exists many open problems for spectrum management techniques. On top of the proposed model, these open issues can be solved from the systematic viewpoint and then provide better traffic-adaptive solutions.

## 9.2 Load-Balancing Spectrum Decision

In this part, an analytical framework has been proposed to design the system parameters for the sensing-based and the probability-based spectrum decision schemes. The proposed model integrated with the PRP M/G/1 queueing systems can evaluate the effects of multiple interruptions from the primary connections and sensing errors (false alarm and missed detection) of the secondary connections on the overall system time for the two considered spectrum decision schemes. Based on this analytical model, the optimal number of candidate channels for the sensing-based spectrum selection method and the optimal channel selection probability for the probability-based spectrum selection method can be obtained analytically for various sensing time and traffic parameters. We found that the probability-based scheme can reduce the overall system time compared to the sensing-based scheme when the traffic loads of the secondary users is light, whereas the sensing-based scheme performs better in the condition of heavy traffic loads. This observation provide an important insight into design a traffic-adaptive spectrum decision scheme in the presence of sensing errors.

### 9.3 Proactive Spectrum Handoff

In this part, we have used the PRP M/G/1 queueing network model to characterize the spectrum usage behaviors with multiple handoffs. We studied the latency performance of the secondary connections by considering the effects of (1) generally distributed service time; (2) various operating channels; and (3) queueing behaviors of multiple secondary connections. The proposed model can accurately estimate the extended data delivery time of different proactively designed target channel sequences. On top of this model, we showed the extended data delivery time of the secondary connections based on the *always-staying* and the *always-changing* sequences in the IEEE 802.22 standard. If the secondary users can adaptively adopt the better target channel sequence according to traffic conditions, the extended data delivery time can be improved significantly compared to the existing target channel selection methods, especially for the heavy traffic loads of the primary users.

### 9.4 Optimal Proactive Spectrum Handoff

In this part, we have investigated the **Cumulative Handoff Delay Minimization Problem**. We formulated an optimization problem of determining a target channel sequence for multiple handoffs with the objective of minimizing the cumulative handoff delay for the newly arriving secondary user's connection. In order to solve this problem, we developed a state diagram to characterize the evolution of the target channel sequence. Based on this model, an optimal solution can be found by the proposed dynamic programming algorithm with time complexity of  $O(LM^2)$ . Furthermore, we suggested a suboptimal greedy strategy to select the target channels for spectrum handoffs with time complexity of  $O(M)$ . We proved that only six permutations of

the target channel sequences are needed to be compared when the suggested greedy strategy is adopted. Numerical results show that the performance of this greedy strategy can approach the optimal solution.

## 9.5 Reactive Spectrum Handoff

In this part, we have investigated the effects of reactive spectrum handoff on the channel utilization and the extended data delivery time of the secondary users' connections by considering the three key design features for spectrum handoffs, consisting of (1) heterogeneous arrival rates of the primary users; (2) various arrival rates of the secondary users; (3) handoff processing time. Firstly, we propose a PRP M/G/1 queueing network model to characterize the spectrum usage behaviors between the primary and the secondary connections with multiple handoffs . Next, we develop a state diagram to characterize the effect of multiple handoff delay on the extended data delivery time of the secondary users' connections. Based on the proposed unifying model, an insightful study to quantify the effect of the three design features on the channel utilizations and the extended data delivery time under various traffic arrival rates and service time distributions can be provided. More importantly, these analytical results can facilitate the designs of admission control rule for the secondary users and can provide a framework to determine whether the spectrum sensing technology can effectively shorten the data delivery time under various sensing time.

## 9.6 Interference-Avoiding Spectrum Sharing

In this part, we proposed an adaptively arrival rate control mechanism by adjusting traffic admission probability of the secondary connections in order to maintain the interference constraint of the primary users and the latency requirement of the secondary users. Although a larger traffic admission probability for the secondary connections can increase channel utilization, it leads to more interference on the primary connections as well as more contention between the secondary connections. In order to find the best traffic admission probability, we formulate this issue as a cross-layer optimization problem by considering the effects of sensing errors and power outage in the physical layer, traffic admission probability in the MAC layer, and the traffic statistics as well as the QoS constraints in the application layer. The analytical results show the optimal traffic admission probabilities under various cross-layer parameters and provide important insight into the design tradeoffs between the system-level performance measure (channel utilization) and the user-level performance measures (interference ratio and transmission latency).

## 9.7 Suggestions for Future Research

The proposed PRP M/G/1 queueing network model provides a systematic method to help the design of spectrum management technologies. It can capture the general behaviors for the connection-based channel usage, including the effects of channel selection, spectrum sensing time, multiple interruptions, channel switching between different channels, and generally distributed service time simultaneously. The contributions of this dissertation are summarized in Table 9.1, where the signs “o” and “x” indicate that the issue “has” and “has not” been discussed, respectively. Specifically, we have investigated

Table 9.1: Summary of This Dissertation

	Spectrum Management Techniques with Multiple Handoffs	
	Non-hopping Model	Hopping Mode
Spectrum Decision (Chapter 4)	○	×
Spectrum Mobility (Chapters 5-7)	○	○
Spectrum Sharing (Chapter 8)	○	×

the spectrum decision, mobility, and sharing issues in the non-hopping mode as well as the spectrum mobility issue in the hopping mode. The spectrum decision and sharing issues in the hopping model are still needed to be solved.

Some interesting research issues that can be extended from the proposed model include the following:

1. For the spectrum sensing issue, an interesting issue is to consider the sequential sensing. For example, in the sensing-based spectrum decision scheme in Chapter 4, we assume that the secondary user performs wide-band sensing to find the idle channel when a new connection request arrives at CR network. In fact, the secondary user can perform sequential sensing to find the idle channel. In this case, the sensing procedures can be terminated once one idle channel is found, and thus the sensing time can be shorter than  $n\tau$ . Furthermore, in Chapters 4 and 8, we assume that the class-A missed detection and false alarm probabilities are constant. In fact, as transmission time increases, missed detection and false alarm probabilities can be reduced because the sensing results at the previous sensing phases can be employed to improve the accuracy of the sensing results at the following sensing phases. Hence, it is also worthwhile to investigate the effects of variable missed detection

and false alarm probabilities in Chapters 4 and 8. Besides, the effects of the class-B missed detection is another important research issue.

2. From the viewpoint of *spectrum decision* issue, it is worthwhile determining the optimal distribution probability vector for the probability-based spectrum decision method when the secondary connections may have different opinions on the observed traffic statistics  $\lambda_p^{(k)}$ ,  $\lambda_s$ ,  $f_p^{(k)}(x)$ , and  $f_s(x)$ . Second, it would be interesting to see how to analyze the latency performance for the spectrum decision methods in the hopping mode.
3. The proposed model assumes that the *spectrum mobility* functionality can help the interrupted secondary user resume its unfinished data transmission on the suitable channel. This resumption policy can be characterized by the preemptive resumption priority queueing network. However, in other scenarios, the interrupted secondary user may need to retransmit the whole connection rather than resuming the unfinished transmission. In this situation, a CR network should be modeled by the preemptive repeat priority queueing network. It is also worthwhile to investigate the latency performances resulted from different transmission policies.
4. For the *spectrum sharing* issue, an interesting issue is to involve the distributed channel contention behaviors into the proposed model. In the proposed model, we assume that the FCFS scheduling policy is adopted. For a distributed medium access control (MAC) protocol such as the carrier sense multiple access (CSMA) protocol, the channel contention time and retransmission in the MAC layer should be taken into account when calculating the latency performance of the secondary



users.

Cognitive radio (CR) is an emerging technique to promote spectrum efficiency. Through the CR technique, we believe that the dream of freely connecting people anywhere anytime is no longer an impossible mission but will be come true in the near future. After all, the development of technology is to satisfy the need that people want.



# Bibliography

- [1] R. W. Brodersen, A. Wolisz, D. Cabric, S. M. Mishra, and D. Willkomm, “CORVUS: A Cognitive Radio Approach for Usage of Virtual Unlicensed Spectrum,” *Berkeley Wireless Research Center (BWRC) White paper*, 2004.
- [2] J. Mitola and G. Q. Maguire, “Cognitive Radio: Making Software Radios More Personal,” *IEEE Personal Communications*, vol. 6, pp. 13–18, Aug. 1999.
- [3] S. Haykin, “Cognitive Radio: Brain-empowered Wireless Communications,” *IEEE Journal on Selected Areas in Communications*, vol. 23, no. 2, pp. 201–220, Feb. 2005.
- [4] R. W. Thomas, L. A. DaSilva, and A. B. MacKenzie, “Cognitive Networks,” *IEEE International Symposium on Dynamic Spectrum Access Networks (DYSPAN)*, Nov. 2005.
- [5] I. F. Akyildiz, W.-Y. Lee, M. C. Vuran, and S. Mohanty, “NeXt Generation/Dynamic Spectrum Access/Cognitive Radio Wireless Networks: A Survey,” *Computer Networks Journal (Elsevier)*, vol. 50, pp. 2127–2159, Sep. 2006.

- [6] P.-Y. Huang and K.-C. Chen, "A Cognitive CSMA-based Multichannel MAC Protocol for Cognitive Radio Networks," *APSIPA Annual Summit and Conference (ASC)*, Oct. 2009.
- [7] D. Shiung and K.-C. Chen, "On the Optimal Power Allocation of a Cognitive Radio Networks," *IEEE International Symposium on Personal, Indoor and Mobile Radio Communications (PIMRC)*, Sep. 2009.
- [8] S.-Y. Lien, C.-C. Tseng, and K.-C. Chen, "Carrier Sensing based Multiple Access Protocols for Cognitive Radio Networks," *IEEE International Conference on Communications (ICC)*, May 2008.
- [9] O. Jo and D.-H. Cho, "Seamless Spectrum Handover Considering Differential Path-loss in Cognitive Radio Systems," *IEEE Communications Letters*, vol. 13, no. 3, pp. 190–192, Mar. 2009.
- [10] M. D. Silviu, R. Rangnekar, A. B. MacKenzie, and C. W. Bostian, "The Smart Radio Channel Change Protocol: A Primary User Avoidance Technique for Dynamic Spectrum Sharing Cognitive Radios to Facilitate Co-existence in Wireless Communication Networks," *International Conference on Cognitive Radio Oriented Wireless Networks and Communications (CrownCom)*, Jun. 2009.
- [11] A. Sgora and D. D. Vergados, "Handoff Prioritization and Decision Schemes in Wireless Cellular Networks: A Survey," *IEEE Communications Surveys and Tutorials*, vol. 11, no. 4, pp. 57–77, 2009.
- [12] I. F. Akyildiz, W.-Y. Lee, and K. R. Chowdhury, "CRAHNs: Cognitive Radio Ad Hoc Networks," *Ad Hoc Networks*, vol. 7, no. 5, pp. 810–836, 2009.

- [13] I. F. Akyildiz, W.-Y. Lee, M. C. Vuran, and S. Mohanty, "A Survey on Spectrum Management in Cognitive Radio Networks," *IEEE Communications Magazine*, vol. 46, no. 4, pp. 40–48, Apr. 2008.
- [14] Q. Zhao and A. Swami, "A Decision-theoretic Framework for Opportunistic Spectrum Access," *IEEE Wireless Communications Magazine*, vol. 14, no. 4, pp. 14–20, Aug. 2007.
- [15] X. Zhu, L. Shen, and T.-S. P. Yum, "Analysis of Cognitive Radio Spectrum Access with Optimal Channel Reservation," *IEEE Communications Letters*, vol. 11, no. 4, pp. 304–306, Apr. 2007.
- [16] C. Zhang, X. Wang, and J. Li, "Cooperative Cognitive Radio with Priority Queueing Analysis," *IEEE International Conference on Communications (ICC)*, Jun. 2009.
- [17] H. Tran, T. Q. Duong, and H.-J. Zepernick, "Average Waiting Time of Packets with Different Priorities in Cognitive Radio Networks," *IEEE International Symposium on Wireless Pervasive Computing (ISWPC)*, May 2010.
- [18] Y. Zhu, Q. Zhang, Z. Niu, and J. Zhu, "On Optimal QoS-aware Physical Carrier Sensing for IEEE 802.11 Based WLANs: Theoretical Analysis and Protocol Design," *IEEE Transactions on Wireless Communications*, vol. 7, no. 4, pp. 1369–1378, April 2008.
- [19] A. Banaei and C. N. Georghiades, "Throughput Analysis of a Randomized Sensing Scheme in Cell-based Ad-hoc Cognitive Networks," *IEEE International Conference on Communications (ICC)*, Jun. 2009.
- [20] J. Gambini, O. Simeone, Y. Bar-Ness, U. Spagnolini, and T. Yu, "Packet-wise Vertical Handover for Unlicensed Multi-standard Spec-

- trum Access with Cognitive Radios,” *IEEE Transactions on Wireless Communications*, vol. 7, no. 12, pp. 5172–5176, Dec. 2008.
- [21] J. Gambini, O. Simeone, U. Spagnolini, Y. Bar-Ness, and Y. Kim, “Cognitive Radio with Secondary Packet-By-Packet Vertical Handover,” *IEEE International Conference on Communications (ICC)*, May 2008.
- [22] G. Noh, J. Lee, and D. Hong, “Stochastic Multichannel Sensing for Cognitive Radio Systems: Optimal Channel Selection for Sensing with Interference Constraints,” *IEEE Vehicular Technology Conference Fall*, Sep. 2009.
- [23] C.-M. Lee, J.-S. Lin, Y.-P. Hsu, and K.-T. Feng, “Design and Analysis of Optimal Channel-hopping Sequence for Cognitive Radio Networks,” *IEEE Wireless Communications and Networking Conference (WCNC)*, Apr. 2010.
- [24] A. T. Chronopoulos, M. R. Musku, S. Penmatsa, and D. C. Popescu, “Spectrum Load Balancing for Medium Access in Cognitive Radio Systems,” *IEEE Communications Letters*, vol. 12, no. 5, pp. 353–355, May 2008.
- [25] I. Malanchini, M. Cesana, and N. Gatti, “On Spectrum Selection Games in Cognitive Radio Networks,” *IEEE Global Communications Conference (GLOBECOM)*, Nov. 2009.
- [26] H.-P. Shiang and M. van der Schaar, “Queuing-based Dynamic Channel Selection for Heterogeneous Multimedia Applications Over Cognitive Radio Networks,” *IEEE Transactions on Multimedia*, vol. 10, no. 5, pp. 896–909, Aug. 2008.

- [27] Y. Song, Y. Fang, and Y. Zhang, "Stochastic Channel Selection in Cognitive Radio Networks," *IEEE Global Communications Conference (GLOBECOM)*, Nov. 2007.
- [28] H.-J. Liu, S.-F. Li, Z.-X. Wang, W.-J. Hong, and M. Yi, "Strategy of Dynamic Spectrum Access Based-on Spectrum Pool," *IEEE International Conference on Wireless Communications, Networking and Mobile Computing (WiCOM)*, Sep. 2008.
- [29] A. W. Min and K. G. Shin, "Exploiting Multi-channel Diversity in Spectrum-agile Networks," *IEEE International Conference on Computer Communications (INFOCOM)*, Apr. 2008.
- [30] B. Hamdaoui, "Adaptive Spectrum Assessment for Opportunistic Access in Cognitive Radio Networks," *IEEE Transactions on Wireless Communications*, vol. 8, no. 2, pp. 922–930, Feb. 2009.
- [31] A. Sabharwal, A. Khoshnevis, and E. Knightly, "Opportunistic Spectral Usage: Bounds and a Multi-band CSMA/CA Protocol," *IEEE/ACM Transactions on Networking*, vol. 15, no. 3, pp. 533–545, 2007.
- [32] J. Jia, Q. Zhang, and X. S. Shen, "HC-MAC: A Hardware-constrained Cognitive MAC for Efficient Spectrum Management," *IEEE Journal on Selected Areas in Communications*, vol. 26, no. 1, pp. 106–117, Jan 2008.
- [33] M. Felegyhazi and J.-P. Hubaux, "Game Theory in Wireless Networks: A Tutorial," *EPFL Technical Report: LCA-REPORT-2006-002*, 2006.
- [34] Q. Zhao, L. Tong, A. Swami, and Y. Chen, "Decentralized Cognitive MAC for Opportunistic Spectrum Access in Ad Hoc Networks: A

- POMDP Framework,” *IEEE Journal on Selected Areas in Communications*, vol. 25, no. 3, pp. 589–600, April 2007.
- [35] Q. Zhao, S. Geirhofer, L. Tong, and B. M. Sadler, “Opportunistic Spectrum Access via Periodic Channel Sensing,” *IEEE Transactions on Signal Processing*, vol. 56, no. 2, pp. 785–796, Feb. 2008.
- [36] O. Mehanna, A. Sultan, and H. E. Gamal, “Blind Cognitive MAC Protocols,” *IEEE International Conference on Communications (ICC)*, Jun. 2009.
- [37] S. Senthuran, A. Anpalagan, and O. Das, “A Predictive Opportunistic Access Scheme for Cognitive Radios,” *IEEE Vehicular Technology Conference Fall*, Sep. 2009.
- [38] L. Yang, L. Cao, and H. Zheng, “Proactive Channel Access in Dynamic Spectrum Networks,” *Physical Communication*, vol. 1, no. 2, pp. 103–111, 2008.
- [39] R.-T. Ma, Y.-P. Hsu, and K.-T. Feng, “A POMDP-based Spectrum Handoff Protocol for Partially Observable Cognitive Radio Networks,” *IEEE Wireless Communications and Networking Conference (WCNC)*, Apr. 2009.
- [40] M. Hoyhtya, S. Pollin, and A. Mammela, “Performance Improvement with Predictive Channel Selection for Cognitive Radios,” *IEEE International Workshop on Cognitive Radio and Advanced Spectrum Management (CogART)*, Feb. 2008.
- [41] S.-U. Yoon and E. Ekici, “Voluntary Spectrum Handoff: A Novel Approach to Spectrum Management in CRNs,” *IEEE International Conference on Communications (ICC)*, May 2010.

- [42] Y. Song and J. Xie, "Common Hopping Based Proactive Spectrum Handoff in Cognitive Radio Ad Hoc Networks," *IEEE Global Communications Conference (GLOBECOM)*, Dec. 2010.
- [43] L.-C. Wang and A. Chen, "On the Performance of Spectrum Handoff for Link Maintenance in Cognitive Radio," *IEEE International Symposium on Wireless Pervasive Computing (ISWPC)*, May 2008.
- [44] B. Wang, Z. Ji, K. J. Ray Liu, and T. C. Clancy, "Primary-prioritized Markov Approach for Dynamic Spectrum Allocation," *IEEE Transactions on Wireless Communications*, vol. 8, pp. 1854–1865, Apr. 2009.
- [45] I. Suliman and J. Lehtomaki, "Queueing Analysis of Opportunistic Access in Cognitive Radios," *IEEE International Workshop on Cognitive Radio and Advanced Spectrum Management (CogART)*, May 2009.
- [46] H. Li, "Queueing Analysis of Dynamic Spectrum Access Subject to Interruptions from Primary Users," *International Conference on Cognitive Radio Oriented Wireless Networks and Communications (CrownCom)*, Jun. 2010.
- [47] P. Zhu, J. Li, and X. Wang, "A New Channel Parameter for Cognitive Radio," *International Conference on Cognitive Radio Oriented Wireless Networks and Communications (CrownCom)*, Aug. 2007.
- [48] S. Wang and H. Zheng, "A Resource Management Design for Cognitive Radio Ad Hoc Networks," *IEEE Military Communications Conference (MILCOM)*, Oct. 2009.
- [49] F. Borgonovo, M. Cesana, and L. Fratta, "Throughput and Delay Bounds for Cognitive Transmissions," *Advances in Ad Hoc Networking*, vol. 265, pp. 179–190, Aug. 2008.



- [50] C.-T. Chou, Sai Shankar N, H. Kim, and K. G. Shin, "What and How Much to Gain from Spectral Agility?" *IEEE Journal on Selected Areas in Communications*, vol. 25, no. 3, pp. 576–588, Apr. 2007.
- [51] J. Heo, J. Shin, J. Nam, Y. Lee, J. G. Park, and H.-S. Cho, "Mathematical Analysis of Secondary User Traffic in Cognitive Radio System," *IEEE Vehicular Technology Conference Fall*, Sep. 2008.
- [52] Y. Zhang, "Spectrum Handoff in Cognitive Radio Networks: Opportunistic and Negotiated Situations," *IEEE International Conference on Communications (ICC)*, Jun. 2009.
- [53] F. Capar, I. Martoyo, T. Weiss, and F. Jondral, "Comparison of Bandwidth Utilization for Controlled and Uncontrolled Channel Assignment in a Spectrum Pooling System," *IEEE Vehicular Technology Conference Spring*, May 2002.
- [54] B. Ishibashi, N. Bouabdallah, and R. Boutaba, "QoS Performance Analysis of Cognitive Radio-based Virtual Wireless Networks," *IEEE International Conference on Computer Communications (INFOCOM)*, Apr. 2008.
- [55] D. Pacheco-Paramo, V. Pla, and J. Martinez-Bauset, "Optimal Admission Control in Cognitive Radio Networks," *International Conference on Cognitive Radio Oriented Wireless Networks and Communications (CrownCom)*, Jun. 2009.
- [56] W. Ahmed, J. Gao, and M. Faulkner, "Performance Evaluation of a Cognitive Radio Network with Exponential and Truncated Usage Models," *IEEE International Symposium on Wireless Pervasive Computing (ISWPC)*, Oct. 2009.

- [57] M. Huang, R. Yu, and Y. Zhang, "Call Admission Control with Soft-QoS Based Spectrum Handoff in Cognitive Radio Networks," *International Conference on Wireless Communications and Mobile Computing (IWCMC)*, Jun. 2009.
- [58] I. Suliman, J. Lehtomaki, T. Braysy, and K. Umebayashi, "Analysis of Cognitive Radio Networks with Imperfect Sensing," *IEEE International Symposium on Personal, Indoor and Mobile Radio Communications (PIMRC)*, Sep. 2009.
- [59] S. Tang and B. L. Mark, "Performance Analysis of a Wireless Network with Opportunistic Spectrum Sharing," *IEEE Global Communications Conference (GLOBECOM)*, Nov. 2007.
- [60] —, "Modeling and Analysis of Opportunistic Spectrum Sharing with Unreliable Spectrum Sensing," *IEEE Transactions on Wireless Communications*, vol. 8, pp. 1934–1943, Apr. 2009.
- [61] —, "Modeling an Opportunistic Spectrum Sharing System with a Correlated Arrival Process," *IEEE Wireless Communications and Networking Conference (WCNC)*, Apr. 2008.
- [62] —, "An Analytical Performance Model of Opportunistic Spectrum Access in a Military Environment," *IEEE Wireless Communications and Networking Conference (WCNC)*, Apr. 2008.
- [63] E. W. M. Wong and C. H. Foh, "Analysis of Cognitive Radio Spectrum Access with Finite User Population," *IEEE Communications Letters*, vol. 13, no. 5, pp. 294–296, May 2009.
- [64] M. M. Rashid, M. J. Hossain, E. Hossain, and V. K. Bhargava, "Opportunistic Spectrum Access in Cognitive Radio Networks: A Queueing

- Analytic Model and Admission Controller Design,” *IEEE Global Communications Conference (GLOBECOM)*, Nov. 2007.
- [65] —, “Opportunistic Spectrum Scheduling for Multiuser Cognitive Radio: A Queueing Analysis,” *IEEE Transactions on Wireless Communications*, vol. 8, no. 10, pp. 5259–5269, Oct. 2009.
- [66] Y. Zhang, “Dynamic Spectrum Access in Cognitive Radio Wireless Networks,” *IEEE International Conference on Communications (ICC)*, May 2008.
- [67] Sai Shankar N, “Squeezing the Most Out of Cognitive Radio: A Joint MAC/PHY Perspective,” *IEEE International Conference on Acoustics, Speech and Signal Processing*, vol. 4, Apr. 2007.
- [68] Sai Shankar N, C.-T. Chou, K. Challapali, and S. Mangold, “Spectrum Agile Radio: Capacity and QoS Implications of Dynamic Spectrum Assignment,” *IEEE Global Communications Conference (GLOBECOM)*, Nov. 2005.
- [69] I. Suliman and J. Lehtomaki, “Optimizing Detection Parameters for Time-slotted Cognitive Radios,” *IEEE Vehicular Technology Conference Spring*, Apr. 2009.
- [70] W. Hu, D. Willkomm, G. Vrantis, M. Gerla, and A. Wolisz, “Dynamic Frequency Hopping Communities for Efficient IEEE 802.22 Operation,” *IEEE Communications Magazine*, vol. 45, no. 5, pp. 80–87, May 2007.
- [71] H.-J. Liu, Z.-X. Wang, S.-F. Li, and M. Yi, “Study on the Performance of Spectrum Mobility in Cognitive Wireless Network,” *IEEE Singapore International Conference on Communication Systems (ICCS)*, Jun. 2008.

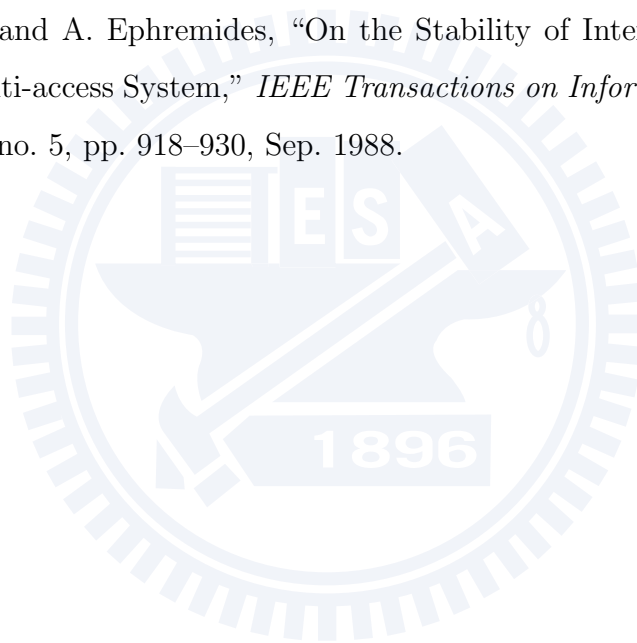
- [72] H. Su and X. Zhang, "Channel-hopping Based Single Transceiver MAC for Cognitive Radio Networks," *IEEE Annual Conference on Information Sciences and Systems (CISS)*, Mar. 2008.
- [73] Y.-C. Liang, Y. Zeng, E. C. Peh, and A. T. Hoang, "Sensing-throughput Tradeoff for Cognitive Radio Networks," *IEEE Transactions on Wireless Communications*, vol. 7, no. 4, Apr. 2008.
- [74] P. Wang, L. Xiao, S. Zhou, and J. Wang, "Optimization of Detection Time for Channel Efficiency in Cognitive Radio Systems," *IEEE Wireless Communications and Networking Conference (WCNC)*, Mar. 2007.
- [75] W.-Y. Lee and I. F. Akyildiz, "Optimal Spectrum Sensing Framework for Cognitive Radio Networks," *IEEE Transactions on Wireless Communications*, vol. 7, no. 10, pp. 3845–3857, Oct. 2008.
- [76] C. R. Stevenson, G. Chouinard, Z. Lei, W. Hu, S. J. Shellhammer, and W. Caldwell, "IEEE 802.22: The First Cognitive Radio Wireless Regional Area Network Standard," *IEEE Communications Magazine*, vol. 47, no. 1, pp. 130–138, Jan. 2009.
- [77] IEEE 802.11, *Part 11: Wireless LAN Medium Access Control (MAC) and Physical Layer (PHY) Specifications*, supplement to IEEE 802.11 Standard, Sept. 1999.
- [78] L. Kleinrock, *Queueing Systems - Volume 2: Computer Applications*. John Wiley & Sons Inc., 1975.
- [79] L.-C. Wang, C.-W. Wang, and F. Adachi, "Load-balancing Spectrum Decision for Cognitive Radio Networks," *accepted by IEEE Journal on Selected Areas in Communications (JSAC)*, 2010.

- [80] X. Liu and Z. Ding, "ESCAPE: A Channel Evacuation Protocol for Spectrum-agile Networks," *IEEE International Symposium on Dynamic Spectrum Access Networks (DYSPAN)*, Apr. 2007.
- [81] C.-W. Wang, L.-C. Wang, and F. Adachi, "Modeling and Analysis of Multi-user Spectrum Selection Schemes in Cognitive Radio Networks," *IEEE International Symposium on Personal, Indoor and Mobile Radio Communications (PIMRC)*, Sep. 2009.
- [82] X. Li and S. A. Zekavat, "Traffic Pattern Prediction and Performance Investigation for Cognitive Radio Systems," *IEEE Wireless Communications and Networking Conference (WCNC)*, Mar. 2008.
- [83] H. Jiang, L. Lai, R. Fan, and H. V. Poor, "Optimal Selection of Channel Sensing Order in Cognitive Radio," *IEEE Transactions on Wireless Communications*, vol. 8, no. 1, pp. 297–307, Jan. 2009.
- [84] C.-W. Wang, L.-C. Wang, and F. Adachi, "Performance Gains for Spectrum Utilization in Cognitive Radio Networks with Spectrum Handoff," *International Symposium on Wireless Personal Multimedia Communications (WPMC)*, Sep. 2009.
- [85] C.-W. Wang and L.-C. Wang, "Modeling and Analysis for Proactive-decision Spectrum Handoff in Cognitive Radio Networks," *IEEE International Conference on Communications (ICC)*, Jun. 2009.
- [86] Chee-Hock Ng and Boon-Hee Soong, *Queueing Modelling Fundamentals with Applications in Communication Networks, 2nd*. John Wiley & Sons Inc., 2008.

- [87] Q. Zhao and B. M. Sadler, "A Survey of Dynamic Spectrum Access: Signal Processing, Networking, and Regulatory Policy," *IEEE Signal Processing Magazine*, pp. 79–89, May 2007.
- [88] N. K. Jaiswal, "Preemptive Resume Priority Queue," *Operations Research*, vol. 9, no. 5, pp. 732–742, Sep./Oct. 1961.
- [89] *Draft Standard for Wireless Regional Area Networks Part 22: Cognitive Wireless RAN Medium Access Control (MAC) and Physical Layer (PHY) Specifications*, IEEE 802.22 Working Group.
- [90] S. Srinivasa and S. A. Jafar, "The Throughput Potential of Cognitive Radio: A Theoretical Perspective," *IEEE Communications Magazine*, pp. 73–79, May 2007.
- [91] Q. Shi, D. Taubenheim, S. Kyperountas, P. Gorday, and N. Correal, "Link Maintenance Protocol for Cognitive Radio System with OFDM PHY," *IEEE International Symposium on Dynamic Spectrum Access Networks (DYSPAN)*, Apr. 2007.
- [92] C.-W. Wang, L.-C. Wang, and F. Adachi, "Modeling and Analysis for Rective-decision Spectrum Handoff in Cognitive Radio Networks," *IEEE GLOBECOM*, Dec. 2010.
- [93] D. Willkomm, J. Gross, and A. Wolisz, "Reliable Link Maintenance in Cognitive Radio Systems," *IEEE International Symposium on Dynamic Spectrum Access Networks (DYSPAN)*, Nov. 2005.
- [94] J. Tian and G. Bi, "A New Link Maintenance and Compensation Model for Cognitive UWB Radio Systems," *International Conference on ITS Telecommunications Proceedings*, Jun. 2006.

- [95] L.-C. Wang and C.-W. Wang, "Spectrum Handoff for Cognitive Radio Networks: Reactive-sensing or Proactive-sensing?" *IEEE International Performance Computing and Communications Conference (IPCCC)*, Dec. 2008.
- [96] L.-C. Wang, Y.-C. Lu, C.-W. Wang, and D. S.-L. Wei, "Latency Analysis for Dynamic Spectrum Access in Cognitive Radio: Dedicated or Embedded Control Channel?" *IEEE International Symposium on Personal, Indoor and Mobile Radio Communications (PIMRC)*, Sep. 2007.
- [97] R. W. Wolff, "Poisson Arrivals See Time Averages," *Operations Research*, vol. 30, no. 2, pp. 223–231, Mar./Apr. 1982.
- [98] S. K. Bose, *An Introduction to Queueing Systems*. Kluwer Academic/Plenum Publishers, New York, 2002.
- [99] ETSI, "Universal Mobile Telecommunications System (UMTS); Selection Procedures for The Choice of Radio Transmission Technologies of The UMTS," *Technical Report UMTS 30.03 version 3.2.0*, April 1998.
- [100] C. R. Stevenson, C. Cordeiro, E. Sofer, and G. Chouinard, "Functional Requirements for The 802.22 WRAN Standard," *IEEE 802.22-05/0007r46*, Sep. 2005.
- [101] C.-W. Wang, L.-C. Wang, and F. Adachi, "Optimal Admission Control in Cognitive Radio Networks with Sensing Errors," *IEICE Tech. Rep.*, vol. 109, no. 440, pp. 491–496, Mar. 2010.
- [102] L.-C. Wang and C.-W. Wang, "Spectrum Management Techniques with QoS Provisioning in Cognitive Radio Networks," *International Symposium on Wireless and Pervasive Computing (ISWPC)*, May 2010.

- [103] L.-C. Wang, C.-W. Wang, and C.-J. Chang, “Modeling and Analysis for Spectrum Handoffs in Cognitive Radio Networks,” *Submitted to IEEE Transactions on Mobile Computing*, 2010.
- [104] M. S. Jang and D. J. Lee, “Optimum Sensing Time Considering False Alarm in Cognitive Radio Networks,” *IEEE International Symposium on Personal, Indoor and Mobile Radio Communications (PIMRC)*, Sep. 2009.
- [105] R. Rao and A. Ephremides, “On the Stability of Interacting Queues in a Multi-access System,” *IEEE Transactions on Information Theory*, vol. 34, no. 5, pp. 918–930, Sep. 1988.





## Appendix

### A Distribution Probability Vector for the Sensing-based Channel Selection Scheme

The probability that a secondary user can select channel  $k$  for its operating channel is determined inherently based on the traffic patterns for the sensing-based spectrum decision scheme. According to the sensing outcomes, this probability consists of three components. First, we consider the case that false alarm does not occur at the idle channel  $k$ . When the channels in  $\mathfrak{S} \subseteq \Omega - \{k\}$  are also actually idle and false alarms do not occur at the channels in  $\mathfrak{R} \subseteq \mathfrak{S}$ , channel  $k$  will be selected with probability  $\frac{1}{1+|\mathfrak{R}|}$ . Secondly, we consider the case when a false alarm occurs at the idle channel  $k$ . If false alarms also occur at all the remaining idle channels, the secondary user will randomly select one channel from all candidate channels to be its operating channel. In this case, channel  $k$  is selected with probability  $1/|\Omega|$ . Thirdly, we consider the case when channel  $k$  is actually busy. With the similar argument in the previous case, the secondary user will randomly select one channel if false alarms occur at all the idle channels. In this case, channel  $k$  will be selected with probability  $1/|\Omega|$ . On the other hand, channel  $k$  cannot

be selected when  $k \notin \Omega$ . From these observations, we can have

$$p_{sb}^{(k)} = \begin{cases} (1 - \rho^{(k)})(1 - P_F) \times \\ \sum_{\mathfrak{S} \subseteq \Omega - \{k\}} \left[ \prod_{i \in \mathfrak{S}} (1 - \rho^{(i)}) \prod_{j \in \Omega - \{k\} - \mathfrak{S}} \rho^{(j)} \sum_{\mathfrak{R} \subseteq \mathfrak{S}} \frac{1}{1 + |\mathfrak{R}|} (1 - P_F)^{|\mathfrak{R}|} (P_F)^{|\mathfrak{S}| - |\mathfrak{R}|} \right] + \\ [(1 - \rho^{(k)})P_F + \rho^{(k)}] \times \\ \sum_{\mathfrak{S} \subseteq \Omega - \{k\}} \left[ \prod_{i \in \mathfrak{S}} (1 - \rho^{(i)}) \prod_{j \in \Omega - \{k\} - \mathfrak{S}} \rho^{(j)} (P_F)^{|\mathfrak{S}|} \right] \times \frac{1}{|\Omega|} , & k \in \Omega \\ 0 , & k \notin \Omega \end{cases}$$

## B Derivation of $\omega_i^{(k)}$

First, we consider the type- $i$  secondary connections whose default channels are channel  $\eta$ . Denote  $\omega_{i,\eta}^{(k)}$  as the arrival rate of these secondary connections at channel  $k$ ,  $p_{i,\eta}^{(k)}$  as the probability that these secondary connections are interrupted again at channel  $k$ , and  $\Phi_{i,\eta}^{(k)}$  as the effective service time of these secondary connections at channel  $k$ . Hence, we have

$$\omega_i^{(k)} = \sum_{\eta=1}^M \omega_{i,\eta}^{(k)} , \quad (\text{B1})$$

$$p_i^{(k)} = \sum_{\eta=1}^M \frac{\omega_{i,\eta}^{(k)}}{\omega_i^{(k)}} p_{i,\eta}^{(k)} , \quad (\text{B2})$$

$$\mathbf{E}[\Phi_i^{(k)}] = \sum_{\eta=1}^M \frac{\omega_{i,\eta}^{(k)}}{\omega_i^{(k)}} \mathbf{E}[\Phi_{i,\eta}^{(k)}] , \quad (\text{B3})$$

and

$$\mathbf{E}[(\Phi_i^{(k)})^2] = \sum_{\eta=1}^M \frac{\omega_{i,\eta}^{(k)}}{\omega_i^{(k)}} \mathbf{E}[(\Phi_{i,\eta}^{(k)})^2] . \quad (\text{B4})$$

Next, we derive  $\omega_{i,\eta}^{(k)}$  as follows. For the type- $i$  secondary connections whose default channels are channel  $\eta$ , their operating channels are channel  $s_{i,\eta}$

after the  $i^{\text{th}}$  interruption. In addition, for the type-0 secondary connections on their default channel  $\eta = s_{0,\eta}$ , we have  $\omega_{0,\eta}^{(\eta)} = \lambda_s^{(\eta)}$ . Moreover, the type- $(i-1)$  secondary connections at channel  $s_{i-1,\eta}$  will turn into the new arrivals of the type- $i$  secondary connections at channel  $s_{i,\eta}$  when they are interrupted again. Hence, we have

$$\begin{aligned}
\omega_{i,\eta}^{(k)} &= \begin{cases} 0 & , \quad k \neq s_{i,\eta} \\ \lambda_s^{(\eta)} & , \quad k = s_{i,\eta}, \text{ and } i = 0 \\ \omega_{i-1,\eta}^{(s_{i-1,\eta})} p_{i-1,\eta}^{(s_{i-1,\eta})} & , \quad k = s_{i,\eta}, \text{ and } i \geq 1 \end{cases} \\
&= \begin{cases} 0 & , \quad k \neq s_{i,\eta} \\ \lambda_s^{(\eta)} \prod_{j=0}^{i-1} p_{j,\eta}^{(s_{j,\eta})} & , \quad k = s_{i,\eta} \end{cases} \\
&= \begin{cases} 0 & , \quad k \neq s_{i,\eta} \\ \lambda_s^{(k)} \prod_{j=0}^{i-1} \lambda_p^{(s_{j,\eta})} \mathbf{E}[\Phi_{j,\eta}^{(s_{j,\eta})}] & , \quad k = s_{i,\eta} \end{cases} . \quad (\text{B5})
\end{aligned}$$

Note that  $p_{j,\eta}^{(s_{j,\eta})} = \lambda_p^{(s_{j,\eta})} \mathbf{E}[\Phi_{j,\eta}^{(s_{j,\eta})}]$  according to (5.18). Because  $\lambda_s^{(k)}$  and  $\lambda_p^{(k)}$  are given in advanced as well as  $\mathbf{E}[\Phi_{j,\eta}^{(s_{j,\eta})}]$  has been derived in Appendix C, we can obtain the closed-form expression for  $\omega_{i,\eta}^{(k)}$ . Finally, substituting (B5) into (B1),  $\omega_i^{(k)}$  in (5.17) can be evaluated.

## C Derivations of $\mathbf{E}[\Phi_i^{(k)}]$ and $\mathbf{E}[(\Phi_i^{(k)})^2]$

Here we only show how to evaluate  $\mathbf{E}[\Phi_{i,\eta}^{(k)}]$  and  $\mathbf{E}[(\Phi_{i,\eta}^{(k)})^2]$  because we can obtain  $\mathbf{E}[\Phi_i^{(k)}]$  and  $\mathbf{E}[(\Phi_i^{(k)})^2]$  in (5.7), (5.12), and (5.3) when  $\mathbf{E}[\Phi_{i,\eta}^{(k)}]$  and  $\mathbf{E}[(\Phi_{i,\eta}^{(k)})^2]$  are known according to (B3) and (B4). Denoted  $f_{i,\eta}^{(k)}(\phi)$  and  $F_{i,\eta}^{(k)}(\phi)$  as the probability density function (pdf) and the cumulative density function (cdf) of  $\Phi_{i,\eta}^{(k)}$  where  $i \geq 0$ , respectively. Moreover, let  $\Gamma_p^{(k)}$  be the inter-arrival time of the primary connections at channel  $k$ . Then, for the type-0 secondary connections whose default channels are channel  $\eta = s_{0,\eta}$ ,

their effective duration at channel  $k$  can be expressed as follows:

$$\Phi_{0,\eta}^{(k)} = \begin{cases} 0 & , \quad k \neq s_{0,\eta} \\ \min(\Gamma_p^{(\eta)}, X_s^{(\eta)}) & , \quad k = s_{0,\eta} \end{cases}, \quad (\text{C1})$$

where  $\min(a, b)$  is the minimum function. It returns the minimal value among  $a$  and  $b$ . Hence, the cdf of  $\Phi_{0,\eta}^{(k)}$  can be expressed as follows:

$$F_{0,\eta}^{(k)}(\phi) = \begin{cases} 0 & , \quad k \neq s_{0,\eta} \\ 1 - [(1 - A_p^{(\eta)}(\phi))(1 - F_s^{(\eta)}(\phi))] & , \quad k = s_{0,\eta} \end{cases}. \quad (\text{C2})$$

where  $A_p^{(k)}(\gamma)$  and  $F_s^{(k)}(\phi)$  are the cdfs of  $\Gamma_p^{(k)}$  and  $X_s^{(k)}$ , respectively. They are system parameters and are known in advance.

Next, let  $\tilde{\Phi}_{i,\eta}^{(k)}$  be the remaining transmission time when a type- $i$  secondary connection whose default channel is channel  $\eta$  is interrupted at channel  $k$ . Furthermore, the pdf and the cdf of  $\tilde{\Phi}_{i,\eta}^{(k)}$  are denoted by  $\tilde{f}_{i,\eta}^{(k)}(\phi)$  and  $\tilde{F}_{i,\eta}^{(k)}(\phi)$ , respectively. According to the definition of  $\tilde{\Phi}_{i,\eta}^{(k)}$ , we have

$$\tilde{\Phi}_{0,\eta}^{(k)} = \begin{cases} 0 & , \quad k \neq s_{0,\eta} \\ X_s^{(\eta)} - \Phi_{0,\eta}^{(\eta)} & , \quad k = s_{0,\eta} \end{cases}. \quad (\text{C3})$$

Because the pdf of  $X_s^{(\eta)}$  has been known and the pdf of  $\Phi_{0,\eta}^{(\eta)}$  can be derived by differentiating (C2), we can derive  $\tilde{F}_{0,\eta}^{(\eta)}(\phi)$  as follows:

$$\begin{aligned} & \tilde{F}_{0,\eta}^{(\eta)}(\phi) \\ &= \Pr(\tilde{\Phi}_{0,\eta}^{(\eta)} \leq \phi) \\ &= \Pr(X_s^{(\eta)} - \Phi_{0,\eta}^{(\eta)} \leq \phi) \\ &= \Pr(X_s^{(\eta)} - \min(\Gamma_p^{(\eta)}, X_s^{(\eta)}) \leq \phi) \\ &= \int \int_{x - \min(\gamma, x) \leq \phi} a_p^{(\eta)}(\gamma) f_s^{(\eta)}(x) \eta \gamma \eta x, \end{aligned} \quad (\text{C4})$$

where  $a_p^{(k)}(\gamma)$  and  $f_s^{(k)}(x)$  are the pdfs of  $\Gamma_p^{(k)}$  and  $X_s^{(k)}$ , respectively. Then, we can obtain  $\tilde{f}_{0,\eta}^{(k)}(\phi)$  by differentiating  $\tilde{F}_{0,\eta}^{(k)}(\phi)$ . Furthermore, according to

the total probability principle, we have

$$\tilde{f}_{0,\eta}^{(k)}(\phi) = \begin{cases} 0 & , \quad k \neq s_{0,\eta} \\ \Pr(N < 1)\tilde{f}_{0,\eta}^{(\eta)}(\phi|N < 1) + \Pr(N \geq 1)\tilde{f}_{0,\eta}^{(\eta)}(\phi|N \geq 1) & , \quad k = s_{0,\eta} \end{cases} . \quad (\text{C5})$$

Because the remaining transmission time is zero when a secondary connection does not encounter any interruption during its transmission period, we have  $\tilde{f}_{0,\eta}^{(\eta)}(\phi|N < 1) = \delta(\phi)$  where  $\delta(\phi)$  is the delta function. Then, we can revise (C5) as follows:

$$\tilde{f}_{0,\eta}^{(\eta)}(\phi|N \geq 1) = \frac{\tilde{f}_{0,\eta}^{(\eta)}(\phi)}{\Pr(N \geq 1)} = \frac{\tilde{f}_{0,\eta}^{(\eta)}(\phi)}{p_{0,\eta}^{(\eta)}} = \frac{\tilde{f}_{0,\eta}^{(\eta)}(\phi)}{\lambda_p^{(\eta)} \mathbf{E}[\Phi_{0,\eta}]} . \quad (\text{C6})$$

When a type-0 secondary connection is interrupted on its default channel  $\eta = s_{0,\eta}$ , its remaining transmission time will turn into the transmission time of the type-1 secondary connection at channel  $s_{1,\eta}$ . That is, the events  $\{\Phi_{1,\eta}^{(s_{1,\eta})} < \phi\}$  and  $\{\min(\Delta_p^{(s_{1,\eta})}, \tilde{\Phi}_{0,\eta}^{(s_{0,\eta})}) < \phi|N \geq 1\}$  are equivalent. Then, following the similar argument as in (C2) and (C6), we can have

$$F_{1,\eta}^{(k)}(\phi) = \begin{cases} 0 & , \quad k \neq s_{1,\eta} \\ 1 - [(1 - A_p^{(s_{1,\eta})}(\phi))(\tilde{F}_{0,\eta}^{(s_{0,\eta})}(\phi|N \geq 1))] & , \quad k = s_{1,\eta} \end{cases} . \quad (\text{C7})$$

and

$$\tilde{f}_{1,\eta}^{(s_{1,\eta})}(\phi|N \geq 2) = \frac{\tilde{f}_{1,\eta}^{(s_{1,\eta})}(\phi)}{\Pr(N \geq 2)} = \frac{\tilde{f}_{1,\eta}^{(s_{1,\eta})}(\phi)}{\prod_{j=0}^1 p_{j,\eta}^{(s_{j,\eta})}} = \frac{\tilde{f}_{1,\eta}^{(s_{1,\eta})}(\phi)}{\prod_{j=0}^1 \lambda_p^{(s_{j,\eta})} \mathbf{E}[\Phi_{j,\eta}^{(s_{j,\eta})}]} , \quad (\text{C8})$$

where  $\tilde{F}_{0,\eta}^{(s_{0,\eta})}(\phi|N \geq 1)$  can be derived by integrating  $\tilde{f}_{0,\eta}^{(s_{0,\eta})}(\phi|N \geq 1)$  in (C6).

Repeating the similar discussions, the general forms of  $F_{i,\eta}^{(k)}(\phi)$  and  $\tilde{f}_{i,\eta}^{(s_{i,\eta})}(\phi|N \geq$

$i + 1$ ) for any  $i$  can be expressed as follows:

$$F_{i,\eta}^{(k)}(\phi) = \begin{cases} 0 & , \quad k \neq s_{i,\eta} \\ 1 - [(1 - A_p^{(s_{i,\eta})}(\phi))(\tilde{F}_{i-1,\eta}^{(s_{i-1,\eta})}(\phi|N \geq i))] & , \quad k = s_{i,\eta} \end{cases} , \quad (\text{C9})$$

and

$$\tilde{f}_{i,\eta}^{(s_{i,\eta})}(\phi|N \geq i+1) = \frac{\tilde{f}_{i,\eta}^{(s_{i,\eta})}(\phi)}{\mathbf{Pr}(N \geq i+1)} = \frac{\tilde{f}_{i,\eta}^{(s_{i,\eta})}(\phi)}{\prod_{j=0}^i p_{j,\eta}^{(s_{j,\eta})}} = \frac{\tilde{f}_{i,\eta}^{(s_{i,\eta})}(\phi)}{\prod_{j=0}^i \lambda_p^{(s_{j,\eta})} \mathbf{E}[\Phi_{j,\eta}^{(s_{j,\eta})}]} , \quad (\text{C10})$$

where  $\tilde{F}_{i-1,\eta}^{(s_{i-1,\eta})}(\phi|N \geq i)$  is the integration of  $\tilde{f}_{i-1,\eta}^{(s_{i-1,\eta})}(\phi|N \geq i)$ . Because the arrivals of the primary connections follow the Poisson process, we have  $A_p^{(k)}(\gamma) = 1 - e^{-\lambda_p^{(k)}\gamma}$ . Based on the relationships of (C9) and (C10), we can derive the functions  $f_{i,\eta}^{(k)}(\phi)$  from  $F_{i,\eta}^{(k)}(\phi)$ , and thus  $\mathbf{E}[\Phi_{i,\eta}^{(k)}]$  and  $\mathbf{E}[(\Phi_{i,\eta}^{(k)})^2]$  can be also evaluated.

## D Derivation of $\mathbf{Pr}(\tilde{X}_p = x)$

Now, we show how to derive  $\mathbf{Pr}(\tilde{X}_p = x)$  from  $f_p(x)$ . Let  $f_p(x) = \mathbf{Pr}(X_p = x)$ . We can have

$$\mathbf{Pr}(\tilde{X}_p = \tilde{x}) = \sum_{x=1}^{\tilde{X}_p} \mathbf{Pr}(\tilde{X}_p = \tilde{x}|X_p = x) \mathbf{Pr}(X_p = x) . \quad (\text{D1})$$

Referring to [79], we find that  $\mathbf{Pr}(\tilde{X}_p = \tilde{x}|X_p = x)$  follows the negative binomial distribution with parameter  $P_M \rho_s$ . That is,

$$\mathbf{Pr}(\tilde{X}_p = \tilde{x}|X_p = x) = \binom{\tilde{x} - 1}{\tilde{x} - x} (1 - P_M \rho_s)^x (P_M \rho_s)^{\tilde{x} - x} . \quad (\text{D2})$$

# Vita

**Chung-Wei Wang** (S'07) received the B.S. degree in electrical engineering from Tamkang University, Taipei, Taiwan, in 2003, and the Minor M.S. and Ph.D. degrees in applied mathematics and communication engineering from the National Chiao-Tung University, Hsinchu, Taiwan, in 2007 and 2010, respectively. From 2009 to 2010, he was also a visiting scholar in Tohoku University, Sendai, Japan. He was awarded the student travel grant from IEEE ICC 2009. His current research interests include cross-layer optimization, MAC protocols design, and radio resource management in wireless sensor networks, ad hoc networks, and cognitive radio networks.

# Publication List

## Journal Paper (published or accepted)

1. Li-Chun Wang, Chung-Wei Wang, and Chuan-Ming Liu, “Optimal Number of Clusters in Dense Wireless Sensor Networks: A Cross-layer Approach,” *IEEE Transactions on Vehicular Technology*, vol. 58, no. 2, pp. 966-976, Feb. 2009.
2. Li-Chun Wang, Chung-Wei Wang, and Fumiyuki Adachi, “Load-Balancing Spectrum Decision for Cognitive Radio Networks,” accepted by *IEEE Journal on Selected Areas in Communications (JSAC)*.

## Journal Paper (submitted)

1. Li-Chun Wang, Chung-Wei Wang, and Yu-Chee Tseng, “Concurrent Transmission MAC Protocols for Multiple-Access-Point Wireless Local Area Networks,” submitted to *IEEE Proceedings*, 2010.
2. Li-Chun Wang, Chung-Wei Wang, and Kai-Ten Feng, “A Queueing-Theoretical Framework for QoS-Enhanced Spectrum Management in Cognitive Radio Networks,” submitted to *IEEE Wireless Communications Magazine*, 2010.



3. Li-Chun Wang, Chung-Wei Wang, and Chung-Ju Chang, “Modeling and Analysis for Spectrum Handoffs in Cognitive Radio Networks,” submitted to *IEEE Transactions on Mobile Computing*, 2010.
4. Li-Chun Wang, Chung-Wei Wang, and Chung-Ju Chang, “Optimal Target Channel Sequence for Multiple Spectrum Handoffs in Cognitive Radio Networks,” submitted to *IEEE Transactions on Communications*, 2010.

## **Journal Paper (to be submitted)**

1. Li-Chun Wang, Chung-Wei Wang, and Fumiyuki Adachi, “Modeling and Analysis for Spectrum Handoffs in Cognitive Radio Networks with On-Demand Channel Search,” to be submitted.
2. Li-Chun Wang, Chung-Wei Wang, and Kwang-Cheng Chen, “Interference-avoiding Admission Control in Cognitive Radio Networks with Imperfect Primary User’s Detection,” to be submitted.
3. Li-Chun Wang, Chung-Wei Wang, and Yin-Chih Lu, “Latency Analysis for Dynamic Spectrum Access in Cognitive Radio: Dedicated or Embedded Control Channel?,” to be submitted.

## **Patent**

1. Li-Chun Wang and Chung-Wei Wang, “Apparatus and method for neighbor-aware concurrent transmission media access control protocol,” filed for the Taiwan, U.S., China, and India patents with ITRI, in Aug. 2009.

## Conference Paper

1. Chung-Wei Wang, Li-Chun Wang, and Fumiyuki Adachi, "Modeling and Analysis for Rective-decision Spectrum Handoff in Cognitive Radio Networks," *IEEE GLOBECOM*, 2010.
2. Li-Chun Wang and Chung-Wei Wang, "Spectrum Management Techniques with QoS Provisioning in Cognitive Radio Networks," *International Symposium on Wireless and Pervasive Computing (ISWPC)*, 2010.
3. Chung-Wei Wang, Li-Chun Wang, and Fumiyuki Adachi, "Optimal Admission Control in Cognitive Radio Networks with Sensing Errors," *IEICE Tech. Rep.*, vol. 109, pp. 491-496, Mar. 2010.
4. Chung-Wei Wang, Li-Chun Wang, and Fumiyuki Adachi, "Probability-based Channel Selection Scheme in Cognitive Radio Networks," *IEICE Tech. Rep.*, vol. 109, pp. 209-212, Dec. 2009.
5. Chung-Wei Wang, Li-Chun Wang, and Fumiyuki Adachi, "Modeling and Analysis for Proactive-decision Spectrum Handoff in Cognitive Radio Network," *IEICE Tech. Rep.*, vol. 109, pp. 13-18, Aug. 2009.
6. Chung-Wei Wang, Li-Chun Wang, and Fumiyuki Adachi, "Performance Gains for Spectrum Utilization in Cognitive Radio Networks with Spectrum Handoff," *International Symposium on Wireless Personal Multimedia Communications (WPMC)*, 2009.
7. Chung-Wei Wang, Li-Chun Wang, and Fumiyuki Adachi, "Modeling and Analysis of Multi-User Spectrum Selection Schemes in Cognitive

- Radio Networks,” *IEEE International Symposium on Personal, Indoor and Mobile Radio Communications (PIMRC)*, 2009.
8. Jia-Ming Liang, Chung-Wei Wang, Li-Chun Wang, and Yu-Chee Tseng, “The Upper Bound of Capacity for A Concurrent-transmission-based Ad-hoc Network with Single Channel,” *IEEE VTS Asia Pacific Wireless Communications Symposium (APWCS)*, 2009.
  9. Chung-Wei Wang and Li-Chun Wang, “Modeling and Analysis for Proactive-decision Spectrum Handoff in Cognitive Radio Networks,” *IEEE International Conference on Communications (ICC)*, 2009.
  10. Li-Chun Wang and Chung-Wei Wang, “Spectrum Handoff for Cognitive Radio Networks: Reactive-Sensing or Proactive-Sensing?,” *IEEE International Performance Computing and Communications Conference (IPCCC)*, 2008.
  11. Li-Chun Wang and Chung-Wei Wang, “Spectrum Handoff for Cognitive Radio Networks with Reactive Sensing,” *IEEE VTS Asia Pacific Wireless Communications Symposium (APWCS)*, 2008.
  12. Li-Chun Wang, Yin-Chih Lu, Chung-Wei Wang, and David S.-L. Wei, “Latency Analysis for Dynamic Spectrum Access in Cognitive Radio: Dedicated or Embedded Control Channel?,” *IEEE International Symposium on Personal, Indoor and Mobile Radio Communications (PIMRC)*, 2007.
  13. Li-Chun Wang, Chung-Wei Wang, Yin-Chih Lu, and Chuan-Ming Liu, “A Concurrent Transmissions MAC Protocol for Enhancing Throughput and Avoiding Spectrum Sensing in Cognitive Radio,” *IEEE Wireless Communications and Networking Conference (WCNC)*, 2007.

14. Li-Chun Wang, Chung-Wei Wang, and Chuan-Ming Liu, "Adaptive Contention Window-based Cluster Head Election Algorithms for Wireless Sensor Networks," *IEEE VTC Fall*, 2005.
15. Li-Chun Wang, Chung-Wei Wang, and Chuan-Ming Liu, "Optimizing the Number of Clusters in a Wireless Sensor Network Using Cross-layer Analysis," *IEEE International Conference on Mobile Ad-hoc and Sensor Systems*, 2004.
16. Li-Chun Wang, Chung-Wei Wang, and Chuan-Ming Liu, "A Cross-Layer Design for Determining the Optimal Number of Clusters in a Wireless Sensor Network," *IEEE International Conference on Computing, Communications and Control Technologies (CCCT)*, 2004.
17. Li-Chun Wang and Chung-Wei Wang, "A Cross-layer Design of Clustering Architecture for Wireless Sensor Networks," *IEEE International Conference on Network, Sensing and Control (ICNSC)*, 2004.
18. Anderson Chen, Li-Chun Wang, Chung-Wei Wang, and David S.L. Wei, "NICER- A Distributed Wireless Medium Access Control Protocol in Mobile Ad Hoc Networks with Multimedia Traffic," *IEEE VTC Fall*, 2003.